A Genetic Strategy for Transsynaptic Tracing Reveals Neural Representations of Taste in *Drosophila*

By

Nathaniel James Snell

B.A., University of Wisconsin – Madison, 2012

Thesis

Submitted in partial fulfillment of the requirements for the

Degree of Doctor of Philosophy in the Department of Neuroscience at Brown University

PROVIDENCE, RHODE ISLAND

FEBRUARY 2021

This dissertation by Nathaniel James Snell is accepted in its present form by the Department of Neuroscience as satisfying the dissertation requirement for the degree of Doctor of Philosophy.

Date_____ _____

Gilad Barnea, Advisor

Recommended to the Graduate Council

Date_____ _____

David Berson, Reader

Date_____ _____

Alexander Fleischmann, Reader

Date_____ _____

Karla Kaun, Reader

Date_____ _____

Mark Stopfer, Reader

Approved by the Graduate Council

Date_____ _____

Andrew Campbell, Dean of the Graduate School

NATHANIEL J. SNELL
Box GL-N, Brown University, Providence, RI 02912 | nathaniel_snell@brown.edu

EDUCATION

Ph.D. candidate, Neuroscience, Brown University (expected, Dec) 2020
B.A., Biology, University of Wisconsin – Madison 2012

RESEARCH

Graduate student researcher, lab of Gilad Barnea, Brown University 2014 – present

- Helped develop and validate *trans*-Tango, a genetic tool for transsynaptic labeling and transgene expression in *Drosophila*
- Identified second-order neurons in *Drosophila* gustatory circuits through immunohistochemistry, mosaic analysis, and computational brain registration
- Characterized representation of taste information by *Drosophila* gustatory projection neurons through *in vivo* two-photon calcium imaging
- Programmed custom scripts for functional imaging analysis in ImageJ and Matlab
- Generated recombinant DNA constructs for transgenic *Drosophila* and cell culture expression through molecular cloning techniques
- Designed and evaluated new variants of *trans*-Tango, including alternative ligand/receptor configurations and variations on ligand expression strategy
- Designed and evaluated new Q-system reporters for *trans*-Tango output, including calcium indicators, effectors for activating and silencing neurons, and strategies for restricting reporter expression to defined subsets of postsynaptic populations
- Assessed effects of genetic manipulation of *trans*-Tango-labeled neural populations in various behavioral assays, including feeding and circadian rhythm assays

Research assistant, lab of Bas Rokers, University of Wisconsin – Madison 2012 – 2013

- Developed psychophysical experiment for assessing rules underlying the transfer of human visual perceptual learning
- Programmed tasks and analyzed data using Psychtoolbox in Matlab
- Coordinated participants in study under IRB guidelines

PUBLICATIONS

Talay M, Richman EB, **Snell NJ**, Hartmann GG, Fisher JD, Sorkaç A, Santoyo JF, Chou-Freed C, Nair N, Johnson M, Szymanski JR, Barnea G. (2017). Transsynaptic Mapping of Second-order Taste Neurons in Flies by *trans*-Tango. **Neuron** 96, 783-795. doi:/10.1016/j.neuron.2017.10.011

Snell N, Kattner F, Rokers B, Green CS. (2015). Orientation Transfer in Vernier and Stereoacuity Training. **PLoS ONE** 10(12): e0145770. doi:10.1371/journal.pone.0145770

AWARDS AND HONORS

National Science Foundation Graduate Research Fellowship recipient 2014
Bachelor's degree awarded with distinction 2012

PATENTS

"Methods for labeling and manipulating a cellular circuit"
U.S. Patent Application No.: 15/558,900
Filing Date: September 15, 2017
Inventors: Gilad Barnea, Mustafa Talay, Ethan Richman, John Szymanski, Mark Johnson, John Fisher, Nathaniel Snell

ORAL PRESENTATIONS

"Neural circuits for taste in *Drosophila*" 2019
Brown Neuroscience departmental in-house seminar
"Neural circuits for taste in *Drosophila*" 2019
Brains n' Roses: International Symposium on Olfaction, Collège de France, Paris, France
"Neural circuits of taste in *Drosophila*" 2018
Brown Neuroscience departmental in-house seminar
"Transsynaptic mapping of *Drosophila* gustatory circuitry" 2017
Brown Neuroscience departmental in-house seminar
"Mapping and manipulating *Drosophila* chemosensory circuits with *trans*-Tango" 2016
Brown Neuroscience departmental in-house seminar
"Expanding the *trans*-Tango toolbox for circuit mapping and manipulation in *Drosophila*" 2015
Brown Neuroscience departmental in-house seminar

TEACHING

Guest lecturer, "Animal Minds" 2019
Summer@Brown (High School Summer Program at Brown University)
Guest lecturer, "Behavioral Neuroscience" 2018
Rhode Island College
Completed certificate program, "Reflective Teaching" 2015
Sheridan Center for Teaching and Learning, Brown University
Teaching assistant, "Neural Systems" 2014
Brown University

CONFERENCES ATTENDED

Brains n' Roses: International Symposium on Olfaction, Collège de France, Paris, France 2019
Boston Area Drosophila Meeting, Providence, RI 2019
Boston Area Drosophila Meeting, Boston, MA 2018
Brains n' Roses: International Symposium on Olfaction, Sant Fruitós de Bages, Spain 2016
Society for Neuroscience, San Diego, CA 2013

COURSES ATTENDED

***Drosophila* Neurobiology: Genes, Circuits & Behavior**, Cold Spring Harbor Laboratory 2017

LEADERSHIP AND OUTREACH

Coordinator, Brown Fly Club	2017 – 2020
Assistant coordinator, Boston Area Drosophila Meeting	2019
Graduate student representative, Brown Neuroscience Department	2016 – 2017
High school science outreach, Shea Senior High School, Pawtucket, RI	2016
Judge, Rhode Island Brain Bee	2016
Transportation coordinator for recruitment, Brown Neuroscience Department	2016
Mentor, Graduate-Undergraduate Mentorship Initiative, Brown University	2014 – 2016
Middle school science outreach, Gordon School, East Providence, RI	2014

MENTORING

Jonathan Huang, Brown Sc.B. '20

- Mentored as an undergraduate researcher in the Barnea Lab
- Currently: Medical student, Northwestern

Sasha Martinez-Machado, Brown Sc.B. '18

- Mentored as an undergraduate researcher in the Barnea Lab
- Currently: Research assistant, Massachusetts General Hospital

Collins Cheruiyot, Brown Sc.B. '16

- Mentored through Graduate-Undergraduate Mentorship Initiative program
- Currently: Ph.D. candidate in Immunology, Harvard

PREFACE

The sense of taste is critical to an animal's survival, as it provides the ability to discriminate nutritive substances from non-nutritive or toxic ones. It is also an unusual sensory modality, in that it is thought to consist of only a small number of discrete categories, known as taste qualities. In humans, these are the five basic tastes: sweet, bitter, salty, sour, and umami. How are these taste qualities encoded by the nervous system? Many other sensory systems are known to represent features of the environment by distinct population-level patterns of neural activity. In this coding scheme, known as distributed coding or population coding, the identity of a stimulus can only be decoded by interpreting the broader pattern of neural activity, not by analyzing the response of any one particular neuron within the population. In contrast, a prominent theory holds that taste quality is encoded not by ensembles of neurons, but through "labeled lines". In this model, there are parallel, segregated neural circuits dedicated to each taste quality, from sensory input to behavioral output. The existence of a labeled-line architecture for taste would entail a significant departure from other sensory systems. Yet determining if the gustatory system is organized in labeled lines requires understanding how taste quality is represented by neurons at each successive level in a neural circuit. This understanding has remained elusive in part because of a lack of tools that could provide this kind of neural circuit tracing.

In this dissertation, I describe the development of such a tool for circuit tracing, and use it to examine how neural circuits represent taste in the fly *Drosophila melanogaster.* In chapter 1, I provide background on what is understood about the neural

circuits of taste, from mammals to insects. In chapter 2, I introduce *trans*-Tango, a novel genetic method for transsynaptic circuit mapping. I demonstrate that *trans*-Tango is a powerful and versatile tool for neural circuit analysis, and reveal the anatomy of second-order neurons in the taste system of *Drosophila*. In chapter 3, I combine *trans*-Tango with *in vivo* imaging of neural calcium responses to investigate how second-order taste neurons in the fly respond to sweet and bitter compounds. I argue that these data support a mixed model of taste coding, in which some neurons are narrowly tuned to distinct taste qualities while others use a distributed coding strategy to represent taste. Finally, in chapter 4 I discuss the implications of these findings, and identify potential directions for future research on the neural underpinnings of taste.

ACKNOWLEDGMENTS

This dissertation would not have been possible without the help of many other people. First, it has been an incredible privilege to spend the last several years learning how to be a scientist in the Barnea lab. From the bench to Barcelona, I have been so fortunate to work with so many intelligent, passionate, creative, dedicated, and fun people in the lab over the years. I especially want to thank my advisor, Gilad Barnea. The sincerity and generosity of his support for each of his trainees, his fostering of a collaborative and egalitarian lab culture, emphasis on values and integrity, and vision of what is important and beautiful in science has made a great impression on me.

Outside the lab, there are many others in the department to whom I owe my gratitude. Thank you to my thesis committee – David Berson, Karla Kaun, and Alex Fleischmann – for all their valuable feedback and willingness to sit down with me and answer my questions over the years. Thanks to David Sheinberg for his advice during my first year of graduate school, and to Chris Moore for the continuing interest in my scientific development. Thank you to the administration, especially Carol Viveiros and Rosanna Cabral, for all their help, from planning the recruitment weekend to all my last-minute questions on the dissertation and everything in between. Finally, I want to thank Mark Stopfer from the NIH for taking the time to serve as my outside reader.

I have been lucky to make so many great friends here in Rhode Island. Thank you to everyone I have met here for all the fun times, from the good old days in the NSGP first-year office, to every game night, beach day, ski trip, brewery visit, trivia competition and food truck festival, and all the great conversation at the GCB and Tea in Sahara.

Most of all, I want to thank my family. To my parents, John and Barbara Snell: thank you for your unconditional love, for your generosity, for encouraging all of my creative pursuits, and for always believing in me from the very beginning. To my brother, Alex: thanks for the Danny DeVito pillowcase. To my wife, Megan: I cannot believe how lucky I am to have met you on day one of this crazy grad school journey. Thank you for your love, patience, and support over the years, for keeping me grounded in hard times and for being my best friend all the time. I could never have made it without you. And to my in-laws, Gary and Donna Leyrer: thank you so much for welcoming me into the family.

TABLE OF CONTENTS

LIST OF ILLUSTRATIONS

CHAPTER 1

An Introduction to the Neural Circuits of Taste

1.1 Introduction

Which of the five senses would you miss the most if you lost it? A recent YouGov poll asked this question (Nguyen, 2018; Purtill & Kopf, 2018), and most people (70%) answered vision. Smell was the least popular response – even less popular than taste. Why would so many people prefer to keep their sense of taste over their sense of smell? Presumably, these people want to continue to enjoy the flavors of food. Yet most of the flavor we experience in food is actually due to our sense of smell. Accurately defined, taste, or gustation, refers only to the sensations of sweet, bitter, salty, and sour, plus the lesser-recognized umami – the savoriness of meat or hearty broth. On the other hand, smell, or olfaction, allows for the perception of a vast range of aromas, and furnishes most of the sensation of flavor that cannot be fit into one of those five simple categories of taste. Our sense of smell is what makes the flavor of orange juice more interesting than a solution of sugar and acid.

Perhaps the survey responders were ignorant of this fact. Surely, knowing this, no one would prefer taste over smell. But for all the pleasure that the smell of food adds to our culinary experience, there is a corollary: it also provides many of the aspects of flavor we find unpleasant. Furthermore, which odors we find pleasant or unpleasant is not predetermined. Rather, we develop positive or negative associations to smells mostly, if not entirely, through experience. Since flavor is dominated by smell, this finding applies to flavor as well. This may not be particularly surprising, since people have such wide-ranging individual preferences and dislikes of different foods. While many of us enjoy the particular richness of chocolate and boldness of coffee, there are others for whom these flavors cause disgust, triggered by the same olfactory cues.

In contrast, the hedonic aspects of taste appear to be innate. It is common knowledge that sweet is a "good" taste, while bitter taste is "bad", and it seems likely that these associations are universal and do not have to be learned. Anthropologists have concluded that sweet foods are preferred in all human cultures studied, and it has been documented that newborn infants make stereotyped facial expressions of happiness or disgust upon tasting a sweet or bitter solution (Myers, 1904; Steiner, 1974). Of course, we can learn to override these innate evaluations to some degree – as any beer or coffee drinker knows – and any taste can be offensive at high intensity. But the conspicuous commonality in our judgments of taste suggests that its connection to pleasure may be predefined and unlearned.

So how do we come to like certain flavors and not others? There are numerous possible reasons: perhaps we like the flavor of a certain food because we associate it with a happy memory, or dislike it because it once made us sick. But for many foods, it is likely that its taste played a significant role in shaping our preference for it. Considering this, let us revisit the original question. If one lost their sense of taste but kept their sense of smell, they might continue to enjoy the distinctive character of the flavors they know and love. But the reason they learned to love those flavors in the first place may have been the tastes that they now have lost! And without taste, they risk losing their ability to learn to enjoy new foods.

Luckily, this is a thought experiment, and we do not really have to make this choice. Yet, as I am writing this in the fall of 2020 – in the midst of the COVID-19 pandemic – it seems appropriate to mention that many people unfortunately do suffer from anosmia, or the loss of the sense of smell. Anosmia is one unusual symptom and

early indicator of COVID-19 infection; case studies have reported various figures between 34% to 98% of patients presenting with anosmia (Pellegrino et al., 2020), while psychophysical tests put the number around 77% (Hannum et al., 2020). While most people who suffer from COVID-induced anosmia regain their sense of smell within a few weeks, some cases last much longer (Boscolo-Rizzo et al., 2020). This kind of prolonged anosmia can be devastating to those who suffer from it (Miwa et al., 2001; Neuland, Bitter, Marschner, Gudziol, & Guntinas-Lichius, 2011). This reality contrasts sharply with the dismissive attitude towards the importance of olfaction that many people have.

Considering the loss of smell and taste has hopefully demonstrated not only how much we take these senses for granted, but also how much our naïve understanding of these senses is insufficient. When it comes to understanding what drives our perceptions, our intuition may not be the best guide. We do not intuitively distinguish the taste and smell components of flavor, for example, despite these components being driven by different sensory modalities. And even when we pay attention to this distinction, simply being aware of the difference does not provide much insight into how these different sensory signals are processed by the brain. How much of the joy of a good meal is driven by the complexities of its aroma, and how much by a few simple taste sensations on the tongue? How do these tastes shape which foods we prefer and which we despise? What else is our sense of taste doing? What hidden roles might it be performing beyond the scope our conscious awareness?

In this dissertation, I present my research on how taste is represented in the brain. While I use the fruit fly *Drosophila melanogaster* to address this question, the findings I present may have general implications for how neural circuits of any species encode

taste. As such, I begin in this chapter with a general background on the study of taste. I first address some basic concepts, and then give a brief tour of the history of gustatory (or taste-related) neuroscience, introducing along the way two competing models for how neural circuits encode taste through the discoveries that seemed to support each one. After establishing these foundations, I survey what is known about the neural basis of taste in mammals, and then compare this to what is known about taste in insects, focusing on *Drosophila*. In Chapter 2, I introduce a novel method our lab developed for transsynaptic tracing and neural circuit manipulation, called *trans*-Tango. In Chapter 3, I present research using *trans*-Tango and functional neural imaging to address how taste information is encoded in the *Drosophila* brain. Finally, in Chapter 4, I discuss the implications of these findings, potential directions for follow-up research, and how these findings may relate to our own sense of taste.

1.2 Basic tastes

Before we explore how molecular mechanisms and neural codes explain how we perceive food on our tongue to have a taste, we must be clear what it is we are trying to explain – the taste perception itself. What perceptions of taste do we have? What counts as taste, and what does not? As mentioned earlier, taste is different from flavor. Flavor is a holistic sensation, incorporating smell, taste, temperature, and texture. In humans, taste, or gustation, is limited to the five qualities we call the *basic tastes*: sweet, bitter, salty, sour, and umami. Why do we consider only these five qualities to count as taste? Why not more, or fewer? Why these categories, and not others? And why split taste into categories at all?

Historical evidence shows that the way we organize taste into basic tastes is not entirely self-evident. If it were, human societies would always identify the same list of five basic tastes. On the contrary, the list has not even always had five members (Beauchamp, 2019). In ancient China, there were five, but not the same five we accept today; they included sweet, bitter, salty, and sour, but also pungent (spicy). In ancient India, there were six: the same five as ancient China, plus astringency (the dry sensation found in wine, tea, or unripe fruit). In ancient Greece, Aristotle taught that there were only two fundamental tastes, sweet and bitter. But in his view, a total of seven tastes could emerge from sweet and bitter as a product of mixing the two in different proportions, like mixing two primary colors to get a spectrum of intermediates (Beauchamp, 2019; Dethier, 1978). These seven tastes comprised the six from ancient India plus another translated as "harsh", and they remained the accepted basic taste categories in Europe through the Middle Ages (Finger, 1994).

Eventually, European scientists changed this list in two ways. Some added even more tastes, such as metallic or insipid (Finger, 1994). All such new candidate tastes would end up being rejected, since it was determined they either could be better explained by olfaction or texture, or they were not truly distinct from the other tastes. Other scientists looked to pare Aristotle's list down. It was apparent that some qualities classified as "tastes" might be better explained by other sensory modalities. Pungency is a painful sensation, and astringency is textural. Since pain and texture are somatosensory qualities, not purely gustatory ones, these became excluded from the list (Beauchamp, 2019). This brought down the number of basic tastes to four: sweet, bitter, salty, and sour.

The fifth taste, umami, is the most recent addition to the basic taste list. The term "umami" was coined in 1908 by the chemist Kikunae Ikeda to describe the savory taste of the broth made from dashi, a Japanese kelp (Ikeda, 2002). He determined that the component of the broth that gave it this taste was glutamate. While some remain skeptical as to whether umami counts as a true basic taste based its relative subtlety (Beauchamp, 2019), several lines of experimental evidence support its inclusion in our list. First, subjects can distinguish umami from the other four tastes (Yamaguchi & Ninomiya, 2000). Second, umami taste is augmented by the addition of ribonucleotides like IMP (inosine monophosphate), an effect specific to umami. Finally, in the early 2000s a molecular mechanism was identified for glutamate detection at the taste bud, and this mechanism recapitulated umami's hallmark synergy with ribonucleotides (Nelson et al., 2002). These facts have proven persuasive, as umami is now widely considered by researchers to be one of the basic tastes.

It has been observed that taste correlates with the chemical identity of the tastant, i.e., the thing being tasted. Glutamate is umami, sugar is sweet, acids are sour, sodium salts are salty, and alkaloids and other types of noxious organic compounds are bitter. This correspondence suggests that taste signals the detection of a particular class of nutrients or, in the case of bitter, toxins. Yet this list does not span the entire range of our dietary needs. For example, fat and calcium are examples of necessary nutrients that do not evoke one of the five basic tastes. Might there be a sixth or seventh taste for these substances? Some have suggested that there are (Running, Craig, & Mattes, 2015; Tordoff, Alarcón, Valmeki, & Jiang, 2012), but these claims are controversial (Beauchamp, 2019). On the one hand, the recent discovery of the subtle taste of umami

makes the idea of additional tastes seem more reasonable. To qualify, these candidates would have to elicit a taste perception that is both distinguishable from the other five tastes and not explained by any olfactory or somatosensory qualities. Fat and calcium produce a sensation like a taste, but these perceptions are mild and potentially explainable either by other tastes or other sensory modalities (Beauchamp, 2019). Thus, while these examples may in fact illustrate new basic tastes, they are not yet widely accepted, so we will not address them further.

Another possible way more than five tastes could exist is if one of the basic tastes could be subdivided into two. For example, if sugar A and sugar B produced slightly different variations of sweet, then sweet would be not one basic taste, but two – sweet A and sweet B. But experimental evidence shows that there is only one kind of sweet: for each pair of sugar compounds, the concentrations of each can be adjusted so that the two are indistinguishable (Breslin, Beauchamp, & Pugh, 1996; Breslin, Kemp, & Beauchamp, 1994). This strategy is called metameric matching. While powerful, it has several limitations which has made it difficult to apply to other taste qualities. For example, some tastants evoke more than one taste sensation, some produce distinct textural sensations, and some trigger taste responses with different temporal properties, meaning that these sensations linger longer on the tongue than others (Beauchamp, 2019). As a result, even very fine distinctions between tastants – distinctions that may not be truly related to taste quality – can be used as cues for discrimination in these studies.

However, some have argued that the concept of four discrete basic taste categories is a mistake. Perhaps taste is a continuous variable, with infinite shades of taste in between each of the primary basic tastes. One early model considered the four basic

tastes (without umami) as four corners of a tetrahedron, with a continuity of taste intermediates in the area between (Finger, 1994). Others have taken this idea further, rejecting the notion that there are any basic tastes, primary tastes, or meaningful taste categories at all (Erickson, 2008). These ideas have remained controversial, in part because this is an unnatural way for most people to think about taste. Proponents of anti-"basic taste" theories have argued that it is our language and our inherited scientific assumptions that constrain our way of thinking in this matter – it is only that scientists have assumed that there are basic tastes, and that we have all been taught to think about taste in terms of our basic taste vocabulary, that we learn to perceive the world through these categories (Erickson, 2008). However, it has also been noted that over 60 languages have specific words for these four basic tastes. If these categories are cultural artifacts, why would so many cultures independently stumble upon the same ones? For this reason and others, many researchers remain skeptical of the anti-"basic taste" position (Beauchamp, 2019).

Here, we assume that there are basic tastes, that humans have five, and that these are sweet, bitter, salty, sour, and umami. Working with these conventions, we now turn to the biology underlying our sense of taste. Before surveying what is known about the neural circuits of the gustatory system, we should first address two prominent models that have been proposed for how the nervous system represents taste quality.

1.3 Labeled lines and population codes: A brief history of taste coding models

Our ability to recognize five different tastes implies that the brain represents these tastes in different ways. How is our nervous system wired to enable these distinct

representations of taste? Two competing models have been proposed to explain how our neural circuits achieve this end: the labeled-line model and the distributed coding (or population coding) model (Scott, 2018; Simon, De Araujo, Gutierrez, & Nicolelis, 2006; Spector & Travers, 2005; Yarmolinsky, Zuker, & Ryba, 2009). The labeled-line model posits that the five tastes are detected on the tongue by separate populations of sensory cells, which activate distinct, parallel neural circuits leading to the brain. In this model, taste information is segregated at each stage of the circuit. In contrast, the distributed coding model proposes that information about different tastes becomes integrated at some stage of the circuit; thus, a single neuron may respond to multiple taste qualities. In this model, it is the larger pattern of activity that distinguishes two tastes, not the activity of single neurons, and higher brain regions decode taste identity by interpreting the pattern of the whole population. While other possibilities have been put forth, such as the theory that the precise temporal pattern of neural activity is critical to representing taste identity, these two models have dominated the scientific discourse. Since the models entail concrete and testable predictions, one might think that the debate would be resolved by now. It is not. To understand why, let us take a brief historical detour, reviewing the major evidence that persuaded the proponents of each theory.

Some of the earliest electrophysiological experiments on mammalian taste were done in the 1940s in the lab of Carl Pfaffmann at Brown University. Pfaffmann's group developed a technique for recording from single taste nerve fibers of an animal while delivering tastants to its tongue. This preparation allowed them to determine the tuning of single neurons to tastants of various qualities. In one experiment, they found that single fibers of the cat could be classified into three groups based on their response properties:

group 1 responded to salt and acid, group 2 to quinine and acid, and group 3 to acid alone (Pfaffmann, 1941). Only one of these three groups, group 3, coincides with a basic taste quality – sour. The second group, for instance, responds to both bitter (quinine) and sour (acid) tastants. To know that the tongue is tasting bitter rather than sour, the brain must analyze the pattern of response across the whole nerve: group 2 alone means bitter, but groups 2 and 3 together mean sour. This is inconsistent with a simple labeled-line model. One caveat to this conclusion is that it relies on the faulty assumption that the animal's basic tastes mirror those of our own. Indeed, we know this is not strictly true, since cats seem to lack sweet taste (and correspondingly, none of the fibers in this experiment responded to sucrose) (X. Li et al., 2005). But while we cannot say that cats perceive sour like we do, the fact that acid excites all three fiber groups implies one of two things: either the labeled-line model is correct and the cat tastes acids as having three taste qualities, or acid taste is not encoded through labeled lines. Pfaffmann concluded the latter – that taste fibers use a population code – and he called this coding scheme the across-fiber pattern.

Follow-up experiments seemed to confirm the across-fiber pattern model, with one qualification. Critical to the across-fiber pattern was the existence of fiber types; in Pfaffmann's cat experiment, these types were the three groups, whose relative activity indicated the quality of the tastant. Such fiber types would consistently be found in later experiments, in a variety of mammalian species (Spector & Travers, 2005). But many fiber types seemed to be "specialists": some responded specifically to sugars, some to sodium salts, some to bitter alkaloids. Other fiber types acted as "generalists", responding to a broad variety of tastants, in a way that did not conform to any basic taste quality

(Frank, 2000). While the existence of specialist and generalist fibers is consistent with an across-fiber pattern model, it could also indicate a kind of mixed model, wherein labeled lines for some taste qualities coexist with a population code for others. Pfaffmann himself eventually suggested such a possibility (Pfaffmann, 1974). Thus, while the evidence for labeled lines of taste appeared weak at first, scientific support for the model began to grow.

But the biggest victory for the labeled line interpretation came in the late 1990s, with a series of discoveries of the molecular mechanisms for taste transduction. The labs of Nicholas Ryba and Charles Zuker identified two G protein-coupled receptors (GPCRs) that were expressed specifically in taste buds (Hoon et al., 1999). This finding was especially exciting because it so closely resembled a seminal discovery made a few years earlier by Linda Buck and Richard Axel (Buck & Axel, 1991). Buck and Axel had set out to identify the genes that encoded olfactory receptors. Buck had several key insights: first, that these receptors likely GPCRs; second, that there were likely to be a family of many receptors, as many odorants with significant differences in chemical structure would need to be recognized; and third, that these would be expressed selectively in the olfactory epithelium. She used RT-PCR (reverse transcription polymerase chain reaction) to isolate gene transcripts specific to olfactory tissue, then amplified out candidate GPCRs from the results. Because there was no foreknowledge of the sequences these candidate olfactory GPCRs would have, Buck needed degenerate primers: mixes of primers that are flexible in the bases they recognize at positions where the target base is unknown. Through this method, she was able to identify a novel GPCR family from olfactory epithelium – the olfactory receptors (ORs).

The Ryba and Zuker labs used a similar strategy to identify candidate taste receptors (Hoon et al., 1999). Like Buck and Axel, they recognized that taste receptors were likely GPCRs, and that they would be expressed in taste bud cells, but not the surrounding tissue. They obtained cDNA libraries from single taste bud cells by RT-PCR and screened these libraries for sequences specific to taste tissue. From these taste-specific gene transcripts, they used degenerate primer strategies to amplify out GPCRs, and obtained two candidates, which they named TR1 and TR2 (later to be renamed T1R1 and T1R2). Interestingly, transcripts of these two receptors were expressed in mostly non-overlapping taste bud cells. If these receptors recognize different categories of tastants, then this result would suggest that taste qualities may be detected by different sensory cells.

Following these findings, another group of taste receptors was discovered – this time with some help from human genetics. For some people, the chemical 6-n-propylthiouracil (PROP) is quite bitter; for others, it is tasteless (Bartoshuk & Beauchamp, 1994). The ability to taste PROP was linked to a specific genetic locus on human chromosome 5p15 (Reed et al., 1999). Similarly, there are several strains of mice with bitter-tasting deficits linked to different regions of the genome. Both the Zuker/Ryba group and the lab of Linda Buck scanned these regions for potential genes encoding GPCRs, and found several belonging to a novel gene family, the T2Rs (Adler et al., 2000; Matsunami, Montmayeur, & Buck, 2000). T2Rs are activated by bitter compounds (Chandrashekar et al., 2000a), suggesting they are the functional bitter taste receptors. Furthermore, the T2Rs are expressed by different taste bud cells from either of the T1Rs (Adler et al., 2000). Thus, a model was emerging in which different taste cells detected

different categories of tastants. In other words, the evidence increasingly seemed to point towards labeled lines.

It should be noted that a third alternative is often discussed in addition to the two models of labeled lines and population coding: temporal coding. Labeled lines and population codes are forms of "spatial" coding models, meaning that the relevant variable in the encoding of taste is *which* cells are active, and how active they are – that is, their firing rate (Spector & Travers, 2005). However, information may be encoded not just through spike rate, but spike *timing*. It has been proposed that sensory systems with low temporal bandwidth – that is, sensory systems in which rapid changes in the environment are not encoded with high fidelity – may allow for such temporal coding. In these systems, fine distinctions in spike timing are not used to represent fine temporal features of the stimulus, and so this temporal dimension is freed up to be used to represent non-temporal features, such as stimulus identity. This argument has been made for olfactory systems (Laurent 1999), and since gustatory systems also do not sample tastants at rapid rates, the argument can be made for taste as well. While there is evidence that central gustatory neurons carry information about stimulus identity in the temporal features of their spike trains (Rosen, Victor, & di Lorenzo, 2011; Roussin, Victor, Chen, & Di Lorenzo, 2008), most work on taste coding has focused on spatial coding models, and those will be our primary focus here. However, it is not necessarily the case that a single model is at work; spatial and temporal coding may be multiplexed within a single circuit (Laurent 1999), and so further roles for temporal coding cannot be dismissed.

1.4 The mammalian gustatory system: Taste buds

These results, that labeled lines and population coding (across-fiber patterning) may both be at work in the gustatory system, appear at first to be contradictory. To attempt to reconcile these findings, I will now survey what is known about the neural circuits of taste in the mammalian brain.

The taste circuit in mammals can be thought of as having four successive stages: taste bud, afferent nerve, brainstem, and forebrain. Taste buds are bulbous structures found on both the tongue and the soft palate. Each bud houses roughly 50-100 sensory cells called taste receptor cells (TRCs), named so because they express taste receptors on microvilli at their apical tip (Chandrashekar, Hoon, Ryba, & Zuker, 2006). The apical tips of the TRCs in a bud converge at the taste pore, a single point exposed to the surface of the tongue. TRCs are epithelial cells, not neurons, but they nevertheless release neurotransmitters upon excitation that activate downstream neurons, those of the afferent nerves (Roper & Chaudhari, 2017).

Three afferent nerves are involved in taste: the chorda tympani (CT), greater superficial petrosal (GSP), and glossopharyngeal (GP) nerves. The CT and GSP are two branches of cranial nerve VII and innervate the taste buds of the anterior tongue and soft palate, respectively, while the GP is cranial nerve IX and innervates the buds of the posterior tongue. The cell bodies of the CT and GSP are found in the geniculate ganglion, while the cell bodies of the GP are found in the petrosal ganglion (Yarmolinsky et al., 2009).

The axons of all these neurons project to one brainstem region, the rostral nucleus of the solitary tract (rNST). Some rNST neurons project locally to other hindbrain regions

involved in reflexive taste responses and the coordination of feeding motor programs. But many rNST neurons send information to regions in the forebrain: to the cortex via the thalamus, to the hypothalamus, and to the amygdala (Spector & Travers, 2005).

At this stage of the circuit, there are important neuroanatomical differences between primates like us and the rodents commonly used as model mammals (Rolls, 2019). In primates, rNST neurons project directly to the ventroposteromedial nucleus of the thalamus (VPN), and VPN neurons target a region of insular cortex called the gustatory cortex (GC). From there, information is broadcast to several cortical regions, as well as subcortical regions such as amygdala and hypothalamus. In rodents, on the other hand, rNST neurons first synapse onto another brainstem area, the parabrachial nucleus (PBN) of the pons. Some PBN neurons target VPN neurons, which in turn target GC, as in primates. But other PBN neurons directly target amygdala and hypothalamus, bypassing the cortex in a way not observed for primates. While these examples illustrate salient differences in circuitry, similar regions of the forebrain receive taste information across mammalian species.

Now that we have established the rough anatomy of the taste circuit, let us return to the taste buds, and investigate step by step how each stage of the circuit encodes the basic tastes. Taste begins at the TRCs, the sensory cells within the taste bud. TRCs extend microvilli into the taste pore at the apical end of the cell. Here, tastants contact the microvilli, where they are transduced into intracellular signals by receptors (Roper & Chaudhari, 2017). Different receptors mediate each of the five tastes. There is substantial evidence that the receptors for each taste are expressed by distinct sets of TRCs, suggesting labeled line coding for taste at the periphery (Yarmolinsky et al., 2009).

While we associate sweet taste with sugar, a variety of other compounds can elicit a sweet taste as well, including artificial sweeteners and some D-amino acids. One might imagine that many receptors would be required to recognize this wide range of chemicals. But evidence suggests that there are only two: T1R2 and T1R3, two GPCRs from the three-member T1R family of receptors (X. Li et al., 2002; Montmayeur, Liberles, Matsunami, & Buck, 2001; Nelson et al., 2001; Zhao et al., 2003). These receptors can heterodimerize, and several experiments suggest that their heterodimer may be the functional sweet receptor. Both are required for normal physiological and behavioral responses to sweet tastants *in vivo*, and both need to be expressed to confer normal sweet sensitivity *in vitro* (Zhao et al., 2003).

There is some evidence that the T1R2/T1R3 heterodimer may not be the only sensor for sweetness. T1R3 alone can detect high concentrations of sugars in cell culture, and TRCs expressing T1R3 alone have been identified (Nelson et al., 2001; Zhao et al., 2003). But even in the absence of T1R3, mice retain some neural responses and behavioral preferences to high concentration sugars (Damak et al., 2003). This effect may be partially explained by the presence of glucose transporters like GLUT4 and SGLT1 in some sweet-sensing TRCs (Yee, Sukumaran, Kotha, Gilbertson, & Margolskee, 2011). But the behavioral effect may also be due to sugar-sensing epithelial cells of the gut, which have been shown to transduce glucose via SGLT1 and promote food preferences (Kaelberer et al., 2018; Tan et al., 2020).

In contrast to sweet, umami taste is produced by a single compound: glutamate. But it is also synergized by the addition of 5' ribonucleotides like inosine monophosphate (IMP). Any candidate receptor for umami must demonstrate these two features.

Interestingly, a pair of T1Rs fulfills these criteria. T1R1 and T1R3 together, but not alone, transduce extracellular glutamate into intracellular G-protein signaling, and this effect is potentiated by IMP (X. Li et al., 2002; Nelson et al., 2002; F. Zhang et al., 2008; Zhao et al., 2003). Knockouts of either receptor sharply diminish behavioral and physiological responses to glutamate as well. Thus, it appears that a T1R1/T1R3 heterodimer forms a functional umami receptor, similar to the T1R2/T1R3 heterodimer for sweet taste. However, there are reports that T1R3 knockouts can continue to detect umami taste (Damak et al., 2003). Since the stimulus most often used for umami taste is monosodium glutamate (MSG), and sodium ions are the drivers of salty taste, these T1R3-independent responses might reflect the stimulus's saltiness. But there is also evidence of another metabotropic glutamate receptor, mGluR4, that is expressed in TRCs (Chaudhari, Landin, & Roper, 2000). Knocking out mGluR4 reduces, but does not abolish, neural responses to glutamate/IMP. These results are consistent with the mGluR4 receptor also having a minor role in umami detection.

Bitter taste is thought to have evolved as a kind of security system, a means for detecting toxic substances in food before they are swallowed and digested (Glendinning, 1994). Potential toxins are not defined by a common chemical structure; rather, they are a vast and diverse group of compounds, produced largely by plants as their own defense system against being eaten (Wittstock & Gershenzon, 2002). As such, bitter taste must recognize a large number of unrelated compounds. In mammals, this goal is accomplished by GPCRs, as it is for sweet and umami taste. But unlike sweet and umami, bitter taste is transduced by a large family of receptors, the T2Rs, which number about 40 in rodents and 25 in humans (Adler et al., 2000; Chandrashekar et al., 2000b; Matsunami

et al., 2000; Mueller et al., 2005). While each T2R has a relatively narrow range of tastants it can detect, a single bitter TRC expresses many T2Rs, enabling it to recognize a broad range of bitter stimuli (Adler et al., 2000; Chandrashekar et al., 2000b). Does each bitter TRC detect *all* bitter tastants? This possibility was suggested by early studies, but it appears that TRCs do not express the full range of T2Rs; in humans, for example, there are about 4-11 T2Rs per bitter TRC (Behrens, Foerster, Staehler, Raguse, & Meyerhof, 2007). Likewise, individual bitter TRCs of the mouse do not respond to every bitter stimulus (Caicedo & Roper, 2001). Although this result shows that individual cells can discriminate between bitter stimuli, there is no clear behavioral evidence that the animal can (Spector & Kopka, 2002).

These three tastes – sweet, umami, and bitter – all rely on GPCRs and share common downstream transduction machinery (Liman, Zhang, & Montell, 2014; Y. Zhang et al., 2003). When the tastant binds to the receptor on the cell surface, it triggers the intracellular release of Gβγ from Gα subunits. Transduction follows through a mostly canonical phospholipase C (PLC) signaling pathway (except for the first step: rather than $G\alpha_q$, it is the Gβγ dimers that activate PLC in these cells) (L. Huang et al., 1999). PIP_2 is hydrolyzed, producing IP_3 that binds IP_3Rs on the ER membrane, raising cytosolic calcium levels. This calcium increase triggers the opening of TRPM5 channels on the cell membrane, allowing sodium ion influx and membrane depolarization. Depolarization causes opening of the voltage-gated CALHM1/3 channels, which release ATP as a neurotransmitter (Ma et al., 2018; Taruno et al., 2013).

Salty taste is based on the detection of sodium ions, in contrast to sweet, bitter, and umami, where larger tastant molecules need to be recognized. As such, the

mechanism of transduction is different. Rather than GPCRs, an epithelial sodium channel (ENaC) is expressed by salty-sensing TRCs (Chandrashekar et al., 2010). Sodium ions flow into the cell through ENaCs, depolarizing the cell and opening voltage-gated sodium channels, which trigger action potentials that open synaptic CALHM1/3 channels through which the neurotransmitter ATP is released (Nomura, Nakanishi, Ishidate, Iwata, & Taruno, 2020). Thus, the salt transduction pathway is different from the previously mentioned three in that neither GPCRs nor intracellular calcium increases are required, but all four tastes share a common output neurotransmitter.

Sour taste, like salty taste, is based on the recognition of ions: for sour, these are the free protons of acids. Likewise, the mechanism for sensing acids is not reliant on GPCRs. But acid-sensing TRCs are different from the other four TRC classes in several other ways. These TRCs are excited by intracellular acidification (Lyall et al., 2001; Ye et al., 2016), use conventional vesicular synapses rather than CALHM1/3 channel synapses (Kinnamon, Taylor, Delay, & Roper, 1985; Larson et al., 2015), and release neurotransmitters such as serotonin and GABA rather than ATP (Y. A. Huang, Pereira, & Roper, 2011). Organic acids can permeate the cell membrane to acidify the cytosol directly; strong acids, on the other hand, cannot permeate and must use a proton channel to acidify the cell (Chang, Waters, & Liman, 2010). This channel was recently discovered to be Otopetrin 1 (Otop1), a protein previously known only for its role in the development of otoconia in the vestibular system (Teng et al., 2019; Tu et al., 2018; J. Zhang et al., 2019). Thus, sour tastants directly acidify the sour TRCs, causing excitation and release of 5HT and GABA.

It appears that these transduction mechanisms for the five taste qualities function in five non-overlapping sets of TRCs. This is consistent with a labeled-line model, wherein the taste buds comprise sweet TRCs, bitter TRCs, and so on – the start points of separate labeled-line circuits. However, there is evidence of more complexity. For example, the sour TRCs express carbonic anhydrase 4 (CAR4), a membrane-anchored enzyme that catalyzes the conversion of carbon dioxide and water into protons and bicarbonate (i.e., dissociated carbonic acid) (Chandrashekar et al., 2009). Carbonation in a tastant solution is converted by CAR4 into free protons at the surface of sour TRCs, which are then activated by the increased acidity. Thus, sour TRCs also encode carbonation. Moreover, water itself can excite sour TRCs (Zocchi, Wennemuth, & Oka, 2017). Saliva is normally slightly basic; water lowers the pH at the TRC surface and activates sour TRCs through CAR4. These results suggest that calling these cells "sour" TRCs is not entirely accurate. While carbonation may have a slightly sour taste, water certainly does not. Water also is not an aversive stimulus, whereas sour tastants generally are. Indeed, ablation of the "sour" TRCs does not reduce the aversiveness of sour stimuli. Therefore, it may be that sour taste involves more than just the activation of the "sour" TRCs.

Furthermore, the encoding of salt is not as simple as previously suggested. There seem to be independent mechanisms for transducing low and high concentrations of salt. Unsurprisingly, animals prefer solutions with low concentrations of sodium, and avoid those with high concentrations. But it turns out that application of amiloride, an ENaC blocker, suppresses only the attractive low-concentration salt response, and does not affect the aversive high-concentration response (Chandrashekar et al., 2010; Heck,

Mierson, & Desimone, 1984; Hettinger & Frank, 1990). This result suggests two separate mechanisms for salt coding: the ENaC mechanism, underlying the attraction at low concentration, and another, mediating the aversion to salt at high concentration. It was discovered that the so-called sour TRCs and bitter TRCs are the cells recognizing high-concentration salts (Oka, Butnaru, Von Buchholtz, Ryba, & Zuker, 2013). The sour TRCs likely detect salts via CAR4, while the bitter TRCs might be using one of the T2Rs.

Calcium imaging of taste buds provides the evidence that is perhaps the most difficult for the labeled line model to explain (Tomchik, Berg, Joung, Chaudhari, & Roper, 2007). The "sour" class of TRCs is distinguishable from the other classes by several aspects of its molecular profile, including the expression of vesicular synaptic machinery and the use of the neurotransmitter GABA. TRCs expressing GAD (glutamic acid decarboxylase), and thus presumably GABA, would be predicted by a labeled-line model to be narrowly tuned to sour (and high salt, water, and carbonation). Instead, GAD+ TRCs seem to be heterogeneous, responding to any number between one and five taste qualities. Sweet, bitter, and umami stimuli excite these cells in ways that cannot clearly be explained by receptor expression or by concentration effects. In contrast, GAD- TRCs are narrowly tuned, which is consistent with the labeled-line model. It has been proposed that interactions between the TRCs within a taste bud may explain this effect; the GAD+ "sour" TRCs express P2Y receptors and can be excited by ATP, the neurotransmitter used by the GAD- TRCs. Thus, it may be that the "sour" cells of the taste bud are better thought of as generalist cells, a finding seemingly at odds with a simple labeled line model of taste (Roper & Chaudhari, 2017).

What can we conclude about taste coding at the level of the taste bud? The existence of distinct taste receptor mechanisms provides a foundation for labeled lines. These receptors recognize classes of tastants that conspicuously align with our perceptual notions of taste quality. Moreover, they are expressed on segregated populations of TRCs. These facts suggest that there are dedicated first-order sensory cells for each basic taste. However, despite the separation of taste receptors onto different cells, the TRC populations representing different tastes technically overlap, since the "sour" cells apparently act as generalists. This may mean that downstream regions interpret the TRC response as a population code. But generalist cells can also be reconciled with the existence of distinct coding channels: a generalist channel alongside specialist channels for sweet, bitter, umami, and salty taste. In this model, only sour taste is decoded by integrating several lines of input, and the other tastes are communicated through labeled lines. Moreover, the fact that generalist cells employ different neurotransmitters may provide a means of discriminating sour from the other tastes: it would be signaled by 5HT, but not ATP.

1.5 The mammalian gustatory system: Afferent nerves

The coexistence of specialist and generalist cells is found not just in the taste bud, but in the postsynaptic nerve fibers as well. As discussed earlier, Pfaffmann's initial experiments recording from taste nerves appeared to show that taste quality information is distributed across the various fibers within the taste nerve. But subsequent work from his group and others produced a more granular model for taste coding, wherein fibers belong to one of a variety of fiber types and exhibit fiber-type-specific tuning to stimuli.

Several fiber types have narrow tuning, while others have broad tuning, mirroring the division of TRCs into specialist and generalist classes.

There are four, or possibly five, fiber types: S-fibers, Q-fibers, N-fibers, A-fibers, and H-fibers (A- and H-fibers may be best combined into one group, A/H-fibers) (Spector & Travers, 2005). S-fibers ("sucrose-best") are narrowly tuned to sweet, and Q-fibers ("quinine-best") are narrowly tuned to bitter (Frank, 1991, 2000; Frank, Bieber, & Smith, 1988). N-fibers ("NaCl-best") are narrowly tuned to sodium salts, and these sodium responses can be prevented by amiloride, the ENaC blocker (Hettinger & Frank, 1990). These specialist fibers mirror the selective responses of TRCs for sweet, bitter, and salty taste. A/H-fibers ("ammonium-best" or "HCl-best") are tuned broadly to acids, salts, and some bitter compounds, and have been referred to as "electrolyte generalists" (Spector & Travers, 2005). Interestingly, some accounts show that the salt response of A/H-fibers are particular to high concentrations of salts. These properties are reminiscent of the "sour"/generalist TRCs. Unfortunately, few electrophysiology studies have addressed umami taste coding in nerve fibers, and those that do have produced mixed results (Spector & Travers, 2005). But apart from umami, the response profiles of afferent taste fiber types appear highly correlated with those of TRC types.

Recent calcium imaging studies have largely corroborated these findings. In these studies, about two thirds of the neurons of the geniculate ganglion – where the cell bodies of many taste fibers reside – responded to a single taste (Barretto et al., 2015). This figure is comparable to the typical number of non-A/H-type fibers, the electrolyte generalists, found in electrophysiological recordings. These reports also demonstrated the presence of umami-selective fibers, although their relative number was low. Interestingly, one study

showed that narrowly tuned neurons often broadened their tuning when high-concentration stimuli were used (A. Wu, Dvoryanchikov, Pereira, Chaudhari, & Roper, 2015). This suggests that the common practice of using a single "representative" stimulus and concentration for each taste quality might potentially bias some of the findings. Nevertheless, a general pattern emerges from these imaging and electrophysiological studies: taste nerves are composed of several cell types, and these types correspond to types of TRCs.

This model is further corroborated by recent single cell RNA sequencing analysis. Geniculate ganglion neurons can be clustered into types based on their transcriptomes, and doing so reveals molecular markers that specifically label particular clusters (J. Zhang et al., 2019). Five of these molecularly-defined clusters seem to correspond to five fiber types (that is, the four fiber types plus an umami type), based on behavioral and functional imaging results. The existence of distinct molecular profiles suggests that these fibers may respond to different sets of guidance cues, allowing them to wire up precisely to TRCs of a given type. It is known that bitter and sweet TRCs express Sema3a and Sema7a respectively, and this expression regulates the tuning of downstream neurons (H. Lee, MacPherson, Parada, Zuker, & Ryba, 2017). Indeed, two of the geniculate neuron cluster markers are cadherins, a family of cell adhesion molecules that are known to regulate circuit assembly. These findings suggest that, not only do TRCs and taste fibers come in molecularly defined types, but that the tuning of taste fibers is maintained by some degree of hardwiring at this early stage of the circuit.

In summary, gustatory nerve fibers exhibit tuning properties quite similar to those of taste bud cells. Just as evidence suggests that some taste buds are specialists and others

are generalists, so the case appears to be for afferent fibers. Does this disprove a labeled line model of taste coding? Perhaps, but there may be other interpretations. Specialist taste pathways might convey information about taste quality to the regions of the brain involved in taste discrimination, while generalist taste pathways may form circuits that mediate behaviors that are not dependent on fine discrimination of taste quality (Spector & Travers, 2005). For example, bitter, salty and sour foods can all elicit reflexive food rejection, and generalist pathways may be involved in driving these reflexes. Because the way that taste is encoded by a peripheral neuron might reflect how the information is used by the downstream circuits it feeds into, we must understand the structure and function of taste circuitry beyond these afferent nerves.

1.6 The mammalian gustatory system: Brainstem nuclei, thalamus, and cortex

Moving onward from the periphery into the brain, the way the circuit encodes taste quality becomes less clear. Before entering the brain, the taste circuit is linear: tastants activate the TRCs of the taste bud, the TRCs release transmitter onto nerve fibers, and the nerve fibers project into the brainstem, targeting the rNST. At this point, the circuitry diverges. Some rNST neurons are projection neurons that target the PBN, a relay in the pathway to the cortex; some rNST neurons project locally, to the reticular formation, the caudal NST, or to salivatory or motor nuclei in the brainstem; some rNST neurons are local interneurons (Spector & Travers, 2005). Evaluating whether this stage of the circuit employs labeled-line or population coding requires more than understanding the tuning properties of these neurons, since the coding models implicitly refer to how information is used by some "output", like a discrimination decision or a taste-evoked

behavior. For a circuit that diverges, as the taste circuit does in the rNST, there are multiple outputs, and these different outputs may use taste information in different ways. Furthermore, the way the local interneurons respond to taste stimuli may not reflect the way taste is represented in these outgoing pathways. Therefore, it would be best to understand how taste coding is implemented in each of these pathways, rather than in the aggregate.

However, most studies on the rNST have looked at the aggregate. From these, a few general patterns emerge. The tuning properties exhibited by rNST neurons resemble those of the nerve fibers – there are cells specifically responding to sweet, bitter, and salty, and cells that respond broadly to acids and salts (Smith, Van Buskirk, Travers, & Bieber, 1983; Travers & Geran, 2009). Yet overall, taste quality tuning is slightly broader at this stage of the circuit (Spector & Travers, 2005; Van Buskirk & Smith, 1981). While there are still sweet-specific and bitter-specific classes of neurons, there are also umami/sweet and umami/sweet/salty cells as well (Travers & Geran, 2009). There are neurons responsive to mechanosensory cues, to taste, and to both (Roussin, D'Agostino, Fooden, Victor, & Di Lorenzo, 2012). There is also evidence that spike timing carries information about taste quality (Di Lorenzo & Victor, 2003). While no clear organizing principle for taste coding in this region is agreed upon, it appears less likely to utilize strict labeled lines.

The following stage in the circuit is the PBN, which exhibits tuning relatively similar to the rNST (Geran & Travers, 2009; M. S. Weiss, Victor, & Di Lorenzo, 2014). Like the rNST, PBN neurons exhibit a wide range of tuning properties, including narrow tuning to taste, broad tuning, and mechanosensory sensitivity (M. S. Weiss et al., 2014).

But the PBN is a sensory relay for several other areas besides the rNST, and as such contains neurons sensitive to temperature, pain, interoception, and more (Palmiter, 2018), suggesting that coding in this region may be more heterogeneous.

Some studies have sought to analyze functional subtypes of the neurons within these brainstem regions. One method used to separate out which rNST neurons are projection neurons is through combining rNST recording with antidromic stimulation of the PBN (Cho, Li, & Smith, 2002). This method revealed that projection neurons overall exhibit taste quality tuning similar to that of the general population, but may be more strongly activated by tastants, and more biased towards sweet-selective tuning. More recently, calcium imaging from molecularly defined cell types has revealed that Pdyn-expressing cells of the rNST are specifically tuned to acids (J. Zhang et al., 2019), while SatB2-expressing cells of the PBN are specifically tuned to sweet (Fu et al., 2019). Intriguingly, while different populations of SatB2+ PBN neurons project to thalamus, amygdala, and hypothalamus, only the thalamus-projecting SatB2+ neurons appear to signal the positive valence associated with sweetness. Using genetic markers to parse the brainstem circuits involved in taste may be a promising direction in understanding taste coding in these areas.

Less is known about taste coding in the next stage of the circuit, the VPM nucleus of the thalamus. One study demonstrated that VPM neurons are heterogeneous in their taste specificity: equal proportions responded to one, two, three, or four taste qualities (H. Liu & Fontanini, 2015). As a result, accurate decoding of stimulus identity from thalamic responses requires a population of neurons. Interestingly, decoding taste quality from thalamic neural responses was more successful when the animal self-administered the

taste stimuli. As many recordings from the other regions in the circuit were collected from anesthetized animals, it is unclear to what extent this kind of active sensation modulates activity throughout the whole circuit.

VPM neurons project to the cortex, and at this stage of the circuit, there is conflicting evidence as to which coding model describes taste responses. On the one hand, broadly-tuned neurons are common, which is not surprising given that their input neurons are broadly tuned, as are the inputs of those neurons. This finding has contributed to the popular theory that the gustatory cortex uses a population code to represent taste quality (Simon et al., 2006). On the other hand, several pieces of evidence support the existence of cortical maps in the cortex for each of the basic tastes. One study found that sweet, bitter, salty, and sour tastes activated stereotyped, but overlapping regions of cortex (Accolla, Bathellier, Petersen, & Carleton, 2007). However, another found spatially distinct representations, claiming that there was a "gustotopic" organization, with hotspots selectively tuned to sweet, bitter, salty, and umami at different stereotyped locations (X. Chen, Gabitto, Peng, Ryba, & Zuker, 2011). Yet others have contested both of these claims, presenting evidence that taste quality representations are not spatially biased (Fletcher, Ogg, Lu, Ogg, & Boughter, 2017).

One group used a strategy based on transsynaptic tracing to address the question of spatial representation of taste, not just in cortex but across all levels of the taste circuit (Sugita & Shiba, 2005). Transgenic mice were generated that expressed a fluorescent-tagged version of wheat germ agglutinin (WGA) specifically in bitter TRCs (labeled by T2R5) or sweet and umami TRCs (labeled by T1R3). WGA is a plant lectin that can be taken up by neurons, trafficked in an anterograde direction, and transferred from neuron

to neuron (Yoshihara et al., 1999). Based on these properties, it has been considered to be a potent tool for anterograde transsynaptic tracing, and further, a tool allowing the tracing of a circuit across multiple synapses. Thus, expressing it specifically in bitter or sweet/umami TRCs would reveal the circuitry of bitter and sweet from taste bud to cortex. Indeed, neurons at each stage of this circuit were labeled by WGA (Sugita & Shiba, 2005). The resulting labeling showed the bitter and sweet/umami circuits beginning as sharply segregated in the rNST, PBN and thalamus, but becoming overlapping at the level of cortex, as well as in the amygdala. While this could be viewed as evidence for labeled lines, there are methodological concerns about WGA that need to be accounted for. WGA has been reported to have low sensitivity, and successful primarily when there are large numbers of input neurons converging onto a single target (Luo, Callaway, & Svoboda, 2008). Moreover, it is also not certain whether plant lectins like WGA function as transsynaptic tracers or as transneuronal tracers – that is, labeling all nearby neurons rather than all postsynaptic ones (Luo, Callaway, & Svoboda, 2018). Despite these caveats, this experiment at the very least demonstrates the potential that effective transsynaptic tracing could have on illuminating the logic of taste circuitry.

It is also important to note that the "gustatory" insular cortex is more than a purely gustatory region. In fact, it is not even just a sensory region; like many regions of cortex, responses in this area can be driven by many different factors. Pain, blood pressure, and arterial chemosensory signals are represented in gustatory cortex (Ogawa & Wang, 2002). Intriguingly, retronasal olfactory perception – a predominant component of flavor – is also dependent on GC (Blankenship, Grigorova, Katz, & Maier, 2019). Other sensory modalities can also evoke activity in GC, an effect seen in the context of food

association (Saddoris, Holland, & Gallagher, 2009; Samuelsen, Gardner, & Fontanini, 2012). When paired with a subsequent food reward, a tone or odor cue can trigger GC neuron firing in anticipation of taste.

Considering the way taste is represented across all stages of the mammalian taste circuit, it is clear that taste coding as a whole does not fit neatly into either a pure labeled line or population coding model. Someone who is motivated to demonstrate the existence of one or the other will be able to draw on evidence that appears to justify their preferred model. But any proponent of an extreme version of either model has difficult data to explain. How should the proponent of population coding explain the selectivity of certain cells, seen at each stage from the taste bud to the "gustotopic" organization in the cortex? And what utility is gained by multiplexing a clean, separated code for quality in the periphery into an amalgamated population code if the goal of the circuit is to discriminate between these qualities? On the other hand, the extreme labeled line model supporter must also address some conflicting evidence. How can this model explain the generalist responses and the complex tuning curves observed at each level of the circuit? What function would be served by having so many stages within a neural circuit that maintains the same representation scheme across each stage?

1.7 The Drosophila *gustatory system: Tastant detection at the periphery*

Perhaps the key to understanding the neural code for mammalian taste is a better understanding of the "parts list" of the circuit. Currently, we know which brain regions the circuit flows through, and we have a statistical sense of the way neurons react at each step in the circuit. We would have a much better model of taste function if we understood

what individual cell types existed at each stage, defined by their connectivity, physiology, and molecular profile. Characterizing the circuit with cell type-specificity would enhance the current statistical level of understanding to one with high resolution, where we know the way the code is implemented in neural pathways involved in different behaviors. New tools can get us closer to this resolution, such as single-cell RNA sequencing or fiber photometry.

Alternatively, progress on taste coding could be made by taking an orthogonal approach – changing model organisms. The problems of assessing the nutritional value of food are common to all animals, and consequently, the sense of taste is maintained across phyla. Rodents are useful and popular model organisms in neuroscience, but their use in research is not without drawbacks. Other animals are often more tractable, and some may prove valuable in understanding general principles of taste coding. Some may raise the objection that research on animal that are evolutionarily distant from mammals may not reflect the way the mammalian nervous system functions. I acknowledge this caveat, but, given that nutritional needs are shared across animals to a remarkable extent, there is reason to believe that the properties of taste – the sense for screening nutrients – may be largely conserved as well. In any case, understanding taste in a simpler model organism can help us elucidate the space of possible solutions for the problem of nutrient selection, and the results will allow us to generate hypotheses for how taste coding may operate in general.

The model organism we turn to here is the fly *Drosophila melanogaster*. *Drosophila* has been a popular model in biological research for over a century (Bellen, Tong, & Tsuda, 2010). There are many advantages to their use, including several factors

of convenience – the ease of breeding them, their short generation time, the low cost of keeping many stocks, etc. One major advantage is that decades of accumulated genetic research on *Drosophila* has produced a wealth of genetic tools for targeted labeling and manipulation of specific cells. Using these tools on one's neuron of choice, one can label, ablate, excite, inhibit, record the neural activity, express a new gene, or silence the expression of a gene, specifically in these target neurons. Furthermore, despite the vast evolutionary difference that separates them, flies and mammals have many striking commonalities. Many of these result from shared strategies animals use to solve common problems: how to develop, reproduce, maintain homeostasis, find nutrients, avoid danger, etc. Whether through deep homology or convergent evolutionary solutions to some of these problems, many vertebrate and invertebrate sensory systems are organized in remarkably similar ways. Similar neural circuit architectures have been described for the visual system (Sanes & Zipursky, 2010) and the olfactory system (Imai, Sakano, & Vosshall, 2010). Could the same be said for the gustatory system?

We normally associate taste with an oral sensation, but for *Drosophila*, taste detection occurs at several locations across the body. Taste neurons are found not only on the mouthparts, but on the legs, ovipositor, and wings (Vosshall & Stocker, 2007). While the positioning of these neurons may at first seem unusual, it makes sense in context with behavior. The leg neurons are activated when the fly steps on a potential food source; the ovipositor neurons may assist the female in choosing an appropriate substrate on which to lay eggs; the wing neurons are involved in pheromonal communication between flies (He, Luo, Shang, Sun, & Carlson, 2019; Vosshall & Stocker, 2007). The neurons of the mouthparts play a similar role to taste neurons in mammals – the sensation of nutrients in

the food prior to and during eating. Just as mammals have chemosensory cells both on the tongue and in the throat, flies have taste neurons on the labellum (the external tip of the proboscis) and in the pharynx (the internal mouthparts).

Most taste neurons in *Drosophila* extend their dendrites into hair-like structures called sensilla. Like taste buds, sensilla house multiple taste cells, shielding them from the environment except at a small taste pore located at the tip (Vosshall & Stocker, 2007). Tastants enter through the pore and bind to receptors on the neurons; many of these receptors belong to the gustatory receptor (GR) family, and as such, the peripheral taste neurons are referred to as gustatory receptor neurons (GRNs). Sensilla contain two to four GRNs, as well as one mechanosensory neuron and three support cells, and are found on each of the peripheral organs of taste previously described. There is also another gustatory structure, the taste peg, found only on the labellum. Taste pegs are shorter than sensilla and house just one GRN each.

Like mammals, *Drosophila* use different types of receptors to detect tastants of different quality. The first such receptor type discovered was the gustatory receptor (GR) gene family (Clyne, Warr, & Carlson, 2000; Dunipace, Meister, Mcnealy, & Amrein, 2001; Scott et al., 2001). The discovery of the GR family was made on the heels of the discoveries of the *Drosophila* olfactory receptor (OR) family and the mammalian T1Rs and T2Rs, which were all based on the insight that chemosensory receptors are likely GPCRs, and therefore 7-transmembrane domain proteins – a structural feature easy to identify based on their amino acid sequence. Indeed, the ORs and GRs are also 7-transmembrane domain proteins and were also identified by this feature. But intriguingly – and what was not realized for several years after their discovery – the insect ORs have

an inverted membrane topology, with their C-terminal domain, which would normally bind to G proteins, facing the outside of the cell (Benton, Sachse, Michnick, & Vosshall, 2006). Thus, these receptors are *not* GPCRs, despite being identified through a search for GPCRs. Rather, it appears that the ORs form heteromultimers and act as ligand-gated ion channels (Butterwick et al., 2018; Sato et al., 2008).

The OR family is a subfamily of the larger GR family (Robertson, Warr, & Carlson, 2003), and so it is possible that these features are hallmarks of GRs in general. Indeed, two distantly related GRs both exhibit this inverted membrane topology (H. J. Zhang et al., 2011), and at least one insect GR has been observed to act as a ligand-gated ion channel (Sato, Tanaka, & Touhara, 2011). However, other evidence suggests that G protein signaling is necessary for GR-expressing neurons to function properly (Kain et al., 2010; Liman et al., 2014; Ueno et al., 2006; Yao & Carlson, 2010). It may be that GRs can act as both ion channels and GPCRs, or that other GPCRs are involved in modulating GR responses. These possibilities have also been raised for the ORs (Nakagawa & Vosshall, 2009).

Whatever the case, the evidence is clear that GRs are tastant detectors, and their expression patterns in GRNs dictate the taste responses of those neurons. Classic electrophysiological studies had demonstrated that many labellar sensilla house four GRNs with four different tuning profiles: one type sensitive to water (W-cells), one to sugars (S-cells), one to low concentrations of salt (L1-cells), and another to bitter compounds and high concentrations of salt (L2-cells) (Meunier, Marion-Poll, Rospars, & Tanimura, 2003; Rodrigues & Siddiqi, 1978). Might these four GRN types show different GR expression profiles? Indeed, early analysis of GR expression demonstrated that some

receptors – like Gr5a and Gr66a – were expressed in non-overlapping sets of GRNs (Wang, Singhvi, Kong, & Scott, 2004). Ablation of Gr5a+ neurons impaired behavioral responses to sugars, and ablation of Gr66a+ neurons impaired the aversion to bitter compounds.

However, these are not the only receptors involved in the detection of these qualities. Based on the fact that mammalian bitter-sensing TRCs use a variety of receptors – in order to ascribe "bitterness" to the wide diversity of potentially toxic compounds – we would expect a similar finding for the bitter GRNs of *Drosophila*. Indeed, this is the case: each bitter GRN expresses a multitude of GRs (Freeman & Dahanukar, 2015; L. A. Weiss, Dahanukar, Kwon, Banerjee, & Carlson, 2011). Yet there is a significant difference between the ways that the receptors of the fly and the mouse detect bitter stimuli. The fly uses GRs, which, in contrast to the mouse's T2Rs, are likely heteromeric ion channels. Thus, while the mouse has a single receptor that can independently detect cycloheximide (Mueller et al., 2005), *Drosophila* uses complexes of multiple GRs to transduce each bitter compound (Dweck & Carlson, 2020; Y. Lee, Moon, & Montell, 2009; Shim et al., 2015). Six of these GRs are expressed across nearly all bitter neurons, suggesting that they form a kind of core complex and may serve a general function, or act as necessary co-receptors (Dweck & Carlson, 2020); other GRs outside this core may be necessary to expand the receptive range to different classes of compounds. Interestingly, these bitter GRs do not confer taste sensitivity in an exclusively additive manner – that is, the addition of a new bitter GR to a neuron does not simply "add on" to the palette of compounds it can detect. Instead, adding GRs may add, remove, or modulate sensitivity to specific compounds; inversely, removal of individual

GRs can actually produce novel sensitivity to individual compounds (Delventhal & Carlson, 2016; Dweck & Carlson, 2020).

Sugar detection in *Drosophila* also relies on a variety of different receptors, not just Gr5a. A total of 9 GRs have been identified in sweet GRNs (Jiao, Moon, & Montell, 2007; Miyamoto, Chen, Slone, & Amrein, 2013), all of which contribute in some way to sugar detection (Fujii et al., 2015). Like the bitter GRs, there seem to be a core of GRs required for sweet taste: in flies lacking just 2 of these GRs – Gr5a and Gr64a – no labellar sensilla responded to any sugars (Dahanukar, Lei, Kwon, & Carlson, 2007). Furthermore, Gr5a+ neurons must also express Gr64f to respond to sugars (Jiao, Moon, Wang, Ren, & Montell, 2008). And just as individual bitter GRs can shape the add, subtract, or modify the responses to particular bitter tastants, individual sweet GRs can do the same (Freeman, Wisotsky, & Dahanukar, 2014; Wisotsky, Medina, Freeman, & Dahanukar, 2011).

Sweet GRNs and bitter GRNs are both heterogeneous in their GR expression profiles, and likewise, there are differences in the tuning profiles within each of these classes (Ling, Dahanukar, Weiss, Kwon, & Carlson, 2014; Miyamoto, Slone, Song, & Amrein, 2012; L. A. Weiss et al., 2011). Might it be that flies detect and represent meaningful subcategories of sweet and bitter? This possibility has been addressed in humans through experiments using metameric matching of sugars, which demonstrated a single type of sweet taste (Breslin et al., 1996, 1994). Similar experiments have been performed on flies using a taste conditioning assay (Masek & Scott, 2010). Flies normally extend their proboscis when they detect sugars, but this behavior can be suppressed by presenting a punishment, such as a laser pulse, after presenting the sugar.

Flies conditioned in this paradigm cannot discriminate between the conditioned sugar and a different one, as long as the two are presented at equivalently effective concentrations. Furthermore, the same pattern was observed for bitter tastants. These results thus demonstrate a lack of evidence for the fly making meaningful distinctions between tastants of either taste quality.

It turns out that GRs are not the only types of receptors involved in tastant detection. Receptors from two other families, the pickpocket channels (PPKs) and ionotropic receptors (IRs), have roles in detecting classes of tastants beyond sweet and bitter. PPKs belong to the family of epithelial sodium channel/degenerin (ENaC/DEG) proteins, the same protein family responsible for salt taste in mammalian taste buds (Chandrashekar et al., 2010). Like the ENaCs in mammalian salt-taste cells, *Drosophila* PPKs function as ion channels and as multimers (Zelle, Lu, Pyfrom, & Ben-Shahar, 2013). Yet unlike in mammals, *Drosophila* PPK channels are implicated in water taste (Cameron, Hiroi, Ngai, & Scott, 2010). PPK28 is expressed in a set of labellar GRNs that do not overlap the sweet and bitter GRNs. The calcium responses of these PPK28+ GRNs are inversely proportional to the osmolarity of the stimulus: they are strongly activated by water, but not by high-osmolarity solutions, such as 20% polyethylene glycol (PEG). Moreover, heterologous expression of PPK28 in cell culture conferred a response to low osmolarity in these cells, demonstrating that this channel is sufficient to explain the water response.

Beyond PPK28, other PPKs are involved in the detection of pheromones. During courtship, male *Drosophila* will use their forelegs to tap the abdomen of the female; in doing so, he uses the gustatory neurons of his legs to sample the female's cuticular

hydrocarbons to determine whether to proceed with courting. Since this is a form of contact chemosensation, such pheromone detection can be considered a form of taste in *Drosophila*. The PPK channels PPK23, PPK25, and PPK29 are expressed in these tarsal GRNs, and have been implicated in the detection of various pheromones (Clowney, Iguchi, Bussell, Scheer, & Ruta, 2015; Thistle, Cameron, Ghorayshi, Dennison, & Scott, 2012; Vijayan, Thistle, Liu, Starostina, & Pikielny, 2014).

Out of the four types of taste neurons identified in the aforementioned "classic" scheme – the W, S, L1, and L2 cells – GRs and PPKs appear to explain the taste sensitivity of three: the W (water), S (sweet), and L2 (bitter/high salt) cells. Further, PPK expression also underlies the responses of pheromone-sensitive cells that were not identified by these classic experiments. The molecular basis of the L1 (low salt) cells' taste responses appears to be based on another type of receptor: the IRs.

IRs are related to ionotropic glutamate receptors (iGluRs), and are expressed in olfactory and other sensory neurons of the fly (Benton, Vannice, Gomez-Diaz, & Vosshall, 2009; Sánchez-Alcañiz et al., 2018). They appear to function as heteromers, complexes of up to 3 different IRs that include at least one obligate co-receptor (IR8a or IR25a) and at least one receptor conferring unique ligand tuning properties (Abuin et al., 2011; Silbering et al., 2011). Interestingly, a clade within the IR gene family has been shown to be widely expressed in GRNs, implicating them in taste sensation as well (Koh et al., 2014).

IRs have been posited to be the receptors mediating the fly's attraction to low concentrations of salt (Y. V. Zhang, Ni, & Montell, 2013). All animals must maintain internal ionic homeostasis, and thus high concentrations of salt may be dangerous to

consume. This reason has been purported to explain the fact that flies, like mammals, find low salt concentrations attractive and high concentrations aversive (Oka et al., 2013). The mechanism for this concentration dependence in attraction may rest on the existence of separate cells for encoding "low salt" and "high salt", which have been observed in both flies and mammals. In this dual-pathway model, low salt cells connect to downstream "attraction" circuits, while high salt cells inhibit these circuits.

Originally, the receptor IR76b was posited to label these low salt (or L1) cells. IR76b mutants lost their attraction to salt, and based on the expression pattern of Ir76b-QF lines, it did not appear to overlap significantly with Gr5a or Gr66a (Y. V. Zhang et al., 2013). However, further reports suggested that Ir76b expression actually did overlap substantially with these other GRNs (Jaeger et al., 2018), and that it was also necessary for high salt avoidance (M. J. Lee et al., 2017). Thus, while IR76b plays a critical role in *Drosophila* salt detection, it is more widely expressed than originally thought. While this may simply indicate that a more specific marker is needed to access these low salt cells, it could also point to a more complex representation of salt than originally expected.

Recent evidence has supported this latter interpretation. In *Drosophila*, salt taste appears to be encoded not through one labeled line or a pair of opposing high-salt/low-salt channels, but rather through a distributed code (Jaeger et al., 2018). Five markers were obtained that, together, covered nearly all GRNs in labellar sensilla: Gr64f (a sweet receptor), Gr66a (bitter), Ppk28 (water), Ppk23 (pheromone), and Ir94e (a specific marker for the low salt cells). Intriguingly, all of these types responded to salts in some way. As expected, the water-sensing Ppk28+ neurons were inhibited by increasing concentrations of salt, the Ir94e+ neurons responded to low concentrations of salt, and the

bitter-sensing Gr66a+ neurons responded to high concentrations of salt as well as bitter. In addition, the sweet-sensing Gr64f+ neurons responded to sodium salts, with stronger responses to higher concentrations. And interestingly, pheromone-sensitive Ppk23+ neurons responded to all salts at high concentration; moreover, these salt responses were much stronger than their responses to pheromones. Attraction to low salt concentrations depended not just on the Ir94e+ "low salt" cells, but also the sweet cells; aversion to high salt depended on both the bitter cells and the Ppk23+ "pheromone" cells. How does Ir76b fit into this picture? Ir76b was necessary for both the appetitive, sweet-neuron responses to salt and the aversive, Ppk23+ "pheromone" neuron responses. Thus, the representation of salt is distributed across GRN classes, and Ir76b (and other IRs) mediate salt reception in many of these classes.

It appears that flies have a kind of "umami-like" taste as well. While the aforementioned five molecular markers label all the sensillar GRNs, there are also GRNs in the taste pegs on the inner surface. Some of these taste pegs respond strongly to yeast (Steck, Walker, Itskov, & Ribeiro, 2018), an essential part of the *Drosophila* diet. Part of this response is likely driven by carbonation, a natural byproduct of yeast, as some taste peg neurons show strong responses to carbonation alone (Fischler, Kong, Marella, & Scott, 2007). However, while deactivated (and thus, decarbonated) yeast also drives taste peg responses, amino acids themselves only weakly excite these neurons. This suggests that other yeast metabolites are the cue being detected by these neurons. Even so, this yeast-sense is likely a cue for amino acids, as dietary amino acid deprivation leads to specific potentiation of the yeast response in these neurons (Steck et al., 2018). Some leg GRNs also respond to yeast, and do so in an Ir76b-dependent manner (Ganguly et al.,

2017). Since the yeast-sensing taste peg GRNs are also Ir76b+, it is likely that IRs mediate this yeast metabolite taste in flies – and a trio of IRs has recently been shown to mediate their carbonation responses (Sánchez-Alcañiz et al., 2018).

Can flies detect other taste qualities? On the one hand, it appears that nearly all GRNs are involved in either sweet, bitter, salty, water, pheromone, carbonation or yeast taste, and thus there are few "orphan GRNs" left to assign a taste response profile to. However, the data demonstrating that salt – an essential nutrient – is encoded in a distributed fashion suggest that GRNs can be involved in representing multiple taste qualities. Indeed, some GRNs have been shown to detect other kinds of compounds, including acids (Charlu, Wisotsky, Medina, & Dahanukar, 2013; Devineni, Sun, Zhukovskaya, & Axel, 2019; Rimal et al., 2019), fatty acids (Kim et al., 2018; Masek & Keene, 2013; Tauber et al., 2017), and calcium (Y. Lee, Poudel, Kim, Thakur, & Montell, 2018). The detection of each of these occurs through GRN classes that have been ascribed to other tastes: calcium is detected by salty/pheromonal Ppk23+ GRNs, fats by sweet Gr64f+ GRNs, and acids by both bitter Gr66a+ and sweet Gr64f+ GRNs. It is not clear whether the fly can discriminate between compounds detected by the same set of cells. Do flies perceive acids as a mixture of sweet and bitter, or as something else entirely? Although distributed coding may possibly allow for a taste perception of acid as something distinct from a mixture of sweet and bitter, there is currently no evidence supporting this hypothesis.

1.8 The Drosophila *gustatory system: Central projections of gustatory receptor neurons*

GRNs of the mouthparts project their axons to a region of the brain called the subesophageal zone. Insects, like humans, have an esophagus – a section of the digestive tract connecting the pharynx to the gut. But quite unlike humans, for many insects (including *Drosophila*) the esophagus travels right through the center of the brain. This feature provides anatomists with a landmark for dividing the brain into two regions: the supraesophgeal zone (i.e. the area of the brain above the esophagus) and the subesophageal zone (i.e. the area of the brain below the esophagus; hereafter referred to as the SEZ).

Alternatively, many anatomists prefer to use a different nomenclature, one based on the development of the nervous system. All *Drosophila* neurons are derived from a small number of embryonic stem cells called neuroblasts. These neuroblasts have precisely specified genetic identities, and are found in repeated, segmental units called neuromeres. The *Drosophila* brain is derived from six neuromeres; from anterior to posterior: the protocerebrum, deutocerebrum, tritocerebrum, and the mandibular, maxillary, and labial neuromeres. These last three neuromeres correspond to three segments of external, movable mouthparts that are found in basal insects: the mandible, maxilla, and labium. *Drosophila* has lost some of these parts and fused together others to form its proboscis, and as these external features have become reduced, so have their corresponding neuromeres. The mandibular, maxillary, and labial neuromeres have lost their distinct segmental boundaries and fused together with the tritocerebrum, and this area corresponds roughly to the SEZ. However, some prefer to maintain a distinction

between the tritocerebrum and the three more posterior, fused-together ganglia; they refer to the fusion of these three as the gnathal ganglion (GNG).

Beyond providing an explanation for the use of the terms SEZ and GNG, the developmental origins of this area can also illuminate why the region has remained so poorly characterized. As previously described, in *Drosophila* the lineages of the SEZ are reduced; moreover, tracts delineating the neuromeres have also been reduced or lost. This pattern has resulted in a neuropil structure that lacks clearly defined boundaries and substructures. This contrasts sharply with other sensory neuropils of the brain, such as the antennal lobe and optic lobe, in which clear delineations within the regions exist and have provided anatomists with clues to these regions' organizational structure (Miyazaki & Ito, 2010).

Despite the overall unstructured appearance of SEZ neuropil, there is a clearer organizational pattern to the sensory nerves that provide input to the region. The labial nerve, which carries input from the GRNs of the labellum, enters the SEZ at a ventral location and splits into three branches: the anterior maxillary sensory (AMS) branch, posterior maxillary sensory (PMS) branch, and labellar sensory (LS) branch (Kendroud et al., 2017; Miyazaki & Ito, 2010). Each of these branches innervates a distinct subregion of the SEZ, and each such region can be divided into 3-5 subcompartments based on GRN innervation patterns. The pharyngeal nerve, which carries the axons of pharyngeal GRNs, projects into a more dorsal region of SEZ and splits into a ventral pharyngeal sensory (VPS) branch and dorsal pharyngeal sensory (DPS) branch. Finally, the anterior cerebrocervical fascicle (aCCF) projects from the ventral nerve cord into the SEZ posteriorly, carrying axons from leg GRNs. (Only some tarsal GRNs send their axons to

the SEZ through this fascicle; others keep their projections within the VNC, terminating in the neuropil of the thoracic ganglion corresponding to the leg they innervate.) In short, there is a topographical organization of GRN axons based on the external sensory organ that their dendrites innervate, which has been confirmed both by sparse labeling of individual neurons and by molecular markers specific to GRNs innervating single body parts (Kwon, Dahanukar, Weiss, & Carlson, 2014; Thorne, Chromey, Bray, & Amrein, 2004; Wang et al., 2004).

Not only are the GRN projections to SEZ organized by their somatotopic origin, but they also cluster according to the taste quality they recognize. Sweet and bitter GRNs of the labellum both project through the PMS branch of the labial nerve, but they arborize in distinct subcompartments. Sweet GRNs innervate lateral and ventromedial regions (PMS4 and PMS5), while bitter GRNs innervate medial and dorsolateral ones (PMS1-3) (Miyazaki & Ito, 2010; Thorne et al., 2004; Wang et al., 2004). Water GRNs appear to arborize in the same regions as sweet neurons (PMS4 and PMS5), and taste peg GRNs project through the AMS branch, innervating region AMS1 (Miyazaki & Ito, 2010). The precise targeting of Ppk23+ (pheromone/high salt) and Ir94e+ (low salt) projections within the SEZ is unclear, but they appear to be part of the PMS branch, and do not show obvious innervation of the medial regions (PMS2 and PMS3) targeted by bitter neurons (Jaeger et al., 2018). Thus, GRNs representing a given taste quality target a stereotyped region within the SEZ, and while some of these representations overlap, some – notably, sweet and bitter – are conspicuously distinct. This anatomical segregation of sweet and bitter projections has led some to postulate that these GRNs synapse onto different

downstream partners, and as a result, sweet and bitter taste may be conveyed through separate, labeled-line circuits (Thorne et al., 2004; Wang et al., 2004).

The GRNs found on parts of the body other than the mouthparts also exhibit somatotopic projection patterns. There are gustatory neurons on the legs, wings, and ovipositor. Those on the legs project axons in one of two patterns: either terminating in the thoracic ganglion of the VNC corresponding to their leg of origin ("segmental"), or passing through the VNC and projecting up to the brain via the aCCF and terminating in the SEZ ("ascending") (Kwon et al., 2014; Miyazaki & Ito, 2010; Thoma et al., 2016). Interestingly, Gal4 drivers under the control of sweet-sensing GRs label both types of neurons, while those under control of bitter-sensing GRs only label the second kind (Kwon et al., 2014), possibly hinting at a difference in how sweet and bitter are processed by local circuits within the VNC. Indeed, the segmental, but not ascending, tarsal sweet GRNs are specifically involved in reducing turning behaviors when the fly moves onto a sugar-laced medium (Thoma et al., 2016). Afferents from the wing terminate in the accessory mesothoracic neuropil (Court et al., 2020; Kwon et al., 2014). Sensory neurons around the ovipositor are thought to be gustatory in nature, but it not clear if they express GRs (Montell, 2009). In addition, there are GR-expressing neurons that innervate the abdomen and reproductive tracts; these neurons project axons to the abdominal ganglion of the VNC (J. H. Park & Kwon, 2011).

Finally, there are GRs expressed on central brain neurons that sense the nutrient content of the circulating hemolymph. Gr43a and Gr64a are both expressed in 2-4 pairs of neurons in the superior lateral protocerebrum (Fujii et al., 2015). Gr43a is a fructose sensor, and endows these neuron with the ability to detect circulating fructose (Miyamoto

et al., 2012). Since an increase in circulating blood sugar reflects the consumption of nutritive carbohydrates, this may be a mechanism for the fly to detect the caloric content of a recent meal. There are other central neurons in the fly's brain that also act as post-ingestive nutrient sensors, but through a non-GR mechanism. These neurons appear to be excited by increases in intracellular pyruvate, which are driven by glucose transport into the cell and subsequent glycolysis (Dus et al., 2015).

Internal nutritional state is not only sensed by neurons, but modulates the responses of many GRNs. Starvation increases the activity of a dopaminergic neuron local to the SEZ (Marella, Mann, & Scott, 2012). Sweet-sensing GRNs are potentiated by this starvation-induced dopamine through DopEcR, thus leading to stronger responses to sugar and increased likelihood of proboscis extension (Inagaki et al., 2012; Marella et al., 2012). Bitter-sensing GRNs are normally potentiated by octopaminergic input, but starvation silences these octopaminergic neurons and excites other GABAergic neurons that inhibit the bitter-sensing neurons (Inagaki, Panse, & Anderson, 2014; LeDue et al., 2016). This leads to reduced sensitivity to bitter tastants when the fly is starved. Further, the salt-tuned Ppk23+ GRNs are selectively modulated by salt deprivation (Jaeger et al., 2018), and the Ir76b+ yeast-sensing GRNs of the taste pegs are potentiated by amino acid deprivation (Steck et al., 2018). These results suggest that the fly has specific hungers for particular nutrient classes, which are manifested as neuromodulatory signals acting on specific classes of GRNs.

1.9 The Drosophila *gustatory system: Organization of the larval gustatory system*

Drosophila are holometabolous insects, meaning that they undergo a complete metamorphosis from a larval form to an adult form via a transitional pupal stage. The pupal transition entails a dramatic transformation, not only for the external anatomy of the insect, but also for its neuroanatomy. Consequently, both the layout of peripheral gustatory organs and the neural circuitry of GRNs are significantly remodeled between the larval and adult stages. Larvae and adult flies have different physiological needs, behaviors, and ecological niches, so this remodeling enables the gustatory system to be initially adapted to serve the needs of the larva, then readapted to serve those of the adult.

As in the adult, there are multiple peripheral organs for taste in the larva. The terminal organ (TO) and the dorsal organ (DO) both house neurons and detect tastants external to the animal; the dorsal, ventral, and posterior pharyngeal sense organs (DPS, VPS, and PPS) detect tastants as they pass through the pharynx. These can be thought of as functionally equivalent to the labellar and pharyngeal organs of the adult fly. However, the neurons in these organs are not exclusively gustatory neurons. Some are known to respond to olfactory, mechanosensory, or thermosensory cues (Python & Stocker, 2002). At most, there are 81 true gustatory neurons in the larva, much fewer than there are for the adult. Because of this low number and the expression profiles of these neurons, it has been proposed that each larval gustatory neuron may have a distinct function (Apostolopoulou, Rist, & Thum, 2015). If true, this would mirror the lack of redundancy in the larval olfactory system, wherein each olfactory glomerulus is innervated by a single first-order sensory neuron and a single second-order projection neuron (Ramaekers et al., 2005).

Yet the coding scheme employed by the 81 or so GRNs of the larva remains less well understood than that of the adult. Many larval GRNs express similar receptor types as in the adult – GRs, IRs, and PPKs – yet some GRNs so far have not been shown to express any of these (Apostolopoulou et al., 2015; Rist & Thum, 2017). Curiously, many of the GRs expressed in the larva are associated with bitter GRNs in the adult, and no expression was observed for nearly all sugar-sensing GRs (Kwon, Dahanukar, Weiss, & Carlson, 2011). This observation was unexpected, given that larvae have a carbohydrate-based diet (Apostolopoulou et al., 2015), and thus would be expected to taste sugars. Indeed, in feeding preference and olfactory conditioning assays, they can (Rohwedder et al., 2012). However, a single sugar-sensing GR – Gr43a – is in fact expressed in both taste organs and the central brain of the larva (Mishra et al., 2013). Curiously, Gr43a expression limited to the brain is sufficient for normal sugar feeding behavior, indicating that post-ingestive signals, and not taste itself, may be the primary means of larval sugar detection. Larvae also exhibit a form of sugar detection not observed in the adult: detection of ribonucleosides and RNA, which is mediated by Gr28-family GRs (Mishra, Thorne, Miyamoto, Jagge, & Amrein, 2018). These ribonucleoside-sensors may provide a critical supplement the larva's sparse population of Gr43a+ sugar-sensing GRNs.

Interestingly, recent microfluidics-based methods for assaying taste responses in larval GRNs have provided evidence suggesting a distributed code for peripheral taste in the larva (Van Giesen et al., 2016). Some larval GRNs exhibited taste response profiles reminiscent of some GRN classes of the adult: one identified as B2 showed selective tuning to some bitter compounds, and another identified as C6 responded to some sugars and salts. However, while adult GRNs tend to respond broadly to tastants of a particular

quality, the larval GRNs appeared to be tuned to particular combinations of chemicals rather than a broad category. One identified neuron in particular, C7, showed a particularly unusual profile, responding to some bitter compounds, high-concentration salts, and also some sugars and amino acids. These data suggest that there are substantial differences between the ways the larva and the adult represent taste stimuli.

1.10 The Drosophila *gustatory system: Beyond first-order neurons*

In the mammalian gustatory system, different taste qualities are represented largely by separate populations of cells at the periphery, but these representations seem to become more complex the further downstream one goes in the circuit. It may be that this pattern is a general feature of gustatory coding across species. If so, then the powerful genetic tools that are available for *Drosophila* hold great potential to address this question. The ability to label and manipulate sparse, defined sets of neurons in *Drosophila* could allow us to unpack the complexities of central taste coding.

So far, little is known about how the *Drosophila* brain represents taste information beyond the first order of the circuit. However, the fact that GRNs encoding different taste qualities project to distinct subregions of the SEZ may indicate that they synapse onto different downstream partners. This would be consistent with a labeled line model of taste: different taste qualities would be detected by different first-order neurons, which would propagate that information to different second-order neurons. But without identifying such second-order neurons, this is only a hypothesis. To test this, gustatory neurons downstream of the GRNs must be identified, and their tuning properties measured.

A few studies have found Gal4 lines labeling putative second-order gustatory neurons. Kain & Dahanukar (2015) identified a neuron (which they call a sweet gustatory projection neuron, or "sGPN") that receives input from labellar sweet GRNs, responds selectively to sweet tastants, projects to the nearby antennal mechanosensory and motor center (AMMC), and is sufficient to drive the proboscis extension response (PER). Miyazaki et al. (2015) identify a different second-order neuron (which they termed a "G2N") that is also postsynaptic to sweet GRNs, but stays local to the SEZ. Yapici et al. (2016) find a cluster of local SEZ neurons ("IN1") that receive input from sweet GRNs of the pharynx but not the labellum, respond to sweet tastants and control sucrose ingestion. Kim et al. (2017) found several types of taste projection neurons ("tPNs"); two of these responded to sweet tastants on the legs, while one (tPN3) responded to bitter tastants applied either to the legs or labellum. Bohra et al. (2017) identified a type of local SEZ interneuron ("bGLN") that receives input from bitter GRNs, responds to bitter tastants but not sweet, and whose activation inhibited PER. Interestingly, in each of these cases, the second-order neurons are narrowly tuned to either bitter or sweet, but not both. It could thus be argued that these data provide support for a labeled line model of taste coding.

In mammals, the taste circuit that is most typically considered is the one from periphery to cortex (despite the existence of other neural pathways to different target brain regions). What is the equivalent circuit in the fly? Or in other words, where in the fly brain does taste information go? While we do not know for sure, there are at least two downstream regions that receive gustatory inputs. The first are the motor neurons that

drive proboscis movement and feeding behavior. The other is the mushroom body, considered the learning and memory center of the fly's brain.

It seems likely that the most direct circuits controlling taste-induced feeding responses are contained wholly within the SEZ. The SEZ is the target of axonal input from GRNs, and the motor neurons innervating the muscles of the proboscis keep their dendrites within the SEZ (McKellar, Siwanowicz, Dickson, & Simpson, 2020). The shortest possible circuits between these two would be either through direct connections from sensory to motor neurons, or through intermediate connections by local interneurons. So far, no GRNs have been found that directly synapse onto motor neurons controlling the proboscis (Gordon & Scott, 2009; McKellar et al., 2020). However, motor neurons of the proboscis do show sugar-induced responses, as expected (Gordon & Scott, 2009). Furthermore, an SEZ interneuron called the Fdg ("feeding") neuron has been identified that responds to sweet taste and whose activation can drive the entire proboscis extension and feeding response (Flood et al., 2013). Because this neuron apparently does not receive input from sweet GRNs, there may be at least two steps in the local SEZ circuit between taste input and motor output. Regardless, there are clear signs that taste information travels through local feeding-related circuitry of the SEZ.

In addition, taste information reaches the mushroom body (MB), a brain region critical for learning and memory. The MB is most often thought of as a center for olfactory associative learning. It contains many intrinsic neurons called Kenyon cells (KCs), which receive input at a region called the calyx from a small number of olfactory projection neurons (OPNs) (Aso, Hattori, et al., 2014). There are roughly 15 times as many KCs as OPNs, and KCs are more sparsely tuned to odors than OPNs are

(Honegger, Campbell, & Turner, 2011; Perez-Orive et al., 2002; Vosshall & Stocker, 2007). Further, the OPN-to-KC connections are semi-random, resulting in a KC representation of odor that is sparse and odor-specific (Caron, Ruta, Abbott, & Axel, 2013; Lin, Lai, Chin, Chen, & Chiang, 2007; Tanaka, Awasaki, Shimada, & Ito, 2004). KCs extend their axons through the lobes of the MB, and along these lobes they make synapses onto a small number of mushroom body output neurons (MBONs), each of which has a stereotyped role in assigning valence within particular contexts (Aso, Sitaraman, et al., 2014). Odors, represented by sparse sets of KCs, can thus drive appetitive or aversive behavioral responses through the synaptic connections from KCs to "appetitive" or "aversive" MBONs. Learning occurs through the reweighting of these synapses, which is driven by dopamine input from the dopaminergic neurons (DANs) of the MB (Cohn, Morantte, & Ruta, 2015; Hige, Aso, Rubin, & Turner, 2015). The specificity of this learning is enabled by compartmentalization: each lobe of the MB is divided into compartments, and each DAN and MBON innervate a particular compartment (Aso, Hattori, et al., 2014; Aso, Sitaraman, et al., 2014). For example, although a single KC extending through a lobe will innervate two adjacent compartments ("A" and "B"), they will contact different MBONs in each, and receive input from different DANs in each as well. Thus, the DAN in "A" may strengthen the KC connection to MBON "A", but it will not affect the connection to MBON "B". If MBON "A" drives appetitive behavior and MBON "B" drives aversive behavior, this change in connection strength will result in the odor represented by that KC becoming more appetitive to the fly. While the circuitry and molecular mechanisms underlying memory formation in the MB are understood in more detail than this example illustrates, this basic

model provides a sufficient background to understand the roles that taste has been shown to have in this region.

As mentioned earlier, flies can be conditioned to reduce their response to sweet stimuli if these tastants are paired with an aversive heat shock stimulus (Masek & Scott, 2010). The MB was found to be necessary for this taste conditioning to have an effect, as blocking synaptic transmission in the Kenyon cells (KCs) prevented this learning. This suggests that KCs, in addition to representing odors, can represent tastants. Indeed, functional imaging studies confirmed this; sweet and bitter tastants drive calcium responses in KCs (Kirkhart & Scott, 2015). Also, in addition to a heat shock punishment, bitter tastants can be used as a punishment (Kirkhart & Scott, 2015; Masek, Worden, Aso, Rubin, & Keene, 2014). Bitter taste activates the PPL1 cluster of DANs, which are known to encode punishments (Aso, Hattori, et al., 2014; Kirkhart & Scott, 2015; Masek & Scott, 2010). Likewise, sugar can be used as a reward in conditioning assays, and sweet taste activates the PAM cluster of DANs, which are known to encode rewards (Burke et al., 2012; C. Liu et al., 2012). Sweet and bitter taste are therefore conveyed to at least two types of MB neurons – the KCs and the DANs. While some central gustatory neurons have been identified that are involved in connecting the GRNs to the MB (Kim, Kirkhart, & Scott, 2017; Otto et al., 2020), the general coding logic of taste at this stage of the circuit still remains unclear.

One study aimed to address this question through a strategy for large-scale calcium imaging of the *Drosophila* brain (Harris, Kallman, Mullaney, & Scott, 2015). In this study, a calcium indicator was expressed panneuronally, sweet and bitter stimuli were delivered to the proboscis, and the resulting calcium responses in cell bodies were

recorded. Responses to sweet and bitter in the cell bodies around the SEZ were found in mostly (but not entirely) segregated populations of neurons. Around the MB, a similar pattern was observed: largely separate group of neurons responded to sweet and bitter stimuli.

While these results may be viewed as evidence for labeled lines, this is not the only interpretation. Because sweet and bitter tastants drive different behaviors, at some point in the circuit – such as the regions that generate these behavioral outputs – the patterns of activity driven by these tastants must be distinct. It may be that intermediate stages of the circuit represent sweet and bitter as a distributed code; in this case, sweet- and bitter-specific behaviors may be generated by downstream regions by reading out over the population of these distributed-coding neurons. To determine whether or not this is the case will require recoding specifically from second-order neurons of the circuit. The previously mentioned studies on individual second-order gustatory neurons have begun to address the question in this way, but because each of these studies only investigated specific types of second-order neurons, they have so far only provided a limited understanding of the situation.

1.11 Insights into taste coding from non-Dipteran insects

Although we have focused on the gustatory system of *Drosophila*, studies on other insects have also revealed interesting insights into taste coding. Of particular relevance are two studies on taste coding in different species of moths (Kvello, Jørgensen, & Mustaparta, 2010; Reiter, Campillo Rodriguez, Sun, & Stopfer, 2015). In the moth *Heliothis virescens*, central neurons innervating the SEZ were tested for their

responses to sucrose, quinine, water, and a mechanosensory stimulus, each applied to one of four locations: left antenna, right antenna, proboscis and tarsi (Kvello et al., 2010). Curiously, a wide variety of tuning curves were observed: responses to multiple qualities, responses to stimuli on multiple appendages, and responses across sensory modality (taste and mechanosensation). The diverse tuning properties of these central neurons cannot be easily explained by a labeled line model.

In a study on the moth *Manduca sexta*, taste responses were recorded from neurons at two levels of the gustatory circuit – first-order GRNs and second-order neurons (SONs) (Reiter et al., 2015). GRNs showed heterogeneous responses to tastants typically assumed to be of the same quality; for example, many responded strongly to sucrose, but not to other sugars. Some GRNs responded to a set of chemicals that crossed taste quality boundaries, including neurons tuned to sweet, salty, and bitter. SONs were more broadly tuned than their presynaptic GRNs: many responded to tastants of multiple taste qualities, even the SONs that received input from selectively-tuned GRNs. Intriguingly, some GRNs and SONs also exhibited peak firing rates at both stimulus onset and offset, suggesting a more complex representation of gustatory stimulus timing than has previously been appreciated.

Thus, in both species of moth, evidence suggests that taste tuning is rather broad at central stages of the gustatory circuit. There appears to be integration across taste quality and heterogeneity within taste quality, two properties that have not yet been reported for second-order taste neurons in *Drosophila*. However, our understanding of *Drosophila* comes from a small number of identified second-order neurons; there are likely many more whose taste response tuning has not been measured. Thus, it remains

unclear whether or not the coding properties observed in these species of moth are also operative in *Drosophila*.

1.12 How do we crack the neural circuits of taste?

How can we determine how taste information is represented at each stage of the neural circuit? Ideally, we would have a complete wiring diagram (or connectome) of the nervous system. Then we would know exactly which neurons were second-order in the circuit, which first-order neurons they receive input from, where in the brain these second-order neurons project, and which third-order neurons they connect to. Thus, knowing the response profiles of particular first order neurons, we could record from their downstream second-order neurons to determine how taste information is transformed from the first to second stage in the circuit. However, achieving this dream is still quite a way off for any mammalian nervous system. But it is nearing a reality for *Drosophila*: recent work from Janelia Research Campus has produced an electron microscopy volume of a complete brain of an individual adult fly (Zheng et al., 2018). A large portion of this volume has been painstakingly analyzed to produce a wiring diagram (Scheffer et al., 2020). Unfortunately, currently missing from this reconstructed area is the entire SEZ, the region that receives inputs from the GRNs.

However, we may be able to circumvent this problem using other techniques for tracing synaptic connections. Strategies to achieve this kind of transsynaptic tracing using viruses have been established for use in mammalian nervous systems. The rabies virus is known to be able to infect neurons, and spread from neuron to neuron by jumping across synapses in a retrograde direction (Wickersham et al., 2007). Through some genetic

modifications to the rabies virus, this fact was leveraged to enable retrograde monosynaptic transsynaptic tracing.

Sadly, methods such as this cannot be used to address taste coding in the fly for two reasons. First, viral injections are not feasible in small insects like *Drosophila*, whose brains are far too small to accurately target the virus to a given location. (In addition, it is not clear whether a fly could survive this procedure.) And second, what is needed is not a retrograde tracing method, but an *anterograde* one: one that labels the neurons downstream to the first-order neurons. Even in the mouse, where viral tracers are used, the few existing methods for viral anterograde tracing have significant limitations: for example, some cause substantial tissue damage (Luo et al., 2018). In addition, some tracing methods are *transneuronal* rather than transsynaptic, and label nearby, but not necessarily synaptically connected, neurons (Luo et al., 2018).

But *Drosophila* has another advantage: it is a model organism with a huge array of genetic tools available, and one in which it is comparatively easy to develop new ones. Could we create a genetic tool to achieve the capability to trace circuits in the fly? In this dissertation, I show that we can. In the next chapter, I describe the development of *trans*-Tango, a novel genetic method for anterograde transsynaptic tracing and circuit manipulation in *Drosophila.* Using *trans*-Tango, I reveal the anatomy of second-order gustatory neurons in the fly, including several newly-discovered classes of gustatory projection neurons. Further, I combine *trans*-Tango with *in vivo* calcium imaging to characterize the representation of taste in these gustatory projection neurons. I argue that our results support a kind of mixed model of taste coding, in which some pathways may act as labeled lines and others appear to employ distributed coding. Finally, I discuss

what kinds of conclusions we can draw from these results, possible directions for future experiments, and the implications for taste coding more generally.

CHAPTER 2

Transsynaptic Mapping of Second-Order Taste Neurons in Flies by *trans*-Tango

This chapter is adapted from published work.

Citation:

Talay, M., Richman, E. B., Snell, N. J., Hartmann, G. G., Fisher, J. D., Sorkaç, A., Santoyo, J. F., Chou-Freed, C., Nair, N., Johnson, M., Szymanski, J. R., Barnea, G. (2017). Transsynaptic Mapping of Second-Order Taste Neurons in Flies by trans-Tango. Neuron, 96(4), 783-795.e4. https://doi.org/10.1016/j.neuron.2017.10.011

Funding Acknowledgements

This work was supported by NIH grants R21DCO14333, R01MH086920, R01MH105368 and R01DC013561 (GB), and by internal funds from Brown University: BIBS Innovation Award and OVPR Salomon and Seed Awards (GB). GB was supported in part by the Pew Charitable Trust. MT was supported by a fellowship from the Suna & İnan Kıraç Foundation and BIBS. EBR, GGH and CC-F were supported in part by a Karen T. Romer UTRA. NJS was supported by grant number DGE1058262 from the National Science Foundation Graduate Research Fellowship Program.

Research Contributions

- I performed dissections, immunohistochemistry, and confocal microscopy to generate data for Figure 2-5 and Figure 2-S1.
- I devised and performed the staining quantification in Figure 2-S3.
- I edited and commented on the manuscript.
- Other experimental design was performed by M.T., E.B.R., G.G.H., J.D.F., A.S., C.C-F., M.J., J.R.S., and G.B.
- Other experiments were performed by M.T., E.B.R., G.G.H., J.D.F., A.S., C.C-F., J.R.S., and N.N.
- Other data analysis was performed by M.T., E.B.R., G.G.H., J.D.F., A.S., J. F. S., C.C-F., and G.B.
- M.T., E.B.R. and G.B. wrote the manuscript.
- G.G.H., J.D.F., A.S., J. F. S., C.C-F., M.J., and J.R.S. also commented on the manuscript.

2.1 Introduction

Neurons are the basic structural and functional units of the nervous system (Ramón y Cajal, 1888; Sherrington, 1906). Individual neurons connect to one another via synapses to form neural circuits (De Robertis & Bennett, 1955), and the concerted activities of neurons within circuits underlie all brain functions, including perception, cognition, and generation of behavior. Our limited ability to specifically map synaptically connected neurons within circuits, or to selectively manipulate their functions, therefore, poses a major obstacle to understanding the workings of the brain. Neuroimaging techniques, such as magnetic resonance imaging, lack the resolution and precision needed to reveal synaptic connectivity, while most molecular genetic techniques are limited to the confines of the neurons for which markers exist. Other methods for circuit mapping, such as paired recording and optogenetic-assisted circuit mapping, are labor intensive and low throughput. Serial electron microscopy is the gold standard for identifying synaptic connections within a circuit, but practical considerations limit the utility of this technique to analyzing small volumes of postmortem tissue. Further, this approach is not suitable for comprehensive analysis of variability among individuals (Briggman & Bock, 2012).

The use of genetically introduced tracers, such as plant lectins and bacterial toxins, has been invaluable towards understanding neuronal connectivity (Huh, Oh, Leblanc, & Kim, 2010). However, the utility of these tracers is limited by the lack of synaptic specificity and directionality. These tracers are further limited by their spread beyond one neuron and by the resulting dilution of the signal. The most commonly used transsynaptic tracing techniques in vertebrates rely on replication-deficient neurotropic viruses that are restricted to specific genetically defined neurons within a circuit

(Callaway & Luo, 2015). While most neurotropic viruses transport only in the retrograde direction, some anterograde viral tracers have been developed (Lo & Anderson, 2011; Zingg et al., 2017). Two major limitations in the use of neurotropic viruses as tracers are the low efficiency of transsynaptic transport and the variability between experiments in the infected neuronal populations (Callaway & Luo, 2015). Another significant problem with some viral tracers is their toxicity to the infected neurons that may lead to cell death and consequent infection of irrelevant bystander neurons (Callaway & Luo, 2015). In spite of these limitations, rabies has been useful for retrograde tracing, but it is restricted to certain model organisms. By contrast, the utility of the anterograde viral tracers has been very limited.

Several techniques use versions of fluorescent proteins to label synaptic connections or to trace circuits. Transsynaptic complementation of a split version of green fluorescent protein (GFP) is used in GRASP (GFP Reconstitution Across Synaptic Partners) to mark synapses (Feinberg et al., 2008; Gordon & Scott, 2009). Each of the two complementary pieces of GFP is expressed by genetically-defined neuronal populations, and functional GFP is reconstituted when both pieces are in close proximity. Modified versions of GRASP have been developed to enhance its synaptic specificity by fusing at least one of the pieces of GFP to a synaptic protein (Fan et al., 2013; Macpherson et al., 2015). Nonetheless, these methods only label synapses rather than whole cells, and it is therefore difficult to relate the GRASP signal to particular neurons. Further, none of the versions of GRASP can be used for tracing the projections of postsynaptic neurons. Another method for circuit tracing uses photoactivatable GFP, which is genetically encoded and locally photoconverted to its high-fluorescence form to

enable labeling of specific neural processes (Clowney et al., 2015; Datta et al., 2008; Patterson & Lippincott-Schwartz, 2002; Ruta et al., 2010). This approach achieves higher spatial specificity than that afforded by genetic markers, but is invasive, can label fibers-of-passage, and does not report connectivity. Finally, a major limitation of all of these tracing techniques is that they do not provide stable genetic access to the postsynaptic partners, and therefore they cannot be used to manipulate the function of the circuit.

Tango-Trace is a technique that was developed to trace projections in the fly visual system (Jagadish, Barnea, Clandinin, & Axel, 2014). It is based on Tango, an *in vitro* assay for recording the activation of receptors by their ligands (Barnea et al., 2008). In Tango, a synthetic signaling pathway consisting of two fusion proteins converts the activation of a cell-surface receptor into reporter expression through site-specific proteolysis (Barnea et al., 2008). Tango-Trace employed a configuration of Tango for detecting release of histamine, the excitatory neurotransmitter released from photoreceptors in the fly retina upon activation (Jagadish et al., 2014). The utility of Tango-Trace has been rather limited because outside of the retina histamine is believed to serve as a neuromodulator rather than a neurotransmitter (S. T. Hong et al., 2006; Nässel, 1999). Further, diffusion of histamine away from the synapse and consequent labeling of non-synaptic neurons is a potential problem with Tango Trace.

Here we describe *trans*-Tango, a new method for anterograde transsynaptic tracing. While *trans*-Tango is also based on the Tango assay, its design is fundamentally different than Tango-Trace in order to generate a general and flexible transsynaptic labeling system. *trans*-Tango employs an exogenous ligand-receptor pair for circuit labeling, so in principle it can be applied to any neural circuit regardless of the

neurotransmitter that it uses and without making any assumptions about the nature of the connection. To present the ligand, we introduce a third fusion protein in which the ligand is tethered to a synaptic protein via an extracellular spacer. This configuration directs the ligand to the synapse and prevents it from diffusing away. In *trans*-Tango, the Tango signaling pathway is introduced into all neurons in the animal. Specific labeling is achieved by presenting the tethered ligand at the synapses of genetically defined neurons, thereby activating the signaling pathway only in their postsynaptic partners. We designed *trans*-Tango in a modular fashion to allow easy integration with other genetic tools for circuit dissection and manipulation. We first validated *trans*-Tango in the olfactory system of the fruit fly *Drosophila melanogaster*, where our experiments recapitulated known connections, but also revealed new ones. We then used *trans*-Tango to identify hitherto unknown second-order neurons in the *Drosophila* gustatory system. Our anatomical tracing experiments revealed that second-order gustatory neurons target brain areas known to be involved in neuromodulation and in controlling feeding behaviors, providing a possible pathway for integrating gustatory signals and the regulation of feeding.

2.2 Transsynaptic labeling by trans-*Tango*

trans-Tango is a transsynaptic labeling system that is based on Tango, a cellular assay for recording the activation of specific receptors by their ligands (Barnea et al., 2008). In Tango, synthetic signaling pathway is activated in response to ligand binding to its receptor through a specific proteolytic event that releases a membrane-tethered transcription factor, allowing it to translocate into the nucleus and induce expression of a

reporter (Barnea et al., 2008). To attain anterograde labeling by *trans*-Tango, the core components of the signaling pathway are expressed panneuronally and the ligand that activates the pathway is presented at presynaptic sites in a neural circuit. Contact between the ligand and its receptor at synaptic sites drives expression of a reporter in postsynaptic neurons. The ligand and its receptor are exogenous to the animal in order to prevent spurious signal. To establish *trans*-Tango in *Drosophila,* we used human glucagon and its receptor as the ligand-receptor pair.

The signaling pathway driving postsynaptic reporter expression consists of three components (Figure 1A). The first is a fusion protein comprising the glucagon receptor, a G protein-coupled receptor, bound at its cytoplasmic tail to the transcriptional activator QF (Potter, Tasic, Russler, Liang, & Luo, 2010) via a linker containing the cleavage site for the highly specific N1a protease from the tobacco etch virus (TEV) (Barnea et al., 2008). The second component, hArr::TEV, is a fusion between TEV and human β-arrestin2, a protein that is specifically recruited to activated G protein-coupled receptors (Barnea et al., 2008). Panneuronal promoters drive expression of these two fusion proteins in all neurons. The third component in the pathway is a reporter, such as mtdTomato, under transcriptional control of QF. In this manner, all neurons in the fly are endowed with the capacity to express the reporter upon activation of the signaling pathway. The pathway is activated only in neurons that are postsynaptic to those that express a membrane-tethered form of glucagon at their presynaptic terminals (see below). In the absence of ligand at a given synapse, QF is sequestered to the membrane, and the reporter is not expressed (Figure 1A, top). By contrast, at synapses where the ligand is expressed, transsynaptic activation of the receptor leads to recruitment of hArr::TEV.

Upon TEV cleavage in its target site, QF is released from the membrane, allowing it to enter the nucleus and induce expression of the reporter (Figure 1A, bottom). The inherent signal amplification by the signaling pathway renders *trans*-Tango very sensitive, and since the components of the signaling pathway are extrinsic to the cell, background noise can be kept low. Thus, *trans*-Tango should label circuits with high signal-to-noise ratios.

In order to localize glucagon to the synapse and present it to postsynaptic receptors, we generated another fusion protein consisting of the cytosolic and transmembrane domains of the synaptic protein *Drosophila* Neurexin1, the large extracellular domain of the human cell adhesion molecule ICAM1, a flexible linker including a myc-tag (Fortin et al., 2009), and a mutated version of the glucagon peptide with high potency for glucagon receptor activation (Krstenansky, Trivedi, Hruby, & Johnson, 1986) (Figures 1A and S1A). The resulting *trans*-Tango ligand, which is sized to extend across the average length of a synapse, is targeted to axon termini (Figure S1B). The expression of the ligand fusion protein is controlled by the Gal4-UAS binary system (Brand & Perrimon, 1993), the most commonly used tool for genetic access in flies.

To introduce the *trans*-Tango components into the fly, we generated a transgenic line bearing all three fusion proteins as a single allele (*trans*-Tango): (i) the receptor fusion, (ii) hArr::TEV, and (iii) the ligand fusion (Figure S1A). We did not detect any effect of panneuronal expression of the *trans*-Tango components on normal life span, development, brain morphology or motor behavior (data not shown). We generated a second transgenic line bearing a reporter allele containing a membrane-associated form of GFP under control of Gal4 (*UAS*-myrGFP) to mark presynaptic neurons, and a membrane-associated form of tdTomato under control of QF (*QUAS*-mtdTomato) to

mark postsynaptic neurons (Figures 1A and S1A). In this manner, any circuit for which a presynaptic Gal4 driver is available can in principle be traced by *trans*-Tango. To achieve this, flies bearing the *trans*-Tango and reporter alleles are crossed to flies bearing the appropriate Gal4 driver, and offspring carrying all three alleles are analyzed.

2.3 Validating trans-*Tango in the olfactory system*

We sought to validate *trans*-Tango in the context of the well-characterized olfactory system. *Drosophila* olfactory receptor neurons (ORNs) express specific receptors and detect volatile odors. ORNs residing in the antenna and maxillary palp project to the antennal lobe (AL), where ORNs expressing a given receptor converge on the same neuropil structures called glomeruli. Axons from ORNs synapse with local interneurons (LNs) and projection neurons (PNs) (Vosshall & Stocker, 2007). LNs project locally to other glomeruli within the AL, while PNs project from the AL to the mushroom body (MB) calyx and the lateral horn (LH) mainly via the medial, mediolateral and lateral antennal lobe tracts (mALT, mlALT and lALT, respectively) (Ito et al., 2014).

We first used *Orco*-Gal4, which is expressed in the majority of ORNs (Vosshall & Stocker, 2007), to drive expression of the *trans*-Tango ligand and myrGFP. In flies bearing the *Orco*-Gal4 driver and the *trans*-Tango components, we observed the typical innervation of the AL by GFP-expressing ORNs and robust mtdTomato labeling in LNs as well as in PNs that target the MB calyx and LH (Figure 1B and Movie S1). In addition, we observed projections descending to the subesophageal zone (SEZ), the first processing center for gustatory information in the brain (Ito et al., 2014; Wang et al., 2004). We

observed a total of 152±6 (mean±s.d.) and 182±17 postsynaptic neurons per hemisphere in females and males, respectively (n=10 ALs per group). By contrast, no signal, except two spots in the ventral SEZ, was detected in the brains of control flies bearing the *trans*-Tango components but no Gal4 driver, which is necessary for *trans*-Tango ligand expression (Figure 1C). The background noise in the ventral SEZ might be due to sporadic leaky expression known to occur in the attP40 genomic locus where we integrated the *trans*-Tango allele (B. D. Pfeiffer et al., 2010). These results demonstrate the tight regulation of ligand-dependent QF release and the consequent high signal-to-noise ratio of *trans*-Tango.

2.4 Specificity of trans-*Tango*

To examine the specificity of *trans*-Tango, we expressed the ligand in individual ORN classes. We started with Or67d-expressing ORNs that target the DA1 glomeruli and mediate sexual behaviors. This is one of the most studied olfactory circuits in flies (Datta et al., 2008; Jefferis et al., 2007; Kurtovic, Widmer, & Dickson, 2007; Ruta et al., 2010). Expression of the *trans*-Tango ligand in Or67d+ ORNs resulted in an extremely dense signal in LNs innervating many glomeruli including DA1, and also led to specific labeling of PNs targeting the MB calyx and LH (Figure 2A). Additionally, we found bilateral descending projections from the AL to the SEZ (Figure 2A, arrows), as we noticed with the broadly expressed *Orco*-Gal4 (Figure 1B). We observed a total of 61±5 and 81±4 postsynaptic neurons per hemisphere in females and males, respectively (n=10 ALs per group). In subsequent experiments, we expressed the ligand in Or42b-expressing ORNs that are important for detecting certain food odors (Root, Ko, Jafari, & Wang,

2011; Semmelhack & Wang, 2009). We observed dense *trans*-Tango dependent signal in LNs innervating many glomeruli, including the cognate DM1 glomerulus, as well as signal in a distinct set of PNs projecting to the MB calyx and LH (Figure 2B). We observed a total of 86±7 and 92±5 postsynaptic neurons per hemisphere in females and males, respectively (n=10 ALs per group). It is noteworthy that the reporter in *trans*-Tango is integrated in the X chromosome, so due to dosage compensation, the signal in males is higher than in heterozygous females. Thus, while the cell number differences between males and females could reflect sexual dimorphism, they could also result from the difference in reporter levels. These results, together with *trans*-Tango labeling of other ORN classes (Figure S2), confirm the high degree of interconnectivity among glomeruli suggested by earlier studies (Y.-H. Chou et al., 2010; Seki, Rybak, Wicher, Sachse, & Hansson, 2010).

While the general patterns of postsynaptic signal were similar for the various ORN populations, careful examination revealed notable differences. Namely, with ligand expressed in Or42b+ ORNs, we did not observe the neurons descending from the AL to the SEZ (Figures 2A and 2B, arrows). In addition, the targeting patterns of the two PN populations within the LH were distinct, with projections from DA1 terminating in the ventral LH and those from DM1 terminating more dorsally (Figure 2A and 2B). These projection patterns are in agreement with the literature (Jefferis et al., 2007; Strutz et al., 2014). Finally, while we observe postsynaptic signal from both DA1 and DM1 throughout the AL, the signal distribution is not homogeneous and is different between the two. The postsynaptic signal from the DA1 glomerulus is sparser in the medial aspect of the AL, an area that includes DM1 among other glomeruli. By contrast, the

postsynaptic signal from DM1 is sparser in the lateral aspect of the AL, an area that includes DA1 (Figures 2A and 2B). The different postsynaptic signal patterns produced by driving *trans*-Tango ligand expression in different classes of ORNs, and the agreement with known projection patterns, suggest that *trans*-Tango reveals specific postsynaptic partners.

In our attempts to optimize *trans*-Tango, we examined the effects of temperature and age on the *trans*-Tango signal. We found an inverse correlation between the *trans*-Tango signal and temperature over the range of 15-25°C, with the best signal-to-noise ratio observed at 18°C (Figure S3), while Gal4-dependent signal increased with temperature in this range as expected (Wilder & Perrimon, 1995). In flies raised at 18°C, *trans*-Tango output labeling for three different populations of ORNs gradually increased with age, starting to saturate at approximately two weeks post-eclosion (Figure S4). We therefore maintained the flies for all of our experiments at 18°C and analyzed them at least two weeks post-eclosion.

It is noteworthy that we observed linkage between the strength of the Gal4 line used to drive the ligand and the intensity of the *trans*-Tango output signal (data not shown). This was apparent even when comparing different genomic integrations of the same Gal4 drivers (data not shown). Hence, the optimal age for analysis should be established empirically for each Gal4 driver of interest. Finally, we wished to examine individual variability in projection patterns among flies of the same genotype. We compared the postsynaptic projections from the DA1 and DM1 glomeruli in age-matched flies and observed consistent projection patterns within groups (Figure S5). These results

showcase the strength of *trans*-Tango as a genetic system to generate reproducible transsynaptic labeling results between individuals.

2.5 Sparse labeling of postsynaptic neurons with trans-*Tango*

The widespread mtdTomato labeling in the AL impeded our ability to determine whether the labeled PNs were indeed receiving input from the proper glomerulus. We therefore pursued mosaic-labeling strategies to isolate individual postsynaptic neurons. We used *trans*-Tango in conjunction with MARCM (T. Lee & Luo, 1999; Potter et al., 2010) to label postsynaptic neurons singly or in small groups. Suppression of the QF-dependent postsynaptic signal was achieved with a pancellular QS repressor allele (Potter et al., 2010) and relieved in stochastic subsets of cells by heat-shock. Importantly, MARCM analysis of postsynaptic neurons that were labeled via ligand expression in Or67d+ ORNs revealed PNs or LNs with dendrites arborizing within the DA1 glomerulus (Figure 3A, data not shown). Likewise, equivalent experiments with Or42b+ ORNs revealed neurons contacting the cognate DM1 glomerulus (data not shown). With both populations, obtaining single cell clones with MARCM was rare. Notably, when the ligand was expressed in Or67d+ ORNs, we obtained brains in which a single neuron projecting between the AL and SEZ was observed. This neuron innervates the DA1 glomerulus along with a number of other glomeruli (Figure 3A).

To further characterize the putative postsynaptic neurons of Or67d+ ORNs, we implemented an intersectional Flp-out strategy for *trans*-Tango, in which QF-dependent reporter expression required the FLP recombinase (Gordon & Scott, 2009; Potter et al., 2010). By combining this intersectional reporter with initiation of *trans*-Tango labeling

from Or67d+ ORNs, we were able to restrict labeling to Fru+ or GH146+ neurons (Figures 3B and 3C, respectively). We observed 10±2 Fru+ PN cell bodies per hemisphere in females and 6±1 in males (n=12 ALs per group), and 23±2 GH146+ PN cell bodies per hemisphere in females and 23±3 in males (n=22 ALs for females and 20 for males). A similar strategy driving the system from Orco+ ORNs revealed 93±7 PN cell bodies per hemisphere in females and 98±6 in males (n=12 ALs per group). Interestingly, these intersectional experiments with ligand expressed in Or67d+ ORNs revealed that the neuron projecting from the AL to the SEZ is Fru+ (Figure 3B, arrows), suggesting that this neuron might play a role in connecting pheromone responses and gustation.

2.6 Sensitivity and versatility of trans-*Tango*

The adult olfactory circuits are characterized by a convergence of many ORNs onto the output neurons in the AL. This architecture results in concentration of the *trans*-Tango ligand from many neurons onto the postsynaptic neurons. Many other circuits are less convergent, and may not yield such concentration of ligand onto postsynaptic receptors. The ability to label postsynaptic partners of a single presynaptic neuron is essential for the precise characterization of circuits. We therefore sought to determine whether *trans*-Tango could illuminate output neurons that receive input from single ligand-expressing neurons. We chose to examine this in the larval olfactory system, in which distinct olfactory receptor genes are expressed by single ORNs (Fishilevich & Vosshall, 2005). However, when we examined larvae carrying the *trans-Tango* allele, we observed mtdTomato expression in the ventral nerve cords (VNCs) of both the

experimental and control larvae (data not shown). Careful examination of the VNCs revealed GFP expression, albeit faint (Figure 4A, asterisk), suggesting that our UAS promoters might be leaky in the larval VNC, leading to Gal4-independent expression of ligand that induces *trans*-Tango mediated mtdTomato expression. This background labeling in the larval VNC is not observed in flies not carrying the *UAS*-glucagon component (data not shown). We therefore decided to use an intersectional approach where the signal is limited to the olfactory system through the use of *GH146*-FLP together with a conditional suppressor (*tubP-FRT-QS-FRT*) that we have generated. In larvae bearing these alleles together with *trans*-Tango driven from Or42a+ ORNs, we observe 3±1 GH146+ PN cell bodies per hemisphere (n=22 ALs). (Figure 4A). These results in the larval olfactory system suggest that *trans*-Tango is sensitive enough to label the outputs of single neurons. We note that because various circuits exhibit a range of densities of synapses, the sensitivity of *trans*-Tango may lessen in circuits with sparser synaptic contacts.

To further determine whether *trans*-Tango could be used in circuits with other architectures, we investigated the peripheral visual system, where the architecture is mostly columnar (Morante & Desplan, 2008). We expressed the *trans*-Tango ligand in lGMR+ photoreceptor cells and observed widespread postsynaptic labeling in the lamina and medulla (Figure 4B). The implementation of *trans*-Tango to label visual circuits illustrates the flexibility of the system and its utility for studying circuits with diverse architectures and properties.

2.7 Identifying second-order taste neurons and their projections in the brain

We next turned our attention to the gustatory system, where relatively little is known about the postsynaptic partners of gustatory receptor neurons (GRNs) (Harris et al., 2015; Kain & Dahanukar, 2015; Kim et al., 2017; Miyazaki, Lin, Ito, Lee, & Stopfer, 2015; Yapici et al., 2016). GRNs express gustatory receptors (GRs) that detect non-volatile chemicals and are dispersed in various parts of the body, including the proboscis (labellum and pharynx), tarsal segments of the legs, wing margins, abdomen, intestine and female genitalia (Clyne et al., 2000; Dunipace et al., 2001; Scott et al., 2001; Vosshall & Stocker, 2007). Each one of these peripheral gustatory organs is thought to contribute distinctly to the overall gustatory response of the fly to tastants (Vosshall & Stocker, 2007). Distinct populations of GRNs respond to sweet and bitter tastants (Harris et al., 2015). Like mammals, flies respond to sweet and bitter tastants with different behavioral outputs: sweet molecules are attractive and elicit acceptance, while bitter compounds are aversive and lead to rejection (Vosshall & Stocker, 2007). The clear linkage between stimulus quality and behavioral response suggests differential representation of taste categories in the brain. Indeed, the projections of GRNs responding to sweet and bitter tastants segregate within the SEZ (Wang et al., 2004). However, little is known about the nature of subsequent projections from the SEZ, or about how gustatory information is processed further to elicit the appropriate behavioral outputs.

Seeking to identify second-order neurons in the gustatory system, we initiated expression of the *trans*-Tango ligand in Gr64f+ sweet GRNs. Expression of the *trans*-Tango ligand in Gr64f+ GRNs revealed extensive postsynaptic signal in the CNS (Figure

5A and 5B, Movie S2). Gr64f+ GRNs are present in each leg and either terminate in the thoracic ganglia or project directly to the posterior SEZ with collaterals in the thoracic ganglia (Figure 5A) (Kwon et al., 2014; Thoma et al., 2016). Gr64f+ GRNs also innervate the abdominal ganglion (Movie S2). Expression of the Tango ligand in Gr64f+ GRNs induced postsynaptic mtdTomato signal in each thoracic neuromere and in the abdominal ganglion in the VNC and in projections to the central brain (Figure 5A and 5B, Movie S2).

In the central brain, expression of the *trans*-Tango ligand in Gr64f+ GRNs revealed a large number of postsynaptic neurons (Figure 5B, Movie S2). The observed signal was saturated in the vicinity of the SEZ, most likely due to dense interconnectivity. It was therefore difficult to precisely discern specific connections. Most of the distinguishable cell bodies of the second order neurons resided external to the SEZ, in the cell body rind of neighboring neuropil structures such as the antennal mechanosensory and motor center (AMMC). Additional groups of cell bodies were located posteroventral and anterodorsal to the SEZ, as well as dorsal to the AL. Due to the intense mtdTomato labeling in the SEZ, we were unable to distinguish cell bodies from cell processes there (Figure 5B).

In addition to the dense signal in the vicinity of the SEZ, we observed projections to distant neuropil structures. These projections appeared to follow three major tracts: (i) an axon bundle that projected along the midline toward the superior medial protocerebrum (SMP), where it arborized away from the midline; (ii) an axon bundle that traveled posterior to the AL and arborized in the superior intermediate protocerebrum (SIP) and superior lateral protocerebrum (SLP); and (iii) a thinner bundle that passed

through the posterior ventrolateral protocerebrum and projected to the SLP and lateral protocerebrum (Figure 5B and 5D, Movie S2). Although the locations of the cell bodies varied across individuals, these projection tracts appeared to be stereotyped. These findings implicate the SMP, SIP and SLP as target areas for second-order neurons in the gustatory circuits. Following the naming convention of second-order olfactory pathways (Ito et al., 2014), we refer to these gustatory tracts as medial, mediolateral, and lateral SEZ tracts (mSEZt, mlSEZt, and lSEZt, respectively).

In order to discern the precise connectivity of second-order gustatory neurons and overcome the dense signal, we combined *trans*-Tango with MARCM, or FLP-out, to stochastically reveal labeling in clonal subsets of neurons postsynaptic to Gr64f+ GRNs (Figure 5C). We observed many local interneurons that exhibited diverse arborizations within the SEZ (Figure 5C). These neurons mainly inhabited the outer layer of the neighboring AMMC and sent diffuse processes that mostly arborized on the ipsilateral side (Figure 5C). Neurons with similar morphology have been described (Kain & Dahanukar, 2015; Miyazaki et al., 2015; Yapici et al., 2016). We also observed clusters of neurons that projected to the SMP, SIP and SLP. Our experiments revealed two distinct clusters of neurons that projected through the mSEZt: a cluster of cell bodies posteroventral to the SEZ and a cluster anterodorsal to the SEZ (Figure 5C). Neurons in the posteroventral cluster received input from the ipsilateral SEZ and projected to the ipsilateral SMP, where they branched laterally. By contrast, neurons in the anterodorsal cluster received input from both sides of the SEZ and projected to the SMP, where they branched bilaterally. We observed a single cluster of neurons that projected through mlSEZt (Figure 5C). The cell bodies of these neurons resided anterodorsal to the AL.

They received input mostly from the contralateral SEZ, with a faint connection to the ipsilateral SEZ, and projected contralaterally, forming crescent-shaped terminals in the SIP/SLP. Interestingly, neurons with similar morphology were previously described as being sexually dimorphic, with females having fewer neurons and lacking input from the ipsilateral SEZ (Chiang et al., 2011; Kimura, Ote, Tazawa, & Yamamoto, 2005). Indeed, comparison between these neurons in female and male brains revealed that their morphology is different; in females the fiber connecting the cell bodies and the ipsilateral SEZ is missing (data not shown). Finally, we observed two clusters of neurons projecting through the lSEZt. The cell bodies of neurons within the first cluster resided in the cell body rind of the AMMC (Figure 5C). These neurons extended dense arborizations into the ipsilateral SEZ and more sparse arborizations into the medial aspect of the contralateral SEZ. Following the lSEZt, they projected largely to the ipsilateral SLP with minor collaterals in the lateral protocerebrum. The cell bodies of the neurons within the second cluster projecting through the lSEZt resided near the abdominal ganglion in the VNC (Figure 5C). These neurons cross the midline and ascend towards the central brain receiving input from each contralateral leg neuromere. In the central brain, they extended dense arborizations into the contralateral SEZ and some continue through the lSEZt to the contralateral SLP with minor collaterals in the lateral protocerebrum (Figure 5C). Similar long-range sweet projection neurons have been recently described (Kim et al., 2017). Interestingly, neurons with similar morphology were also described for pheromone detection (Clowney et al., 2015; Yu, Kanai, Demir, Jefferis, & Dickson, 2010). It is noteworthy that we observed that each cluster of postsynaptic neurons receiving input from the SEZ projected along a single tract, and we never observed a neuron with parallel

projections through multiple tracts (Figure 5C). While we have described here the most common projections, we also observed other projection neurons from the SEZ to the protocerebrum that did not fit in these clusters (Movie S2 and data not shown). Neurons with similar morphologies to all of the classes of second-order gustatory neurons that we have identified had been described in single cell resolution (Chiang et al., 2011).

2.8 Discussion

In this study, we describe *trans*-Tango, a new method that we have developed for transsynaptic mapping and manipulation of neural circuits in the anterograde direction. The design of *trans*-Tango is based on the Tango assay for recording ligand-receptor interactions (Barnea et al., 2008). The Tango assay was also the basis for two earlier *in vivo* systems in *Drosophila*: TANGO-map, a method for identifying sites of neuromodulation (Inagaki et al., 2012), and Tango-Trace, which was used to functionally map projections in the visual system (Jagadish et al., 2014). Both of these techniques used the Tango design for detecting endogenous ligands (dopamine in TANGO-map, histamine in Tango-Trace). Unlike these earlier Tango based systems, *trans*-Tango employs exogenous ligand and receptor for circuit labeling, so in principle it can be applied to any neural circuit regardless of the neurotransmitter that it uses. Further, since in *trans*-Tango the ligand is tethered to a synaptic protein it does not diffuse away from the synapse, a potential problem with Tango-Trace (Jagadish et al., 2014). Thus, *trans*-Tango is truly a general and flexible transsynaptic labeling technique that allows discovery of unknown synaptic partners and circuit elements without any assumptions or previous knowledge about the nature of these connections. In this manner, *trans*-Tango is

a powerful tool for generating hypotheses regarding potential connectivity. Unlike other techniques for anterograde tracing, such as dye injection or the use of neurotropic viruses, *trans*-Tango is immune to signal diffusion. Further, as it can be readily combined with mosaic approaches for sparse labeling of postsynaptic neurons, *trans*-Tango is especially suitable for tracing projections within dense neuropil.

Our experiments revealed an inverse correlation between the intensity of the postsynaptic *trans*-Tango signal and the temperature in which the flies were raised over the range of 15-25°C. To maximize the signal-to-noise ratio, we maintained the flies for all of our experiments at 18°C. It is noteworthy that this inverse correlation extends beyond signal intensity per neuron. Indeed, we consistently observe signal in more neurons at lower temperatures (15-18°C) than at 25°C. We believe that as flies are ectotherms this difference could reflect the effect of the low temperature on biological processes, such as pruning. Alternatively, this phenomenon could be directly related to features of *trans*-Tango. For example, it is conceivable that the folding of the synthetic fusion proteins in *trans*-Tango is more efficient at lower temperature, or that their turnover is slower, such that the concentrations of the various components are higher. Otherwise, perhaps the kinetics of the various interactions in *trans*-Tango (*e.g.* ligand-receptor interaction, recruitment of β-arrestin to the activated receptor, processivity of TEV, interaction between QF and QUAS, etc.) is differentially affected by temperature such that the signaling pathway is sensitized. In both cases, the overall sensitivity of the system would be much higher at lower temperatures. Consequently, even transient interactions between axons during development might result in some signal. Whatever the explanation, this phenomenon could in fact act as a knob that controls the gain of the

system, and it should be considered when using it. When the goal is to reveal as many potential postsynaptic partners as possible, the flies should be raised at 15-18°C, but when a more stringent assessment of connectivity is desired, the flies should be raised at 25°C. This phenomenon also impacted the interpretation of the numbers of postsynaptic neurons that we observed compared to the literature, as most published data are obtained at 25°C.

Comparison of the numbers of postsynaptic neurons that we have observed with the available published numbers revealed that in some cases, our numbers corresponded with the published numbers while in others, our numbers were higher. For example, earlier studies revealed that Or67d+ ORNs provide input onto six Fru+ PNs both in females and males (Datta et al., 2008; Ruta et al., 2010). In our experiments driving *trans*-Tango from Or67d+ ORNs and restricting the signal to Fru+ neurons, we observed 10±2 Fru+ PN cell bodies per hemisphere in females and 6±1 in males, suggesting thorough labeling of postsynaptic partners by *trans*-Tango. However, we observed 23±2 GH146+ PN cell bodies per hemisphere in females and 23±3 in males. These numbers are higher than the numbers published recently: 8±2 uniglomerular PNs in females and 10±1 uniglomerular PNs in males (Grabe et al., 2016). This trend extends to the number of PNs associated with other glomeruli (data not shown). Similarly, when we drive *trans*-Tango from Or42a+ ORNs in larvae, we observed 3±1 GH146+ PN cell bodies per hemisphere compared to the suggested one PN (Ramaekers et al., 2005). There are several potential explanations to this discrepancy. Our numbers could be inflated by the fact that we intentionally counted cells in a non-stringent manner; we counted cells even if the signal in them was faint in order to reveal any potential post-synaptic neurons. This

was especially significant in the anterodorsal cluster of PNs in the olfactory system where we often saw weak signal. The difference in numbers could also be explained by the experimental approach: our numbers resulted from intersectional experiments where FLP was used, while the published numbers were generated using Gal4. As we have discussed earlier, temperature could be a major factor: all of our experiments were conducted at 18°C where the signal-to-noise with *trans*-Tango is optimal, but the system is more sensitive. When the flies were raised at 25°C, the numbers that we observed were closer to the published numbers (data not shown). The choice of the reporter used to reveal the postsynaptic signal is another technical factor that affects the numbers. In our attempts to optimize *trans*-Tango, we tested several available QUAS reporters as well as a few that we generated (data not shown). In our experiments, we chose to use the reporter that we generated because it yielded the best signal-to-noise ratio. The use of other reporters led to higher non-specific background noise as well as to signal in more neurons. In our intersectional experiments in the adult, we wished to achieve a sufficiently strong signal in order to obtain comprehensive labeling of potential postsynaptic partners. To avoid underrepresentation, we chose to use one of the more sensitive reporters (Potter et al., 2010) that consistently labeled more neurons even at the expense of potential false-positive signal. The use of this reporter could have contributed to the higher cell numbers observed. These explanations notwithstanding, the higher numbers observed with *trans*-Tango could of course represent false-positive signal that could have resulted from inefficient synaptic localization of the ligand due to its overexpression, as was observed for synaptic GRASP (Y. Chen et al., 2014). Such ligand mislocalization could have been exacerbated by the relatively late age in which we analyze the flies. It is worth noting that

a recent EM study revealed occasional bilateral variability within the same animal in the number of PNs receiving input from the same pair of glomeruli (Tobin, Wilson, & Allen Lee, 2017). Thus, the number of PNs per glomeruli is most likely less stereotyped than previously thought, though this variability is much lower than the differences between the numbers that we observed and the published numbers. In conclusion, *trans*-Tango is a powerful tool for generating hypotheses regarding connectivity. Like any other technique, connections revealed by *trans*-Tango will require further functional validation. Since *trans*-Tango provides genetic access to the postsynaptic neurons, future versions of *trans*-Tango incorporating calcium indicators, such as GCaMP6 (T.-W. Chen et al., 2013), as readout might facilitate such validation in circuits of interest.

When we assessed the age-dependence of the *trans*-Tango signal, we observed three additional glomeruli in young animals when the ligand was driven in Or42b+ ORNs (Figure S4A). By contrast, we never saw additional glomeruli when we analyzed Or67d+ ORNs (Figure S4B). Careful examination of both the antennae and the AL revealed that these supernumerary glomeruli correspond to the neighboring neurons of Or42b+ ORNs within the ab1 sensilla (Or10a→DL1, Or92a→VA2, Gr21a→V), suggesting interactions between axons within the bundle. These interactions could be biologically significant or simply an artifact/noise of *trans*- Tango. Interestingly, when we drove ligand expression from Or92a+ ORNs that also reside in ab1 sensilla, we did not observe signal in the glomeruli of the other ORNs (Figure S4C). Importantly, the strength of the *Or42b*-Gal4 and *Or92a*-Gal4 drivers is similarly high. The different patterns of staining with these ORN populations might therefore reflect their biology.

In our validation experiments in the olfactory system, we induced ligand expression in different populations of ORNs and observed postsynaptic signal spanning the entire AL, as expected due to the panglomerular LNs (Y.-H. Chou et al., 2010). However, we noticed that the postsynaptic signal is not homogeneously distributed throughout the AL (Figures 2 and S2). Closer inspection revealed that the two classes of ORNs that detect pheromones (Or67d- and Or47b-expressing ORNs, targeting DA1 and VA1v, respectively) share the pattern of postsynaptic signal with sparser labeling of the medial aspect of the AL, an area that includes DM1 and VA2 (cognate glomeruli of Or42b and Or92a, respectively). By contrast, the two classes of ORNs known to detect food odors (Or42b and Or92a) share a different pattern of postsynaptic signal that is sparser in the lateral aspect of the AL, an area that includes DA1 and VA1v. The differences in postsynaptic patterns between the classes of glomeruli suggest that the segregation of food and pheromone channels observed in the targeting patterns of PNs in the LH (Jefferis et al., 2007) might be extended back to the AL, particularly to LNs. Such LNs that avoid certain glomeruli have been described (Y.-H. Chou et al., 2010). Interestingly, there is an inverse correlation between the odor-evoked firing rates of an LN and the number of glomeruli connected to it (Y.-H. Chou et al., 2010). It is conceivable that this inverse correlation is reflected in connectivity and extends to the numbers or sizes of synapses with ORNs. Therefore, it is possible that the connections between panglomerular LNs and ORNs are not strong enough to elicit robust *trans*-Tango signal. Notably, the synapses of panglomerular LNs were only revealed using a presynaptic marker (synaptotagmin-HA) and not by a post-synaptic marker (Y.-H. Chou et al., 2010). Therefore, it is conceivable that at least some of these LNs send output to all

glomeruli while not receiving input from all glomeruli. Such LNs would not be detected by *trans*-Tango.

We revealed a connection between some glomeruli in the antennal lobe, including DA1 and VA1v, and the SEZ (Figures 1B, 2A, S2A, and Movie S1). These glomeruli are involved in pheromone detection, and the neuron connecting the two brain areas is Fru+ (Figure 3B and data not shown). Our observations could implicate this neuron in connecting olfactory pheromone responses and gustation. Other functional connections between pheromone detection and gustatory behavior have been recently reported (Clowney et al., 2015). The new features that we have identified in the well-studied olfactory circuits illustrate the power of *trans*-Tango to provide a comprehensive map of projections from a given neuron while maintaining the capacity to integrate clonal analysis for sparse labeling.

The implementation of *trans*-Tango in the gustatory system enabled us to identify previously unknown second-order neurons and trace their projections. Our study identified different areas in the protocerebrum (SMP, SIP and SLP) as the targets of the second-order neurons in the gustatory circuits. The SMP is associated with neuroendocrine centers, such as the pars intercerebralis (PI), which regulate various behaviors including feeding (Nässel, Kubrak, Liu, Luo, & Lushchak, 2013). Several neuropeptides that control feeding behaviors are secreted from cells associated with the SMP (Nässel et al., 2013). For example, insulin-producing cells located in the PI have dendritic branches in the dorsal SMP (Kapan, Lushchak, Luo, & Nässel, 2012). Thus, the direct input from the SEZ to the SMP via the mSEZt (Figure 5, Movie S2) provides a possible pathway for integrating gustatory signals and the regulation of feeding behavior.

The SMP is also a target of the MB output neurons (MBONs) and it harbors the dendrites of dopaminergic neurons (DANs) that terminate in the MB (Aso, Hattori, et al., 2014). Similarly, the SIP and SLP contain processes of MBONs and DANs (Aso, Hattori, et al., 2014). In the MB, MBONs integrate dopamine input from DANs to mediate behavioral output. Several studies revealed that sugar-induced activity in a subset of DANs elicits appetitive memory (Burke et al., 2012; C. Liu et al., 2012). Remarkably, the projections through the three main gustatory tracts do not innervate the MB. This is in stark contrast to the olfactory circuits where second-order neurons massively project to the MB. Thus, gustatory information might be relayed into the MB at a higher level in the gustatory circuits. The direct input from the SEZ to the SMP, SIP and SLP could provide the anatomical framework for gustatory learning. However, it is possible that such second-order gustatory neurons with termini in the MB do exist, but for some reason *trans*-Tango fails to reveal them.

The design of *trans*-Tango is modular, so it is not limited to tracing experiments. Since the readout of *trans*-Tango is transcription of a reporter gene, the system can be readily configured for functional experiments in which the activity of second-order neurons is altered (e.g. by incorporating optogenetic proteins as the reporter) or monitored (e.g. by incorporating calcium sensors as the reporter). Further, the *trans*-Tango design could be implemented in other organisms via viral delivery of the necessary components or by introducing them through genome editing techniques. In essence, *trans*-Tango provides genetic access to cells on the basis of their connectivity. Thus, *trans*-Tango expands the utility of molecular genetic techniques beyond the confines of a given cell. Finally, though we have presented *trans*-Tango as a neural

circuit tracing technique, the same design could be used, with minor modifications, to study transient interactions between cells in other contexts, such as during development, in the immune system, or in cancer.

2.9 Methods

Fly strains

All fly lines used in this study were maintained at either 18°C or 21°C on standard cornmeal agar-molasses media. Unless otherwise stated, crosses and the resulting progeny that were analyzed for this study were maintained at 18°C in humidity-controlled chambers under 12-hr light/dark cycles. The fly lines used in this study are as follows: *Or42a-Gal4* (BDSC#9969), *Or42b-Gal4* (BDSC#9971), *Or47b-Gal4* (BDSC#9983), *Or92a-Gal4* (BDSC#23140) (Fishilevich & Vosshall, 2005); $Or67d^{Gal4}$ (Kurtovic et al., 2007); *Orco-Gal4* (Or83b-Gal4; BDSC#23292) (Kreher, Kwon, & Carlson, 2005); *Gr64f-Gal4* (BDSC#57669) (Dahanukar et al., 2007); *lGMR-Gal4* (BDSC#8121); *MB247-Gal4* (BDSC#50742) (Aso et al., 2009); FRT^{G13} (BDSC#1956) (Wilder & Perrimon, 1995); FRT^{G13}, *tubP-QS*(5A) (BDSC#30133) (Potter et al., 2010); *hsFLP* (BDSC#7), *hsFLP* (BDSC#1813) (T. B. Chou & Perrimon, 1992); *GH146-*$FLP^{3xP3\text{-}DsRED}$ (W. Hong et al., 2009); fru^{FLP} (Yu et al., 2010); *UAS-syt::GFP* (BDSC#6924) (Y. Q. Zhang, Rodesch, & Broadie, 2002); *UAS-syt::GFP, UAS-DenMark* (BDSC#33065) (Nicolaï et al., 2010); *QUAS-FRT-STOP-FRT-mCD8::GFP* (BDSC#30136), *hsFLP, UAS-mCD8::GFP, QUAS-mtdTomato(3xHA)* (BDSC#30118) (Potter et al., 2010); *UAS-mtdTomato* (BDSC#32221) (B. D. Pfeiffer et al., 2010); *UAS-*

myrGFP, QUAS-mtdTomato(3xHA); tubP-FRT-QS-FRT and *trans-Tango* (described below).

A list of the full genotypes for the flies used in each figure is as follows:

Figure #	Genotype
1B	UAS-myrGFP, QUAS-mtdTomato(3xHA)/+; *trans*-Tango/+; Orco-Gal4/+
1C	UAS-myrGFP, QUAS-mtdTomato(3xHA)/+; *trans*-Tango/+;
2A	UAS-myrGFP, QUAS-mtdTomato(3xHA); *trans*-Tango/+; Or67d-Gal4/+
2B	UAS-myrGFP, QUAS-mtdTomato(3xHA); *trans*-Tango/Or42b-Gal4;
3A	hsFLP, UAS-myrGFP, QUAS-mtdTomato(3xHA)/+; *trans*-Tango, FRT^{G13}, tubP-QS(5A)/FRT^{G13}; Or67d-Gal4/+
3B	; *trans*-Tango/+; QUAS-FRT-STOP-FRT-mCD8::GFP, UAS-mtdTomato/Or67d-Gal4, fru-FLP
3C	; *trans*-Tango, GH146-FLP/+; QUAS-FRT-STOP-FRT-mCD8::GFP, UAS-mtdTomato/Or67d-Gal4
4A	UAS-myrGFP, QUAS-mtdTomato(3xHA); *trans*-Tango, GH146-FLP, tubP-FRT-QS-FRT/Or42a-Gal4;
4B	hsFLP, UAS-mCD8::GFP, QUAS-mtdTomato(3xHA); *trans*-Tango (earlier version)/+; lGMR-Gal4/+
5A	UAS-myrGFP, QUAS-mtdTomato(3xHA)/+; *trans*-Tango/Gr64f-Gal4;
5B	UAS-myrGFP, QUAS-mtdTomato(3xHA)/+; *trans*-Tango/Gr64f-Gal4;
5C	UAS-myrGFP, QUAS-mtdTomato(3xHA), hsFLP/+; *trans*-Tango, FRT^{G13}, tubP-QS(5A)/Gr64f-Gal4, FRT^{G13}; UAS-myrGFP, QUAS-mtdTomato(3xHA), hsFLP; *trans*-Tango, FRT^{G13}, tubP-QS(5A)/Gr64f-Gal4, FRT^{G13}; UAS-myrGFP, QUAS-mtdTomato(3xHA); *trans*-Tango, tubP-FRT-QS-FRT/Gr64f-Gal4, hsFLP;
S1B	; *trans*-Tango/+; UAS-syt::GFP, UAS-DenMark/MB247-Gal4
S1C	UAS-syt::GFP; *trans*-Tango/+; Or67d-Gal4/+
S2A	UAS-myrGFP, QUAS-mtdTomato(3xHA)/+; *trans*-Tango/Or47b-Gal4;
S2B	UAS-myrGFP, QUAS-mtdTomato(3xHA)/+; *trans*-Tango/Or92a-Gal4;
S3	UAS-myrGFP, QUAS-mtdTomato(3xHA)/+; *trans*-Tango/+; Or67d-Gal4/+ UAS-myrGFP, QUAS-mtdTomato(3xHA)/+; *trans*-Tango/+;
S4A	UAS-myrGFP, QUAS-mtdTomato(3xHA)/+; *trans*-Tango/Or42b-Gal4;
S4B	UAS-myrGFP, QUAS-mtdTomato(3xHA)/+; *trans*-Tango/+; Or67d-Gal4/+
S4C	UAS-myrGFP, QUAS-mtdTomato(3xHA)/+; *trans*-Tango/Or92a-Gal4;
S5A, B	UAS-myrGFP, QUAS-mtdTomato(3xHA)/+; *trans*-Tango/+; Or67d-Gal4/+
S5C, D	UAS-myrGFP, QUAS-mtdTomato(3xHA)/+; *trans*-Tango/Or42b-Gal4;

Generation of transgenic fly lines

Plasmids used in this study to generate transgenic fly lines (described in Figure S1A in detail) were constructed using standard cloning techniques including restriction digest and ligation, PCR assembly and Gibson Assembly, and were sequenced before injection. The plasmid used for the generation of *trans*-Tango transgenic flies was constructed by standard molecular cloning techniques. A scaffold of unique restriction sites was ligated into pBluescript KS+ (pBS KS+; Agilent). The following DNA sequences were PCR amplified to add appropriate restriction sites and ligated into the pJET1.2 vector (Thermo Fisher Scientific): the Elav promoter, obtained from *Drosophila* genomic DNA; the Arrestin::TEV protease fusion (hArr::TEV) (Barnea et al., 2008); the SV40 polyadenylation sequence (SV40pA), which was obtained from pUASTattB vector (Bischof, Maeda, Hediger, Karch, & Basler, 2007); the nSyb promoter; the *Drosophila* Synthetic Core Promoter (DSCP) (B. D. Pfeiffer et al., 2008); human glucagon receptor; the serine TEV cleavage site (TEVcs); QF, obtained from pattB-QF-hsp70 (Addgene, 24368) (Potter et al., 2010), and the hsp70 polyadenylation sequence (hsp70pA), obtained from pattBQF-hsp70. These sequences were digested from pJET1.2 and ligated into the pBS KS+ scaffold in a hierarchical manner, resulting in two cassettes from 50 to 30: Elav-hArr::TEV-SV40pA, nSyb-DSCP-hGCGR::TEVcs::QF hsp70pA (panneuronal cassettes). A second scaffold of unique restriction sites was generated and ligated into pUASTattB between the white gene and the attB sequence. The panneuronal cassettes were digested and ligated in an inverted manner (30 to 50) into the modified pUASTattB scaffold. To assemble the *trans*-Tango ligand, the following DNA sequences were amplified with overlapping 50 and 30 sequences: 10xUAS-IVS-Syn21, obtained from

pJFRC81 (Addgene, 36432) (B. D. Pfeiffer, Truman, & Rubin, 2012); trypsin signal peptide, followed by human glucagon peptide, six Glycine-Asparagine (GN) repeats, myc-tag, and nine GN repeats (Fortin et al., 2009); the extracellular domain of human ICAM1, from the last isoleucine residue of the transmembrane domain to the N terminus of the extracellular domain, obtained from cDNA (VersaClone); *Drosophila* Neurexin1, from the C-terminal cytosolic tail through the transmembrane domain (not including the last isoleucine residue), obtained from *Drosophila* genomic DNA, and the p10 polyadenylation sequence, obtained from pJFRC81. These sequences were covalently fused to each other by Gibson Assembly (New England Biolabs) (Gibson et al., 2009). They were subsequently amplified in two pieces to introduce super-agonist mutations to the glucagon peptide (Krstenansky et al., 1986), and were finally assembled by Gibson Assembly, from 50 to 30, into the pUASTattB scaffold containing the panneuronal cassettes in the opposite orientation.

The plasmid used for the generation of reporter flies, *UAS-myrGFP* and *QUAS-mtdTomato(3xHA)*, was constructed by Gibson Assembly. The 5xQUAS-mtdTomato(3xHA) sequence, obtained from pQUAST-mtdT-3xHA (Addgene, 24354) (Potter et al., 2010), and the hsp70pA sequence were amplified by PCR with appropriate overlaps. These sequences were assembled into the pJFRC12 plasmid (Addgene, 26222) (B. D. Pfeiffer et al., 2010) following the existing GFP cassette and in the reverse orientation.

The plasmid used to generate *tubP-FRT-QS-FRT* conditional suppressor transgenic flies was constructed by Gibson Assembly. The tubulin promoter and the first FRT site, as well as the WPRE, the SV40pA and the second FRT site were amplified

from tubPFRT>GAL80-6-FRT> (Addgene, 63173) (Nern, Pfeiffer, & Rubin, 2015), and the QS sequence was amplified from ptubP-QS (Addgene, 24352) (Potter et al., 2010). All PCR amplifications were performed with the appropriate overlaps and the pieces were assembled into the pUASTattB vector.

Lines of transgenic flies were generated by site-directed genomic integration of constructs using the PhiC31 system (Groth, Fish, Nusse, & Calos, 2004; Markstein, Pitsouli, Villalta, Celniker, & Perrimon, 2008). The *trans*-Tango construct containing ligand, synthetic receptor and hArr::TEV genes was incorporated at the attP40 site. The construct containing the reporter genes, UAS-myrGFP and QUAS-mtdTomato(3xHA), was incorporated at the su(Hw)attP8 site. The conditional suppressor construct, tubP-FRT-QS-FRT, was incorporated at the VK00018 site.

Mosaic analysis

MARCM experiments for postsynaptic signal in the olfactory and gustatory systems were performed as described previously (T. Lee & Luo, 1999; Potter & Luo, 2011). Briefly, flies of genotype *UAS-myrGFP, QUAS-mtdTomato(3xHA), hsFLP (X); trans-Tango, FRTG13, tubP-QS(5A)/FRTG13 (II); Or67d-Gal4/+ (III)*, and *UAS-myrGFP, QUAS-mtdTomato(3xHA), hsFLP (X); trans-Tango, FRTG13, tubP-QS(5A)/FRTG13, Gr64f-Gal4 (II)* were raised at 18°C and transiently heat-shocked in a 37°C water bath for 2 min to 1 hr during early third instar larval stage.

Intersectional analysis of postsynaptic signal of Or67d+ neurons was performed using flies of the following genotypes: *w (X); trans-Tango, GH146-FLP/+ (II); Or67d-Gal4/QUAS-FRT-STOP-FRT-mCD8::GFP, UAS-mtdTomato (III)*, and *w (X); trans-*

Tango/+ (II); Or67d-Gal4, fru-FLP/QUAS-FRT-STOP-FRT-mCD8::GFP, UAS-mtdTomato (III).

Intersectional FLP-out analysis of postsynaptic signal of Or42a+ neurons was performed using larvae of the following genotypes: *UAS-myrGFP, QUAS-mtdTomato(3xHA) (X); trans-Tango, GH146-FLP, tubP-FRT-QS FRT/Or42a-Gal4 (II)*.

Clonal FLP-out analysis of postsynaptic signal of Gr64f+ neurons was performed using flies of the following genotypes: *UAS-myrGFP, QUAS-mtdTomato(3xHA) (X); trans-Tango, tubP-FRT-QS-FRT/Gr64f-Gal4, hsFLP (II)*. Flies were raised at 18°C and transiently heat-shocked in a 37°C water bath for 5 to 15 min during late pupal stages to generate random clones that lack QS expression.

Immunohistochemistry and data processing

Immunohistochemistry experiments were performed as described previously (J. S. Wu & Luo, 2006) with minor modifications. Briefly, either adult flies that are 15-20 days old (unless otherwise noted) or third instar wandering larvae were cold anaesthetized on ice and dissected in PBS or 0.03%PBST (T stands for Triton X-100; Fisher Bioreagents, BP151-500). After a 30 min fixation of samples in 4% PFA/0.3%PBST at room temperature (RT) or an overnight fixation in 2%PFA/0.3%PBST at 4°C, samples were washed four times for 15 min in 0.3%PBST at RT, blocked in 5% heat-inactivated donkey or equine serum (diluted from 100% with 0.3% PBST) for 30 min at RT, and incubated with primary antibodies for two overnights at 4°C. Samples were washed again four times for 15 min at RT and incubated with secondary antibodies for two overnights at 4°C. The samples were then washed again four times for 15 min at RT and mounted on

a slide (Fisherbrand Superfrost Plus, 12-550-15) using Fluoromount-G mounting medium (SouthernBiotech, 0100-01). Samples used for generating supplemental videos and cell-counting data were cleared as described previously (Nern et al., 2015). The primary and secondary antibodies were diluted in blocking solution. The primary antibodies used in this study were anti-GFP rabbit (Thermo Fisher Scientific, A11122; 1:1,000), anti-HA mouse (Covance, MMS-101P; 1:250), anti-HA rat (Roche,11867423001; 1:100), anti-myc mouse (Covance, MMS-150P; 1:250), anti-Brp mouse (nc82; DSHB; 1:50) and anti-Ncad rat (DSHB; 1:20). Secondary antibodies were diluted at 1:1,000 and were as follows: donkey anti-rabbit Alexa Fluor 488, donkey anti-mouse Alexa Fluor 555, goat anti-rat Alexa Fluor 555, donkey anti-mouse Alexa Fluor 647 and goat anti-rat Alexa Fluor 647. Images were taken using confocal microscopy (Zeiss, LSM800) with ZEN software (Zeiss, version 2.1) with auto Z brightness correction to generate a homogeneous signal where it seemed necessary, and were formatted using Fiji software (http://fiji.sc) or Adobe Photoshop CC. Supplemental videos were generated using Imaris software (Bitplane AG, version 8.4.1) with tiled confocal images taken with low laser settings. Figures were generated using Adobe Illustrator CC.

Quantification of postsynaptic neurons

Confocal images taken with laser and microscope settings held constant within groups were used to quantify the postsynaptic neurons revealed by *trans*-Tango. Cell bodies were counted manually using cell counter plugin in Fiji in a non-stringent manner: cells were counted even if the signal in them was weak in order to reveal any potential

connection. Number of samples used for cell-counting data is reported in the results and discussion sections.

Pixel intensity measurement

HA and myc immunofluorescence were imaged in separate channels using confocal microscopy, and all laser and microscope settings were held constant for all brains. Pixel intensities were calculated using Fiji. For a given z stack of a brain, the selection brush feature was used to draw a circular ROI of fixed diameter over either the entire left antennal lobe (to quantify HA staining) or the entire left DA1 glomerulus (to quantify myc staining). For each frame of the stack, average pixel intensity within the ROI was calculated. For myc, this average pixel intensity in each frame was normalized by subtracting out the average pixel intensity of an unstained region within the antennal lobe. The maximum value of this average pixel intensity across all frames of the stack was determined and reported. Number of samples used to determine the average pixel intensity is reported in the figure legend.

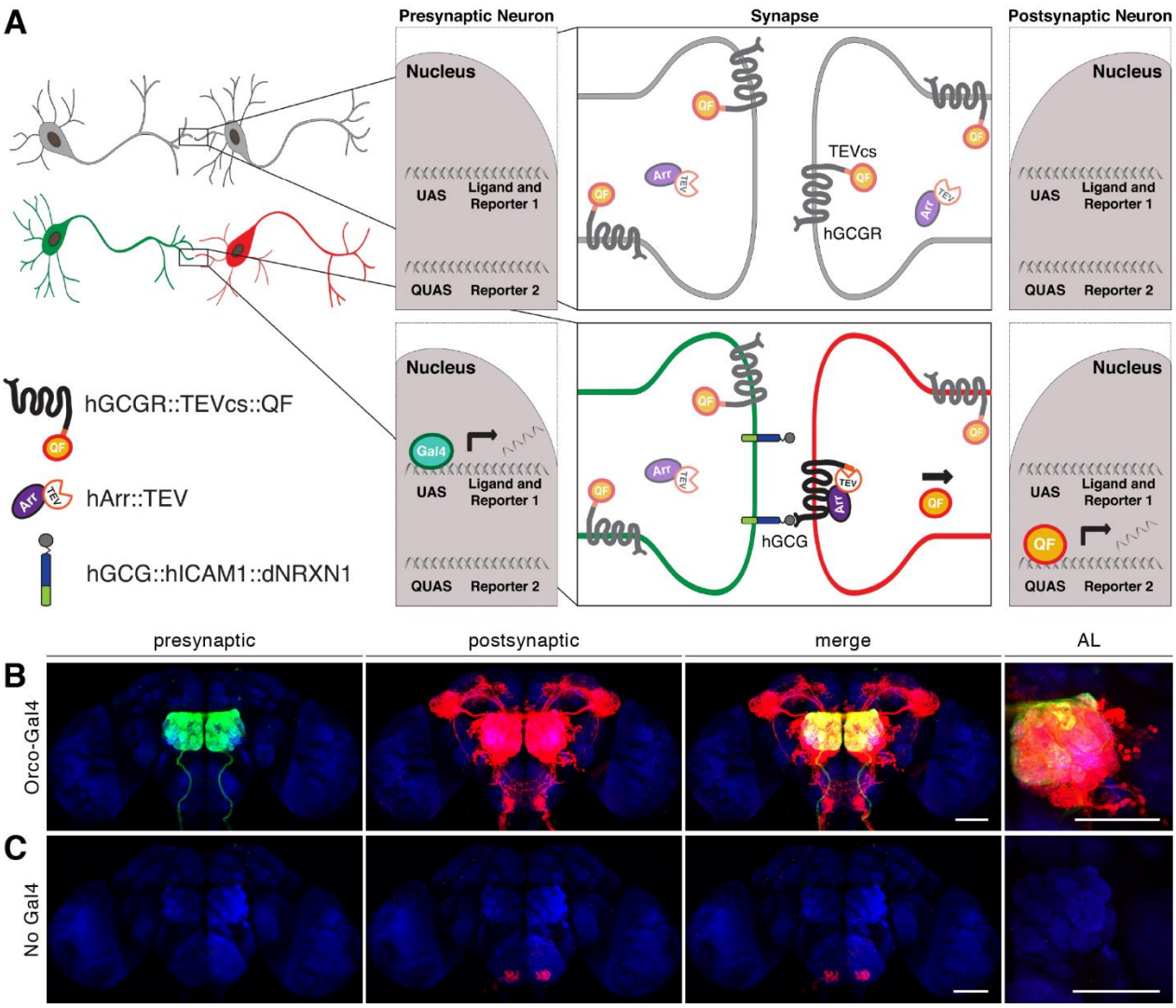

Figure 2-1. Design and implementation of *trans*-Tango in the fly olfactory system.

(A) Schematic design of *trans*-Tango. The general design of *trans*-Tango is based on the Tango assay in a configuration for human glucagon. In *trans*-Tango, the components of the Tango signaling pathway (hGCGR::TEVcs::QF and hArr::TEV) are expressed in all neurons, rendering them competent for QF-dependent expression of Reporter 2 (red). The signaling pathway is transsynaptically activated by a membrane-tethered form of glucagon that is fused to the transmembrane and cytoplasmic domains of the *Drosophila* synaptic protein Neurexin1 via a spacer consisting of the extracellular domain of the human cell

adhesion molecule ICAM1 and a flexible linker (hGCG::hICAM1::dNRXN1). Expression of the ligand fusion and Reporter 1 (green - to mark the presynaptic neuron) are Gal4 dependent. In the absence of ligand, the transcription factor QF stays tethered to the receptor; hence, there is no expression of Reporter 2 (top). Ligand expression in the presynaptic neuron activates the signaling pathway in the postsynaptic neuron, releasing QF to translocate into the nucleus and initiate Reporter 2 expression from QUAS (bottom). (B) In flies bearing the *trans*-Tango components, driving ligand and myrGFP expression in the majority of ORNs targeting the AL by Orco-Gal4 (green) results in mtdTomato expression in postsynaptic LNs and PNs (red). (C) No signal is observed in flies bearing the *trans*-Tango components without a Gal4 driver, except for some background noise in the ventral SEZ. (B and C) The right panels are zoom-in on the AL. Max-projection pictures of whole-mount brains are shown. Blue, neuropil counterstain. Scale bars, 50 μm.

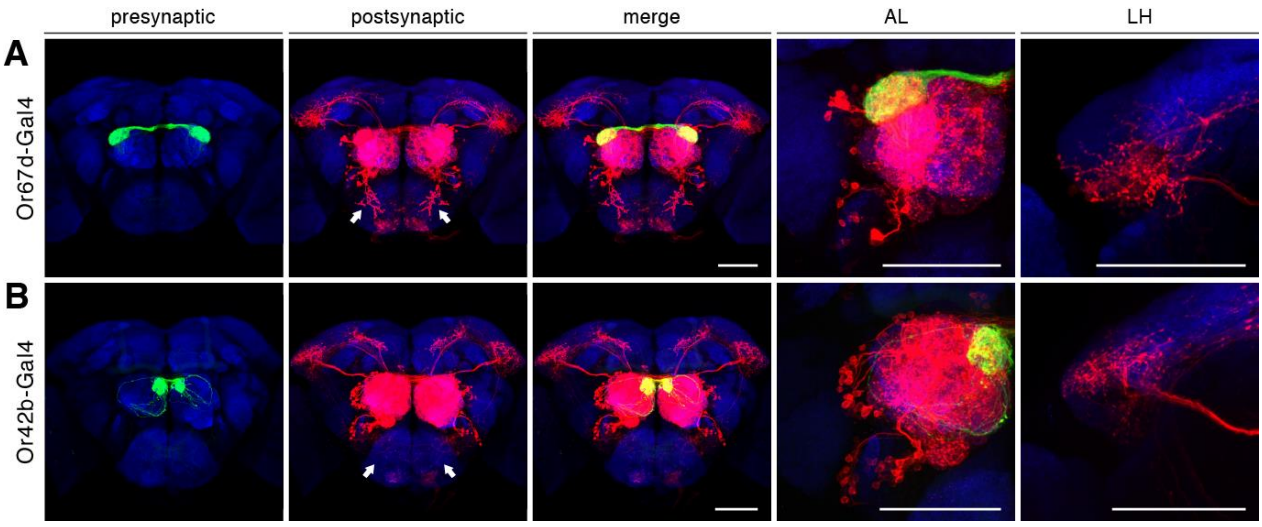

Figure 2-2. Specificity of *trans*-Tango.

Expression of the *trans*-Tango ligand in Or67d+ (A) and in Or42b+ (B) ORNs (green) reveals distinct projection patterns (red). (A and B) Note the postsynaptic signal of Or67d+ ORNs that descends to the SEZ (arrows) and is absent when the ligand is expressed in Or42b+ ORNs. The right panels are zoom-in on the AL and LH. Max-projection pictures of whole-mount brains are shown. Blue, neuropil counterstain. Scale bars, 50 μm.

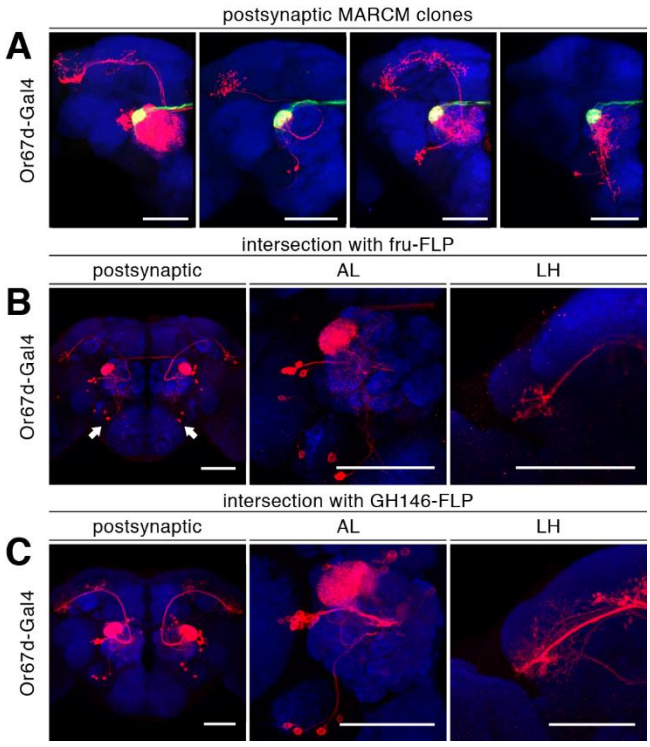

Figure 2-3. Sparse labeling of postsynaptic neurons with *trans*-Tango.

(A) Sparse labeling of postsynaptic neurons through combining *trans*-Tango with MARCM. Clones of different postsynaptic neurons (red) receiving input from the DA1 glomerulus (green) are shown for four different individuals. (B and C) Sparse labeling of genetically-defined postsynaptic neurons via FLP recombination. Combining *trans*-Tango with FLP recombination enables intersectional labeling of FLP+ postsynaptic neurons. Postsynaptic signal is expressed by removing the stop cassette in the conditional reporter (red) using fru-FLP (B), and GH146-FLP (C). Arrows in (B) point to the neurons descending to the SEZ. The right panels are zoom-in on the AL and LH. (A-C) Max-projection pictures of whole-mount brains are shown. Blue, neuropil counterstain. Scale bars, 50 μm.

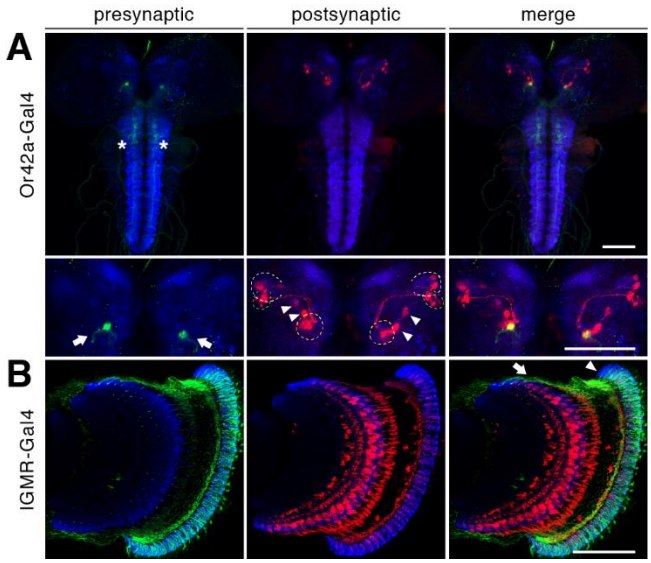

Figure 2-4. Sensitivity of *trans*-Tango.

(A) Expression of the *trans*-Tango ligand in Or42a+ ORNs in the larva (a single ORN per side, green, arrows) leads to labeling of PNs (red, arrowheads). *trans*-Tango is combined with intersectional genetics to restrict the postsynaptic signal to GH146-FLP+ PNs, as the leakiness of the UAS promoter in the larval ventral nerve cord (green, asterisks) results in background noise (data not shown). In the lower zoom-in panels of the larval central brain, the AL, MB calyx and LH are indicated by dashed lines in yellow, white and green, respectively. Max-projection pictures of whole-mount brains are shown. (B) Implementation of *trans*-Tango in the visual system. Expression of the ligand in lGMR+ photoreceptor cells (green) induces postsynaptic signal (red) in the lamina (arrowhead) and medulla (arrow). A single optical section through the adult optic lobe is shown. (A and B) Blue, neuropil counterstain. Scale bars, 50 μm.

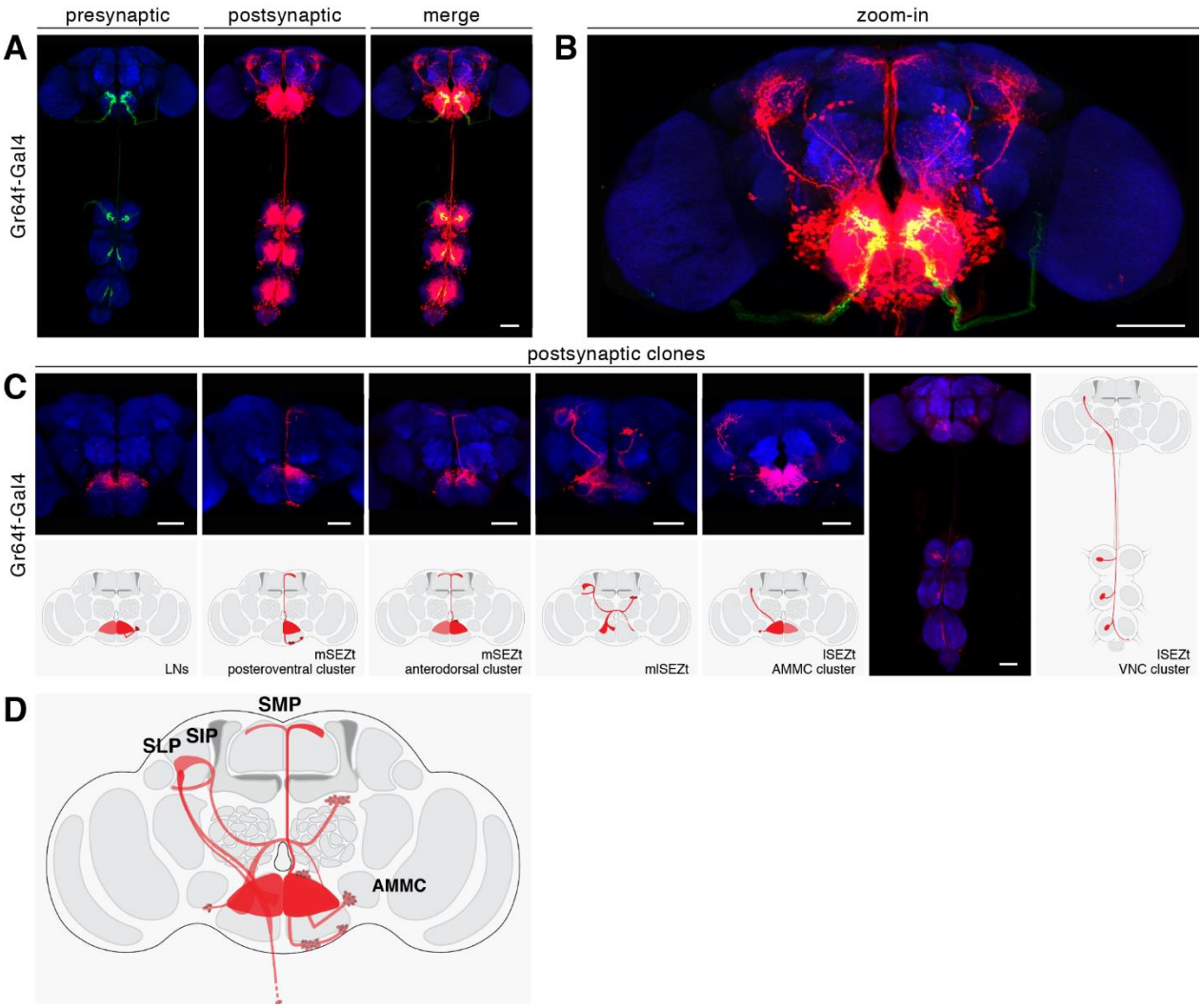

Figure 2-5. Second-order neurons of the gustatory system revealed by *trans*-Tango.

(A) Expression of the *trans*-Tango ligand in Gr64f+ sweet sensory neurons (green) reveals second-order neurons of the gustatory system (red) targeting the VNC and the central brain. (B) Zoomed-in picture of the central brain. (C) Sparse labeling of second-order neurons of Gr64f+ GRNs by clonal analysis restricts the postsynaptic signal (red) to distinct neuronal clusters. Representative clones from distinct pathways are shown in each panel and these pathways are illustrated unilaterally for simplicity. (D) Schematic

summary of a unilateral representation of the various projections shown in (B and C). See text for details. (A, B and C) Max-projection pictures of whole-mount brains are shown. Blue, neuropil counterstain. Scale bars, 50 μm.

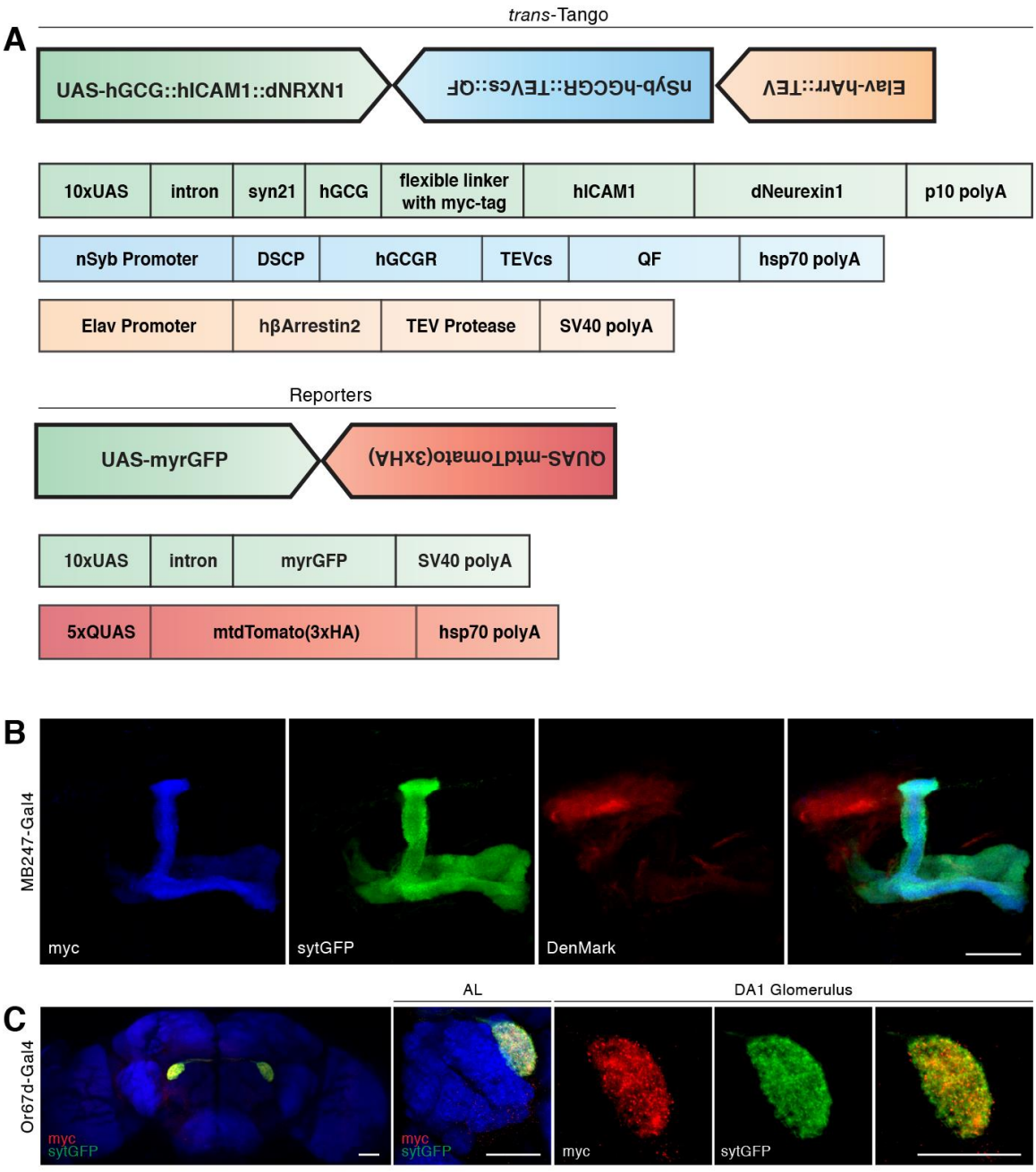

Figure 2-S1. Components of *trans*-Tango.

(A) Genetic components in detail. Inverted blocks indicate genes placed in a 3' to 5' orientation to minimize genetic crosstalk. hGCG: human Glucagon analogue with enhanced receptor binding (Krstenansky et al., 1986); hICAM1: extracellular domain of human ICAM1; dNRX1: trans-membrane and intracellular domains of *Drosophila*

Neurexin1; hArr: human β-Arrestin2 (Barnea et al., 2008); TEV: N1a protease from the Tobacco Etch Virus (Barnea et al., 2008); TEVcs: cleavage site for TEV (Barnea et al., 2008); hGCGR: human Glucagon Receptor; QF: transcription factor (Potter et al., 2010); Elav and nSyb: panneuronal promoters; syn21: a synthetic 21bp sequence (Pfeiffer et al., 2012b); polyA: polyadenylation signal; DSCP: *Drosophila* Synthetic Core Promoter (Pfeiffer et al., 2008); UAS: Upstream Activating Sequence; QUAS: Upstream Activating Sequence for QF (Potter et al., 2010). Schematics are not drawn to scale. (B) Enrichment of the ligand in axons. Immunostaining against the myc tag (blue) embedded in the flexible linker of the ligand reveals enrichment of the ligand at presynaptic sites in MB247+ neurons marked by synaptotagmin-GFP (sytGFP, green), compared to their dendrites (DenMark, red). (C) Presence of the ligand on axon terminals. Immunostaining against the myc tag (red) reveals the presynaptic localization of ligand expressed in Or67d+ ORNs. Presynaptic sites in these neurons are marked by sytGFP (green). The whole brain is shown on the left, zoom-in panels on the AL and the DA1 glomerulus are shown in the middle and on the right, respectively. (A and B) Max-projection pictures of whole-mount brains are shown. Blue, neuropil counterstain. Scale bars, 25 μm.

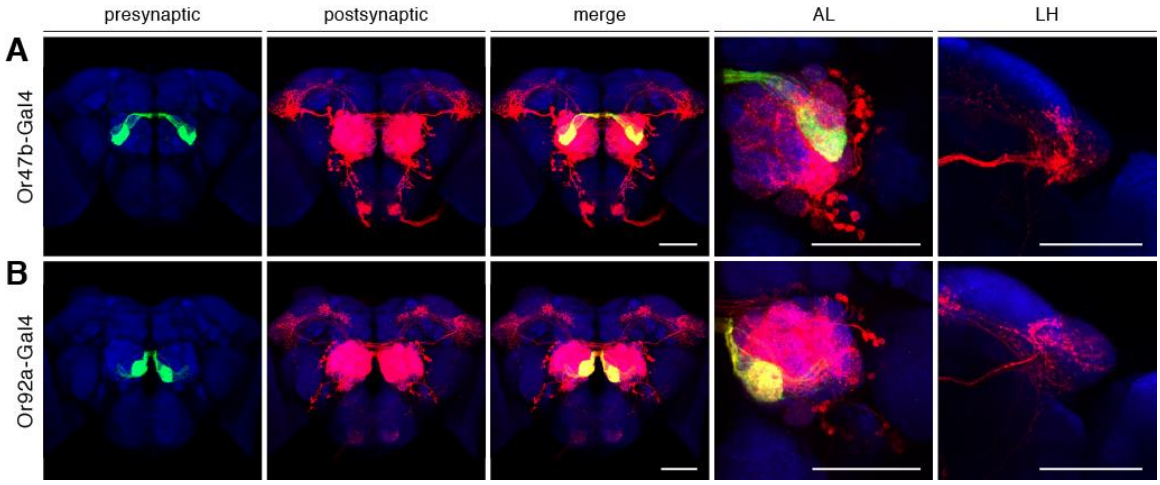

Figure 2-S2. Second-order neurons of additional ORNs.

Ligand expressed in Or47b+ (A), and Or92a+ (B) ORNs (green) induced specific *trans*-Tango signal in the postsynaptic neurons (red). The right panels are zoom-in on the AL and LH. Max-projection pictures of whole-mount brains are shown. Blue, neuropil counterstain. Scale bars, 50 μm.

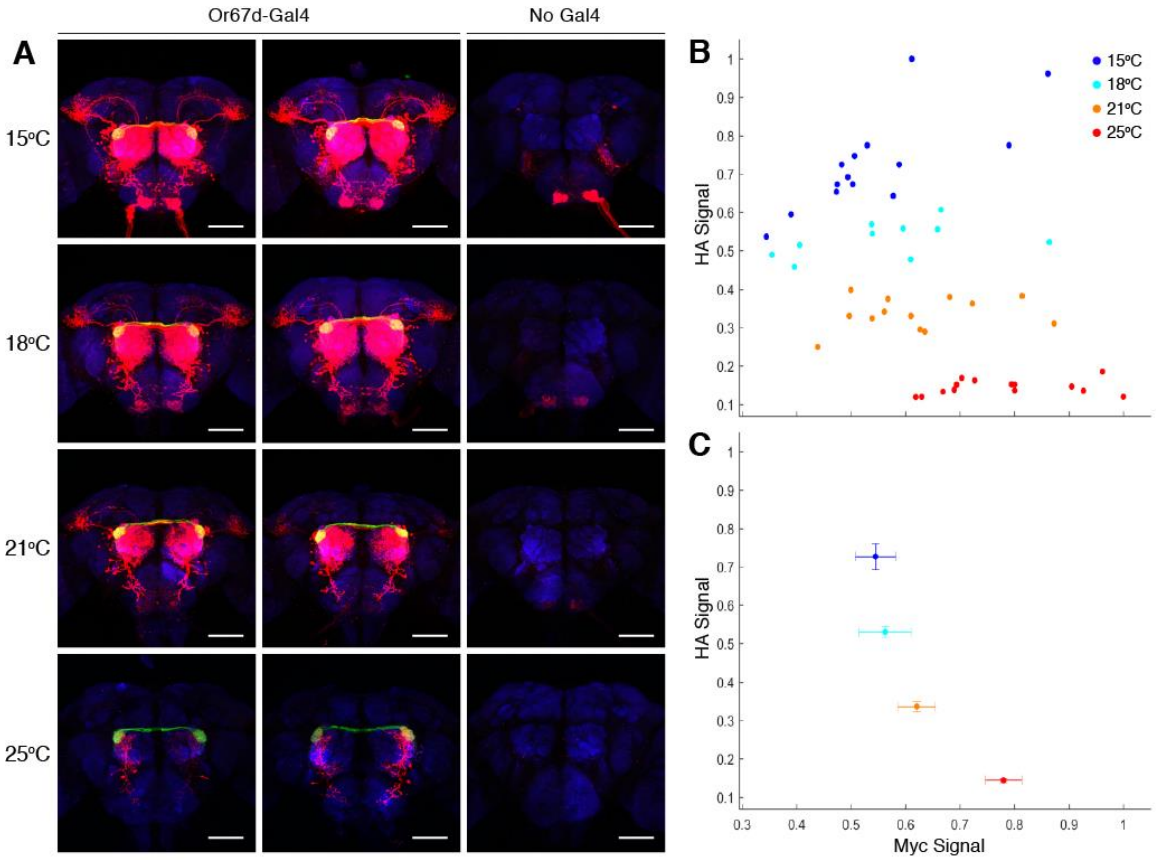

Figure 2-S3. Temperature-dependence of the *trans*-Tango signal.

Max-projections of brains of age-matched flies expressing the *trans*-Tango ligand in Or67d+ ORNs (green) reveal that the postsynaptic signal (red) is stronger in flies raised at lower temperatures. Two representative experimental brains and a control brain for each temperature are shown. Blue, neuropil counterstain. Scale bars, 50 □m. (B) Pixel intensity of HA and myc immunofluorescence (postsynaptic reporter and ligand tag, respectively) in brains of flies raised at different temperatures. Each point represents the maximum value of average pixel intensity in an ROI across all z-stack frames in a single brain. The ROI for HA was the left antennal lobe, and the ROI for myc was the left DA1 glomerulus. n=10-14 per group, colors represent different temperatures. Pixel intensity units are normalized

to the highest value across all brains. For further details on quantification procedure, see methods section. (C) Group means of individual data presented in (B). Error bars represent standard error of the mean.

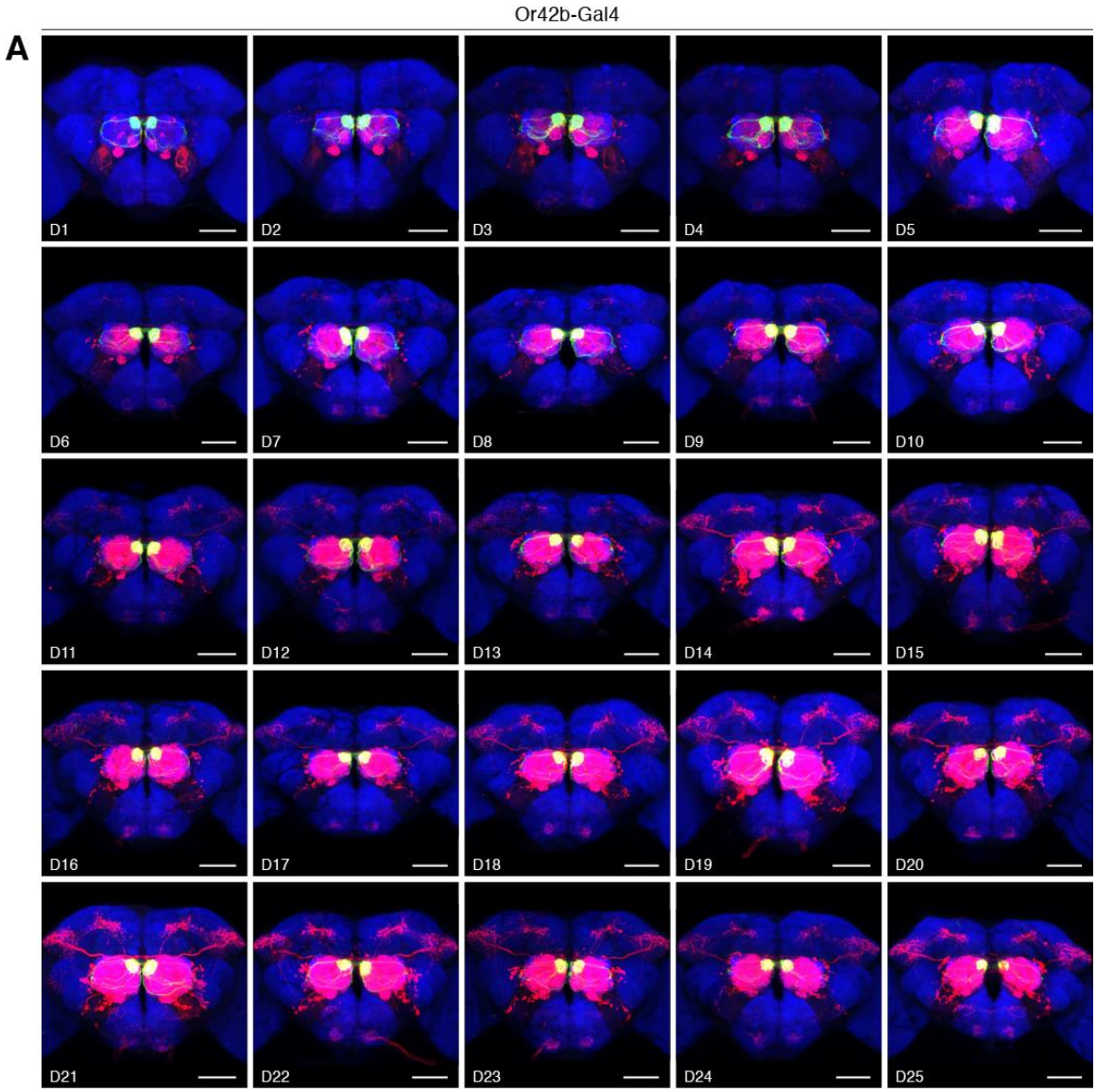
A
Or42b-Gal4
D1
D2
D3
D4
D5
D6
D7
D8
D9
D10
D11
D12
D13
D14
D15
D16
D17
D18
D19
D20
D21
D22
D23
D24
D25

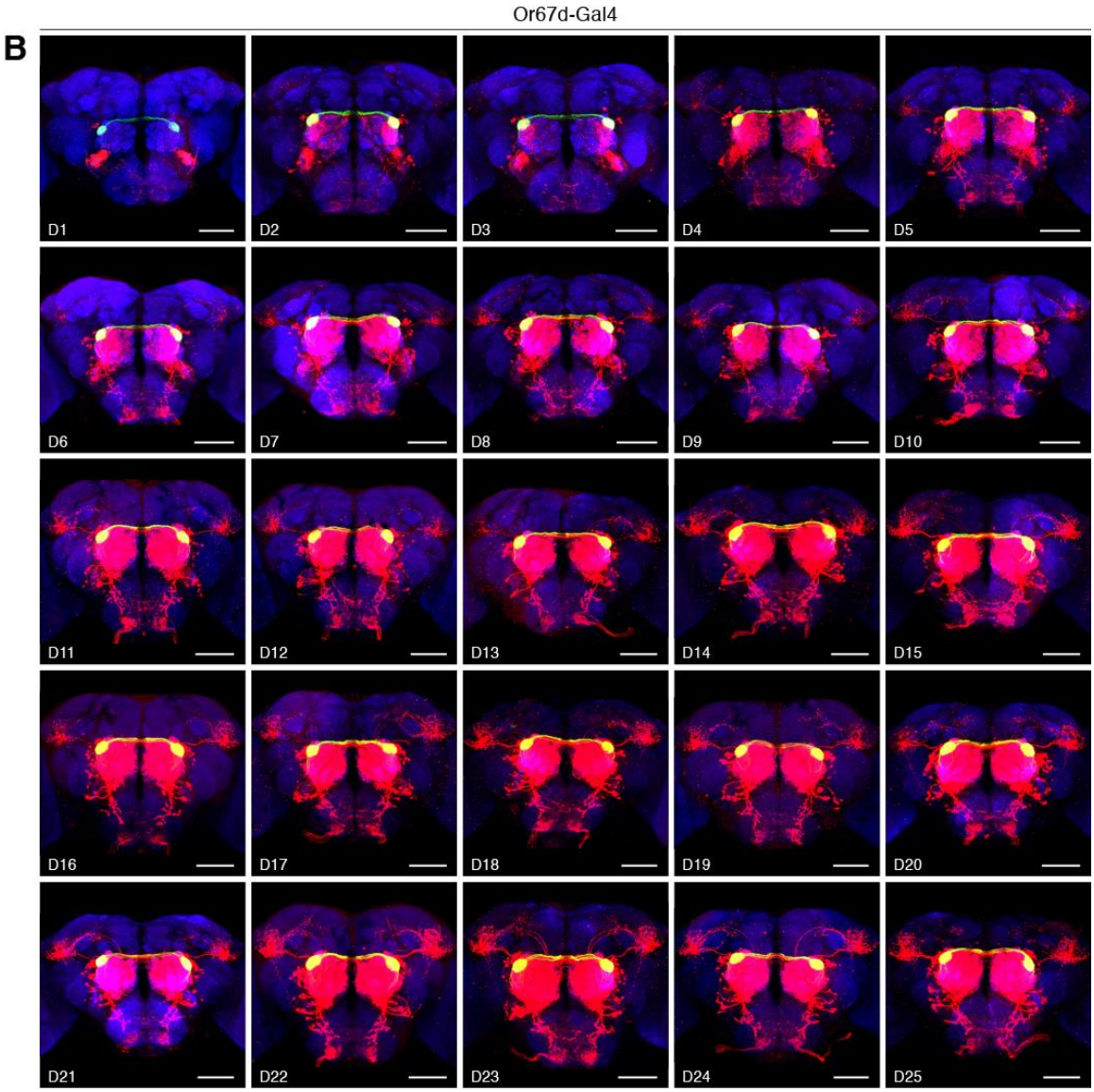
B
Or67d-Gal4
D1
D2
D3
D4
D5
D6
D7
D8
D9
D10
D11
D12
D13
D14
D15
D16
D17
D18
D19
D20
D21
D22
D23
D24
D25

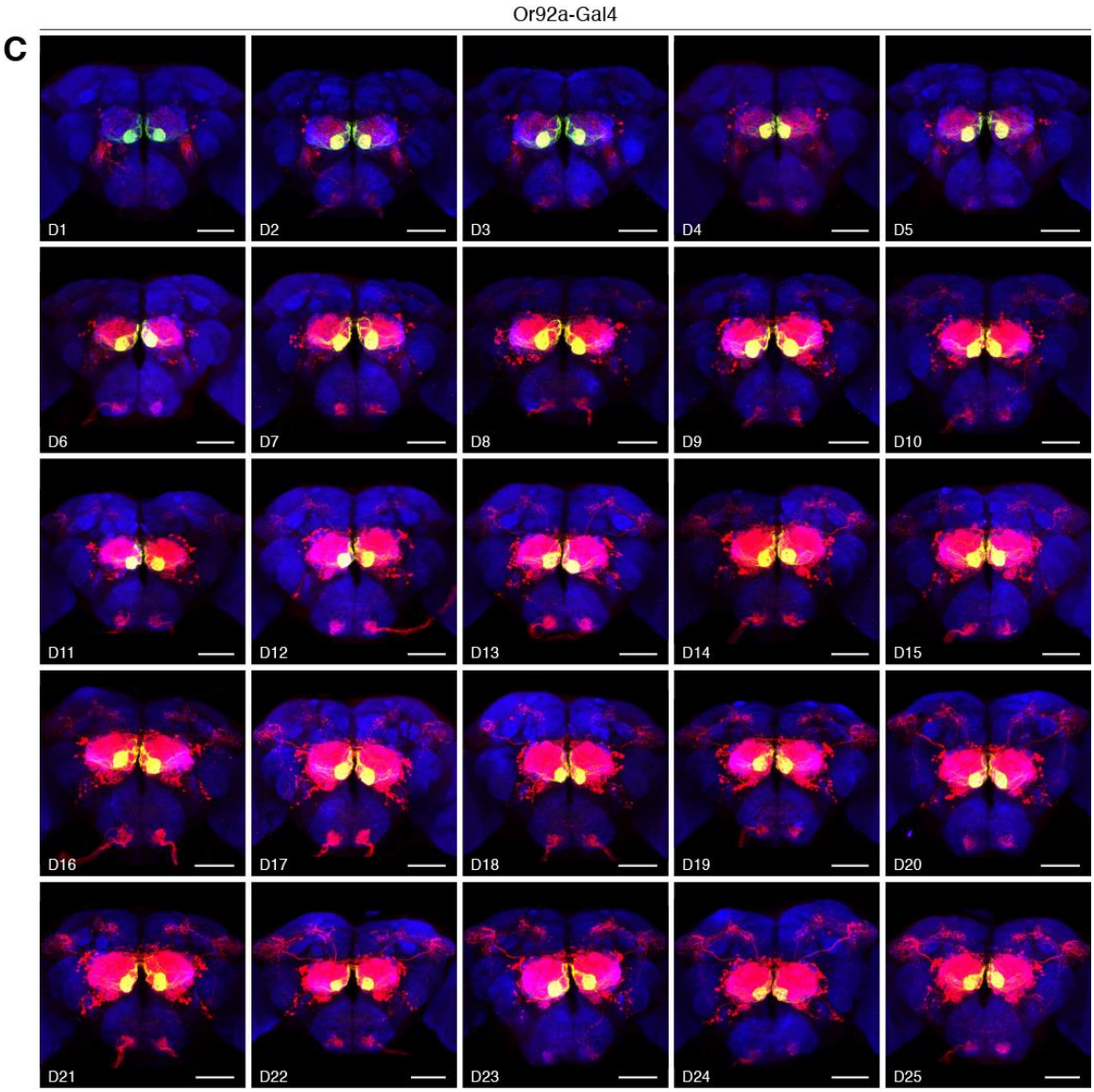

Figure 2-S4. Age-dependence of the *trans*-Tango signal.

trans-Tango signal (red) elicited by ligand expression in Or42b+ (A), Or67d+ (B), and Or92a+ (C) ORNs (green) was monitored at single-day resolution over 25 days (D1 to D25) post-eclosion. *trans*-Tango output labeling increases gradually with the age of the individual, starting to saturate at approximately two weeks post-eclosion in flies raised at

18°C. Max-projection pictures of whole-mount brains are shown. Blue, neuropil counterstain. Scale bars, 50 μm.

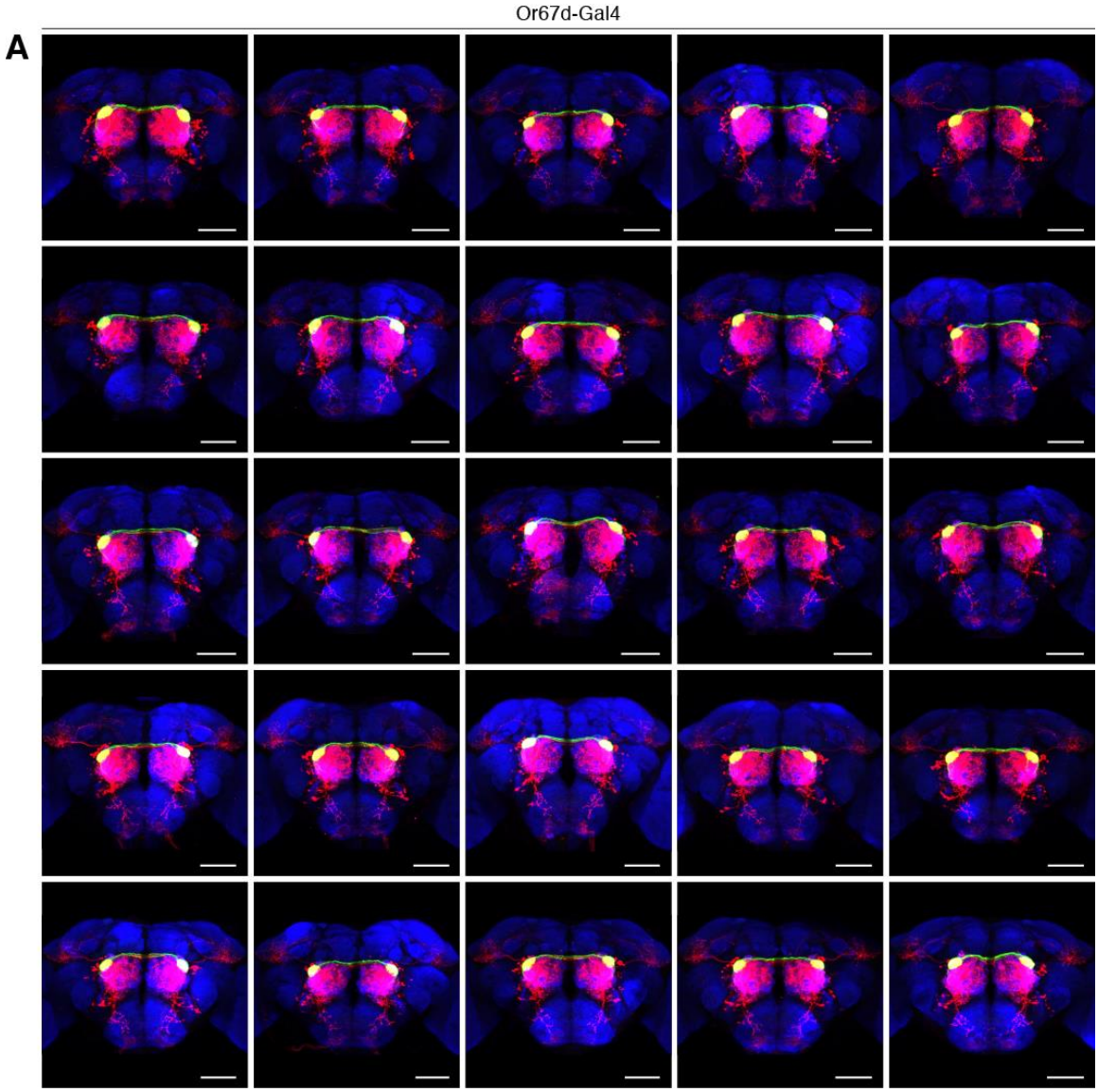
A
Or67d-Gal4

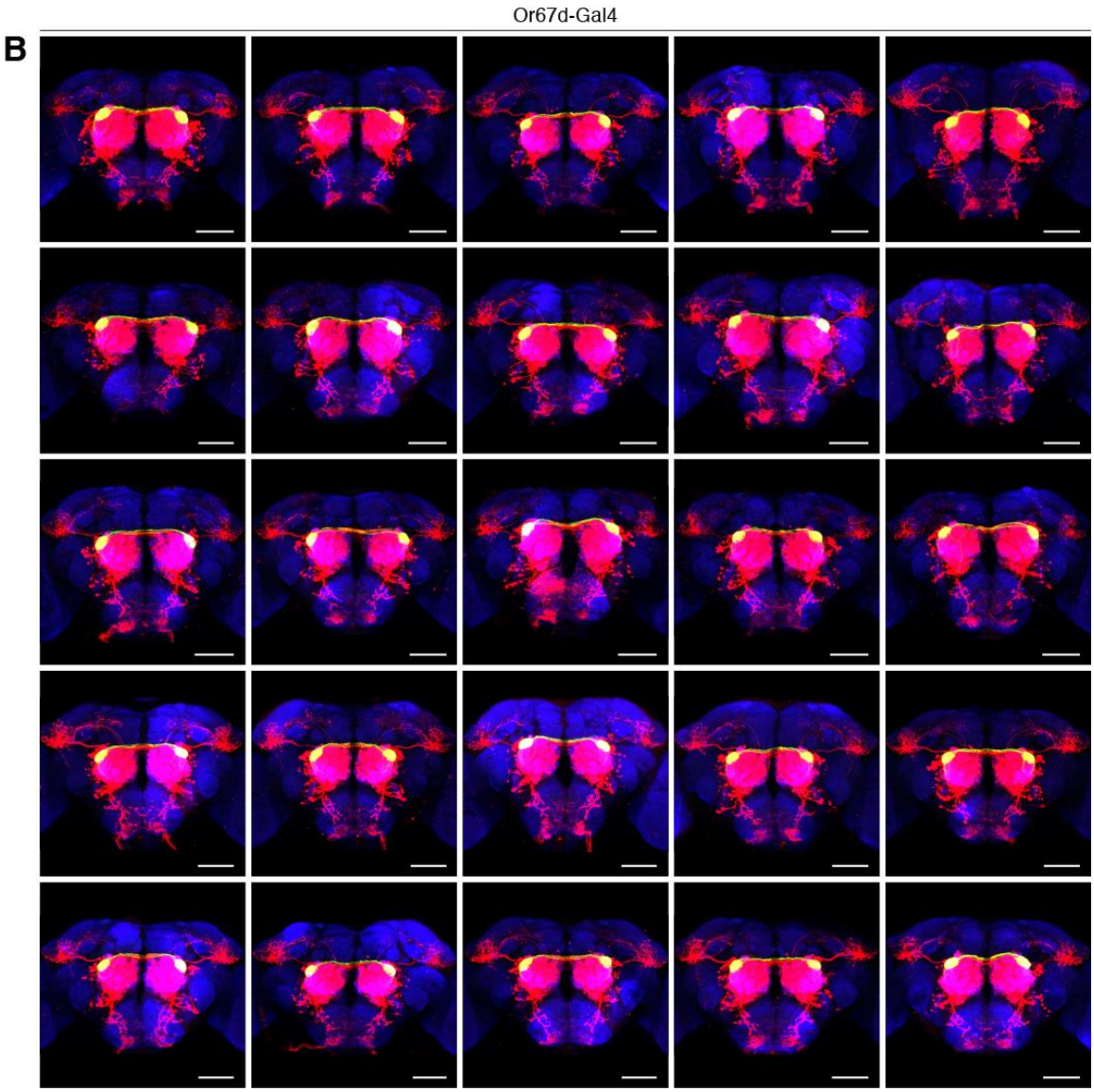
B
Or67d-Gal4

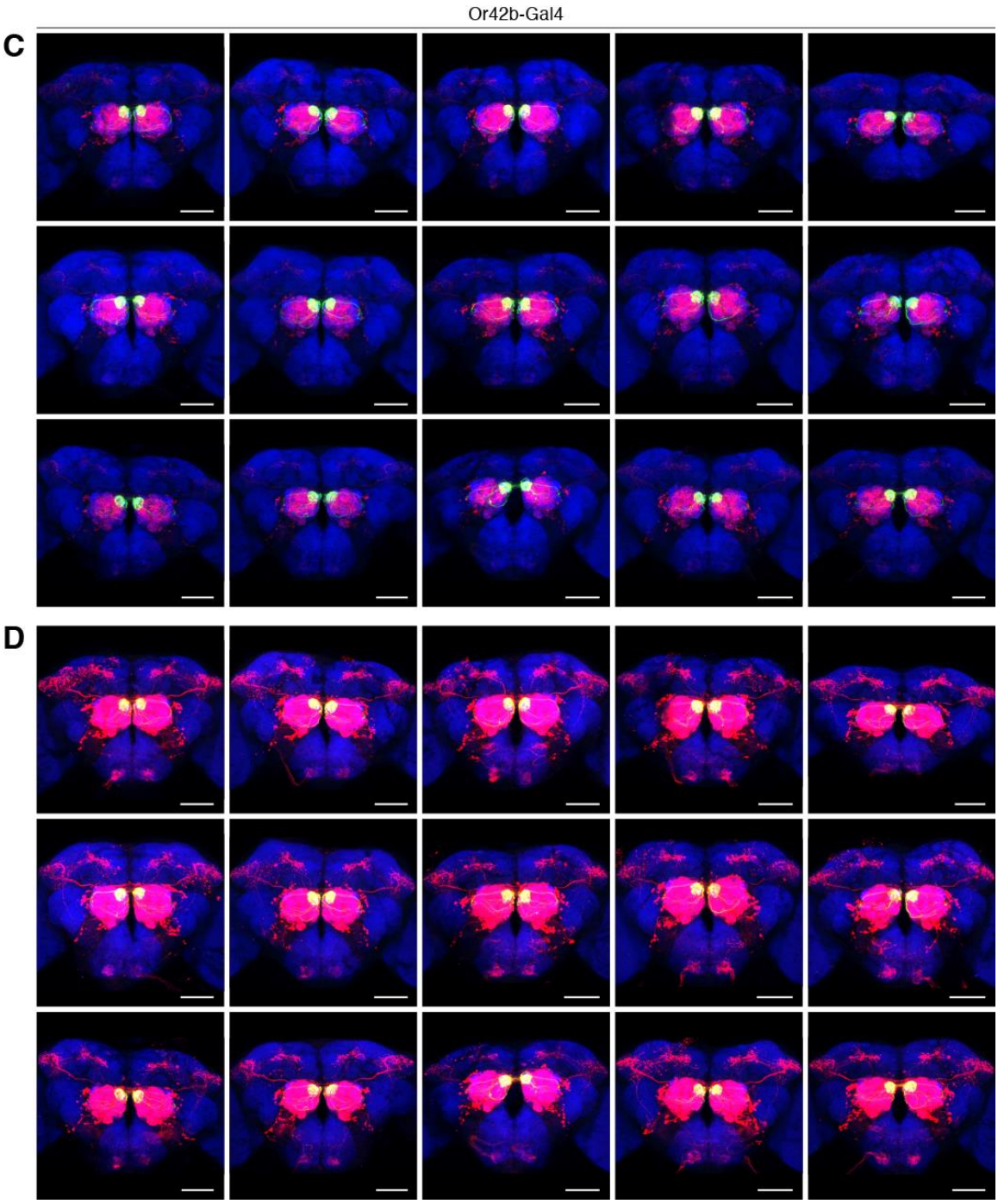

Figure 2-S5. Consistency of the *trans*-Tango signal between individual flies.

(A and B) *trans*-Tango signal (red) elicited by ligand expression in Or67d+ ORNs (green) was monitored in 25 age-matched individual flies (20 days old). The same 25 brains are

shown in (A) and (B), with imaging settings adjusted uniformly across brains in each panel to highlight either the antennal lobe in (A) or the projection targets in (B). Crosses were set 5 times in parallel, and 5 brains from the offspring of each cross are shown in the same row. (C and D) The same analysis was performed in 15 age-matched individual flies (16 days old) collected from a single cross in which *trans*-Tango is driven from Or42b+ ORNs (green). (A-D) Max-projection pictures of whole-mount brains are shown. Blue, neuropil counterstain. Scale bars, 50 μm.

CHAPTER 3

Distributed Representation of Taste Quality by Second-Order Gustatory Projection Neurons in *Drosophila*

Funding Acknowledgements

This work was supported by NIH grants R01DC017146 and R01MH105368 as well as by internal funds from Brown University: Carney Innovation Award and OVPR Seed Award (Gilad Barnea). I was supported by grant number DGE1058262 from the National Science Foundation Graduate Research Fellowship Program.

Research Contributions

- I performed dissections, immunohistochemistry and confocal microscopy for Figure 3-1.
- I performed all two-photon calcium imaging and data analysis.
- John D. Fisher performed additional dissections, immunohistochemistry, and confocal microscopy.
- Griffin G. Hartmann generated the 10xQUAS-GCaMP6s construct.
- I conceived of the idea for the project with Mustafa Talay and Gilad Barnea.
- I designed all experiments with Gilad Barnea.
- I wrote the manuscript with Gilad Barnea, with input from John D. Fisher, Griffin G. Hartmann, and Mustafa Talay.

3.1 Introduction

Taste enables animals to assess the nutritional value of food prior to ingestion. Sweet and bitter tastes respectively signal the presence of potentially calorie-rich sugars or toxic compounds. Accordingly, sweet tastants elicit food acceptance behaviors and bitter tastants elicit rejection, an innate behavioral response conserved between humans and the fly *Drosophila* melanogaster (Liman et al., 2014). Yet, despite the importance of taste in shaping feeding behavior, the neural circuits and codes linking taste sensation to behavioral response are not well understood.

The neural representation of taste begins with the detection of tastants by peripheral sensory cells. Humans can distinguish five taste qualities – sweet, bitter, salty, sour, and umami – and there are five distinct populations of taste bud cells, each tuned to one of these qualities (Yarmolinsky et al., 2009). In flies, the detection of sweet and bitter tastants is similarly performed by distinct populations of gustatory receptor neurons (GRNs) (Marella et al., 2006; Thorne et al., 2004; Wang et al., 2004). GRNs innervate hair-like sensilla on the tip of the proboscis, or labellum, where food intake occurs; they are also found in the pharynx and on the legs, wings, and ovipositor (Vosshall & Stocker, 2007). Sweet and bitter GRNs express different repertoires of gustatory receptors (GRs) (Clyne et al., 2000; Dunipace et al., 2001; Scott et al., 2001), endowing them with their tastant sensitivity (Dahanukar, Foster, Van der Goes van Naters, & Carlson, 2001; Moon, Köttgen, Jiao, Xu, & Montell, 2006). Segregation of sweet and bitter GR expression enables genetic access to these populations: Gr64f and Gr66a are expressed in all sweet and bitter GRNs of the labellum, respectively (Dahanukar et al., 2007; L. A. Weiss et al., 2011). GRN axons project to a region of the brain called the subesophageal zone (SEZ),

and intriguingly, axons of sweet and bitter GRNs terminate in different areas of the SEZ, suggesting that they may synapse onto different downstream circuits (Thorne et al., 2004; Wang et al., 2004).

Two predominant models have been proposed for the circuit logic that underlies taste information processing from the peripheral taste cells to higher brain regions (Simon et al., 2006; Yarmolinsky et al., 2009). The labeled line model posits that taste information is relayed through parallel, segregated channels from the periphery to central brain. By contrast, the distributed coding model holds that different tastes activate overlapping neuronal ensembles, which are read out by downstream brain areas as a population code. The existence of separate sweet and bitter GRN populations with distinct projection patterns within the SEZ is consistent with a labeled line model (Thorne et al., 2004; Wang et al., 2004). Labeled line coding in peripheral neurons is further supported by behavioral evidence. Optogenetically activating sweet GRNs is sufficient to drive proboscis extension and feeding behaviors, while silencing or ablating these neurons strongly suppresses these behaviors; likewise, activation of bitter GRNs prevents feeding, while silencing or ablating these neurons promotes proboscis extension and feeding responses to sweet tastants even in the presence of aversive bitter compounds (Moreira et al., 2019; Musso et al., 2019; Thorne et al., 2004; Wang et al., 2004). Moreover, several putative second-order gustatory neurons respond to either sweet or bitter, but not both (Bohra, Kallman, Reichert, & VijayRaghavan, 2018; Kain & Dahanukar, 2015; Kim et al., 2017; Miyazaki et al., 2015; Yapici et al., 2016). In other insect species, however, recordings from second-order neurons have revealed complex tuning properties that seem inconsistent with labeled lines (Kvello et al., 2010; Reiter et

al., 2015). Beyond the second order of the circuit, data suggests that sweet and bitter activate separate central neuronal populations (Harris et al., 2015). Yet, since these tastes evoke different behavioral responses, at some point in the circuit the responding neuronal populations must be different. Determining which model is operative therefore requires understanding the tuning of gustatory neurons at each successive stage in the circuit.

We recently developed *trans*-Tango, a genetic technique for transsynaptic tracing and circuit manipulation, and used it to identify several types of second-order gustatory neurons that are postsynaptic to sweet GRNs (Talay et al., 2017). The transsynaptic output of *trans*-Tango is transcription of a marker protein; by changing the identity of this protein, *trans*-Tango can be used for purposes beyond anatomical tracing. For example, using a genetically encoded calcium indicator as the transsynaptic reporter would enable one to measure neural activity across a population of second-order neurons in a circuit.

Here, we establish a configuration of *trans*-Tango enabling in vivo calcium imaging of transsynaptically labeled neurons. We use this strategy to examine the taste coding models by determining how sweet and bitter are encoded by second-order gustatory projection neurons (GPNs) in *Drosophila*. We find that sweet and bitter tastants excite different GPNs innervating distinct regions of the superior protocerebrum. These GPNs respond similarly to stimuli of the same taste quality, although for sweet tastants, the degree of this similarity is modulated by hunger state. While these findings are consistent with a labeled line model, we report that water also drives activity across the bitter-responsive region of GPNs. Although bitter taste and water thus activate similar GPNs, we discover a property of taste coding that may distinguish these stimuli: bitter tastants alone activate GPNs upon both their presentation (stimulus onset) and removal

(stimulus offset). This bitter offset response originates in the first-order GRNs encoding bitter onset, but in second-order GPNs, bitter offset activity is distributed beyond the bitter onset-responsive region. Our results support a mixed model of taste coding, wherein some neurons are selective for a single taste quality while distributed populations are recruited to represent others.

3.2 Anatomy of second-order neurons in the sweet and bitter circuits

Sweet and bitter tastants activate separate classes of GRNs, but it is not clear whether this labeled line representation is maintained beyond the first order of the circuit. If labeled lines are maintained, one possibility is an extreme case, wherein the second-order neurons of the sweet and bitter circuits are completely distinct. To test this, we used *trans*-Tango to compare the neural populations postsynaptic to Gr64f+ sweet GRNs and Gr66a+ bitter GRNs. Surprisingly, similar patterns of labeling were observed in both conditions, including dense innervation of the SEZ and multiple tracts projecting to the superior neuropils, to which we refer here as the lateral, mediolateral, and medial SEZ tracts (lSEZt, mlSEZt, mSEZt) (Talay et al., 2017; Figures 1A-1B). While the overall labeling from each genotype is similar, there may be subtle distinctions. For example, Gr66a>*trans*-Tango appears to label the mlSEZt more strongly than the lSEZt, while Gr64f>*trans*-Tango labels both tracts at comparable levels. Nevertheless, the morphology of projection terminals in and around the superior lateral protocerebrum (SLP) is similar in these two strains (Figure 1D). It is unlikely that completely distinct populations are labeled in these two strains, since driving *trans*-Tango from both Gal4 drivers simultaneously did not appear to label a substantially greater number of neurons (Figure

1C). However, from these results we cannot conclude the degree to which these second-order neuron populations overlap.

3.3 Sweet and bitter stimuli activate different GPNs

Understanding the neural representation of taste requires determining not just the anatomy of relevant neurons, but also their tuning properties. Thus, we decided to perform in vivo calcium imaging of second-order gustatory neurons using *trans*-Tango, a strategy we term *trans*-Tango(activity). The modular design of *trans*-Tango enables the expression of any reporter protein, not just a fluorescent marker, in the second-order neurons of a circuit. The combination of cell-type-specific Gal4, *trans*-Tango, and a calcium indicator under QUAS control as the readout of *trans*-Tango would allow calcium imaging of the neurons postsynaptic to the Gal4+ starter neurons. However, calcium imaging of neuropil requires high levels of calcium indicator expression, and *trans*-Tango reporter levels can take weeks to accumulate to saturation (Talay et al., 2017). To overcome this challenge, we generated new QUAS-GCaMP6 reagents with significantly boosted expression levels (see details in Methods). As an output of *trans*-Tango, these reporters enabled robust in vivo calcium imaging of second-order neurons in flies as young as 10 days post-eclosion.

Previously, we used mosaic analysis to identify several classes of second-order GPNs that comprise the three SEZ tracts as well as local interneurons of the SEZ (Talay et al., 2017). Our objective here is to understand how taste is represented in the circuits connecting peripheral neurons to central brain regions, so we limited our investigation to GPNs rather than local interneurons. To simultaneously image all GPNs of the sweet and

bitter circuits, we expressed GCaMP6s under control of *trans*-Tango initiated from both Gr64f-Gal4 and Gr66a-Gal4 together. We recorded calcium responses of GPNs to the presentation of tastants to the labellum. We imaged the neuropil of GPN arborizations in the SLP, a region previously implicated in innate behaviors. Because GPNs targeting the SLP project to several planes of depth along the anterior-posterior axis, we imaged a volume of several planes that captured the full population.

Two sweet tastants (maltose and sucrose) and two bitter tastants (denatonium and papaverine) all evoked strong activity in GPNs, but the calcium responses to these tastants were distributed unevenly among the GPN terminals. Both maltose and sucrose evoked activity most prominently in dorsal and lateral regions within the anterior planes of the volume, while both denatonium and papaverine drove activity in more ventral and medial posterior areas (Figure 2A and 2C). Thus, patterns of GPN activity were similar within a taste quality, but dissimilar between qualities. These response patterns were consistent across multiple trials and across flies (Figure S1A-B). Correlations between responses further supported the separation of sweet and bitter representations: GPN responses to tastants of the same quality were highly correlated, but responses to tastants of different qualities were not (Figure 2B and S1D).

While sweet and bitter responses were distinct at the population level, we considered the possibility that a subset of the GPN population might respond to both qualities. To identify whether any such regions were present in our volume, we determined the spatial patterns of the activity evoked by each tastant within each plane of depth, and assessed the degree of overlap between the patterns for different tastants. Minimal overlap was observed between sweet and bitter regions in any single plane

(Figure 2C). In contrast, tastants of the same quality often activated nearly completely overlapping regions (Figure S1E). This trend held across flies: most pixels, but not all, responded selectively to only one taste quality in every fly tested (Figure S1C).

Typically, the pixels that showed significant responses to both taste qualities did not cluster together in space, but rather were scattered within areas selective for just one quality. We wondered whether these pixels represented weak responses to the opposite taste quality or just noise. To investigate this, we used the spatial response patterns we derived for each tastant to delineate ROIs in single planes that corresponded to different sweet-responsive or bitter-responsive regions of the volume (Figure 2C). We considered two ROIs in the anterior sweet-responsive region: one corresponding to a projection along the dorsal edge of the region (S_D), and another corresponding to a region along the lateral edge (S_L). While these two regions are located near each other, they likely comprise separate GPNs, as the time courses of their responses were distinct: the time to peak response was shorter for S_L than S_D, and the sweet response in S_L adapted faster than the response in S_D (Figure 2D). Furthermore, while S_D was selective for sweet tastants, S_L responded to both sweet and bitter tastants, though the magnitude of the bitter responses was lower (Figure 2D). We performed a similar analysis for the bitter-responsive region, defining ROIs within this region at three levels of depth within the volume. We refer to these as the anterior (B_A), intermediate (B_I), and posterior (B_P) bitter areas, and based the demarcation of these ROIs on stereotyped morphology of the bitter-responsive neuropil to ensure consistency across individual flies (Figure S1E). Within each of these ROIs, both bitter tastants elicited strong activation at comparable levels. While both sweet tastants also produced minor responses within each of these regions,

these were significantly weaker than the bitter-evoked responses (Figure 2E). Thus, each GPN region responded primarily to only one of the two taste qualities.

We considered the possibility that sweet GPNs might be specifically labeled by *trans*-Tango initiated from the sweet GRN Gal4 driver, and likewise for bitter GPNs and the bitter GRN driver. To test this possibility, we expressed GCaMP6s in the GPNs labeled in each of these strains and imaged their responses to sweet and bitter tastants. Surprisingly, whether we used either the sweet driver or the bitter driver, we observed responses to both sweet and bitter tastants in the GPNs labeled by *trans*-Tango (Figure S2A-D). However, the GPN region responsive to sweet tastants was markedly diminished in the bitter Gal4-driven *trans*-Tango flies, as was the region responsive to bitter tastants in the sweet Gal4-driven *trans*-Tango flies (Figure S2E-F). This result is consistent with different but overlapping subsets of GPNs that are labeled in the two cases, with each GRN type preferentially targeting GPNs tuned to the same taste quality.

3.4 Water and bitter stimuli activate similar GPNs

Apart from sweet and bitter GRNs, the labellum contains both water-sensing GRNs and mechanoreceptors, so we next asked if mechanical stimulation or osmolarity contributed to the responses that we observed. To assess whether this was the case, we compared GPN responses to sucrose and denatonium to those elicited by water and polyethylene glycol (PEG; 3,350 g/mol; 20% w/v), a stimulus that does not excite water-sensing GRNs (Cameron et al., 2010). Both stimuli evoked GPN activity, indicating that these neurons are not activated strictly by sweet and bitter taste (Figure 3A). Moreover,

the water and PEG response was highly correlated, suggesting that this water-evoked activity may largely be a mechanosensory response (Figure 3B and S3B).

Intriguingly, GPN responses to water and PEG also exhibited high correlation with the denatonium response, but no correlation with the sucrose response (Figure 3B and S3B). The spatial patterns of these responses reflected these correlations: water-responsive regions had minimal overlap with sucrose-responsive regions, but substantial overlap with areas responding to PEG and denatonium (Figure 3C and S3A). In each of the three ROIs in the bitter-responsive region, activity was observed in response to both water and PEG. However, denatonium drove stronger responses in these areas than either water or PEG; this difference in magnitude was largest in area B_A, but was observed in areas B_I and B_P as well. Interestingly, the response to sucrose in each of these ROIs was comparable in magnitude to the water and PEG responses, indicating that the sucrose-driven activity in these regions may not be caused by the sweetness of the stimulus (Figure 3D-E). In contrast, neither water nor PEG produced significant activation of area S_D, suggesting that this region selectively responds to sweet tastants. Water and PEG did elicit activity within area S_L, but the magnitude of this activity was much smaller than sucrose-evoked activity, and comparable to denatonium-evoked activity.

3.5 GPNs respond similarly to multiple tastants of the same taste quality

While our initial experiments demonstrate that GPNs respond similarly to two tastants of the same quality, this pattern may not generalize. Indeed, in some insects, different sweet tastants evoke substantially different patterns of neural activity (Reiter et al., 2015). To test this, we imaged GPN calcium responses to a panel of five sweet tastants: fructose,

glucose, maltose, sucrose, and trehalose, and included water as a control. Each of these stimuli elicited a response in GPNs (Figure 4A). However, there was substantial heterogeneity in the spatial patterns of these responses. Tastants produced responses that generally matched one of two spatial patterns: one in which activity was strongest in areas S_D and S_L, and another in which activity was predominantly observed in more medial, water-responsive regions. As such, population-level responses to some sweet tastants were correlated with the water response (Figure 4C). These tastants did not exclusively activate the water-responsive region, as excluding the water-responsive pixels revealed substantial activity outside this area for all sweet tastants (Figure S4A). The heterogeneity in the response patterns of GPNs to the different sweet tastants was even more apparent after removing water-responsive pixels from the analysis (Figure S4C). Furthermore, the magnitude of responses in areas S_D and S_L varied substantially between stimuli (Figure S5A-B).

While the heterogeneity of GPN responses to sweet tastants might indicate distinct spatial representations of different sugars, there are other possible explanations. In particular, maltose and sucrose may drive more robust activity in sweet-responsive areas because these sugars are more potent activators of GRNs than most others (Dahanukar et al., 2007), and perhaps a threshold of GRN activity must be reached to robustly drive activity in sweet-responsive GPNs. Since starvation potentiates both sweet GRNs and some sweet-responsive second-order gustatory neurons (Inagaki et al., 2012; Kain & Dahanukar, 2015), we wondered if starved flies would exhibit stronger GPN responses to sweet tastants. Indeed, flies starved for 24 hours exhibited equal or stronger correlations between GPN responses for every pair of sweet tastants (Figure 4B and 4D

and S5C). Excluding water-responsive pixels from the analysis enhanced this effect, both in the visibility of these responses (Figure S4B) and in the inter-trial correlations (Figure S4D). Correspondingly, responses to sweet tastants in areas S_D and S_L were equal or stronger in starved flies than in fed flies (Figure S5A-B).

We performed the equivalent experiments with a panel of bitter tastants: caffeine, denatonium, lobeline, papaverine, and quinine, with water included again as a control. As was the case for sweet compounds, each of these stimuli evoked activity in GPNs (Figure 5A). However, unlike for sweet tastants, GPN responses to bitter tastants were highly correlated with one another (Figure 5B and S6C). Moreover, all bitter responses (except papaverine) were significantly correlated with the water response, as was previously observed for denatonium. The spatial pattern of responses to each bitter stimulus nearly completely overlapped the pattern of the water response across each plane of the volume (Figure 5C). However, bitter tastants generally drove stronger responses than water in this region. This pattern was most pronounced in area B_A, but was observed across planes of depth (Figure S6A-B). These results indicate that the spatial overlap between denatonium and water responses generalizes to bitter tastants as a group.

3.6 GRNs and GPNs respond to bitter offset in a concentration-dependent manner

The finding that bitter tastants and water evoke responses within similar GPN regions raises the question of how these signals might be distinguished by downstream neurons. Because the observed magnitude of the bitter response was typically greater than that of water (Figure S6B), it is possible that relative activity levels are used to differentiate the two types of stimulus. However, this difference in magnitude was rather

small for some bitter tastants, even though the concentrations we used are known to be highly aversive (Sellier, Reeb, & Marion-Poll, 2011; L. A. Weiss et al., 2011). Thus, the magnitude of GPN response alone is unlikely to provide enough information to reliably discriminate bitter from water, a critical ability for survival.

Interestingly, we observed that denatonium evoked a GPN response upon both the delivery of the stimulus (stimulus onset) and its removal (stimulus offset) (Figure 6A, left). This offset response was time-locked to the removal of the stimulus: when we held the bitter stimulus on the labellum for varying lengths of time, the second activity peak consistently followed stimulus offset, rather than a fixed time delay from the onset (Figure 6A, right). While responses to stimulus offset have been observed in the moth *Manduca sexta* (Reiter et al., 2015), no such effect has been reported in *Drosophila*. We wondered whether this effect emerged at the second order of the circuit or if it was initiated in the GRNs. To test this, we performed similar experiments while imaging calcium activity in bitter GRNs. We observed an offset response to denatonium in these first-order neurons as well (Figure 6B). Besides denatonium, we observed offset responses to lobeline and quinine in both GRNs and GPNs, suggesting that this offset response is a general property of bitter representation (Figure S7A-B). Furthermore, this response is specific to bitter; no offset response to water or sucrose was observed at either stage of the circuit (Figures 6C, 7A and data not shown).

The concentrations of bitter tastants we initially used to evoke the offset responses were relatively high (10 mM for denatonium and lobeline, 100 mM for quinine). We next tested whether the concentration threshold for the offset response matched that of the onset response. GRNs exhibited a significant response to bitter onset at concentrations as

low as 100 μM for denatonium ($p<.05$, two-sample one-tailed t-test with Bonferroni correction, denatonium response greater than water response, see Methods; Figure 6C). However, at this concentration, no offset response was clearly visible. A slight albeit visible activity peak at stimulus offset was detected at 1 mM, and a strong and significant offset response was seen at 10 mM ($p<.05$, two-sample one-tailed t-test with Bonferroni correction, denatonium response greater than water response; Figure 6E). The concentration thresholds obtained for onset and offset responses to lobeline were the same as for denatonium (Figure S7C).

We next sought to examine whether the responses to bitter onset and offset were similarly concentration-dependent in GPNs. We performed the equivalent set of experiments, imaging GPN activity to determine thresholds for the bitter onset and offset responses within bitter-responsive ROIs in anterior, intermediate, and posterior frames (Figure 6D-E). Denatonium onset produced a significantly stronger response than water in each of these ROIs at concentrations as low as 100 μM ($p<.05$). Thus, the onset response threshold matched that which we observed in GRNs. At a concentration of 1 mM, an offset response to denatonium was observed in area B_A ($p<.05$), but no significant response was observed in the more posterior B_I and B_P areas. At a concentration of 10 mM, however, the offset response was clearly observed in all ROIs ($p<.05$). For lobeline, 100 μM evoked onset activity in areas B_A and B_P, and 1 mM was sufficient to drive a significant offset response in all three ROIs ($p<.05$; Figure S7D).

3.7 GPN representation of bitter offset extends beyond the bitter onset-responsive region

In addition to observing a bitter offset response within the bitter onset-responsive GPN region, we noticed a separate region in which the responses to bitter offset were conspicuously strong. This area was located lateral and slightly ventral to the onset-responsive region, and typically spanned posterior to intermediate planes within the volume. Spatial overlays of bitter offset-responsive regions with those of bitter onset or water suggested that this region, which we call B_L, did not respond significantly to these stimuli, and thus may be selective for bitter offset (Figure 6D). Indeed, the magnitude of bitter onset and water responses within B_L was small, while the magnitude of the offset response was much greater (Figure 6E, bottom row). As in areas B_I and B_P, the threshold for denatonium offset responses in B_L was 10 mM ($p<.05$).

Intriguingly, the spatial pattern of the GPN bitter offset response also appeared to include a region of neuropil resembling the sweet-responsive area S_L. However, without a sweet stimulus response to provide a benchmark, we could not delineate this region in our bitter concentration experiments. We therefore performed an experiment comparing bitter onset and offset responses to the response to sucrose (Figure 7A). As we previously observed, the offset-responsive region overlapped the onset-responsive region throughout the imaging volume (Figure 7B, top row). However, in anterior planes, the offset-responsive region also overlapped with the sucrose-responsive region (Figure 7B, bottom row). The spatial overlap between sucrose-responsive and bitter offset-responsive areas appeared restricted to S_L and did not extend to S_D (Figure 7B, bottom row).

To verify this, we compared the magnitude and time course of the responses to sucrose, denatonium, and water within multiple ROIs: the bitter-responsive B_P, the bitter

offset-responsive B_L, and the sweet-responsive S_L and S_D (Figure 7C-D). As expected, sucrose drove strong responses in S_L and S_D, with temporal dynamics matching those observed in earlier experiments. While sucrose also elicited activity in areas B_P and B_L, this activity was comparable in magnitude to the water response or weaker than it, and thus not likely to be a response to sweetness. Denatonium onset drove a strong response in area B_P and a mild response in area S_L, but this S_L response was comparable to the water response in this region, and thus not likely to reflect a bitter response. Denatonium offset evoked strong activity in both regions B_P and B_L, as previously observed. Further, it elicited a strong response in area S_L, but only a mild response in area S_D (Figure 7C-D). These results suggest that the response to bitter offset involves multiple GPN types, including both bitter onset-responsive GPNs and GPNs specifically tuned to bitter offset, and may potentially include a subset of sweet-responsive GPNs as well.

3.8 Discussion

A central question in taste coding is how the neural representation of sweet and bitter is maintained beyond the sensory neurons at the first order of the circuit. The present study is the first to investigate taste responses selectively in second-order neurons in *Drosophila*, a strategy enabled by a novel configuration of *trans*-Tango. We found evidence that sweet and bitter tastants activate distinct second-order GPNs, just as they do for first-order GRNs. Yet we also found evidence that the representation of bitter in GPNs is somewhat complex. While the GPN response to bitter tastants is strikingly similar to the response to water, bitter tastants are distinguished by their ability to evoke activity upon both onset and offset. The spatial distribution of this offset response is

restricted to bitter GRNs in the first order but extends beyond the onset region in the second order, and may recruit GPNs that also respond to sweet. Our results are consistent with a mixed model of taste coding, in which some GPNs may function as labeled lines for particular taste qualities, while others respond to multiple qualities of the stimulus.

Beyond these findings on taste coding, our study demonstrates more generally that *trans*-Tango can fill a niche in analyzing neural circuit function. While a plethora of genetic tools exist for probing circuit function in *Drosophila*, they are limited by the expression patterns of Gal4 driver lines. There is an obvious use in having a line that labels a broad population of neurons at a defined stage of the circuit; for example, the GH146-Gal4 driver has been extensively used because it labels a broad set of second-order olfactory projection neurons with little background expression (Heimbeck, Bugnon, Gendre, Keller, & Stocker, 2001). In many other circuits, though, no comparable driver exists. Using *trans*-Tango initiated from a sparse set of starter neurons, one can selectively image the calcium responses of their downstream projection neurons, as we have done here in the gustatory system. The increasing availability of highly specific split-Gal4 drivers will enable this strategy in a wide variety of systems (Dionne, Hibbard, Cavallaro, Kao, & Rubin, 2018).

Our results suggest that there are GPNs with tuning properties not observed in first-order sensory neurons. For example, some GPNs appear to encode both bitter and water, and thereby integrate signals from different classes of first-order neurons. Further, the water responses of these neurons may be mechanosensory in origin, as PEG elicited similar levels of activation; these GPNs might therefore be integrating across sensory modalities. Other GPNs respond only to bitter offset, which is encoded together with

onset by first-order bitter neurons. Thus, some GPNs appear to selectively extract one temporal component of a signal from a single class of first-order neurons. These results suggest that substantial signal convergence and divergence occurs in the transition from the first to the second order of the taste circuit.

We also identified neurons that do not exhibit signatures of such circuit convergence – namely, GPNs selective for sweet taste. Dedicated central pathways for sweet taste may reflect the outsize role sugar has for the animal's survival. Interestingly, we also found evidence that GPNs represent sweet tastants with both sustained and more transient responses. While it is not immediately apparent what relevance these different temporal patterns may have for behavior, the fact that these two types of responses segregate within the imaging plane suggests that their downstream circuits are distinct as well.

The fact that the fly actively encodes bitter offset raises questions about the relevance of this response for the animal. Distinct onset and offset responses have been observed in other sensory modalities, such as vision (Behnia, Clark, Carter, Clandinin, & Desplan, 2014; Schiller, Sandell, & Maunsell, 1986; Strother, Nern, & Reiser, 2014). In vision, stimulus offset may serve as a cue for the motion of an object, for example. Bitter offset might similarly signal a change in the fly's gustatory environment. In the wild, flies can encounter a mixture of noxious and nutritious substances at a single feeding site: *Drosophila* feed on microbes that grow on decaying plant matter, and some of these microbes metabolize plant-derived compounds that are normally toxic to flies, and thereby make them safe for the fly's consumption (Markow & O'Grady, 2008). Since many plant toxins are bitter, a fly sampling such a food source would encounter a series

of bitter and non-bitter patches; a bitter offset response could thus signal movement off of a toxic substrate and onto a nutritive microbial one.

While we do not know the precise number of GPN types involved in the bitter offset response, the distribution of the offset response within areas B_L, S_L, and the bitter onset-responsive areas B_A, B_I and B_P strongly suggests that several second-order neuron types encode this feature. What function could be served by the distribution of this signal among several channels, rather than keeping it in one, as is the case in the first order? One possibility is that the separation of onset and offset components of the bitter response may endow the fly with greater sensitivity to changes in bitter concentration. In primate vision, separate ON and OFF pathways have been proposed to enable metabolically efficient coding of intensity changes to enhance contrast sensitivity (Schiller et al., 1986) and increase the dynamic range of the system (Kremkow et al., 2014). Likewise, the cockroach has separate olfactory sensory neurons tuned to odor onset and offset, which increase the animal's ability to detect small concentration changes (Burgstaller & Tichy, 2011). The bitter offset pathway in *Drosophila* might perform a similar function, enabling the fly to efficiently navigate concentration gradients of bitter compounds on heterogeneous food sources. Finally, since this parallel ON/OFF pathway circuit motif has been observed in several sensory systems, including vision (Schiller et al., 1986; Strother et al., 2014), olfaction (Burgstaller & Tichy, 2011; Chalasani et al., 2007), touch (Iggo & Ogawa, 1977), and thermosensation (Gallio, Ofstad, Macpherson, Wang, & Zuker, 2011), it may have general utility in sensory coding.

Another possibility is that bitter onset and offset may have opposing hedonic valences to the fly. The cessation of punishment is known to act as a reward in

conditioning experiments (Gerber et al., 2014). Because bitter taste is aversive, bitter offset may thus be interpreted as rewarding. Separating these components of the bitter taste response may allow for differential input to dopaminergic neurons of the mushroom body that mediate aversive and appetitive conditioning. The intriguing observation that the bitter offset response overlaps with the sweet response in the area we call S_L is consistent with this idea. If there is a GPN that underlies both the bitter offset and sweet responses in this area, this neuron may functionally encode the valence of the stimulus. Yet even if these responses are caused by separate sweet and bitter offset GPNs, their overlapping projections in this region may indicate that these GPNs converge onto common third-order neurons in the circuit.

Together, our results revealed a hybrid model of taste quality coding in the *Drosophila* gustatory system. The GPN population we studied includes both labeled line and convergent representations of taste, and distributes information about stimulus timing across multiple neural pathways. It remains to be seen how this manner of encoding gustatory information is used by downstream circuits to sculpt the behavior of the fly.

3.9 Methods

Fly strains

Drosophila melanogaster lines used in this study were raised on standard cornmeal-agar media (with tegosept anti-fungal agent). Flies were maintained in humidity-controlled chambers kept at 18°C and set to a 12-hour light/dark cycle. The following fly lines were used: Gr64f-Gal4 (Dahanukar et al., 2007), Gr66a-Gal4 (Scott et al., 2001), *trans*-Tango (Talay et al., 2017), UAS-myrGFP, QUAS-mtdTomato(3xHA)

(Talay et al., 2017), 20xUAS-IVS-jGCaMP7b (Dana et al., 2019), QUAS-GCaMP6s (this study).

Genotypes

The genotypes used in each figure are as follows:

Figure 1A and 1D (top row)	*w, P{UAS-myrGFP, QUAS-mtdTomato(3xHA)}su(Hw)attP8; P{Gr64f-Gal4}/P{trans-Tango}attP40*
Figure 1B and 1D (bottom row)	*w, P{UAS-myrGFP, QUAS-mtdTomato(3xHA)}su(Hw)attP8; P{Gr66a-Gal4}/P{trans-Tango}attP40*
Figure 1C	*w, P{UAS-myrGFP, QUAS-mtdTomato(3xHA)}su(Hw)attP8; P{Gr64f-Gal4}, P{Gr66a-Gal4}/P{trans-Tango}attP40*
Figures 2-5, 6A, 6D-E, 7, S1, S3-S6, S7A and S7D	*w, P{QUAS-GCaMP6s}su(Hw)attP8; P{Gr64f-Gal4}, P{Gr66a-Gal4}/P{trans-Tango}attP40*
Figure 6B-C and S7B-C	*w; P{Gr66a-Gal4}/P{20xUAS-IVS-jGCaMP7b}su(Hw)attP5*

Generation of transgenic fly strains

The QUAS-GCaMP6s construct was designed with several elements included to boost reporter expression levels (B. D. Pfeiffer et al., 2010, 2012): a 10xQUAS site,

5'UTR intervening sequence (IVS), 5'UTR syn21 sequence, codon optimized GCaMP6s, and a p10 terminator. The plasmid used to generate reporter flies was constructed by PCR, restriction digest and Gibson Assembly. The IVS, syn21 and p10 sequences, obtained from pJFRC81 (Addgene, 36432), and 10xQUAS site and GCaMP6s codon optimized sequences, obtained by synthesis (GeneArt, Thermo Fisher; seed sequence: (T.-W. Chen et al., 2013)), were amplified with the appropriate Gibson overlaps. The plasmid backbone was obtained by digesting UAS-myrGFP-QUAS-mtdTomato(3xHA) (Talay et al., 2017) to replace the UAS-myrGFP and mtdTomato(3xHA) components. These fragments were assembled by Gibson assembly (New England Biolabs) cloned and sequence verified before injection.

Immunohistochemistry

Immunohistochemistry was performed as previously described (Talay et al., 2017). Images are of brains of adult males aged 15-20 days. The following primary antibodies were used: rabbit anti-GFP (Thermo Fisher Scientific, A11122; 1:1,000), rat anti-HA (Roche, 11867423001; 1:100), mouse anti-Brp (nc82; DSHB; 1:50). The following secondary antibodies were used, all at 1:1000 dilution: donkey anti-rabbit (Alexa Fluor 488), goat anti-rat (Alexa Fluor 555), donkey anti-mouse (Alexa Fluor 647). Imaging was performed with a Zeiss confocal microscope (LSM800) using ZEN software (Zeiss, version 2.1). Images were further formatted using Fiji software (http://fiji.sc).

Calcium imaging

All imaging was performed on adult male flies. All flies were aged 10-15 days to maximize *trans*-Tango-dependent GCaMP signal. In starvation experiments, flies were wet-starved in a vial with a wet Kimwipe for 22-26 hours before imaging.

Preparation of flies for calcium imaging was based on previously described methods (Yapici et al., 2016). An imaging chamber was created by drilling a hole into a small plastic tissue culture dish. A piece of clear packing tape was used to cover the hole so that the non-adhesive side formed the basin of the dish. Flies were anesthetized with CO_2 and placed onto the sticky side of the tape. A human hair placed across the neck secured the fly in place; the hair was held in place using thin strips of tape. Flies extend their proboscis as they recover from CO_2 anesthesia, and during this process the proboscis was glued in an extended position using UV-curing glue (Loctite). Forelegs were removed along with tarsi of other legs to prevent both interference with the stimulus and accidental activation of tarsal gustatory neurons. A window was cut into the tape using a syringe needle, and the head capsule was inserted through the window and glued into place with UV-curing glue. The dish was filled with artificial hemolymph-like (AHL) solution (108 mM NaCl, 5 mM KCl, 2 mM $CaCl_2$, 8.2 mM $MgCl_2$, 4 mM $NaHCO_3$, 1mM NaH_2PO_4, 15 mM ribose, 5 mM HEPES, pH adjusted to 7.2-7.5, osmolarity adjusted to ~275 mOsm). Ribose was substituted for other sugars in the AHL to avoid spurious activation of sugar-sensing neurons (Marella et al., 2006). A small window was cut into the fly cuticle to expose the imaging area, and obstructing tissue and air sacs were removed. Antennae and muscle 16 were removed to reduce motion. When imaging the SEZ, the esophagus was cut to reduce motion and expose the imaging area.

Two-photon calcium imaging was performed on a Scientifica multiphoton galvo system. The excitation wavelength used was 920 nm, and laser power at the objective was kept between 15-20 mW. Imaging data was collected using SciScan software (Scientifica). A water-immersion objective (Nikon, 16x, 0.8 NA) was used and imaging volumes consisting of 12 planes of depth with 8-9 μm spacing between planes were acquired with 256x256 pixel resolution per plane, using 391 nm pixel size for GPN imaging and 521 nm pixel size for GRN imaging. Volumes were collected at a ~0.5 Hz volume rate (~6 Hz frame rate).

Each imaging session consisted of three trials per tastant, where each trial consisted of one stimulus delivery, held for several seconds. For experiments in which stimulus offset was monitored, the stimulus hold time was varied between 20, 25, and 30 seconds; for all other experiments, hold time was 8-10 seconds. To ensure the fly remained responsive throughout the imaging session, overall imaging time per fly was kept under 2 hours. Trials using the same tastant were therefore performed consecutively to reduce overall imaging time. Stimulus presentations were spaced out by ~2 minutes to minimize habituation.

Tastant solutions were delivered to the proboscis during imaging using a Drummond Nanoject II microinjector mounted on a micromanipulator (Scientifica). In each trial, stimuli were manually delivered after collecting at least 10 baseline imaging volumes. Tastant delivery to the proboscis was monitored using a Point Grey Firefly camera equipped with an Infinistix lens and a shortpass IR filter (850nm OD 4.0 shortpass filter, Edmund Optics). An LED flash was triggered by the software upon the start of an imaging trial, and the frame of tastant delivery was calculated for each trial

based on elapsed time since the flash. Tastant solutions used for imaging were used at the following concentrations: polyethylene glycol (3,350 g/mol) (20% w/v); fructose, glucose, maltose, sucrose, trehalose (1 M); caffeine, papaverine hydrochloride, quinine hydrochloride dihydrate (10 mM); denatonium benzoate and lobeline hydrochloride were used at 10 μM, 100 μM, 1 mM, and 10 mM for concentration experiments and at 1 mM for bitter panel experiments; denatonium was used at 10 mM in experiments in Figure 2 and Figure 7.

Calcium imaging analysis

Raw images were preprocessed using Fiji functions "Subtract Background" (rolling ball radius of 50 pixels) and "Gaussian Blur" (radius of 2 standard deviations). In MATLAB, motion correction was performed on each plane in the imaging volume using the NoRMCorre algorithm (Pnevmatikakis & Giovannucci, 2017).

We performed imaging analysis in MATLAB, using a strategy inspired by a previously described method (Liang et al., 2013). We limited our analysis to a general ROI within the imaging volume consisting only of responsive pixels. We determined this ROI in three steps. First, for each trial we determined which pixels in the imaging volume showed a significant response to the stimulus. For each pixel, we defined a significant response as three standard deviations above its baseline fluorescence level. We considered the three imaging volumes following stimulus delivery to comprise the response to stimulus onset, and used the mean of ten volumes before stimulus as the baseline. To reduce noise, we considered only those pixels that showed significant responses in all three volumes following stimulus delivery. Second, we defined specific

ROIs for each tastant, representing the average region activated by that tastant across trials. We considered only those pixels showing significant responses in two out of three trials for that tastant, then median filtered the resulting image and removed from consideration any border pixels that did not remain in frame for all trials in the experiment. Third, we created the general ROI consisting of all responsive pixels in an experiment by taking the union of all tastant-specific ROIs.

To determine peak responses for each trial, we took the three post-stimulus volumes and considered only those pixels within the general ROI, calculated the maximum ΔF/F across these volumes for each pixel showing a significant response, then median filtered the resulting image. To display this peak response as a heatmap, we exported the image to Fiji, created a maximum Z projection, and used the "physics" LUT with a max of 300% ΔF/F. To calculate correlations between trials, we took the peak responses for each trial, converted ΔF/F values of all pixels within the general ROI to vectors, and computed Pearson's correlation coefficient between these vectors. This produced correlation values for every trial pair for each fly; the correlation matrices displayed in each figure depicts the mean of these inter-trial correlation values across all flies. To generate maps of spatial patterns of tastant responses, we displayed all pixels that were active in any of the three trials for a given tastant. To define ROIs for calculating fluorescence traces and response magnitude, we took motion-corrected single imaging planes and used the maps of spatial patterns of responses as a guide to manually draw boundaries around regions that exhibited significant responses to a tastant.

For trials where we analyzed both stimulus onset and offset, the method for defining the general ROI was slightly modified. Stimulus onset-responsive regions and

ROIs were calculated the same way. In addition to determining stimulus onset-responsive pixels, we also determined offset-responsive pixels. The analysis period for defining offset-responsive pixels was the volume when stimulus removal occurred plus the following three volumes; significant responses were considered to be those exhibiting activity greater than three standard deviation above baseline level. The offset baseline level was defined as the mean pixel fluorescence of the five volumes prior to stimulus removal. In the onset/offset experiments, we generated ROIs for each tastant-on/off pairing (e.g. separate ROIs for denatonium-on and denatonium-off), and considered the union of all tastant-on/off ROIs as the general ROI for that experiment. For first-order experiments, to reduce background noise we only used tastant-on ROIs to construct the general ROI; there is no apparent subregion of GRN axons that is selectively offset-tuned, so this modification did not exclude any responsive areas.

Statistics

To determine whether correlations between responses to two tastants were statistically significant, we computed Pearson's r between each pair of trials for those tastants; since we ran three trials for each tastant during an imaging session, for every pair of tastants there were nine pairs of trials, and we took the mean of these nine Pearson's r values to determine a correlation value for that tastant pair for each fly. We ran a one sample t-test on these correlation values against a mean of 0 for each tastant pair and used a Bonferroni correction to account for multiple comparisons. To determine whether differences between taste responses within an ROI were statistically significant, we performed one-way ANOVA tests with Tukey post-hoc tests to account for multiple

comparisons. To determine significant concentration threshold levels for bitter onset and offset responses, we performed two-sample one-tailed t-tests with Bonferroni correction, where the experimental hypothesis was that the bitter response was greater than the water response within the ROI. All statistics were performed in MATLAB.

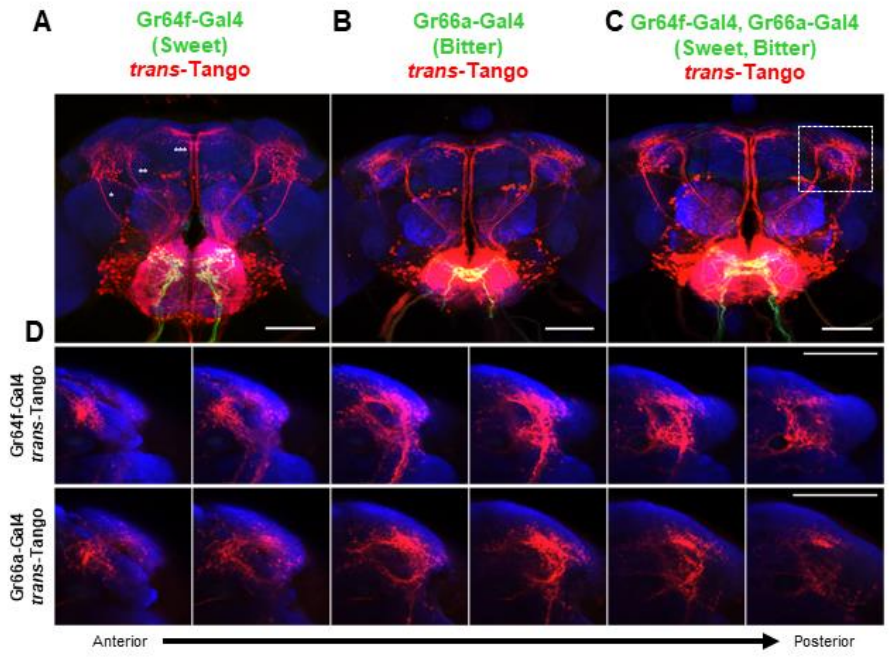

Figure 3-1. Anatomy of second-order gustatory neurons revealed by *trans*-Tango.

(A) Anatomy of second-order gustatory neurons postsynaptic to sweet GRNs, as revealed by *Gr64f-Gal4* > *trans*-Tango, with three SEZ tracts labeled: * = lSEZt; ** = mlSEZt; *** = mSEZt. (B) Anatomy of second-order gustatory neurons postsynaptic to bitter GRNs, as revealed by *Gr66a-Gal4* > *trans*-Tango. (C) Anatomy of second-order gustatory neurons postsynaptic to both sweet and bitter GRNs, revealed by *Gr64f-Gal4*, *Gr66a-Gal4* > *trans*-Tango. (D) Projection neurons targeting SLP labeled by *trans*-Tango initiated by either *Gr64f-Gal4* or Gr66a-Gal4 have similar overall morphology. Images correspond to area within white dotted line in C; sections from left to right depict progressively more posterior planes of depth. In all panels, first-order neurons are labeled by GFP (green) and second-order neurons by tdTomato (red). Scalebars in all panels 50 μm; for D, scalebar in rightmost image applies to entire row.

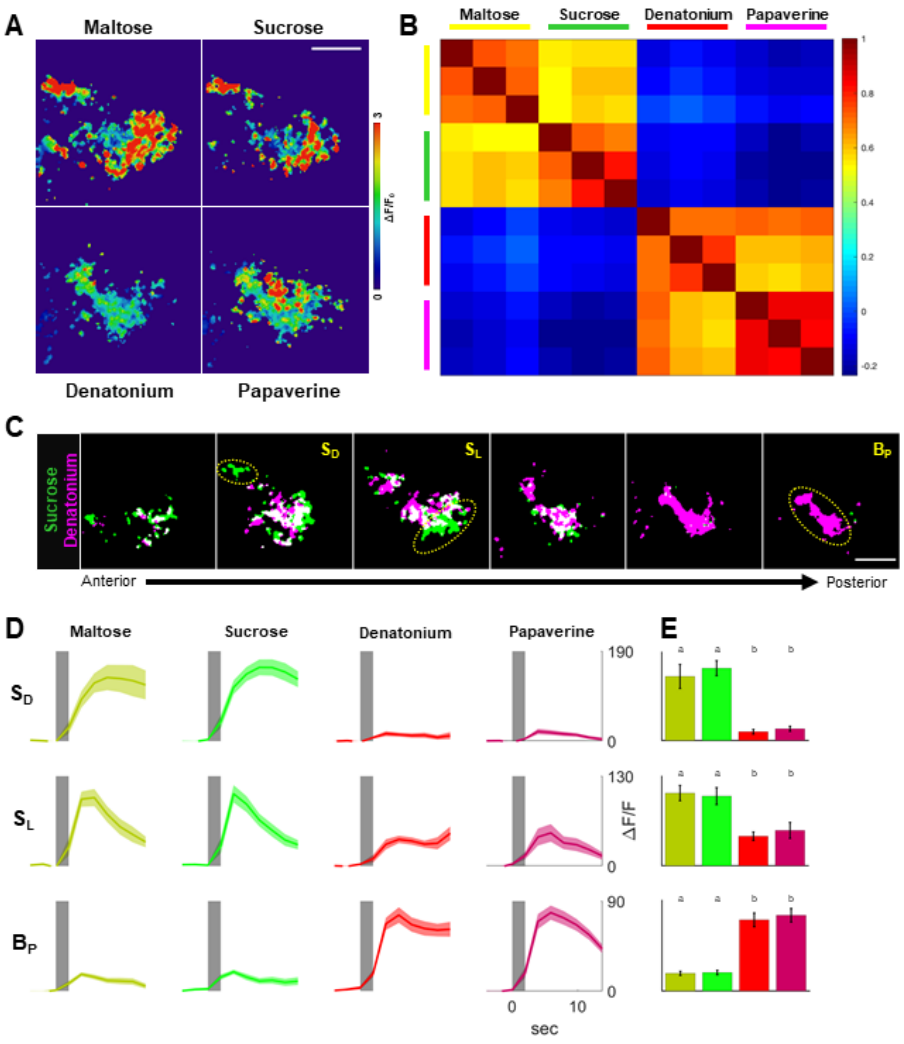

Figure 3-2. Sweet and bitter tastants excite different populations of GPNs.

(A) Representative heatmaps of GPN responses to sweet (maltose, sucrose) and bitter (denatonium, papaverine) tastants. Heatmaps are maximum projections over all planes in the volume; each image represents the response during one trial, and all images are from the same experiment. Heatmaps show ΔF/F value from 0 to 3 as indicated by legend on the right. (B) Pairwise peak response correlations (Pearson's r) between trials, group-averaged (n = 11 flies). Each group of three rows/columns represents three consecutive trials of the tastant indicated above matrix. Colors represent correlation coefficient value according to

legend on the right. (C) Representative images of spatial patterns of significant GPN responses to sucrose (green) and denatonium (magenta) in individual planes. Images are ordered from anterior to posterior; white indicates overlap between areas of significant response to each tastant. Yellow dotted ovals indicate locations of ROIs S_L, S_D, and B_P. (D) Fluorescence traces showing magnitude and time course of responses within each ROI. Responses are color-coded by tastant as follows: maltose, yellow; sucrose, green; denatonium, red; papaverine, magenta. Bold trace denotes mean and shaded region denotes SEM. Gray bar denotes time of stimulus onset. Y axis is ΔF/F; scale is same for panels within a row. X axis is time; scale is same for all panels. (E) Peak responses to each tastant within each ROI. Colors represent tastants with same color scheme as D. Y axis is maximum ΔF/F; scale is same as 2D. Error bars denotes SEM. Letters represent statistically significant differences between groups ($p < .05$, one-way ANOVA with Tukey post-hoc test). All scalebars 30 μm; scalebar applies to all images in a panel.

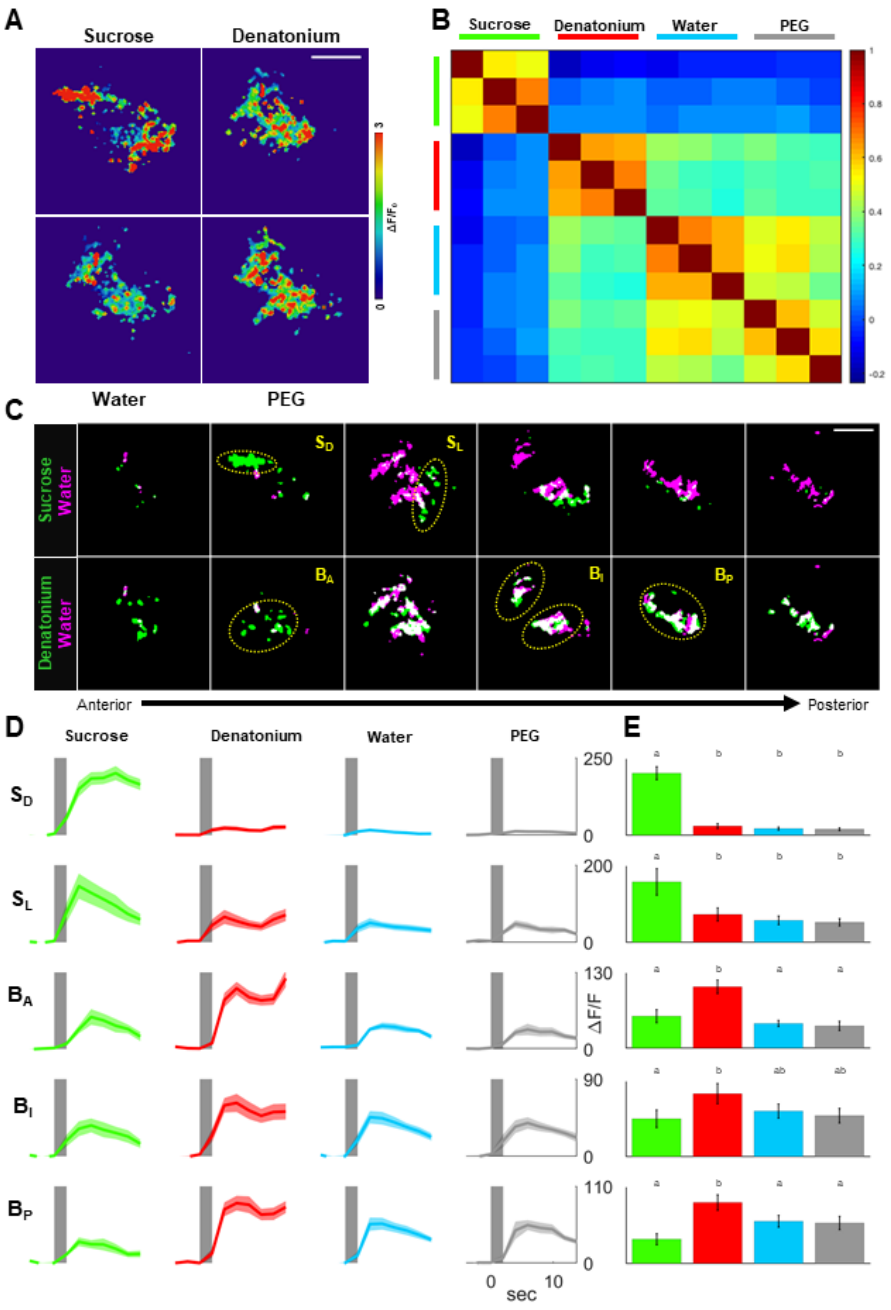

Figure 3-3. GPNs responding to bitter also respond to water and PEG.

(A) Representative heatmaps of GPN responses to sucrose, denatonium, water, and PEG. Heatmaps are maximum projections over all planes in the volume; each image represents the response during one trial, and all images are from the same experiment. Heatmaps show

ΔF/F value from 0 to 3 as indicated by legend on the right. (B) Pairwise peak response correlations (Pearson's r) between trials, group-averaged (n = 8 flies). (C) Representative images of spatial response patterns to water (magenta) and either sucrose (green, top row) or denatonium (green, bottom row) in individual planes. Yellow dotted ovals indicate locations of ROIs S_D, S_L, B_A, B_I, and B_P. (D) Fluorescence traces showing magnitude and time course of responses within each ROI. Responses are color-coded by tastant as follows: sucrose, green; denatonium, red; water, cyan; PEG, light gray. (E) Peak responses to each tastant within each ROI. Colors represent tastants with same color scheme as D. Y axis is maximum ΔF/F; scale is same as D. Error bars denote SEM. Letters represent statistically significant differences between groups ($p < .05$, one-way ANOVA with Tukey post-hoc test). All scalebars 30 μm; scalebar applies to all images in a panel.

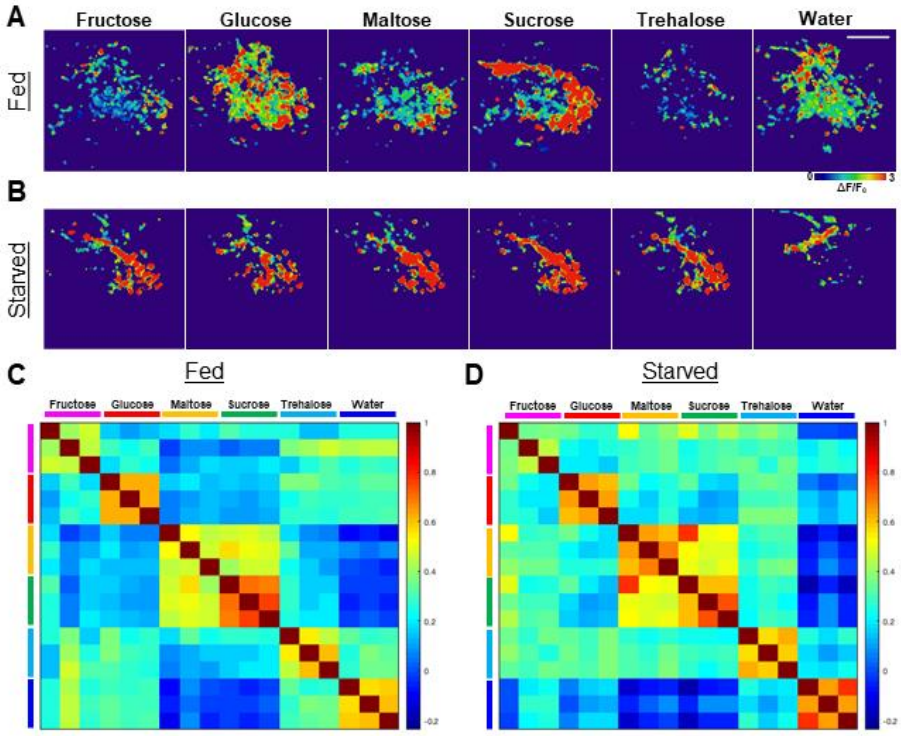

Figure 3-4. GPN responses to sweet vary between tastants, but are more consistent after starvation.

(A) Heatmaps from a fed fly showing responses to a panel of sweet tastants. Heatmaps are maximum projections over all planes in the volume; each image represents the response during one trial, and all images are from the same experiment. Heatmaps show ΔF/F value from 0 to 3 as indicated by legend on the right. (B) Heatmaps as in A, but for a fly wet-starved for 1 day. (C) Matrix of inter-trial correlations for fed flies, group averaged (n = 8 flies). (D) Matrix of inter-trial correlations for starved flies, group averaged (n = 8 flies). Scalebar marks 30 μm and applies throughout figure.

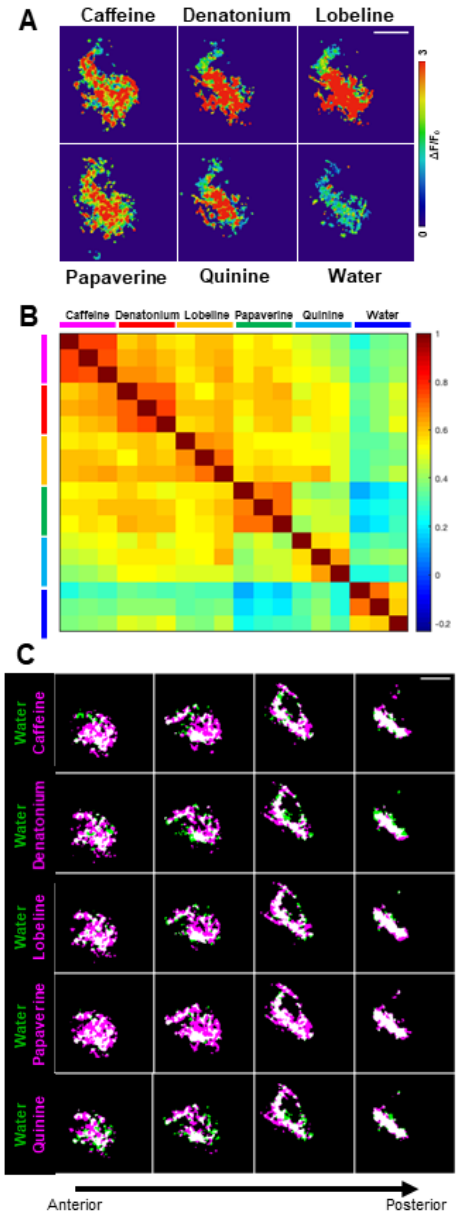

Figure 3-5. GPN responses to bitter are similar between tastants as well as to water.

(A) Heatmaps showing peak responses to five bitter tastants and water. Heatmaps are maximum projections over all planes in the volume; each image represents the response during one trial, and all images are from the same experiment. Heatmaps show ΔF/F value from 0 to 3 as indicated by legend on the right. (B) Matrix of inter-trial correlations, group

averaged (n = 8). (C) Spatial patterns of bitter-responsive areas (magenta) overlaid with the water-responsive area (green); white denotes overlap. All scalebars 30 μm; scalebar applies to all images in a panel.

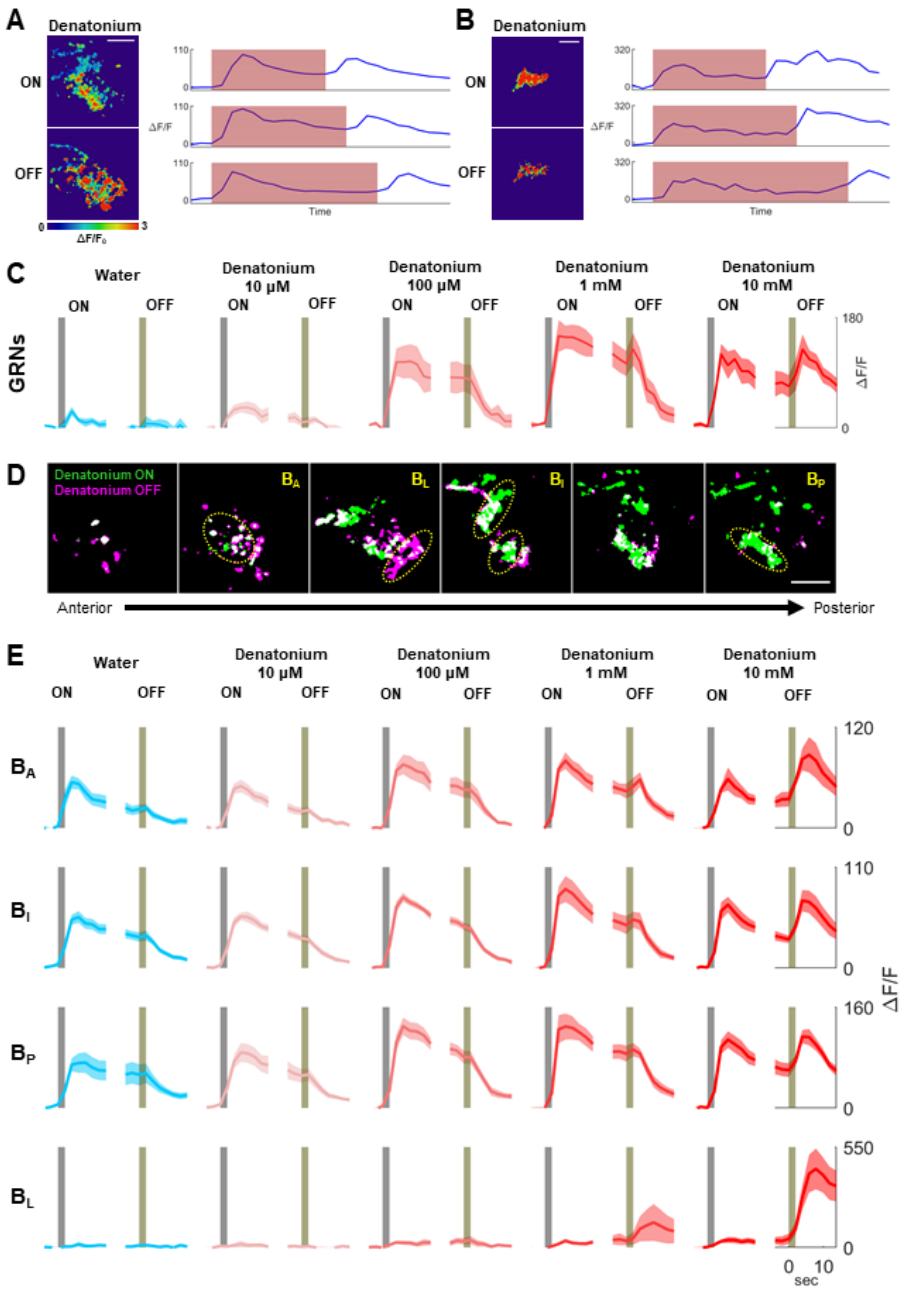

Figure 3-6. GRNs and GPNs respond to bitter stimulus offset.

(A) GPN response to denatonium onset and offset. Left, representative heatmaps of onset and offset responses. Right, traces showing response to denatonium applied for different lengths of time. In traces, red shading denotes the time interval during which the stimulus was applied. Top row, time is approximately 20 sec; middle row, 25 sec; bottom row, 30

sec. (B) Same as A, but for Gr66a+ GRNs. (C) Gr66a+ GRN responses to increasing concentrations of denatonium. For each concentration, left plot shows responses aligned to stimulus onset (gray bar) and right plot shows responses aligned to offset (yellow bar). Plots show mean (bold trace) and SEM (shaded area; n = 5 flies, 3 trials per concentration). (D) Spatial maps of onset (green) and offset (magenta) responses to denatonium in GPNs across individual planes. Yellow dotted circles denote ROIs B_A, B_L, B_I, and B_P. (E) GPN responses to increasing concentrations of denatonium in four ROIs depicted in Figure D. Color scheme follows that of panel C (n = 6 flies, 3 trials per concentration). All scalebars 30 μm; scalebar applies to all images in a panel.

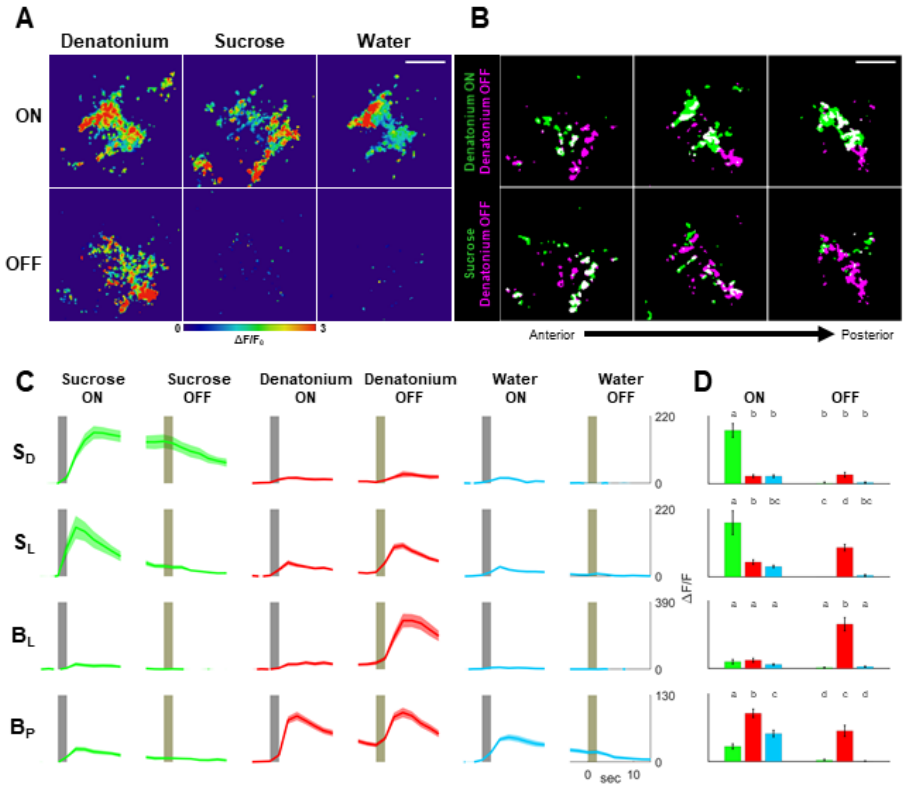

Figure 3-7. Bitter offset activates a broader set of GPNs than bitter onset.

(A) Representative heatmaps showing GPN responses to onset (top row) and offset (bottom row) of denatonium, sucrose, and water. Heatmaps are maximum projections over all planes in the volume; each image represents the response during one trial, and all images are from the same experiment. Heatmaps show ΔF/F value from 0 to 3 as indicated by legend on the right. (B) Representative spatial response maps showing overlap between denatonium offset (magenta) and either denatonium onset (green, top row) or sucrose onset (green, bottom row); overlap is shown in white. (C) GPN responses to onset and offset of sucrose, denatonium, and water within each of four ROIs (n = 10 flies, 3 trials per tastant). (D) Peak responses to onset and offset of each tastant within each ROI. Error bars denote SEM. Letters represent statistically significant differences between groups ($p < .05$, one-

way ANOVA with Tukey post-hoc test). All scalebars 30 μm; scalebar applies to all images in a panel.

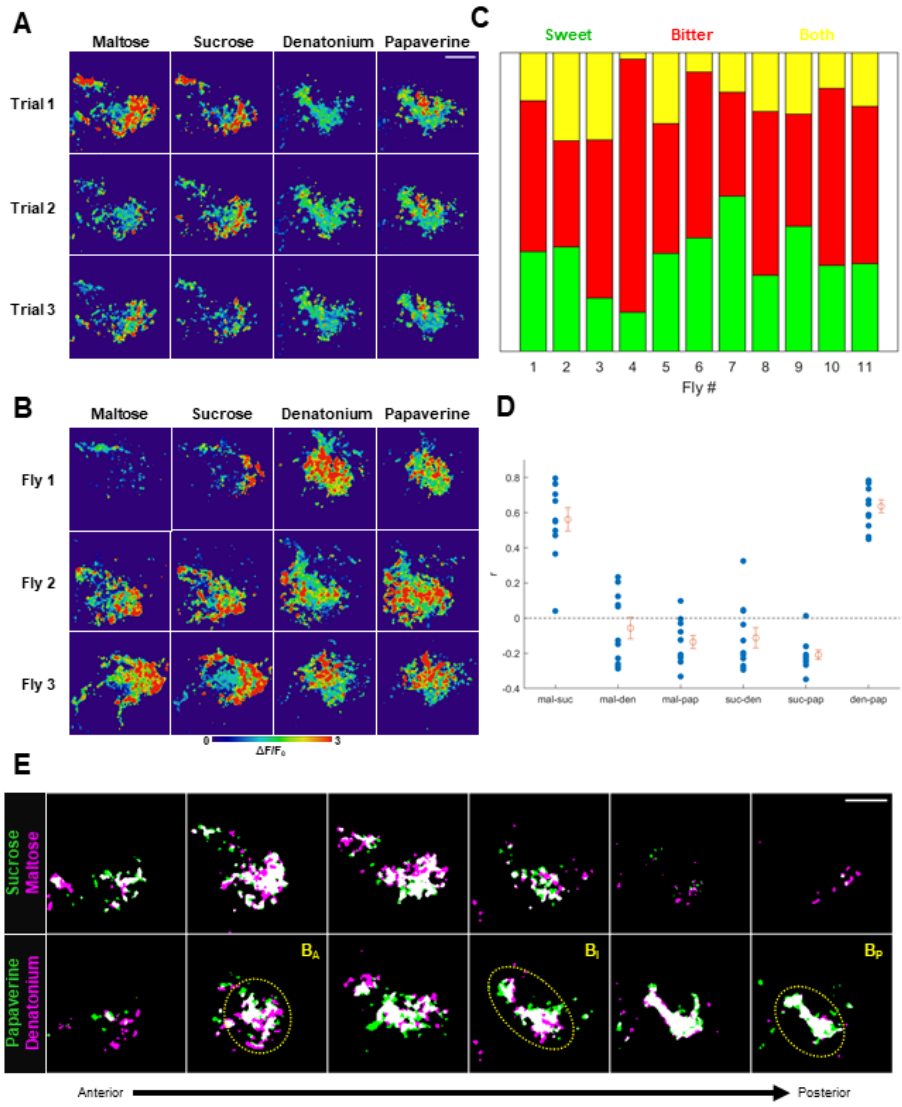

Figure 3-S1. Consistency of GPN responses between trials and tastants.

(A) Heatmaps of peak responses to a tastant during each of three trials for an example fly. Top row is the first trial, middle row is second, bottom row is third. Heatmaps are maximum projections over all planes in the volume. Heatmaps show ΔF/F value from 0 to 3 as indicated by legend. (B) Heatmaps for three different flies. (C) Proportion of pixels responding to each taste quality. Green: proportion of pixels only responding to sweet stimuli; red: proportion only responding to bitter; yellow: proportion responding to both

sweet and bitter. Each column shows results for one fly. (D) Inter-tastant correlations for individual flies. Each blue dot represents average correlation between trials of a given tastant pair for a single fly. Orange dot denotes mean; error bars denote SEM. Sucrose/maltose and denatonium/papaverine correlations are significantly greater than zero ($p < .05$, one sample t-test, Bonferroni correction). (E) Overlaid spatial response maps for tastants of the same quality. Top row: sucrose (green) and maltose (magenta), bottom row: papaverine (green) and denatonium (magenta); overlap shown in white. ROIs for areas B_A, B_I, and B_P shown on bottom row. All scalebars 30 μm; scalebar in A applies to A and B, and scalebar in D applies to all images in the panel.

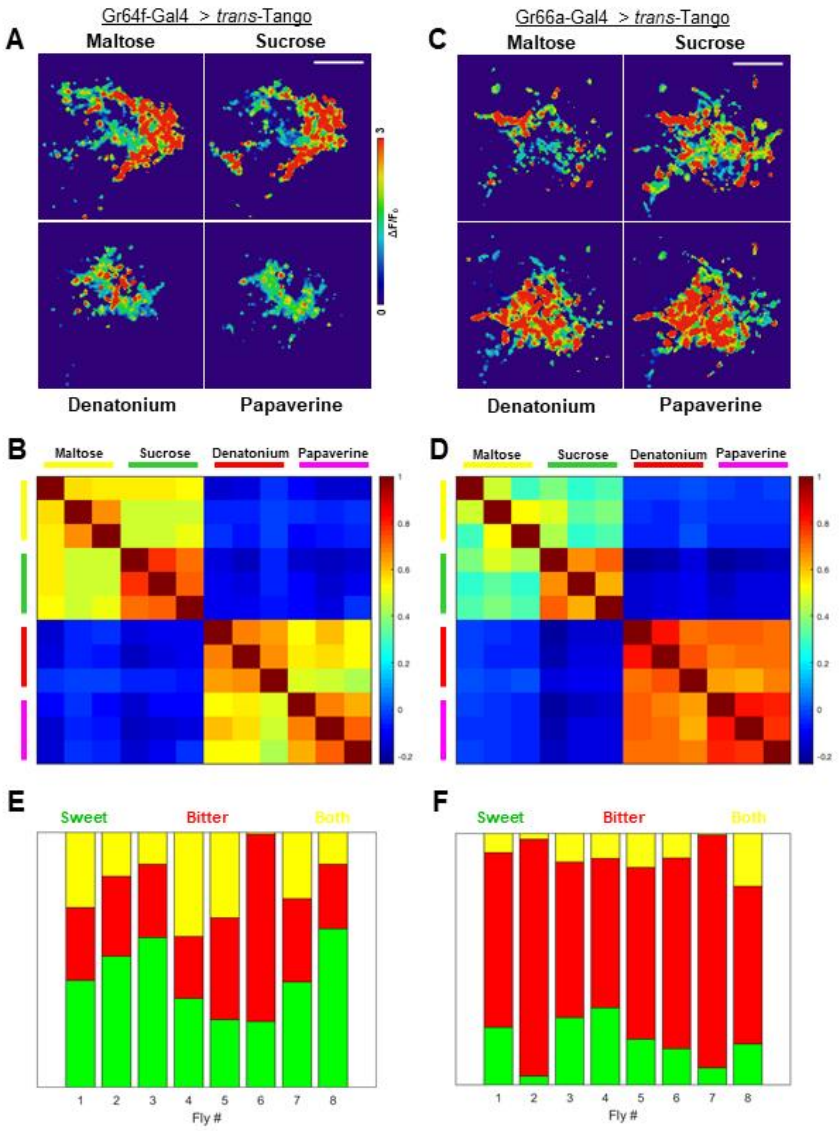

Figure 3-S2. Taste responses of GPNs labeled by *trans*-Tango driven by either *Gr64f-Gal4* or *Gr66a-Gal4*.

(A) Representative heatmaps showing responses of GPNs labeled by *Gr64f-Gal4* > *trans*-Tango to sweet (maltose, sucrose) and bitter (denatonium, papaverine) tastants. (B) Correlation matrix showing pairwise inter-trial correlations of peak responses of GPNs labeled by *Gr64f-Gal4* > *trans*-Tango; group-averaged (n = 8 flies). (C) Heatmaps as in A, but for GPNs labeled by *Gr66a-Gal4* > *trans*-Tango. (D) Correlation matrix as in B, but

for GPNs labeled by *Gr64f-Gal4* > *trans*-Tango (n = 8 flies). (E) Proportion of pixels responding to each taste quality, for *Gr64f-Gal4* > *trans*-Tango. Green: proportion of pixels only responding to sweet stimuli; red: proportion only responding to bitter; yellow: proportion responding to both sweet and bitter. Each column shows results for one fly. (F) Proportion of pixels responding to each taste quality, as in E, for *Gr66a-Gal4* > *trans*-Tango. All scalebars 30 μm; scalebar applies to all images in a panel. Colors same as in E.

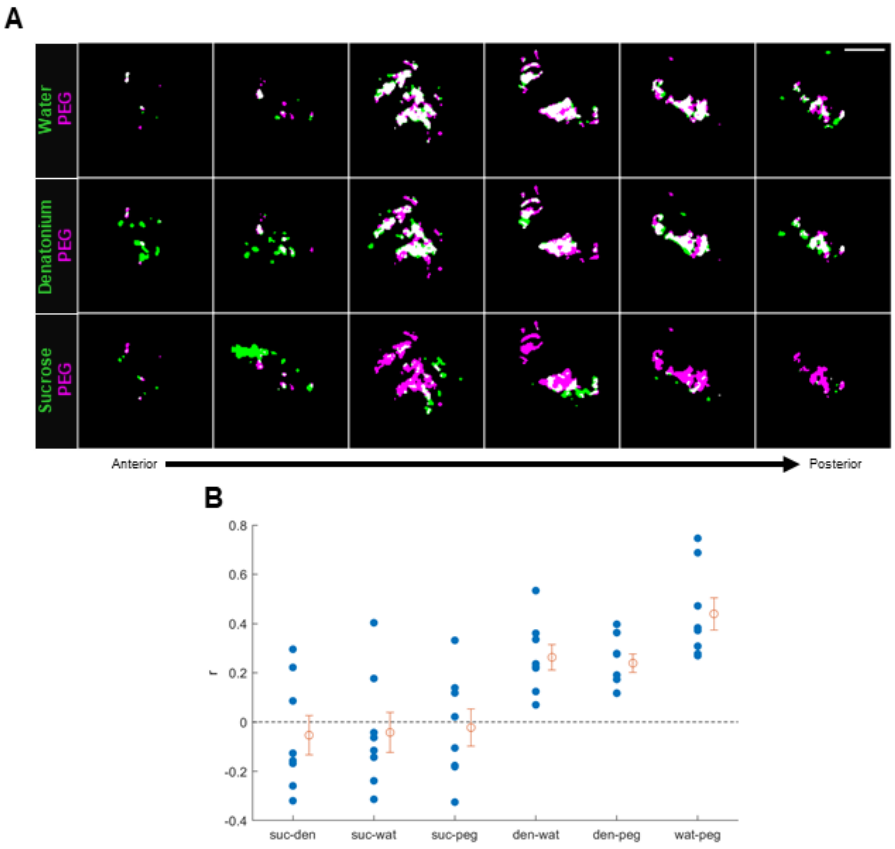

Figure 3-S3. PEG and water activate similar GPNs.

(A) Representative overlaid spatial maps of PEG-evoked responses (magenta) with those of water (green, top row), denatonium (green, middle row), and sucrose (green, bottom row). (B) Inter-tastant correlations for individual flies. Each blue dot represents average correlation between trials of a given tastant pair for a single fly. Orange dot denotes mean; error bars denote SEM. Denatonium/water, denatonium/PEG, and water/PEG correlations are significantly greater than zero ($p < .05$, one sample t-test, Bonferroni correction). Scalebar 30 μm and applies to all panels.

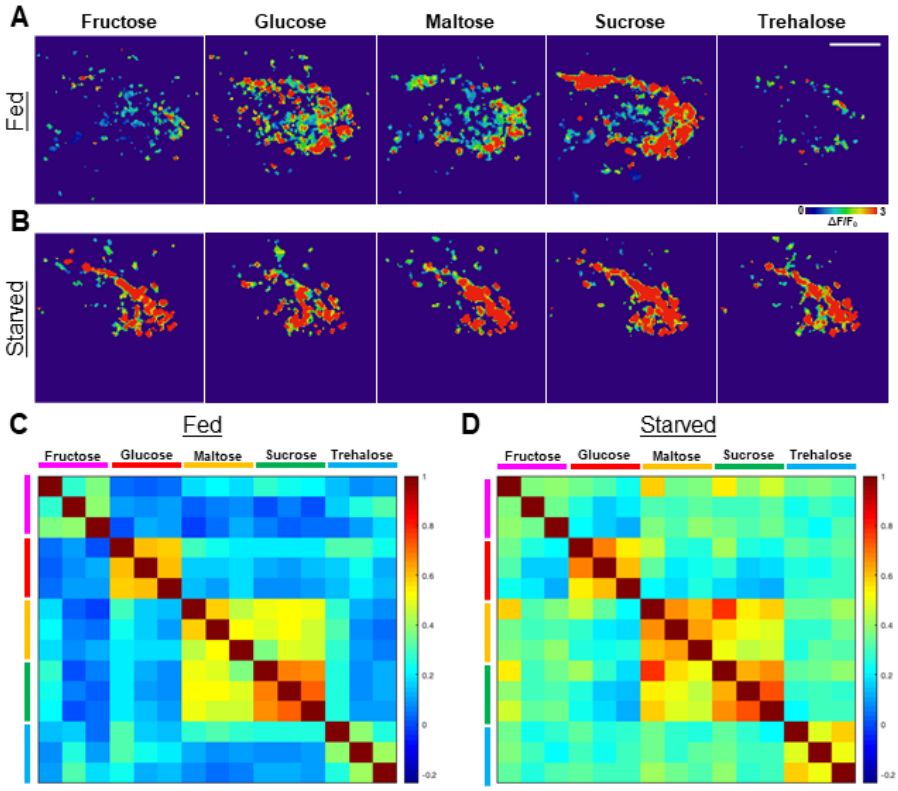

Figure 3-S4. Responses to sweet tastants excluding water-responsive pixels.

(A) Heatmaps of same responses to sweet tastants shown in Figure 4A, but excluding the water-responsive pixels. (B) Heatmaps of same responses to sweet tastants shown in Figure 4B, but excluding the water-responsive pixels. (C) Correlation matrix of GPN responses to sweet tastants in fed flies, as shown in Figure 4C, but limited to region excluding water-responsive pixels. (D) Correlation matrix of GPN responses to sweet tastants in starved flies, as shown in Figure 4D, but limited to region excluding water-responsive pixels. Scalebar 30 μm and applies to all panels in figure.

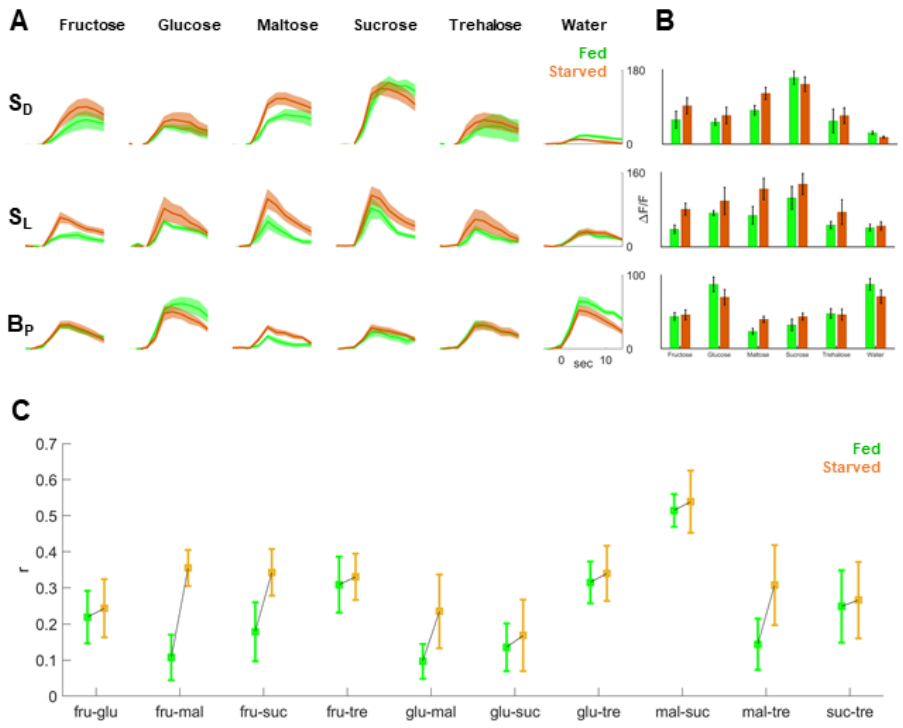

Figure 3-S5. Effects of starvation on GPN responses to sweet tastants.

(A) Reponses to sweet tastants in the two sweet-responsive regions, S_D and S_L, and water/bitter-responsive region B_P. Green traces indicate responses for fed flies, orange traces indicate responses for starved flies (n = 8 fed; n = 8 starved). (B) Max ΔF/F for each tastant in each ROI. (C) Inter-tastant correlations are equal or greater for starved flies than fed flies. Squares denote mean correlation across individuals; error bars denote SEM. Green: values for fed flies, orange: values for starved flies.

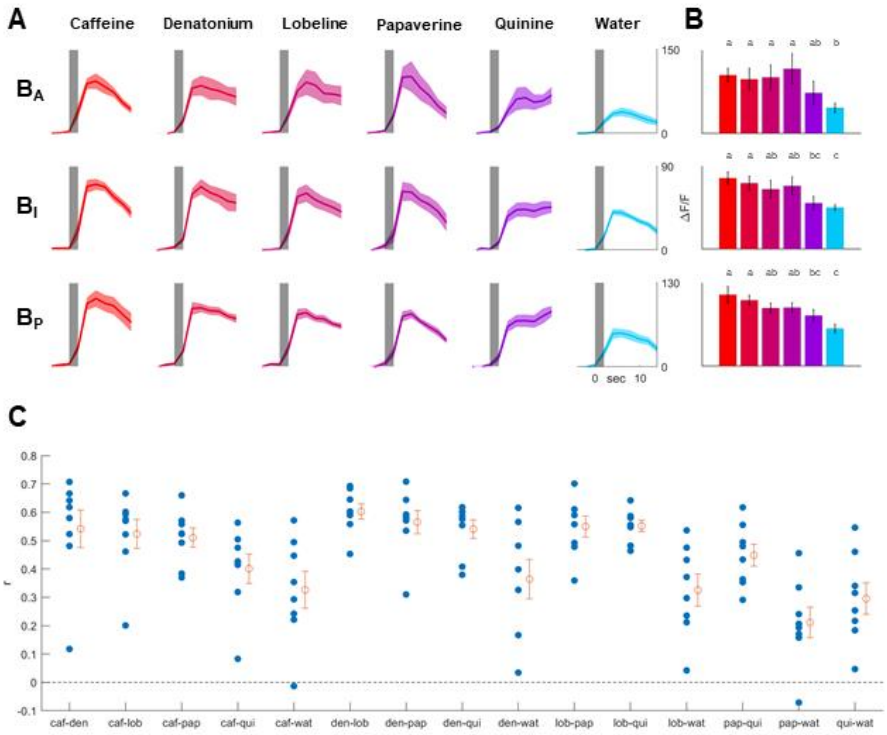

Figure 3-S6. Responses to bitter tastants within each bitter ROI.

(A) Reponses to bitter tastants in each of three bitter ROIs (n = 8). (B) Max ΔF/F for each tastant in each ROI. Letters represent statistically significant differences between groups ($p < .05$, one-way ANOVA with Tukey post-hoc test). (C) Inter-tastant correlations for individual flies. Each blue dot represents average correlation between trials of a given tastant pair for a single fly. Orange dot denotes mean; error bars denote SEM. Except for papaverine/water, correlations for all pairs were significantly greater than zero ($p < .05$, one sample t-test compared to 0, Bonferroni correction).

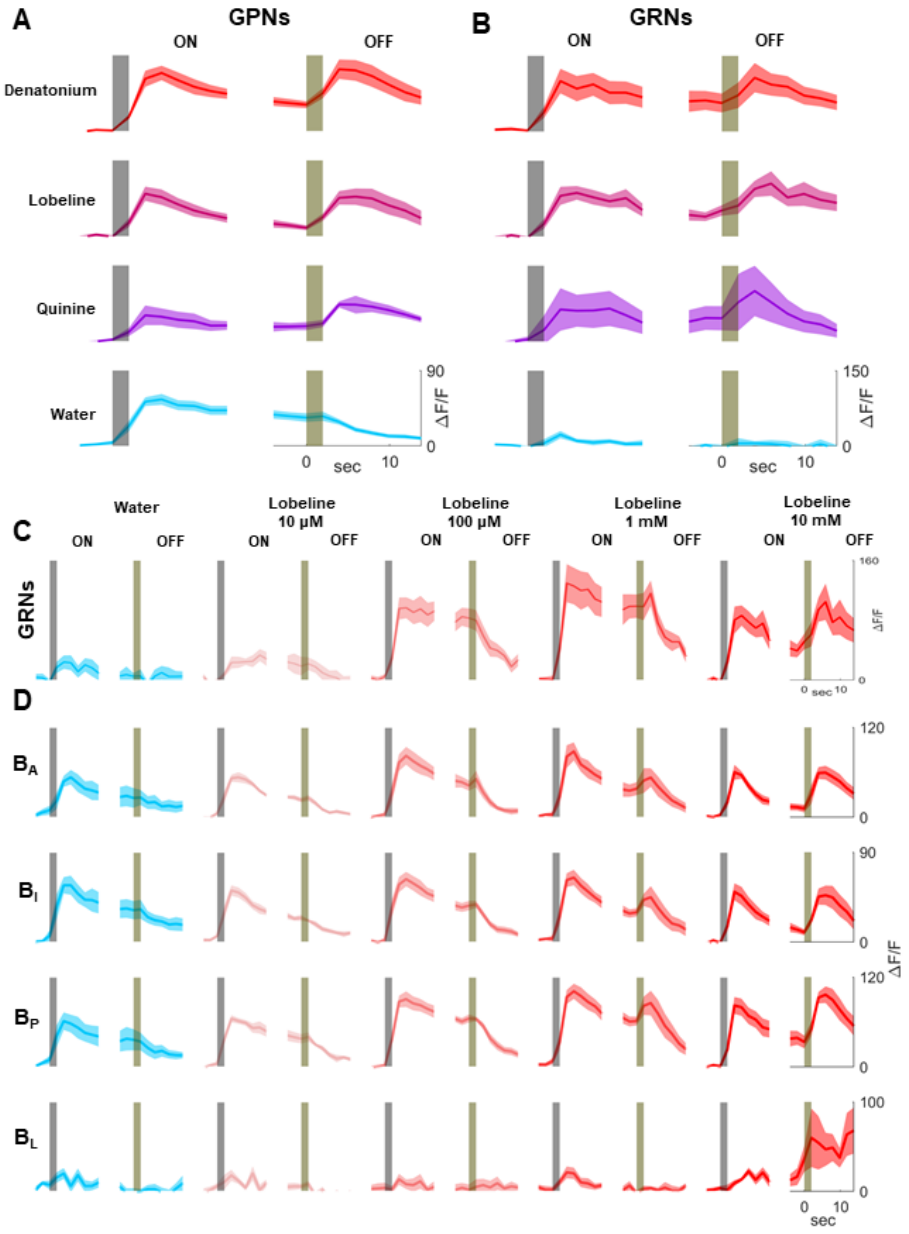

Figure 3-S7. Bitter offset response to various bitter tastants.

(A) GPN responses to onset and offset of bitter compounds and water (denatonium: n = 6; lobeline: n = 6; quinine: n = 3, water: n = 6). (B) GRN responses to onset and offset of bitter compounds and water (denatonium: n = 5; lobeline: n = 6; quinine: n = 2, water: n =

5). (C) GRN responses to increasing concentrations of lobeline (n = 6). (D) GPN responses to increasing concentrations of lobeline in different ROIs (n = 6).

CHAPTER 4

Conclusion

4.1 A mixed model of taste coding

In this dissertation, I have introduced a genetic technique for transsynaptic circuit mapping and demonstrated its utility in addressing a longstanding question in taste coding. While these findings answer some questions, they also raise many new ones. Here, I discuss the broader implications of this work, and consider some interesting directions in which future research can build upon these discoveries.

I proposed in the previous chapter that the gustatory system of *Drosophila melanogaster* adheres to a mixed model of taste coding, as opposed to strict versions of labeled line or population coding. While the question of coding models is often posed as a binary choice, it may very well be that different circuits use different strategies to represent taste. Our data suggests that this is the case for GPNs in *Drosophila*, and that strict versions of the pure labeled line or population coding models are insufficient to explain what we observed. To explore this argument more closely, let us assume that each one of the more extreme models holds true, then attempt to explain our results.

In a labeled line view, our finding that area S_D is selective for sweet is unsurprising. The bitter offset response of area B_L technically fits into such a view as well, as these responses are bitter-specific. The other areas, however, present some difficulty. Area S_L's responses may be consistent with this model if the GPNs responding to sweet and bitter offset in this area are distinct. Likewise, GPN responses in areas B_A, B_I, and B_P may be explainable only if the water/mechanosensory responses of these areas are contributed by distinct neurons than the bitter responses. However, this last possibility does not seem very likely, as our spatial maps consistently revealed a coterminous distribution of water and bitter responses throughout these regions, a finding further

substantiated by our correlation analyses. To produce such an effect with separate classes of neurons would require the existence of functionally distinct GPNs with uncannily similar arborization patterns. While we cannot rule out this possibility, it is not the most parsimonious explanation of our results.

In a population coding view, neurons co-tuned to water and bitter are, in contrast, expected. Rather, it is the narrowly tuned GPNs that are more difficult to reconcile with this model. However, they are not necessarily inconsistent. Population coding simply requires that the downstream neurons in the circuit that effect taste quality-dependent behaviors achieve their quality specificity by reading out over a population of inputs, rather than relying solely on a single input channel. If the downstream neurons that drive bitter-responsive aversive behaviors do so by integrating over both bitter-selective and non-selective GPNs, this would fulfill the criteria for a population coding model. Indeed, this may very well be the case: bitter signals from the non-selective GPN region spanning B_A, B_I, and B_P might be disambiguated from water by downstream regions in part through integration of their activity with offset responses from area B_L. Similarly, perhaps responses in S_L are integrated with responses in S_D to distinguish between sweet onset and bitter offset. This possibility seems less convincing, however, since any neurons downstream of both S_L and S_D could more easily decode sweetness by just receiving input from S_D and ignoring S_L. Thus, it is not clear that population coding is the simplest way for downstream neurons to decipher taste quality from GPN responses.

It might be more helpful to understand our results on the fly's gustatory system in terms of feature detectors rather than either labeled lines or population codes. Indeed, bitter offset, which we have mentioned often, is not a taste quality *per se*, but a kind of

gustatory "feature". Offset timing is not taste quality, but it is the critical aspect of the area's responsiveness. Yet taste quality reflects an innately relevant feature of the tastant – the chemical properties that afford it some use by the organism. Thus, in a feature coding view, it makes sense that some neurons might act as apparent "labeled lines", dedicating themselves to encoding a particular taste quality of the stimulus; the sweet-tuned GPNs innervating area S_D are an obvious example. Feature detection can therefore serve as an umbrella concept, explaining neurons either with labeled line-like properties or more sophisticated tuning properties.

What features might the other GPN response types we observed be representing? In the previous chapter, we speculated on the possibility that area S_L – in which transient responses were observed to both sweet onset and bitter offset – may comprise GPNs tuned to hedonic valence. While we do not have definitive proof that these responses are caused by a single class of neurons, it is certainly a possibility. If such neurons exist, they might reasonably be considered to be a kind of valence detector. It would further be interesting to determine if this valence encoding is restricted to sweet onset and bitter offset, or if it generalizes to other tastes as well. For instance, low concentrations of salt are appetitive to flies (especially salt-starved flies), and amino acids are appetitive, especially to mated females. If this hypothetical GPN responded to these other tastants at appetitive concentrations, it would provide a stronger case that the neuron was tuned to hedonic valence.

What about the neurons that make up areas B_A, B_I, and B_P? Assuming that a single GPN type underlies the responses in these areas, these neurons respond to all tastants tested, with strongest responses to bitter tastants (both onset and offset). Sweet

tastants evoked activity in these areas as well, although this activity was comparable to or less than that of water. This suggests that sweet tastants may inhibit the activity of these neurons, while bitter tastants enhance it. The activity of these neurons is thus inversely correlated to the palatability of the tastant. What function might a representation of "inverse palatability" serve? One possibility is that these neurons are GABAergic, and inhibit areas involved in driving behaviors. Thus, these neurons might serve as a "brake" on feeding. As for the neurons innervating area S_L, it would be interesting to determine the responses of these neurons to other tastants (like salt, for example) correlates with these tastants' respective palatability.

4.2 Possible roles of GPN responses in generating behavior

How might the features encoded by GPNs be used by downstream areas? And which downstream areas are receiving information from GPNs? The GPNs we studied project to the SLP and neighboring areas, but the SLP is an area whose function remains poorly characterized. Previous studies have implicated it as a site of fourth-order neurons of the olfactory circuit: third-order lateral horn neurons send projection to SLP, as well as to SIP and SMP, two other regions that are targeted by GPNs. Several types of sexually dimorphic neurons involved in driving courtship and aggression behaviors are also found in the SLP (Hoopfer, Jung, Inagaki, Rubin, & Anderson, 2015; Yu et al., 2010). Interestingly, some of these neurons are known to respond to gustatory inputs (Clowney et al., 2015; Kallman, Kim, & Scott, 2015). Furthermore, the dopaminergic neurons (DANs) that innervate the mushroom body have dendrites in the SLP, and several mushroom body output neurons (MBONs) send outputs to SLP as well (Aso, Hattori, et

al., 2014). Several types of neurons of the central complex, a structure involved in spatial representation and motor coordination, also receive inputs from superior protocerebrum (K. Pfeiffer & Homberg, 2014). And finally, a connectome of the *Drosophila* hemibrain was recently reconstructed from an electron microscopy volume, revealing that neurons of SLP receive inputs from and send outputs to nearly every other brain region (Scheffer et al., 2020). Altogether, these findings suggest that SLP is likely not a specialized sensory area, but rather one involved in multimodal or other more abstract processing.

What possible functions might gustatory signals perform for the animal? Since gustation signals the nutritive quality of the food, the most obvious function is to guide feeding. The feeding behavior of the fly has been proposed to consist of six consecutive subprograms: foraging, cessation of locomotion, meal initiation, ingestion, meal termination, and disengagement (Pool & Scott, 2014). In which of these six stages of feeding does taste play a role? The first and last stages – foraging and disengagement – are driven by non-gustatory cues, such as odor, wind direction, and hunger/satiety state. In contrast, taste has a decisive role in stages two through five. A walking fly stops moving and begins feeding when it contacts a source of nutrients – specifically, when the gustatory sensilla on the tarsi are excited by tastants. Tarsal contact with an appetitive tastant drives not just this cessation step, but also meal initiation: a fly with its back glued to a surface will extend its proboscis when a sweet solution is applied only to its legs. Appetitive tastants applied to the labellum can also drive proboscis extension, and further, the ingestion of these tastants. The persistence of feeding bouts, and therefore meal termination, is also influenced by taste-sensitive local interneurons of the SEZ

(Yapici et al., 2016). Thus, taste information drives or modulates at least four separate feeding subprograms.

Consequently, different neural circuits must exist to connect tastant sensation at the periphery to the motor neurons that drive these different subprograms. Most of these subprograms are carried out by the muscles of the proboscis: initiation and termination of a meal consists of the extension and retraction of the proboscis, and ingestion involves the pumping of food through the esophagus. There are 16 muscle types in the *Drosophila* proboscis, and it has been predicted that half of these are involved in each of these two programs: 8 muscles for extending and retracting the proboscis, and 8 for the driving the pumping that underlies ingestion (McKellar et al., 2020). Each proboscis muscle is innervated by only one or a very small number of motor neurons, all of which extend their dendrites into the SEZ. These motor neurons compartmentalize within the SEZ in a way that mirrors the function of the muscles they innervate: by and large, those responsible for moving the proboscis have dendrites and cell bodies in the ventral region, while those innervating pharyngeal muscles (and presumably driving ingestion) have dendrites and cell bodies in the dorsal region. This anatomical separation between motor neurons involved in different aspects of feeding may enable taste sensation (or other cues) to differentially control these behavioral subprograms.

However, evidence suggests that gustatory sensory neurons do not directly connect to any of these motor neurons. The axon terminals of sweet and bitter sensory neurons do not appear to overlap with the dendritic fields of any of these motor neurons (although they may overlap with the dendrites of a motor neuron innervating the salivary gland) (McKellar et al., 2020). Likewise, synaptic GRASP has not revealed any direct

connections between taste sensory neurons and motor neurons (Gordon & Scott, 2009). Experiments on the blowfly *Phormia regina* have suggested that at least one interneuron, and likely two, exist in between labellar gustatory neurons and their downstream motor neurons (Getting, 1971). This model was based on the observation that temporal and/or spatial summation of gustatory neuron spikes were required to drive the motor response, and the threshold for this summation was lowered by starvation. It was therefore deemed likely that an interneuron existed in this circuit that integrated sensory information and was modulated by internal state.

More recent data from *Drosophila* are consistent with the idea that SEZ interneurons are intermediates between sensory and motor stages of these gustatory circuits. While no monosynaptic connection between GRNs and MNs has been observed, synaptic GRASP experiments have revealed several types of local interneurons that apparently receive direct input from GRNs (Bohra et al., 2018; Chu, Chui, Mann, & Gordon, 2014; Kain & Dahanukar, 2015; Kim et al., 2017; Miyazaki et al., 2015; Yapici et al., 2016). Each of these local second-order neurons extends processes solely within the SEZ. Most receive taste information of just one quality – either sweet or bitter – with the exception of some local GABAergic neurons (Chu et al., 2014). Several of these second-order neurons responsive to either sweet or bitter have been shown to affect particular aspects of feeding behavior in a way that aligns with expectations based on their tuning to taste quality (Bohra et al., 2018; Kain & Dahanukar, 2015; Kim et al., 2017; Yapici et al., 2016).

While the circuits for meal initiation and ingestion are likely contained within the SEZ, it is not clear that the same is true for the prerequisite step in the feeding process,

the cessation of locomotion. When a hungry, walking fly contacts a food source with its tarsi, it must stop walking before it begins meal initiation. Gustatory information from the legs must therefore switch off the motor commands to continue moving. How might this occur? One model is that gustatory signals from tarsal GRNs, which synapse in the VNC, trigger local inhibitory networks within the VNC to silence central pattern generators and/or leg motor neurons. An alternative model is that these gustatory signals ascend to the brain to inhibit higher motor areas involved in coordinating these behaviors, such as the central complex. This second model may be more parsimonious, as it involves a single hub to control behavior; the first model, by contrast, would seem to require many direct inhibitory connections from all potential gustatory inputs to all outputs to be inhibited. However, there is evidence that sugar induces a reduction in the fly's locomotion through the tarsal GRNs that stay local to the VNC – the segmental tarsal GRNs – but not those that ascend to the SEZ (Thoma et al., 2016). Whether all taste-induced cessation of locomotion is controlled by local circuits or if ascending circuits (perhaps postsynaptic to the local, segmental tarsal GRNs) are also involved is not established.

If there is an ascending circuit that links tarsal taste information to central motor control areas to inhibit locomotion, what region might they target? The most likely candidate is the central complex, a set of connected central neuropil structures (such as the ellipsoid body and the fan-shaped body) that are involved in visuospatial representation and sensorimotor integration (Haberkern & Jayaraman, 2016; K. Pfeiffer & Homberg, 2014). Intriguingly, there is accumulating evidence that circuits of the central complex are involved in feeding regulation. A sodium/solute co-transporter-like

protein, *cupcake*, regulates the fly's preference for caloric foods independent of their taste, and is required specifically in R4 neurons of the ellipsoid body for this taste-independent preference (Dus, Ai, & Suh, 2013; J. Y. Park et al., 2016). In addition, another type of neuron that projects to the fan-shaped body is specifically involved in driving yeast consumption (Q. Liu et al., 2017). There are also reports of other fan-shaped body neurons that mediate the choice between sweet and bittersweet food options (Sareen, McCurdy, & Nitabach, 2020). These circuits appear to have at least some role in representing hunger state, nutrient and taste information; it is therefore quite possible that they have an even greater and, as of yet, unexplored role in gustatory processing.

Feeding and foraging decisions are also not hardwired, but flexible and subject to learning; as such, taste information must be integrated in central memory formation areas as well. As described in the introduction, the mushroom body (MB) is a critical brain region for memory in *Drosophila*. In conditioning experiments, when an animal is presented with a stimulus paired with a reward or punishment, it learns to associate the two, and the stimulus becomes more attractive or aversive. It has been shown in *Drosophila* that taste can act as either the conditioned stimulus, the reward, or the punishment in this paradigm (Burke et al., 2012; Kirkhart & Scott, 2015; C. Liu et al., 2012; Masek et al., 2014). In the MB, the conditioned stimulus is represented by the Kenyon cells (KCs), and the reward and punishment are represented by the dopaminergic neurons (DANs) – specifically, the PAM and PPL1 clusters of DANs, respectively (Aso, Hattori, et al., 2014; Aso et al., 2010). Taste is represented by each of these neuron types, but the circuitry linking the GRNs to each of these neurons has not yet been established.

Because the effects of taste on locomotion and learning require the central complex and mushroom body, local circuitry of the SEZ appears insufficient to explain all the roles that taste plays in behavior. However, the GPNs that we have identified may be critical components in linking the GRNs to these higher brain regions. Thus, our results on the coding strategy employed by GPNs may lend insight into how these behaviors are modulated by taste. For example, GPNs innervating region S_L – in which we observed responses to both sweet onset and bitter offset – might convey a reward signal to the mushroom body, as we postulated in the previous chapter. GPNs of the regions B_A, B_I, and B_P may likewise convey a punishment; although, if this is the case, it is curious that they also respond to water, a stimulus that is not thought to be aversive. The GPNs we studied may also be involved in circuits leading to the central complex, as it is known that central complex neurons receive inputs from the superior protocerebrum, which are targeted by all classes of GPNs – mSEZt, mlSEZt, and lSEZt. It will be interesting to trace these circuits further into the brain to address this possibility.

4.3 The bitter offset response

The idea that taste plays unintuitive roles for the animal is reinforced by the unexpected occurrence of a bitter offset response. Prior to the discovery of this response, made independently by us and another group (Devineni, Deere, Sun, & Axel, 2020), it was not appreciated that the gustatory system of *Drosophila* might encode the offset of a taste stimulus (though see Reiter et al. 2015). Hence, there is no prior literature on the particular behaviors that might be driven by this offset activity, nor on the ecological importance of taste offset for the animal. Yet, because these offset responses have

evolved, the fly's nervous system must be utilizing them for some adaptive function. Here, we consider the features of the bitter offset response that we observed, and speculate on what their function may be.

The bitter offset response is akin to the ON and OFF responses observed in several other sensory systems, including vision (Joesch, Schnell, Raghu, Reiff, & Borst, 2010; Schiller et al., 1986; Strother et al., 2014), olfaction (Burgstaller & Tichy, 2011; Chalasani et al., 2007), somatosensation (Iggo & Ogawa, 1977), thermosensation (Gallio et al., 2011), and audition (Scholl, Gao, & Wehr, 2010). In many of these systems, ON and OFF responses are split into separate, parallel pathways. This pathway splitting has been proposed to benefit the animal by allowing it to convey small changes in stimulus intensity through a lower number of spikes than purely through ON pathways, and thus, a lower metabolic cost (Gjorgjieva, Sompolinsky, & Meister, 2014). In the first order of the bitter circuit, however, ON and OFF responses are exhibited by the same set of neurons; only in the second order are neurons responding exclusively to the OFF component found. It could be that the energetic efficiency of pathway splitting drove evolution to develop a circuit mechanism for extracting just the OFF component of the GRN response. While this idea is attractive, it is quite speculative, since we currently do not know for sure what downstream function the bitter offset response performs for the animal.

However, the possibility that bitter offset encoding evolved to enable the animal to track bitter concentration gradients does suggest a hypothesis. Animals that use taste to sample continuous food sources, like flies, would be served by such a function. In contrast, animals that consume food in discrete quantities, like mammals who eat their food in bites, would not benefit from this: knowing that the food in your mouth has a

bitter gradient is no more informative of its unpleasantness than simply knowing it is bitter. Thus, if bitter offset responses evolved to guide an animal across a heterogeneous food source, we can hypothesize that only those animals that use taste to sample their environment will exhibit taste offset responses. We would not, for example, expect humans' gustatory neurons to actively encode bitter offset.

It is well known that the repertoire of gustatory receptors an animal expresses evolves with the dietary habits of the animal. Cats, for example, are carnivores whose diets do not include sugary foods, and have likewise lost their functional sweet receptors (X. Li et al., 2005). In contrast, pandas do not eat meat, and have lost their umami receptor (R. Li et al., 2010). Many birds do not have high-sugar diets, and have thus lost functional expression of their sweet receptor; but interestingly, hummingbirds, which feed on nectar, have regained this lost ability to taste sweetness through an evolution of their ancestral umami receptor into a form that detects sugars (Baldwin et al., 2014). Thus, evolution has repeatedly worked at the level of receptor expression and function to shape taste responses to match the dietary needs of an animal. Intriguingly, data from Devineni et al. (2020) suggests that the dual onset/offset response which we observe in the first-order bitter neurons of *Drosophila* is likely driven by the bitter receptors themselves. Perhaps taste offset responses are a gain-of-function receptor-level adaptation to specific foraging behaviors – and if so, they share much in common with these other examples of taste receptor evolution.

However, as highlighted earlier, the heightened contrast sensitivity conferred by ON and OFF pathways requires these signals to be relayed in *opposing* channels, a phenomenon that we report emerges at the second order of the circuit in *Drosophila*.

Thus, the bifunctional ON/OFF responses of the gustatory receptors themselves may not be sufficient to provide the adaptive function for the fly. It appears that it is also necessary to have circuit mechanisms that separate out the offset component of the signal in the transformation from the first to second order of the circuit. The loci of the evolution of this response therefore might not be limited to the receptors, but may also include regulatory regions specifying the circuit motifs underlying this signal transformation. While it may at first seem less parsimonious for evolution to act at the circuit level than the receptor level, evolution at the circuit level may be more common than presumed. For example, two closely related species of *Drosophila, D. melanogaster* and *D. simulans*, have opposite behavioral responses to the same pheromone, yet this difference is not driven by loss of function in the pheromone receptor; rather, it may result from a change in the strength of inhibition at a synapse between third- and fourth-order neurons in the circuit (Seeholzer, Seppo, Stern, & Ruta, 2018).

It is also unknown when in history these bitter offset responses evolved. The only other report of such responses in insects is in *Manduca sexta*, a lepidopteran (Reiter et al., 2015). The lepidopteran and dipteran (including *Drosophila*) lineages diverged ~290 million years ago (Misof et al., 2014); it would be interesting to know if more distantly related arthropods also exhibit bitter offset responses. As previously mentioned, it is likely that the offset responses in first-order neurons are receptor-dependent. Determining which receptors – and moreover, which domains and residues within these receptors – are responsible for the offset response may provide clues to the evolutionary origin of bitter offset coding. Phylogenetic relationships of the "offset receptor" gene family could potentially reveal the time this function developed and any lineages in which it might

have been lost. It would be intriguing if these timepoints coincided with the development of "exploratory tasting" behavior (or perhaps some other aspect of the animals' chemical ecology). As a specific example, damselflies and dragonflies of the order Odonata do not use this feeding strategy, but rather hunt live prey, and thus would not be expected to exhibit bitter offset responses (Olberg, Worthington, & Venator, 2000).

However, it may be that this hypothesis does not stand up, and that the bitter offset response has nothing to do with sensing concentration differences in the gustatory environment. What else might it possibly be doing for the fly? One possibility is that the temporal aspect is irrelevant, and the real benefit is producing twice the number of neural responses. Bitter tastants are potentially toxic, and the less of them the fly ingests, the lower the chances it poisons itself. Perhaps, by doubling the number of times that contact with the bitter tastant is encoded into neural activity, the fly gains a multiplier effect toward the detection of these noxious stimuli, and becomes sensitized to their presence. While this explanation cannot account for GPNs that selectively encode bitter offset, it could account for the dual onset/offset response seen in GRNs and other GPNs.

The microstructure of the fly's feeding behavior may support this "multiplier effect" explanation. Flies feed in one of two different modes, based on the solidity of the food source: they take long, sustained "drinks" on liquid food, and feed in bursts of short, rhythmic "sips" on more solid food (Itskov et al., 2014). It may be that the bitter offset response provides a particular advantage during the sip mode of feeding, since in this mode the proboscis makes numerous repeated contacts with the food source. Thus, when sipping on something bitter, GRNs will produce twice as many activity peaks as they

would without the offset response, perhaps facilitating downstream circuits to inhibit feeding more promptly.

If this model is accurate, the timing of stimulus offset is not the critical signal conveyed by the offset response. Yet it may still be that the temporal dynamics are quite important. Sips and inter-sip intervals have stereotyped durations: around 130-160 ms for sip length, and 80-90 ms between individual sips within a burst (Itskov et al., 2014). Moreover, these durations are not modulated by hunger state, which suggests that they are driven by a central pattern generator. This timing may have a relation to the dynamics of the bitter offset response. If the sip lengths and inter-sip intervals were much shorter, onset and offset activity peaks would become indistinguishable. Thus, the tempo of the central pattern generator may create a permissive window for offset response timing. Perhaps the kinetics of bitter offset transduction evolved to stay within the constraints of the CPG tempo, or perhaps the tempo evolved to match constraints of the receptors – or both.

4.4 Connections to the mammalian gustatory system

What insights into mammalian taste might we be able to draw from our work on *Drosophila*? Similarities between mammalian and insect gustatory systems suggest that there may be general lessons to be learned from our data. Mammalian and insect lineages are separated by approximately 670 million years of evolution (Ayala, Rzhetsky, & Ayala, 1998), yet they recognize similar categories of tastants (i.e. taste qualities), and employ a similar logic for the detection and encoding of these qualities at the periphery. This perhaps is not incredibly surprising, since taste qualities tend to reflect the

nutritional properties of the stimulus – sweet for carbohydrates, umami for protein, salty for salt – and animals across phyla require from their environment sources of calories and essential amino acids, and must maintain osmotic homeostasis. Yet sensing these factors in the environment is not sufficient; if an animal is to remedy its hunger, neural circuits must connect the sensation of nutrients to brain regions controlling ingestion. Thus, the circuits connecting sensation to behavior are just as vital. It may be that these basic metabolic requirements of animals have put selective pressure not only on the mechanisms of peripheral taste detection, but on downstream gustatory circuit architecture as well.

A major caveat in extrapolating general mechanisms of taste coding from our work is that we currently do not know which aspects of behavior are being driven by the taste signals encoded by GPNs. Ideally, we would be able to identify a complete circuit in the fly's brain linking taste to a certain aspect of behavior, and illustrate how taste information is encoded in that circuit to bring about the appropriate behavioral response. Then we could ask if this coding scheme was also used in the circuit performing the equivalent (or similar) function in the mouse's brain. For example, if we knew for sure that GPNs responding to both sweet onset and bitter offset were used to convey positive valence to the mushroom body to serve as a reward signal, we could ask if the taste circuit known to connect the PBN to the amygdala in the mouse perhaps operates along the same coding principles.

One significant advantage of our work is that we are able to distinguish the morphologies and relative projection targeting of the subsets of GPNs in our population. In contrast, a major limitation of many electrophysiological studies of the mammalian

rNST and PBN is the lack of knowledge about the types of neurons being recorded from. In particular, local neurons and projection neurons are usually not distinguished in these experiments, and may follow different patterns of tuning. Furthermore, it has been noted that many electrophysiology studies may suffer from bias in terms of the neurons recorded from. Smaller cells may be more likely to be missed, and it appears that smaller cells are more likely to be bitter-tuned, resulting in systematic bias away from identifying these cells (Spector & Travers, 2005).

Calcium imaging methods in the mouse may be able to remedy both of these problems. It would enable imaging of neurons regardless of size, resolving the second issue. And it could also resolve the first issue through strategic use of viral methods. For instance, projection neurons from the PBN could be targeted by injecting a retrogradely transported virus into one of their downstream targets, then imaging the labeled neurons in the PBN. Furthermore, gustatory projection neurons of the PBN target multiple downstream sites, including the thalamus, hypothalamus, and amygdala. It may be that isolating the neurons projecting to each of these region would reveal interesting differences in coding strategies used in these different circuits.

There may be other critical distinctions within this rNST population apart from the local vs. projection neuron difference. Specifically, molecular markers may delineate subtypes of rNST neurons with similar circuit functions and similar tuning. A recent study used the Allen Brain Atlas to identify a molecular marker, Pdyn, expressed in a subset of rNST neurons (J. Zhang et al., 2019); further, these Pdyn+ rNST neurons were reported to be narrowly tuned to sour stimuli. This strategy or similar strategies – like single-cell RNA sequencing-based transcriptomic methods – may reveal other markers.

Such transcriptionally-defined cell types may align with functional cell types, and provide a better understanding of the logic of taste coding in this region.

Our data also suggest some other stimulus features besides taste quality that may be encoded by rNST neurons. Taste offset coding, for example, may be present in the rNST. Most studies on this region have used extracellular recordings, which would have revealed such offset tuning. However, such offset responses have either not been discovered in these regions, or at least have not been widely reported. In addition, we discovered GPNs in *Drosophila* that respond to sweet tastants with different kinetics; there may be similar distinctions in the temporal dynamics of rNST neurons as well.

All in all, there are many possible directions for future research on the neural circuits of taste, in mammals as well as flies. In this work, I have shown how *Drosophila* can be of great utility in addressing longstanding questions about neural circuits and neural coding. I have demonstrated the function of a novel genetic method for transsynaptic tracing, and used it to identify second-order neurons in a defined neural circuit. Further, by combining this method with calcium imaging, I have found that projection neurons downstream of sweet and bitter neurons appear to employ a hybrid model of taste coding, where some neurons function like labeled lines for single taste qualities, while others respond to tastants across multiple qualities. I have further shown how an unexpected feature – bitter taste offset – is encoded by these circuits, raising question about the relevant features that are detected by the gustatory system. There is still much more to be discovered regarding how these neurons represent taste, how other circuits in the fly encode taste, how taste information in each of these circuits is processed by downstream neurons to drive behaviors, and more. But even though there is

still much left to understand about these circuits, the discoveries made here will hopefully spark new ideas and generate new hypotheses for how brains of all species – from fly to human – create this mysterious and misunderstood sense of taste.

BIBLIOGRAPHY

Abuin, L., Bargeton, B., Ulbrich, M. H., Isacoff, E. Y., Kellenberger, S., & Benton, R. (2011). Functional Architecture of Olfactory Ionotropic Glutamate Receptors. *Neuron*, *69*(1), 44–60. https://doi.org/10.1016/j.neuron.2010.11.042

Accolla, R., Bathellier, B., Petersen, C. C. H., & Carleton, A. (2007). Differential spatial representation of taste modalities in the rat gustatory cortex. *Journal of Neuroscience*, *27*(6), 1396–1404. https://doi.org/10.1523/JNEUROSCI.5188-06.2007

Adler, E., Hoon, M. A., Mueller, K. L., Chandrashekar, J., Ryba, N. J. ., & Zuker, C. S. (2000). A Novel Family of Mammalian Taste Receptors. *Cell*, *100*(6), 693–702. https://doi.org/10.1016/S0092-8674(00)80705-9

Apostolopoulou, A. A., Rist, A., & Thum, A. S. (2015). Taste processing in Drosophila larvae. *Frontiers in Integrative Neuroscience*, *9*(OCT), 1–9. https://doi.org/10.3389/fnint.2015.00050

Aso, Y., Grübel, K., Busch, S., Friedrich, A. B., Siwanowicz, I., & Tanimoto, H. (2009). The mushroom body of adult Drosophila characterized by GAL4 drivers. *Journal of Neurogenetics*, *23*(1–2), 156–172. https://doi.org/10.1080/01677060802471718

Aso, Y., Hattori, D., Yu, Y., Johnston, R. M., Iyer, N. a, Ngo, T.-T., … Rubin, G. M. (2014). The neuronal architecture of the mushroom body provides a logic for associative learning. *ELife*, *3*, 1–47. https://doi.org/10.7554/eLife.04577

Aso, Y., Sitaraman, D., Ichinose, T., Kaun, K. R., Vogt, K., Belliart-Guérin, G., … Rubin, G. M. (2014). Mushroom body output neurons encode valence and guide memory-based action selection in Drosophila. *ELife*, *3*(3), 1–42. https://doi.org/10.7554/eLife.04580

Aso, Y., Siwanowicz, I., Bräcker, L., Ito, K., Kitamoto, T., & Tanimoto, H. (2010). Specific dopaminergic neurons for the formation of labile aversive memory. *Current Biology : CB*, *20*(16), 1445–1451. https://doi.org/10.1016/j.cub.2010.06.048

Ayala, F. J., Rzhetsky, A., & Ayala, F. J. (1998). Origin of the metazoan phyla: Molecular clocks confirm paleontological estimates. *Proceedings of the National Academy of Sciences of the United States of America*, *95*(2), 606–611. https://doi.org/10.1073/pnas.95.2.606

Baldwin, M. W., Toda, Y., Nakagita, T., O'Connell, M. J., Klasing, K. C., Misaka, T., … Liberles, S. D. (2014). Evolution of sweet taste perception in hummingbirds by transformation of the ancestral umami receptor. *Science*, *345*(6199), 929–933. https://doi.org/10.1126/science.1255097

Barnea, G., Strapps, W., Herrada, G., Berman, Y., Ong, J., Kloss, B., … Lee, K. J. (2008). The genetic design of signaling cascades to record receptor activation. *Proceedings of the National Academy of Sciences of the United States of America*, *105*(1), 64–69. https://doi.org/10.1073/pnas.0710487105

Barretto, R. P. J., Gillis-smith, S., Chandrashekar, J., Yarmolinsky, D. A., Schnitzer, M. J., Ryba, N. J. P., & Zuker, C. S. (2015). The neural representation of taste quality at the periphery. *Nature*, *517*(7534), 373–376. https://doi.org/10.1038/nature13873

Bartoshuk, L. M., & Beauchamp, G. K. (1994). Chemical senses. *Annual Review of Psychology*, (45), 419–449. https://doi.org/10.4324/9781351320047-28

Beauchamp, G. K. (2019). Basic Taste: A Perceptual Concept. *Journal of Agricultural and Food Chemistry*, *67*(50), 13860–13869. https://doi.org/10.1021/acs.jafc.9b03542

Behnia, R., Clark, D. A., Carter, A. G., Clandinin, T. R., & Desplan, C. (2014). Processing properties of on and off pathways for Drosophila motion detection. *Nature*, *512*(7515), 427–430. https://doi.org/10.1038/nature13427

Behrens, M., Foerster, S., Staehler, F., Raguse, J. D., & Meyerhof, W. (2007). Gustatory expression pattern of the human TAS2R bitter receptor gene family reveals a heterogenous population of bitter responsive taste receptor cells. *Journal of Neuroscience*, *27*(46), 12630–12640. https://doi.org/10.1523/JNEUROSCI.1168-07.2007

Bellen, H. J., Tong, C., & Tsuda, H. (2010). 100 Years of Drosophila Research and Its Impact on Vertebrate Neuroscience: a History Lesson for the Future. *Nature Reviews Neuroscience*, *11*, 514–522. https://doi.org/10.1038/nrn2839

Benton, R., Sachse, S., Michnick, S. W., & Vosshall, L. B. (2006). Atypical membrane topology and heteromeric function of Drosophila odorant receptors in vivo. *PLoS Biology*, *4*(2), 240–257. https://doi.org/10.1371/journal.pbio.0040020

Benton, R., Vannice, K. S., Gomez-Diaz, C., & Vosshall, L. B. (2009). Variant Ionotropic Glutamate Receptors as Chemosensory Receptors in Drosophila. *Cell*, *136*(1), 149–162. https://doi.org/10.1016/j.cell.2008.12.001

Bischof, J., Maeda, R. K., Hediger, M., Karch, F., & Basler, K. (2007). An optimized transgenesis system for Drosophila using germ-line-specific phiC31 integrases. *Proceedings of the National Academy of Sciences of the United States of America*, *104*(9), 3312–3317. https://doi.org/10.1073/pnas.0611511104

Blankenship, M. L., Grigorova, M., Katz, D. B., & Maier, J. X. (2019). Retronasal Odor Perception Requires Taste Cortex, but Orthonasal Does Not. *Current Biology*, *29*(1),

62-69.e3. https://doi.org/10.1016/j.cub.2018.11.011

Bohra, A. A., Kallman, B. R., Reichert, H., & VijayRaghavan, K. (2018). Identification of a Single Pair of Interneurons for Bitter Taste Processing in the Drosophila Brain. *Current Biology*, 1–12. https://doi.org/10.1016/j.cub.2018.01.084

Boscolo-Rizzo, P., Borsetto, D., Fabbris, C., Spinato, G., Frezza, D., Menegaldo, A., … Hopkins, C. (2020). Evolution of Altered Sense of Smell or Taste in Patients with Mildly Symptomatic COVID-19. *JAMA Otolaryngology - Head and Neck Surgery*, *146*(8), 1–5. https://doi.org/10.1001/jamaoto.2020.1379

Brand, A. H., & Perrimon, N. (1993). Targeted gene expression as a means of altering cell fates and generating dominant phenotypes. *Development (Cambridge, England)*, *118*(2), 401–415. Retrieved from http://www.ncbi.nlm.nih.gov/pubmed/8223268

Breslin, P. A. S., Beauchamp, G. K., & Pugh, E. N. (1996). Monogeusia for fructose, glucose, sucrose, and maltose. *Perception and Psychophysics*, *58*(3), 327–341. https://doi.org/10.3758/BF03206809

Breslin, P. A. S., Kemp, S., & Beauchamp, G. K. (1994). Single sweetness signal. *Nature*, *369*(6480), 447–448. https://doi.org/10.1038/369447a0

Briggman, K. L., & Bock, D. D. (2012). Volume electron microscopy for neuronal circuit reconstruction. *Current Opinion in Neurobiology*, *22*(1), 154–161. https://doi.org/10.1016/j.conb.2011.10.022

Buck, L., & Axel, R. (1991). A novel multigene family may encode odorant receptors: a molecular basis for odor recognition. *Cell*, *65*(1), 175–187. Retrieved from http://www.ncbi.nlm.nih.gov/pubmed/1840504

Burgstaller, M., & Tichy, H. (2011). Functional asymmetries in cockroach ON and OFF

olfactory receptor neurons. *Journal of Neurophysiology*, *105*(2), 834–845. https://doi.org/10.1152/jn.00785.2010

Burke, C. J., Huetteroth, W., Owald, D., Perisse, E., Krashes, M. J., Das, G., … Waddell, S. (2012). Layered reward signalling through octopamine and dopamine in Drosophila. *Nature*, *492*(7429), 433–437. https://doi.org/10.1038/nature11614

Butterwick, J. A., del Mármol, J., Kim, K. H., Kahlson, M. A., Rogow, J. A., Walz, T., & Ruta, V. (2018). Cryo-EM structure of the insect olfactory receptor Orco. *Nature*. https://doi.org/10.1038/s41586-018-0420-8

Caicedo, A., & Roper, S. D. (2001). Taste receptor cells that discriminate between bitter stimuli. *Science*, *291*(5508), 1557–1560. https://doi.org/10.1126/science.1056670

Callaway, E. M., & Luo, L. (2015). Monosynaptic circuit tracing with glycoprotein-deleted rabies viruses. *Journal of Neuroscience*, *35*(24), 8979–8985. https://doi.org/10.1523/JNEUROSCI.0409-15.2015

Cameron, P., Hiroi, M., Ngai, J., & Scott, K. (2010). The molecular basis for water taste in Drosophila. *Nature*, *465*(7294), 91–95. https://doi.org/10.1038/nature09011

Caron, S. J. C., Ruta, V., Abbott, L. F., & Axel, R. (2013). Random convergence of olfactory inputs in the Drosophila mushroom body. *Nature*, *497*(7447), 113–117. https://doi.org/10.1038/nature12063

Chalasani, S. H., Chronis, N., Tsunozaki, M., Gray, J. M., Ramot, D., Goodman, M. B., & Bargmann, C. I. (2007). Dissecting a circuit for olfactory behaviour in Caenorhabditis elegans. *Nature*, *450*(7166), 63–70. https://doi.org/10.1038/nature06292

Chandrashekar, J., Hoon, M. A., Ryba, N. J. P., & Zuker, C. S. (2006). The receptors and

cells for mammalian taste. *Nature*, *444*(7117), 288–294. https://doi.org/10.1038/nature05401

Chandrashekar, J., Kuhn, C., Oka, Y., Yarmolinsky, D. A., Hummler, E., Ryba, N. J. P., & Zuker, C. S. (2010). The cells and peripheral representation of sodium taste in mice. *Nature*, *464*(7286), 297–301. https://doi.org/10.1038/nature08783

Chandrashekar, J., Mueller, K. L., Hoon, M. A., Adler, E., Feng, L., Guo, W., … Ryba, N. J. . (2000a). T2Rs Function as Bitter Taste Receptors. *Cell*, *100*(6), 703–711. https://doi.org/10.1016/S0092-8674(00)80706-0

Chandrashekar, J., Mueller, K. L., Hoon, M. A., Adler, E., Feng, L., Guo, W., … Ryba, N. J. P. (2000b). T2Rs function as bitter taste receptors. *Cell*, *100*(6), 703–711. https://doi.org/10.1016/S0092-8674(00)80706-0

Chandrashekar, J., Yarmolinsky, D., Von Buchholtz, L., Oka, Y., Sly, W., Ryba, N. J. P., & Zuker, C. S. (2009). The taste of carbonation. *Science*, *326*(5951), 443–445. https://doi.org/10.1126/science.1174601

Chang, R. B., Waters, H., & Liman, E. R. (2010). A proton current drives action potentials in genetically identified sour taste cells. *Proceedings of the National Academy of Sciences of the United States of America*, *107*(51), 22320–22325. https://doi.org/10.1073/pnas.1013664107

Charlu, S., Wisotsky, Z., Medina, A., & Dahanukar, A. (2013). Acid sensing by sweet and bitter taste neurons in Drosophila melanogaster. *Nature Communications*, *4*(May), 1–10. https://doi.org/10.1038/ncomms3042

Chaudhari, N., Landin, A. M., & Roper, S. D. (2000). A metabotropic glutamate receptor variant functions as a taste receptor. *Nature Neuroscience*, *3*(2), 113–119.

https://doi.org/10.1038/72053

Chen, T.-W., Wardill, T. J., Sun, Y., Pulver, S. R., Renninger, S. L., Baohan, A., … Kim, D. S. (2013). Ultrasensitive fluorescent proteins for imaging neuronal activity. *Nature*, *499*(7458), 295–300. https://doi.org/10.1038/nature12354

Chen, X., Gabitto, M., Peng, Y., Ryba, N. J. P., & Zuker, C. S. (2011). A Gustotopic Map of Taste Qualities in the Mammalian Brain, (September), 1262–1267.

Chen, Y., Akin, O., Nern, A., Tsui, C. Y. K., Pecot, M. Y., & Zipursky, S. L. (2014). Cell-type-specific labeling of synapses in vivo through synaptic tagging with recombination. *Neuron*, *81*(2), 280–293. https://doi.org/10.1016/j.neuron.2013.12.021

Chiang, A.-S., Lin, C.-Y., Chuang, C.-C., Chang, H.-M., Hsieh, C.-H., Yeh, C.-W., … Hwang, J.-K. (2011). Three-dimensional reconstruction of brain-wide wiring networks in Drosophila at single-cell resolution. *Current Biology : CB*, *21*(1), 1–11. https://doi.org/10.1016/j.cub.2010.11.056

Cho, Y. K., Li, C. S., & Smith, D. V. (2002). Gustatory projections from the nucleus of the solitary tract to the parabrachial nuclei in the hamster. *Chemical Senses*, *27*(1), 81–90. https://doi.org/10.1093/chemse/27.1.81

Chou, T. B., & Perrimon, N. (1992). Use of a yeast site-specific recombinase to produce female germline chimeras in drosophila. *Genetics*, *131*(3), 643–653.

Chou, Y.-H., Spletter, M. L., Yaksi, E., Leong, J. C. S., Wilson, R. I., & Luo, L. (2010). Diversity and wiring variability of olfactory local interneurons in the Drosophila antennal lobe. *Nature Neuroscience*, *13*(4), 439–449. https://doi.org/10.1038/nn.2489

Chu, B., Chui, V., Mann, K., & Gordon, M. D. (2014). Presynaptic Gain Control Drives Sweet and Bitter Taste Integration in Drosophila. *Current Biology*, *24*(17), 1978–1984. https://doi.org/10.1016/j.cub.2014.07.020

Clowney, E. J., Iguchi, S., Bussell, J. J., Scheer, E., & Ruta, V. (2015). Multimodal Chemosensory Circuits Controlling Male Courtship in Drosophila. *Neuron*, *87*(5), 1036–1049. https://doi.org/10.1016/j.neuron.2015.07.025

Clyne, P. J., Warr, C. G., & Carlson, J. R. (2000). Candidate taste receptors in Drosophila. *Science*, *287*(5459), 1830–1834. https://doi.org/10.1126/science.287.5459.1830

Cohn, R., Morantte, I., & Ruta, V. (2015). Coordinated and Compartmentalized Neuromodulation Shapes Sensory Processing in Drosophila. *Cell*, *163*(7), 1742–1755. https://doi.org/10.1016/j.cell.2015.11.019

Court, R., Namiki, S., Armstrong, J. D., Börner, J., Card, G., Costa, M., … Shepherd, D. (2020). A Systematic Nomenclature for the Drosophila Ventral Nerve Cord. *Neuron*, *107*(6), 1071-1079.e2. https://doi.org/10.1016/j.neuron.2020.08.005

Dahanukar, A., Foster, K., Van der Goes van Naters, W. M., & Carlson, J. R. (2001). A Gr receptor is required for response to the sugar trehalose in taste neurons of Drosophila. *Nature Neuroscience*, *4*(12), 1182–1186. https://doi.org/10.1038/nn765

Dahanukar, A., Lei, Y. T., Kwon, J. Y., & Carlson, J. R. (2007). Two Gr Genes Underlie Sugar Reception in Drosophila. *Neuron*, *56*(3), 503–516. https://doi.org/10.1016/j.neuron.2007.10.024

Damak, S., Rong, M., Yasumatsu, K., Kokrashvili, Z., Varadarajan, V., Zou, S., … Margolskee, R. F. (2003). Detection of sweet and umami taste in the absence of taste

receptor T1r3. *Science*, *301*(5634), 850–853. https://doi.org/10.1126/science.1087155

Dana, H., Sun, Y., Mohar, B., Hulse, B. K., Kerlin, A. M., Hasseman, J. P., … Kim, D. S. (2019). High-performance calcium sensors for imaging activity in neuronal populations and microcompartments. *Nature Methods*, *16*(7), 649–657. https://doi.org/10.1038/s41592-019-0435-6

Datta, S. R., Vasconcelos, M. L., Ruta, V., Luo, S., Wong, A., Demir, E., … Axel, R. (2008). The Drosophila pheromone cVA activates a sexually dimorphic neural circuit. *Nature*, *452*(7186), 473–477. https://doi.org/10.1038/nature06808

De Robertis, E. D., & Bennett, H. S. (1955). Some features of the submicroscopic morphology of synapses in frog and earthworm. *The Journal of Biophysical and Biochemical Cytology*, *1*(1), 47–58. https://doi.org/10.1083/jcb.1.1.47

Delventhal, R., & Carlson, J. R. (2016). Bitter taste receptors confer diverse functions to neurons. *ELife*, *5*(FEBRUARY2016), 1–23. https://doi.org/10.7554/eLife.11181

Dethier, V. G. (1978). Other tastes, other worlds. *Science*, *201*(4352), 224–228. https://doi.org/10.1126/science.663651

Devineni, A. V, Deere, J. U., Sun, B., & Axel, R. (2020). Individual bitter-sensing neurons in Drosophila exhibit both ON and OFF responses that influence synaptic plasticity.

Devineni, A. V, Sun, B., Zhukovskaya, A., & Axel, R. (2019). Acetic acid activates distinct taste pathways in Drosophila to elicit opposing, state-dependent feeding responses. *ELife*, *8*, 1–23. https://doi.org/10.7554/eLife.47677.001

Di Lorenzo, P. M., & Victor, J. D. (2003). Taste response variability and temporal coding

in the nucleus of the solitary tract of the rat. *Journal of Neurophysiology*, *90*(3), 1418–1431. https://doi.org/10.1152/jn.00177.2003

Dionne, H., Hibbard, K. L., Cavallaro, A., Kao, J. C., & Rubin, G. M. (2018). Genetic reagents for making split-GAL4 lines in Drosophila. *Genetics*, *209*(1), 31–35. https://doi.org/10.1534/genetics.118.300682

Dunipace, L., Meister, S., Mcnealy, C., & Amrein, H. (2001). Spatially restricted expression of candidate taste receptors in the. *Current Biology*, (11), 822–835.

Dus, M., Ai, M., & Suh, G. S. B. (2013). Taste-independent nutrient selection is mediated by a brain-specific Na+ /solute co-transporter in Drosophila. *Nature Neuroscience*, *16*(5), 526–528. https://doi.org/10.1038/nn.3372

Dus, M., Lai, J. S., Gunapala, K. M., Geraud, E., Joseph, C. M., Suh, G. S. B., … Suh, G. S. B. (2015). Nutrient Sensor in the Brain Directs the Action of the Brain-Gut Axis in Drosophila. *Neuron*, *87*(1), 139–151. https://doi.org/10.1016/j.neuron.2015.05.032

Dweck, H. K. M., & Carlson, J. R. (2020). Molecular Logic and Evolution of Bitter Taste in Drosophila. *Current Biology*, *30*(1), 17-30.e3. https://doi.org/10.1016/j.cub.2019.11.005

Erickson, R. (2008). A study of the science of taste: On the origins and influence of the core ideas. *Behavioral and Brain Sciences*, *31*(1), 59–105. https://doi.org/10.1017/S0140525X08003348

Fan, P., Manoli, D. S., Ahmed, O. M., Chen, Y., Agarwal, N., Kwong, S., … Shah, N. M. (2013). Genetic and neural mechanisms that inhibit drosophila from mating with other species. *Cell*, *154*(1), 89–102. https://doi.org/10.1016/j.cell.2013.06.008

Feinberg, E. H., VanHoven, M. K., Bendesky, A., Wang, G., Fetter, R. D., Shen, K., & Bargmann, C. I. (2008). GFP Reconstitution Across Synaptic Partners (GRASP) Defines Cell Contacts and Synapses in Living Nervous Systems. *Neuron*, *57*, 353–363. https://doi.org/10.1016/j.neuron.2007.11.030

Finger, S. (1994). *Origins of Neuroscience*. New York: Oxford University Press.

Fischler, W., Kong, P., Marella, S., & Scott, K. (2007). The detection of carbonation by the Drosophila gustatory system. *Nature*, *448*(7157), 1054–1057. https://doi.org/10.1038/nature06101

Fishilevich, E., & Vosshall, L. B. (2005). Genetic and functional subdivision of the Drosophila antennal lobe. *Current Biology : CB*, *15*(17), 1548–1553. https://doi.org/10.1016/j.cub.2005.07.066

Fletcher, M. L., Ogg, M. C., Lu, L., Ogg, R. J., & Boughter, J. D. (2017). Overlapping Representation of Primary Tastes in a Defined Region of the Gustatory Cortex. *The Journal of Neuroscience*, *37*(32), 7595–7605. https://doi.org/10.1523/jneurosci.0649-17.2017

Flood, T. F., Iguchi, S., Gorczyca, M., White, B., Ito, K., & Yoshihara, M. (2013). A single pair of interneurons commands the Drosophila feeding motor program. *Nature*, *499*(7456), 83–87. https://doi.org/10.1038/nature12208

Fortin, J.-P., Zhu, Y., Choi, C., Beinborn, M., Nitabach, M. N., & Kopin, A. S. (2009). Membrane-tethered ligands are effective probes for exploring class B1 G protein-coupled receptor function. *Proceedings of the National Academy of Sciences of the United States of America*, *106*(19), 8049–8054. https://doi.org/10.1073/pnas.0900149106

Frank, M. E. (1991). Taste-responsive neurons of the glossopharyngeal nerve of the rat, *65*(6), 1452–1463.

Frank, M. E. (2000). Neuron types, receptors, behavior, and taste quality. *Physiology and Behavior*, *69*(1), 53–62. https://doi.org/10.1016/S0031-9384(00)00188-8

Frank, M. E., Bieber, S. L., & Smith, D. V. (1988). The organization of taste sensibilities in hamster chorda tympani nerve fibers. *Journal of General Physiology*, *91*(6), 861–896. https://doi.org/10.1085/jgp.91.6.861

Freeman, E. G., & Dahanukar, A. (2015). Molecular neurobiology of Drosophila taste. *Current Opinion in Neurobiology*, *34*, 140–148. https://doi.org/10.1016/j.conb.2015.06.001

Freeman, E. G., Wisotsky, Z., & Dahanukar, A. (2014). Detection of sweet tastants by a conserved group of insect gustatory receptors. *Proceedings of the National Academy of Sciences of the United States of America*, *111*(4), 1598–1603. https://doi.org/10.1073/pnas.1311724111

Fu, O., Iwai, Y., Kondoh, K., Misaka, T., Minokoshi, Y., & Nakajima, K. (2019). SatB2-Expressing Neurons in the Parabrachial Nucleus Encode Sweet Taste. *Cell Reports*, *27*(6), 1650-1656.e4. https://doi.org/10.1016/j.celrep.2019.04.040

Fujii, S., Yavuz, A., Slone, J., Jagge, C., Song, X., & Amrein, H. (2015). Drosophila Sugar Receptors in Sweet Taste Perception, Olfaction, and Internal Nutrient Sensing. *Current Biology*, *25*(5), 621–627. https://doi.org/10.1016/j.cub.2014.12.058

Gallio, M., Ofstad, T. A., Macpherson, L. J., Wang, J. W., & Zuker, C. S. (2011). The coding of temperature in the Drosophila brain. *Cell*, *144*(4), 614–624.

https://doi.org/10.1016/j.cell.2011.01.028

Ganguly, A., Pang, L., Duong, V. K., Lee, A., Schoniger, H., Varady, E., & Dahanukar, A. (2017). A Molecular and Cellular Context-Dependent Role for Ir76b in Detection of Amino Acid Taste. *Cell Reports*, *18*(3), 737–750. https://doi.org/10.1016/j.celrep.2016.12.071

Geran, L. C., & Travers, S. P. (2009). Bitter-responsive gustatory neurons in the rat parabrachial nucleus. *Journal of Neurophysiology*, *101*(3), 1598–1612. https://doi.org/10.1152/jn.91168.2008

Gerber, B., Yarali, A., Diegelmann, S., Wotjak, C. T., Pauli, P., & Fendt, M. (2014). Pain-relief learning in flies, rats, and man: Basic research and applied perspectives. *Learning and Memory*, *21*(4), 232–252. https://doi.org/10.1101/lm.032995.113

Getting, P. A. (1971). The sensory control of motor output in fly proboscis extension. *Zeitschrift Für Vergleichende Physiologie*, *74*(1), 103–120. https://doi.org/10.1007/BF00297793

Gibson, D. G., Young, L., Chuang, R. Y., Venter, J. C., Hutchison, C. A., & Smith, H. O. (2009). Enzymatic assembly of DNA molecules up to several hundred kilobases. *Nature Methods*, *6*(5), 343–345. https://doi.org/10.1038/nmeth.1318

Gjorgjieva, J., Sompolinsky, H., & Meister, M. (2014). Benefits of pathway splitting in sensory coding. *Journal of Neuroscience*, *34*(36), 12127–12144. https://doi.org/10.1523/JNEUROSCI.1032-14.2014

Glendinning, J. I. (1994). Is the bitter rejection response always adaptive? *Physiology and Behavior*, *56*(6), 1217–1227. https://doi.org/10.1016/0031-9384(94)90369-7

Gordon, M. D., & Scott, K. (2009). Motor control in a Drosophila taste circuit. *Neuron*,

61(3), 373–384. https://doi.org/10.1016/j.neuron.2008.12.033

Grabe, V., Baschwitz, A., Dweck, H. K. M., Lavista-Llanos, S., Hansson, B. S., & Sachse, S. (2016). Elucidating the Neuronal Architecture of Olfactory Glomeruli in the Drosophila Antennal Lobe. *Cell Reports*, *16*(12), 3401–3413. https://doi.org/10.1016/j.celrep.2016.08.063

Groth, A. C., Fish, M., Nusse, R., & Calos, M. P. (2004). Construction of Transgenic Drosophila by Using the Site-Specific Integrase from Phage φC31. *Genetics*, *166*(4), 1775–1782. https://doi.org/10.1534/genetics.166.4.1775

Haberkern, H., & Jayaraman, V. (2016). Studying small brains to understand the building blocks of cognition. *Current Opinion in Neurobiology*, *37*, 59–65. https://doi.org/10.1016/j.conb.2016.01.007

Hannum, M. E., Ramirez, V. A., Lipson, S. J., Herriman, R. D., Toskala, A. K., Lin, C., … Reed, D. R. (2020). Objective sensory testing methods reveal a higher prevalence of olfactory loss in COVID-19–positive patients compared to subjective methods: A systematic review and meta-analysis. *Chemical Senses*. https://doi.org/10.1093/chemse/bjaa064

Harris, D. T., Kallman, B. R., Mullaney, B. C., & Scott, K. (2015). Representations of Taste Modality in the Drosophila Brain. *Neuron*, *86*(6), 1449–1460. https://doi.org/10.1016/j.neuron.2015.05.026

He, Z., Luo, Y., Shang, X., Sun, J. S., & Carlson, J. R. (2019). Chemosensory sensilla of the Drosophila wing express a candidate ionotropic pheromone receptor. *PLoS Biology*, *17*(5), 1–27. https://doi.org/10.1371/journal.pbio.2006619

Heck, G. L., Mierson, S., & Desimone, J. A. (1984). Salt taste transduction occurs

through an amiloride-sensitive sodium transport pathway. *Science*, *223*(4634), 403–405. https://doi.org/10.1126/science.6691151

Heimbeck, G., Bugnon, V., Gendre, N., Keller, a, & Stocker, R. F. (2001). A central neural circuit for experience-independent olfactory and courtship behavior in Drosophila melanogaster. *Proceedings of the National Academy of Sciences of the United States of America*, *98*(26), 15336–15341. https://doi.org/10.1073/pnas.011314898

Hettinger, T. P., & Frank, M. E. (1990). Specificity of amiloride inhibition of hamster taste responses. *Brain Research*, *513*(1), 24–34. https://doi.org/10.1016/0006-8993(90)91085-U

Hige, T., Aso, Y., Rubin, G. M., & Turner, G. C. (2015). Plasticity-driven individualization of olfactory coding in mushroom body output neurons. *Nature*. https://doi.org/10.1038/nature15396

Honegger, K. S., Campbell, R. a a, & Turner, G. C. (2011). Cellular-resolution population imaging reveals robust sparse coding in the Drosophila mushroom body. *The Journal of Neuroscience : The Official Journal of the Society for Neuroscience*, *31*(33), 11772–11785. https://doi.org/10.1523/JNEUROSCI.1099-11.2011

Hong, S. T., Bang, S., Paik, D., Kang, J., Hwang, S., Jeon, K., … Kim, J. (2006). Histamine and its receptors modulate temperature-preference behaviors in Drosophila. *The Journal of Neuroscience : The Official Journal of the Society for Neuroscience*, *26*(27), 7245–7256. https://doi.org/10.1523/JNEUROSCI.5426-05.2006

Hong, W., Zhu, H., Potter, C. J., Barsh, G., Kurusu, M., Zinn, K., & Luo, L. (2009).

Leucine-rich repeat transmembrane proteins instruct discrete dendrite targeting in an olfactory map. *Nature Neuroscience*, *12*(12), 1542–1550. https://doi.org/10.1038/nn.2442

Hoon, M. A., Adler, E., Lindemeier, J., Battey, J. F., Ryba, N. J. P., & Zuker, C. S. (1999). Putative mammalian taste receptors: A class of taste-specific GPCRs with distinct topographic selectivity. *Cell*, *96*(4), 541–551. https://doi.org/10.1016/S0092-8674(00)80658-3

Hoopfer, E. D., Jung, Y., Inagaki, H. K., Rubin, G. M., & Anderson, D. J. (2015). P1 interneurons promote a persistent internal state that enhances inter-male aggression in Drosophila. *ELife*. https://doi.org/10.1017/CBO9781107415324.004

Huang, L., Shanker, Y. G., Dubauskaite, J., Zheng, J. Z., Yan, W., Rosenweig, S., … Margolskee, R. F. (1999). Gγ13 colocalizes with gustducin in taste receptor cells and mediates IP3 responses to bitter denatonium. *Nature Neuroscience*, *2*(12), 1055–1062. https://doi.org/10.1038/15981

Huang, Y. A., Pereira, E., & Roper, S. D. (2011). Acid stimulation (sour taste) elicits GABA and serotonin release from mouse taste cells. *PLoS ONE*, *6*(10). https://doi.org/10.1371/journal.pone.0025471

Huh, Y., Oh, M. S., Leblanc, P., & Kim, K. S. (2010). Gene transfer in the nervous system and implications for transsynaptic neuronal tracing. *Expert Opinion on Biological Therapy*, *10*(5), 763–772. https://doi.org/10.1517/14712591003796538

Iggo, A., & Ogawa, H. (1977). Correlative physiological and morphological studies of rapidly adapting mechanoreceptors in cat's glabrous skin. *The Journal of Physiology*, *266*(2), 275–296. https://doi.org/10.1113/jphysiol.1977.sp011768

Ikeda, K. (2002). New Seasonings. *Chemical Senses*, *27*(9), 847–849. https://doi.org/10.1093/chemse/27.9.847

Imai, T., Sakano, H., & Vosshall, L. B. (2010). Topographic mapping--the olfactory system. *Cold Spring Harb Perspect Biol*, *2*(8), a001776. https://doi.org/10.1101/cshperspect.a001776

Inagaki, H. K., Ben-Tabou de-Leon, S., Wong, A. M., Jagadish, S., Ishimoto, H., Barnea, G., … Anderson, D. J. (2012). Visualizing neuromodulation in vivo: TANGO-mapping of dopamine signaling reveals appetite control of sugar sensing. *Cell*, *148*(3), 583–595. https://doi.org/10.1016/j.cell.2011.12.022

Inagaki, H. K., Panse, K. M., & Anderson, D. J. (2014). Independent, Reciprocal Neuromodulatory Control of Sweet and Bitter Taste Sensitivity during Starvation in Drosophila. *Neuron*, *84*(4), 806–820. https://doi.org/10.1016/j.neuron.2014.09.032

Ito, K., Shinomiya, K., Ito, M., Armstrong, J. D., Boyan, G., Hartenstein, V., … Vosshall, L. B. (2014). A systematic nomenclature for the insect brain. *Neuron*, *81*(4), 755–765. https://doi.org/10.1016/j.neuron.2013.12.017

Itskov, P. M., Moreira, J. M., Vinnik, E., Lopes, G., Safarik, S., Dickinson, M. H., & Ribeiro, C. (2014). Automated monitoring and quantitative analysis of feeding behaviour in Drosophila. *Nature Communications*, *5*. https://doi.org/10.1038/ncomms5560

Jaeger, A. H., Stanley, M., Weiss, Z. F., Musso, P., Chan, R. C. W., Zhang, H., … Gordon, M. D. (2018). A complex peripheral code for salt taste in Drosophila, 1–30.

Jagadish, S., Barnea, G., Clandinin, T. R., & Axel, R. (2014). Identifying Functional Connections of the Inner Photoreceptors in Drosophila using Tango-Trace. *Neuron*,

83(3), 630–644. https://doi.org/10.1016/j.neuron.2014.06.025

Jefferis, G. S. X. E., Potter, C. J., Chan, A. M., Marin, E. C., Rohlfing, T., Maurer, C. R., & Luo, L. (2007). Comprehensive maps of Drosophila higher olfactory centers: spatially segregated fruit and pheromone representation. *Cell*, *128*(6), 1187–1203. https://doi.org/10.1016/j.cell.2007.01.040

Jiao, Y., Moon, S. J., & Montell, C. (2007). A Drosophila gustatory receptor required for the responses to sucrose, glucose, and maltose identified by mRNA tagging. *Proceedings of the National Academy of Sciences*, *104*(35), 14110–14115. https://doi.org/10.1073/pnas.0702421104

Jiao, Y., Moon, S. J., Wang, X., Ren, Q., & Montell, C. (2008). Gr64f Is Required in Combination with Other Gustatory Receptors for Sugar Detection in Drosophila. *Current Biology*, *18*(22), 1797–1801. https://doi.org/10.1016/j.cub.2008.10.009

Joesch, M., Schnell, B., Raghu, S. V., Reiff, D. F., & Borst, A. (2010). ON and off pathways in Drosophila motion vision. *Nature*, *468*(7321), 300–304. https://doi.org/10.1038/nature09545

Kaelberer, M. M., Buchanan, K. L., Klein, M. E., Barth, B., Montoya, M., Shen, X., & Bohórquez, D. V. (2018). A gut-brain neural circuit for nutrient sensory transduction. *Science*, *In Press*. https://doi.org/10.1126/science.aat5236

Kain, P., Badsha, F., Hussain, S. M., Nair, A., Hasan, G., & Rodrigues, V. (2010). Mutants in phospholipid signaling attenuate the behavioral response of adult Drosophila to trehalose. *Chemical Senses*, *35*(8), 663–673. https://doi.org/10.1093/chemse/bjq055

Kain, P., & Dahanukar, A. (2015). Secondary Taste Neurons that Convey Sweet Taste

and Starvation in the Drosophila Brain. *Neuron*, *85*(4), 1–14. https://doi.org/10.1016/j.neuron.2015.01.005

Kallman, B. R., Kim, H., & Scott, K. (2015). Excitation and inhibition onto central courtship neurons biases drosophila mate choice. *ELife*, *4*(NOVEMBER2015), 1–18. https://doi.org/10.7554/eLife.11188

Kapan, N., Lushchak, O. V., Luo, J., & Nässel, D. R. (2012). Identified peptidergic neurons in the Drosophila brain regulate insulin-producing cells, stress responses and metabolism by coexpressed short neuropeptide F and corazonin. *Cellular and Molecular Life Sciences*, *69*(23), 4051–4066. https://doi.org/10.1007/s00018-012-1097-z

Kendroud, S., Bohra, A. A., Kuert, P. A., Nguyen, B., Guillermin, O., Sprecher, S. G., … Hartenstein, V. (2017). Structure and development of the subesophageal zone of the Drosophila brain. II. Sensory compartments, (May), 33–58. https://doi.org/10.1002/cne.24316

Kim, H., Kim, H., Kwon, J. Y., Seo, J. T., Shin, D. M., & Moon, S. J. (2018). Drosophila Gr64e mediates fatty acid sensing via the phospholipase C pathway. *PLoS Genetics*, *14*(2), 1–16. https://doi.org/10.1371/journal.pgen.1007229

Kim, H., Kirkhart, C., & Scott, K. (2017). Long-range projection neurons in the taste circuit of Drosophila. *ELife*, *6*, e23386. https://doi.org/10.7554/eLife.23386

Kimura, K. I., Ote, M., Tazawa, T., & Yamamoto, D. (2005). Fruitless specifies sexually dimorphic neural circuitry in the Drosophila brain. *Nature*, *438*(7065), 229–233. https://doi.org/10.1038/nature04229

Kinnamon, J. C., Taylor, B. J., Delay, R. J., & Roper, S. D. (1985). Ultrastructure of

mouse vallate taste buds. I. Taste cells and their associated synapses. *Journal of Comparative Neurology*, *235*(1), 48–60. https://doi.org/10.1002/cne.902350105

Kirkhart, C., & Scott, K. (2015). Gustatory learning and processing in the Drosophila mushroom bodies. *The Journal of Neuroscience : The Official Journal of the Society for Neuroscience*, *35*(15), 5950–5958. https://doi.org/10.1523/JNEUROSCI.3930-14.2015

Koh, T. W., He, Z., Gorur-Shandilya, S., Menuz, K., Larter, N. K., Stewart, S., & Carlson, J. R. (2014). The Drosophila IR20a Clade of Ionotropic Receptors Are Candidate Taste and Pheromone Receptors. *Neuron*, *83*(4), 850–865. https://doi.org/10.1016/j.neuron.2014.07.012

Kreher, S. A., Kwon, J. Y., & Carlson, J. R. (2005). The molecular basis of odor coding in the Drosophila larva. *Neuron*, *46*(3), 445–456. https://doi.org/10.1016/j.neuron.2005.04.007

Kremkow, J., Jin, J., Komban, S. J., Wang, Y., Lashgari, R., Li, X., … Alonso, J. M. (2014). Neuronal nonlinearity explains greater visual spatial resolution for darks than lights. *Proceedings of the National Academy of Sciences of the United States of America*, *111*(8), 3170–3175. https://doi.org/10.1073/pnas.1310442111

Krstenansky, J. L., Trivedi, D., Hruby, V. J., & Johnson, D. (1986). Conformational Considerations in the Design of a Glucagon Analogue with Increased Receptor Binding and Adenylate Cyclase Potencies. *Journal of the American Chemical Society*, *108*(7), 1696–1698. https://doi.org/10.1021/ja00267a053

Kurtovic, A., Widmer, A., & Dickson, B. J. (2007). A single class of olfactory neurons mediates behavioural responses to a Drosophila sex pheromone. *Nature*,

446(March), 542–546. https://doi.org/10.1038/nature05672

Kvello, P., Jørgensen, K., & Mustaparta, H. (2010). Central gustatory neurons integrate taste quality information from four appendages in the moth Heliothis virescens. *Journal of Neurophysiology*, *103*(6), 2965–2981. https://doi.org/10.1152/jn.00985.2009

Kwon, J. Y., Dahanukar, A., Weiss, L. A., & Carlson, J. R. (2011). Molecular and cellular organization of the taste system in the Drosophila larva. *Journal of Neuroscience*, *31*(43), 15300–15309. https://doi.org/10.1523/JNEUROSCI.3363-11.2011

Kwon, J. Y., Dahanukar, A., Weiss, L. A., & Carlson, J. R. (2014). A map of taste neuron projections in the Drosophila CNS. *J Biosci*, *39*(4), 565–574.

Larson, E. D., Vandenbeuch, A., Voigt, A., Meyerhof, W., Kinnamon, S. C., & Finger, T. E. (2015). The role of 5-HT3 receptors in signaling from taste buds to nerves. *Journal of Neuroscience*, *35*(48), 15984–15995. https://doi.org/10.1523/JNEUROSCI.1868-15.2015

LeDue, E. E., Mann, K., Koch, E., Chu, B., Dakin, R., & Gordon, M. D. (2016). Starvation-Induced Depotentiation of Bitter Taste in Drosophila. *Current Biology*, *26*(21), 2854–2861. https://doi.org/10.1016/j.cub.2016.08.028

Lee, H., MacPherson, L. J., Parada, C. A., Zuker, C. S., & Ryba, N. J. P. (2017). Rewiring the taste system. *Nature*, *548*(7667), 330–333. https://doi.org/10.1038/nature23299

Lee, M. J., Sung, H. Y., Jo, H., Kim, H. W., Choi, M. S., Kwon, J. Y., & Kang, K. J. (2017). Ionotropic receptor 76b is required for gustatory aversion to excessive na+

in drosophila. *Molecules and Cells*, *40*(10), 787–795. https://doi.org/10.14348/molcells.2017.0160

Lee, T., & Luo, L. (1999). Mosaic analysis with a repressible neurotechnique cell marker for studies of gene function in neuronal morphogenesis. *Neuron*, *22*(3), 451–461. https://doi.org/10.1016/S0896-6273(00)80701-1

Lee, Y., Moon, S. J., & Montell, C. (2009). Multiple gustatory receptors required for the caffeine response in Drosophila. *Proceedings of the National Academy of Sciences of the United States of America*, *106*(11), 4495–4500. https://doi.org/10.1073/pnas.0811744106

Lee, Y., Poudel, S., Kim, Y., Thakur, D., & Montell, C. (2018). Calcium Taste Avoidance in Drosophila. *Neuron*, *97*(1), 67-74.e4. https://doi.org/10.1016/j.neuron.2017.11.038

Li, R., Fan, W., Tian, G., Zhu, H., He, L., Cai, J., … Wang, J. (2010). The sequence and de novo assembly of the giant panda genome. *Nature*, *463*(7279), 311–317. https://doi.org/10.1038/nature08696

Li, X., Li, W., Wang, H., Cao, J., Maehashi, K., Huang, L., … Brand, J. G. (2005). Pseudogenization of a sweet-receptor gene accounts for cats' indifference toward sugar. *PLoS Genetics*, *1*(1), 0027–0035. https://doi.org/10.1371/journal.pgen.0010003

Li, X., Staszewski, L., Xu, H., Durick, K., Zoller, M., & Adler, E. (2002). Human receptors for sweet and umami taste. *Proceedings of the National Academy of Sciences of the United States of America*, *99*(7), 4692–4696. https://doi.org/10.1073/pnas.072090199

Liang, L., Li, Y., Potter, C. J., Yizhar, O., Deisseroth, K., Tsien, R. W., & Luo, L. (2013). GABAergic projection neurons route selective olfactory inputs to specific higher-order neurons. *Neuron*, *79*(5), 917–931. https://doi.org/10.1016/j.neuron.2013.06.014

Liman, E. R., Zhang, Y. V, & Montell, C. (2014). Peripheral coding of taste. *Neuron*, *81*(5), 984–1000. https://doi.org/10.1016/j.neuron.2014.02.022

Lin, H.-H., Lai, J. S.-Y., Chin, A.-L., Chen, Y.-C., & Chiang, A.-S. (2007). A map of olfactory representation in the Drosophila mushroom body. *Cell*, *128*(6), 1205–1217. https://doi.org/10.1016/j.cell.2007.03.006

Ling, F., Dahanukar, A., Weiss, L. a, Kwon, J. Y., & Carlson, J. R. (2014). The molecular and cellular basis of taste coding in the legs of Drosophila. *The Journal of Neuroscience : The Official Journal of the Society for Neuroscience*, *34*(21), 7148–7164. https://doi.org/10.1523/JNEUROSCI.0649-14.2014

Liu, C., Plaçais, P. Y., Yamagata, N., Pfeiffer, B. D., Aso, Y., Friedrich, A. B., … Tanimoto, H. (2012). A subset of dopamine neurons signals reward for odour memory in Drosophila. *Nature*, *488*(7412), 512–516. https://doi.org/10.1038/nature11304

Liu, H., & Fontanini, A. (2015). State dependency of chemosensory coding in the gustatory thalamus (VPMpc) of alert rats. *Journal of Neuroscience*, *35*(47), 15479–15491. https://doi.org/10.1523/JNEUROSCI.0839-15.2015

Liu, Q., Tabuchi, M., Liu, S., Kodama, L., Horiuchi, W., Daniels, J., … Wu, M. N. (2017). Branch-specific plasticity of a bifunctional dopamine circuit encodes protein hunger. *Science*, *539*(May), 534–539. https://doi.org/10.1126/science.aal3245

Lo, L., & Anderson, D. J. (2011). A cre-dependent, anterograde transsynaptic viral tracer for mapping output pathways of genetically marked neurons. *Neuron*, *72*(6), 938–950. https://doi.org/10.1016/j.neuron.2011.12.002

Luo, L., Callaway, E. M., & Svoboda, K. (2008). Genetic dissection of neural circuits. *Neuron*, *57*(5), 634–660. https://doi.org/10.1016/j.neuron.2008.01.002

Luo, L., Callaway, E. M., & Svoboda, K. (2018). Genetic Dissection of Neural Circuits: A Decade of Progress. *Neuron*, *98*(2), 256–281. https://doi.org/10.1016/j.neuron.2018.03.040

Lyall, V., Alam, R. I., Phan, D. Q., Ereso, G. L., Phan, T. H. T., Malik, S. A., … DeSimone, J. A. (2001). Decrease in rat taste receptor cell intracellular pH is the proximate stimulus in sour taste transduction. *American Journal of Physiology - Cell Physiology*, *281*(3 50-3), 1005–1013. https://doi.org/10.1152/ajpcell.2001.281.3.c1005

Ma, Z., Taruno, A., Ohmoto, M., Jyotaki, M., Lim, J. C., Miyazaki, H., … Foskett, J. K. (2018). CALHM3 Is Essential for Rapid Ion Channel-Mediated Purinergic Neurotransmission of GPCR-Mediated Tastes. *Neuron*, *98*(3), 547-561.e10. https://doi.org/10.1016/j.neuron.2018.03.043

Macpherson, L. J., Zaharieva, E. E., Kearney, P. J., Alpert, M. H., Lin, T.-Y., Turan, Z., … Gallio, M. (2015). Dynamic labelling of neural connections in multiple colours by trans-synaptic fluorescence complementation. *Nature Communications*, *6*(May), 10024. https://doi.org/10.1038/ncomms10024

Marella, S., Fischler, W., Kong, P., Asgarian, S., Rueckert, E., & Scott, K. (2006). Imaging taste responses in the fly brain reveals a functional map of taste category

and behavior. *Neuron*, *49*(2), 285–295. https://doi.org/10.1016/j.neuron.2005.11.037

Marella, S., Mann, K., & Scott, K. (2012). Dopaminergic modulation of sucrose acceptance behavior in Drosophila. *Neuron*, *73*(5), 941–950. https://doi.org/10.1016/j.neuron.2011.12.032

Markow, T. A., & O'Grady, P. (2008). Reproductive ecology of Drosophila. *Functional Ecology*, *22*(5), 747–759. https://doi.org/10.1111/j.1365-2435.2008.01457.x

Markstein, M., Pitsouli, C., Villalta, C., Celniker, S. E., & Perrimon, N. (2008). Exploiting position effects and the gypsy retrovirus insulator to engineer precisely expressed transgenes. *Nature Genetics*, *40*(4), 476–483. https://doi.org/10.1038/ng.101

Masek, P., & Keene, A. C. (2013). Drosophila Fatty Acid Taste Signals through the PLC Pathway in Sugar-Sensing Neurons. *PLoS Genetics*, *9*(9). https://doi.org/10.1371/journal.pgen.1003710

Masek, P., & Scott, K. (2010). Limited taste discrimination in Drosophila. *Proceedings of the National Academy of Sciences of the United States of America*, *107*(33), 14833–14838. https://doi.org/10.1073/pnas.1009318107

Masek, P., Worden, K., Aso, Y., Rubin, G. M., & Keene, A. C. (2014). A Dopamine-Modulated Neural Circuit Regulating Aversive Taste Memory in Drosophila. *Current Biology*, *25*(11), 1535–1541. https://doi.org/10.1016/j.cub.2015.04.027

Matsunami, H., Montmayeur, J. P., & Buck, L. B. (2000). A family of candidate taste receptors in human and mouse. *Nature*, *404*(6778), 601–604. https://doi.org/10.1038/35007072

McKellar, C. E., Siwanowicz, I., Dickson, B. J., & Simpson, J. H. (2020). Controlling

motor neurons of every muscle for fly proboscis reaching, 1–34.

Meunier, N., Marion-Poll, F., Rospars, J. P., & Tanimura, T. (2003). Peripheral coding of bitter taste in Drosophila. *Journal of Neurobiology*, *56*(2), 139–152. https://doi.org/10.1002/neu.10235

Mishra, D., Miyamoto, T., Rezenom, Y. H., Broussard, A., Yavuz, A., Slone, J., … Amrein, H. (2013). The Molecular Basis of Sugar Sensing in Drosophila Larvae. *Current Biology*, *23*(15), 1466–1471. https://doi.org/10.1016/j.cub.2013.06.028

Mishra, D., Thorne, N., Miyamoto, C., Jagge, C., & Amrein, H. (2018). The taste of ribonucleosides: Novel macronutrients essential for larval growth are sensed by Drosophila gustatory receptor proteins. *PLOS Biology*, *16*(8), e2005570. https://doi.org/10.1371/journal.pbio.2005570

Misof, B., Liu, S., Meusemann, K., Peters, R. S., Donath, A., Mayer, C., … Zhou, X. (2014). Phylogenomics resolves the timing and pattern of insect evolution. *Science*, *346*(6210), 763–767. https://doi.org/10.1126/science.1257570

Miwa, T., Furukawa, M., Tsuhatani, T., Costanzo, R. M., DiNardo, L. J., & Reiter, E. R. (2001). Impact of olfactory impairment on quality of life and disability. *Archives of Otolaryngology - Head and Neck Surgery*, *127*(5), 497–503. https://doi.org/10.1001/archotol.127.5.497

Miyamoto, T., Chen, Y., Slone, J., & Amrein, H. (2013). Identification of a Drosophila Glucose Receptor Using Ca2+ Imaging of Single Chemosensory Neurons. *PLoS ONE*, *8*(2), 1–8. https://doi.org/10.1371/journal.pone.0056304

Miyamoto, T., Slone, J., Song, X., & Amrein, H. (2012). A fructose receptor functions as a nutrient sensor in the drosophila brain. *Cell*, *151*(5), 1113–1125.

https://doi.org/10.1016/j.cell.2012.10.024

Miyazaki, T., & Ito, K. (2010). Neural architecture of the primary gustatory center of Drosophila melanogaster visualized with GAL4 and LexA enhancer-trap systems. *Journal of Comparative Neurology*, *518*(20), 4147–4181. https://doi.org/10.1002/cne.22433

Miyazaki, T., Lin, T.-Y., Ito, K., Lee, C.-H., & Stopfer, M. (2015). A gustatory second-order neuron that connects sucrose-sensitive primary neurons and a distinct region of the gnathal ganglion in the *Drosophila* brain. *Journal of Neurogenetics*, 1–12. https://doi.org/10.3109/01677063.2015.1054993

Montell, C. (2009). A taste of the Drosophila gustatory receptors. *Current Opinion in Neurobiology*, *19*(4), 345–353. https://doi.org/10.1016/j.conb.2009.07.001

Montmayeur, J. P., Liberles, S. D., Matsunami, H., & Buck, L. B. (2001). A candidate taste receptor gene near a sweet taste locus. *Nature Neuroscience*, *4*(5), 492–498. https://doi.org/10.1038/87440

Moon, S. J., Köttgen, M., Jiao, Y., Xu, H., & Montell, C. (2006). A Taste Receptor Required for the Caffeine Response In Vivo. *Current Biology*, *16*(18), 1812–1817. https://doi.org/10.1016/j.cub.2006.07.024

Morante, J., & Desplan, C. (2008). The Color-Vision Circuit in the Medulla of Drosophila. *Current Biology*, *18*(8), 553–565. https://doi.org/10.1016/j.cub.2008.02.075

Moreira, J. M., Itskov, P. M., Goldschmidt, D., Baltazar, C., Steck, K., Tastekin, I., … Ribeiro, C. (2019). Optopad, a closed-loop optogenetics system to study the circuit basis of feeding behaviors. *ELife*, *8*, 1–19. https://doi.org/10.7554/eLife.43924.001

Mueller, K. L., Hoon, M. A., Erlenbach, I., Chandrashekar, J., Zuker, C. S., & Ryba, N. J. P. (2005). The receptors and coding logic for bitter taste. *Nature*, *434*(March), 225–229. https://doi.org/10.1038/nature03366.1.

Musso, P. Y., Junca, P., Jelen, M., Feldman-Kiss, D., Zhang, H., Chan, R. C. W., & Gordon, M. D. (2019). Closed-loop optogenetic activation of peripheral or central neurons modulates feeding in freely moving Drosophila. *ELife*, *8*, 1–23. https://doi.org/10.7554/eLife.45636

Myers, C. S. (1904). The taste-names of primitive peoples. *Br. J. Psychol. 1904−1920*, *1*(2), 118–126.

Nakagawa, T., & Vosshall, L. B. (2009). Controversy and consensus: noncanonical signaling mechanisms in the insect olfactory system. *Current Opinion in Neurobiology*, *19*(3), 284–292. https://doi.org/10.1016/j.conb.2009.07.015

Nässel, D. R. (1999). Histamine in the brain of insects: A review. *Microscopy Research and Technique*, *44*(2–3), 121–136.

Nässel, D. R., Kubrak, O. I., Liu, Y., Luo, J., & Lushchak, O. V. (2013). Factors that regulate insulin producing cells and their output in drosophila. *Frontiers in Physiology*, *4 SEP*(September), 1–12. https://doi.org/10.3389/fphys.2013.00252

Nelson, G., Chandrashekar, J., Hoon, M. A., Feng, L., Zhao, G., Ryba, N. J. P., & Zuker, C. S. (2002). An amino-acid taste receptor. *Nature*, *416*(6877), 199–202. https://doi.org/10.1038/nature726

Nelson, G., Hoon, M. a, Chandrashekar, J., Zhang, Y., Ryba, N. J. P., & Zuker, C. S. (2001). Mammalian Sweet Taste Receptors. *Cell*, *106*, 381–390. https://doi.org/10.1016/S0092-8674(03)00844-4

Nern, A., Pfeiffer, B. D., & Rubin, G. M. (2015). Optimized tools for multicolor stochastic labeling reveal diverse stereotyped cell arrangements in the fly visual system. *Proceedings of the National Academy of Sciences of the United States of America*, *112*(22), E2967–E2976. https://doi.org/10.1073/pnas.1506763112

Neuland, C., Bitter, T., Marschner, H., Gudziol, H., & Guntinas-Lichius, O. (2011). Health-related and specific olfaction-related quality of life in patients with chronic functional anosmia or severe hyposmia. *Laryngoscope*, *121*(4), 867–872. https://doi.org/10.1002/lary.21387

Nguyen, H. (2018). Of the five senses, a majority would miss sight the most. Retrieved from https://today.yougov.com/topics/health/articles-reports/2018/07/25/five-senses-majority-would-miss-sight-most

Nicolaï, L. J. J., Ramaekers, A., Raemaekers, T., Drozdzecki, A., Mauss, A. S., Yan, J., … Hassan, B. a. (2010). Genetically encoded dendritic marker sheds light on neuronal connectivity in Drosophila. *Proceedings of the National Academy of Sciences of the United States of America*, *107*(47), 20553–20558. https://doi.org/10.1073/pnas.1010198107

Nomura, K., Nakanishi, M., Ishidate, F., Iwata, K., & Taruno, A. (2020). All-electrical Ca2+-independent signal transduction mediates attractive sodium taste in taste buds. *Neuron*, 1–14. https://doi.org/10.1016/j.neuron.2020.03.006

Ogawa, H., & Wang, X. D. (2002). Neurons in the cortical taste area receive nociceptive inputs from the whole body as well as the oral cavity in the rat. *Neuroscience Letters*, *322*(2), 87–90. https://doi.org/10.1016/S0304-3940(02)00099-X

Oka, Y., Butnaru, M., Von Buchholtz, L., Ryba, N. J. P., & Zuker, C. S. (2013). High salt

recruits aversive taste pathways. *Nature*, *494*(7438), 472–475. https://doi.org/10.1038/nature11905

Olberg, R. M., Worthington, A. H., & Venator, K. R. (2000). Prey pursuit and interception in dragonflies. *Journal of Comparative Physiology - A Sensory, Neural, and Behavioral Physiology*, *186*(2), 155–162. https://doi.org/10.1007/s003590050015

Otto, N., Pleijzier, M. W., Morgan, I. C., Edmondson-Stait, A. J., Heinz, K. J., Stark, I., … Waddell, S. (2020). Input Connectivity Reveals Additional Heterogeneity of Dopaminergic Reinforcement in Drosophila. *Current Biology*, 1–12. https://doi.org/10.1016/j.cub.2020.05.077

Palmiter, R. D. (2018). The Parabrachial Nucleus: CGRP Neurons Function as a General Alarm. *Trends in Neurosciences*, *41*(5), 280–293. https://doi.org/10.1016/j.tins.2018.03.007

Park, J. H., & Kwon, J. Y. (2011). A systematic analysis of drosophila gustatory receptor gene expression in abdominal neurons which project to the central nervous system. *Molecules and Cells*, *32*(4), 375–381. https://doi.org/10.1007/s10059-011-0128-1

Park, J. Y., Dus, M., Kim, S., Abu, F., Kanai, M. I., Rudy, B., & Suh, G. S. B. (2016). Drosophila SLC5A11 Mediates Hunger by Regulating K+ Channel Activity. *Current Biology*, *26*(15), 1965–1974. https://doi.org/10.1016/j.cub.2016.05.076

Patterson, G. H., & Lippincott-Schwartz, J. (2002). A photoactivatable GFP for selective photolabeling of proteins and cells. *Science*, *297*(5588), 1873–1877. https://doi.org/10.1126/science.1074952

Pellegrino, R., Cooper, K. W., Pizio, A. Di, Joseph, P. V., Bhutani, S., & Parma, V.

(2020). Coronaviruses and the Chemical Senses: Past, Present, and Future. *Chemical Senses*, *45*(6), 415–422. https://doi.org/10.1093/chemse/bjaa031

Perez-Orive, J., Mazor, O., Turner, G. C., Cassenaer, S., Wilson, R. I., & Laurent, G. (2002). Oscillations and sparsening of odor representations in the mushroom body. *Science*, *297*(5580), 359–365. https://doi.org/10.1126/science.1070502

Pfaffmann, C. (1941). Gustatory afferent impulses. *Journal of Cellular and Comparative Physiology*, *17*(2), 243–258. https://doi.org/10.1002/jcp.1030170209

Pfaffmann, C. (1974). Specificity of the sweet receptors of the squirrel monkey. *Chemical Senses and Flavor*, *1*(1), 61–67. https://doi.org/10.1093/chemse/1.1.61

Pfeiffer, B. D., Jenett, A., Hammonds, A. S., Ngo, T.-T. B., Misra, S., Murphy, C., … Rubin, G. M. (2008). Tools for neuroanatomy and neurogenetics in Drosophila. *Proceedings of the National Academy of Sciences of the United States of America*, *105*(28), 9715–9720. https://doi.org/10.1073/pnas.0803697105

Pfeiffer, B. D., Ngo, T.-T. B., Hibbard, K. L., Murphy, C., Jenett, A., Truman, J. W., & Rubin, G. M. (2010). Refinement of tools for targeted gene expression in Drosophila. *Genetics*, *186*(2), 735–755. https://doi.org/10.1534/genetics.110.119917

Pfeiffer, B. D., Truman, J. W., & Rubin, G. M. (2012). Using translational enhancers to increase transgene expression in Drosophila. *Proceedings of the National Academy of Sciences of the United States of America*, *109*(17), 6626–6631. https://doi.org/10.1073/pnas.1204520109

Pfeiffer, K., & Homberg, U. (2014). Organization and functional roles of the central complex in the insect brain. *Annual Review of Entomology*, *59*, 165–184. https://doi.org/10.1146/annurev-ento-011613-162031

Pnevmatikakis, E. A., & Giovannucci, A. (2017). NoRMCorre: An online algorithm for piecewise rigid motion correction of calcium imaging data. *Journal of Neuroscience Methods*, *291*, 83–94. https://doi.org/10.1016/j.jneumeth.2017.07.031

Pool, A. H., & Scott, K. (2014). Feeding regulation in Drosophila. *Current Opinion in Neurobiology*, *29*, 57–63. https://doi.org/10.1016/j.conb.2014.05.008

Potter, C. J., & Luo, L. (2011). Using the Q system in Drosophila melanogaster. *Nature Protocols*, *6*(8), 1105–1120. https://doi.org/10.1038/nprot.2011.347

Potter, C. J., Tasic, B., Russler, E. V, Liang, L., & Luo, L. (2010). The Q system: a repressible binary system for transgene expression, lineage tracing, and mosaic analysis. *Cell*, *141*(3), 536–548. https://doi.org/10.1016/j.cell.2010.02.025

Purtill, C., & Kopf, D. (2018). Which of the five senses do you value most? The answer may change as you age. Retrieved from https://qz.com/1343746/as-you-age-the-sense-you-value-the-most-changes/

Python, F., & Stocker, R. F. (2002). Adult-like complexity of the larval antennal lobe of D. melanogaster despite markedly low numbers of odorant receptor neurons. *Journal of Comparative Neurology*, *445*(4), 374–387. https://doi.org/10.1002/cne.10188

Ramaekers, A., Magnenat, E., Marin, E. C., Gendre, N., Jefferis, G. S. X. E., Luo, L., & Stocker, R. F. (2005). Glomerular maps without cellular redundancy at successive levels of the Drosophila larval olfactory circuit. *Current Biology*, *15*(11), 982–992. https://doi.org/10.1016/j.cub.2005.04.032

Ramón y Cajal, S. (1888). Estructura de los centros nerviosos de las aves. *Rev. Trim. Histol. Norm. Pat*, (1), 1–10.

Reed, D. R., Nanthakumar, E., North, M., Bell, C., Bartoshuk, L. M., & Price, R. A. (1999). Localization of a Gene for Bitter-Taste Perception to Human Chromosome 5p15. *Am. J. Hum. Genet.*, (64), 1478–1480. https://doi.org/10.2460/javma.245.5.484

Reiter, S., Campillo Rodriguez, C., Sun, K., & Stopfer, M. (2015). Spatiotemporal Coding of Individual Chemicals by the Gustatory System. *Journal of Neuroscience*, *35*(35), 12309–12321. https://doi.org/10.1523/JNEUROSCI.3802-14.2015

Rimal, S., Sang, J., Poudel, S., Thakur, D., Montell, C., Rimal, S., … Lee, Y. (2019). Mechanism of Acetic Acid Gustatory Repulsion in Article Mechanism of Acetic Acid Gustatory Repulsion in Drosophila. *CellReports*, *26*(6), 1432-1442.e4. https://doi.org/10.1016/j.celrep.2019.01.042

Rist, A., & Thum, A. S. (2017). A map of sensilla and neurons in the taste system of drosophila larvae. *Journal of Comparative Neurology*, *525*(18), 3865–3889. https://doi.org/10.1002/cne.24308

Robertson, H. M., Warr, C. G., & Carlson, J. R. (2003). Molecular evolution of the insect chemoreceptor gene superfamily in Drosophila melanogaster. *Proceedings of the National Academy of Sciences of the United States of America*, *100*(24), 14537–14542. https://doi.org/10.1073/pnas.2335847100

Rodrigues, V., & Siddiqi, O. (1978). Genetic analysis of chemosensory pathway. *Proceedings of the Indian Academy of Sciences - Section B, Experimental Biology*, *87*(7), 147–160. https://doi.org/10.1007/BF03178976

Rohwedder, A., Pfitzenmaier, J. E., Ramsperger, N., Apostolopoulou, A. A., Widmann, A., & Thum, A. S. (2012). Nutritional value-dependent and nutritional value-

independent effects on Drosophila melanogaster larval behavior. *Chemical Senses*, *37*(8), 711–721. https://doi.org/10.1093/chemse/bjs055

Rolls, E. T. (2019). *Taste and smell processing in the brain*. *Handbook of Clinical Neurology* (1st ed., Vol. 164). Elsevier B.V. https://doi.org/10.1016/B978-0-444-63855-7.00007-1

Root, C. M., Ko, K. I., Jafari, A., & Wang, J. W. (2011). Presynaptic facilitation by neuropeptide signaling mediates odor-driven food search. *Cell*, *145*(1), 133–144. https://doi.org/10.1016/j.cell.2011.02.008

Roper, S. D., & Chaudhari, N. (2017). Taste buds: Cells, signals and synapses. *Nature Reviews Neuroscience*, *18*(8), 485–497. https://doi.org/10.1038/nrn.2017.68

Rosen, A. M., Victor, J. D., & di Lorenzo, P. M. (2011). Temporal coding of taste in the parabrachial nucleus of the pons of the rat. *Journal of Neurophysiology*, *105*(4), 1889–1896. https://doi.org/10.1152/jn.00836.2010

Roussin, A. T., D'Agostino, A. E., Fooden, A. M., Victor, J. D., & Di Lorenzo, P. M. (2012). Taste Coding in the Nucleus of the Solitary Tract of the Awake, Freely Licking Rat. *Journal of Neuroscience*, *32*(31), 10494–10506. https://doi.org/10.1523/JNEUROSCI.1856-12.2012

Roussin, A. T., Victor, J. D., Chen, J. Y., & Di Lorenzo, P. M. (2008). Variability in responses and temporal coding of tastants of similar quality in the nucleus of the solitary tract of the rat. *Journal of Neurophysiology*, *99*(2), 644–655. https://doi.org/10.1152/jn.00920.2007

Running, C. A., Craig, B. A., & Mattes, R. D. (2015). Oleogustus: The unique taste of fat. *Chemical Senses*, *40*(7), 507–516. https://doi.org/10.1093/chemse/bjv036

Ruta, V., Datta, S. R., Vasconcelos, M. L., Freeland, J., Looger, L. L., & Axel, R. (2010). A dimorphic pheromone circuit in Drosophila from sensory input to descending output. *Nature*, *468*(7324), 686–690. https://doi.org/10.1038/nature09554

Saddoris, M. P., Holland, P. C., & Gallagher, M. (2009). Associatively learned representations of taste outcomes activate taste-encoding neural ensembles in gustatory cortex. *Journal of Neuroscience*, *29*(49), 15386–15396. https://doi.org/10.1523/JNEUROSCI.3233-09.2009

Samuelsen, C. L., Gardner, M. P. H., & Fontanini, A. (2012). Effects of Cue-Triggered Expectation on Cortical Processing of Taste. *Neuron*, *74*(2), 410–422. https://doi.org/10.1016/j.neuron.2012.02.031

Sánchez-Alcañiz, J. A., Silbering, A. F., Croset, V., Zappia, G., Sivasubramaniam, A. K., Abuin, L., … Benton, R. (2018). An expression atlas of variant ionotropic glutamate receptors identifies a molecular basis of carbonation sensing. *Nature Communications*, *9*(1). https://doi.org/10.1038/s41467-018-06453-1

Sanes, J. R., & Zipursky, S. L. (2010). Design Principles of Insect and Vertebrate Visual Systems. *Neuron*, *66*(1), 15–36. https://doi.org/10.1016/j.neuron.2010.01.018

Sareen, P., McCurdy, L. Y., & Nitabach, M. N. (2020). A neuronal ensemble encoding adaptive choice during sensory conflict. *BioRxiv*, *1*(2), 40–48.

Sato, K., Pellegrino, M., Nakagawa, T., Nakagawa, T., Vosshall, L. B., & Touhara, K. (2008). Insect olfactory receptors are heteromeric ligand-gated ion channels. *Nature*, *452*(April), 1002–1006. https://doi.org/10.1038/nature06850

Sato, K., Tanaka, K., & Touhara, K. (2011). Sugar-regulated cation channel formed by an insect gustatory receptor. *Proceedings of the National Academy of Sciences of the*

United States of America, *108*(28), 11680–11685. https://doi.org/10.1073/pnas.1019622108

Scheffer, L., Xu, C. S., Januszewski, M., Lu, Z., Takemura, S., Hayworth, K., … Plaza, S. (2020). A Connectome and Analysis of the Adult Drosophila Central Brain. *BioRxiv*, 1–57. https://doi.org/10.1101/2020.04.07.030213

Schiller, P. H., Sandell, J. H., & Maunsell, J. H. R. (1986). Functions of the ON and OFF channels of the visual system. *Nature*, *322*(28), 824–825. https://doi.org/10.1016/1350-9462(95)00009-7

Scholl, B., Gao, X., & Wehr, M. (2010). Nonoverlapping Sets of Synapses Drive On Responses and Off Responses in Auditory Cortex. *Neuron*, *65*(3), 412–421. https://doi.org/10.1016/j.neuron.2010.01.020

Scott, K. (2018). Gustatory Processing in Drosophila melanogaster. *Annual Review of Entomology*, *63*, 15–30. https://doi.org/10.1146/annurev-ento-020117-043331

Scott, K., Brady, R., Cravchik, a, Morozov, P., Rzhetsky, a, Zuker, C., & Axel, R. (2001). A chemosensory gene family encoding candidate gustatory and olfactory receptors in Drosophila. *Cell*, *104*(5), 661–673. Retrieved from http://www.ncbi.nlm.nih.gov/pubmed/11257221

Seeholzer, L. F., Seppo, M., Stern, D. L., & Ruta, V. (2018). Evolution of a central neural circuit underlies Drosophila mate preferences. *Nature*. https://doi.org/10.1038/s41586-018-0322-9

Seki, Y., Rybak, J., Wicher, D., Sachse, S., & Hansson, B. S. (2010). Physiological and morphological characterization of local interneurons in the Drosophila antennal lobe. *Journal of Neurophysiology*, *104*(2), 1007–1019.

https://doi.org/10.1152/jn.00249.2010

Sellier, M. J., Reeb, P., & Marion-Poll, F. (2011). Consumption of bitter alkaloids in Drosophila melanogaster in multiple-choice test conditions. *Chemical Senses*, *36*(4), 323–334. https://doi.org/10.1093/chemse/bjq133

Semmelhack, J. L., & Wang, J. W. (2009). Select Drosophila glomeruli mediate innate olfactory attraction and aversion. *Nature*, *459*(7244), 218–223. https://doi.org/10.1038/nature07983

Sherrington, C. S. (1906). Observations on the scratch-reflex in the spinal dog. *The Journal of Physiology*, *34*(1–2), 1–50. https://doi.org/10.1113/jphysiol.1906.sp001139

Shim, J., Lee, Y., Jeong, Y. T., Kim, Y., Lee, M. G., Montell, C., & Moon, S. J. (2015). The full repertoire of Drosophila gustatory receptors for detecting an aversive compound. *Nature Communications*, *6*, 1–8. https://doi.org/10.1038/ncomms9867

Silbering, A. F., Rytz, R., Grosjean, Y., Abuin, L., Ramdya, P., Jefferis, G. S. X. E., & Benton, R. (2011). Complementary function and integrated wiring of the evolutionarily distinct Drosophila olfactory subsystems. *The Journal of Neuroscience : The Official Journal of the Society for Neuroscience*, *31*(38), 13357–13375. https://doi.org/10.1523/JNEUROSCI.2360-11.2011

Simon, S. A., De Araujo, I. E., Gutierrez, R., & Nicolelis, M. A. L. (2006). The neural mechanisms of gustation: A distributed processing code. *Nature Reviews Neuroscience*, *7*(11), 890–901. https://doi.org/10.1038/nrn2006

Smith, D. V., Van Buskirk, R. L., Travers, J. B., & Bieber, S. L. (1983). Gustatory neuron types in hamster brain stem. *Journal of Neurophysiology*, *50*(2), 522–540.

https://doi.org/10.1152/jn.1983.50.2.522

Spector, A. C., & Kopka, S. L. (2002). Rats fail to discriminate quinine from denatonium: Implications for the neural coding of bitter-tasting compounds. *Journal of Neuroscience*, *22*(5), 1937–1941. https://doi.org/10.1523/jneurosci.22-05-01937.2002

Spector, A. C., & Travers, S. P. (2005). The representation of taste quality in the mammalian nervous system. *Behavioral and Cognitive Neuroscience Reviews*, *4*(3), 143–191. https://doi.org/10.1177/1534582305280031

Steck, K., Walker, S. J., Itskov, P. M., & Ribeiro, C. (2018). Internal amino acid state modulates yeast taste neurons to support protein homeostasis in Drosophila, 1–29.

Steiner, J. E. (1974). Discussion Paper: Innate, Discriminative Human Facial Expressions To Taste and Smell Stimulation. *Annals of the New York Academy of Sciences*, *237*(1), 229–233. https://doi.org/10.1111/j.1749-6632.1974.tb49858.x

Strother, J. A., Nern, A., & Reiser, M. B. (2014). Direct observation of on and off pathways in the drosophila visual system. *Current Biology*, *24*(9), 976–983. https://doi.org/10.1016/j.cub.2014.03.017

Strutz, A., Soelter, J., Baschwitz, A., Farhan, A., Grabe, V., Rybak, J., … Sachse, S. (2014). Decoding odor quality and intensity in the Drosophila brain. *ELife*, *3*, 1–21. https://doi.org/10.7554/eLife.04147

Sugita, M., & Shiba, Y. (2005). Neuroscience: Genetic tracing shows segregation of taste neuronal circuitries for bitter and sweet. *Science*, *309*(5735), 781–785. https://doi.org/10.1126/science.1110787

Talay, M., Richman, E. B., Snell, N. J., Hartmann, G. G., Fisher, J. D., Sorkaç, A., …

Barnea, G. (2017). Transsynaptic Mapping of Second-Order Taste Neurons in Flies by trans-Tango. *Neuron*, *96*(4), 783-795.e4. https://doi.org/10.1016/j.neuron.2017.10.011

Tan, H., Sisti, A. C., Jin, H., Vignovich, M., Villavicencio, M., Tsang, K. S., … Zuker, C. S. (2020). The gut – brain axis mediates sugar preference. *Nature*, (April 2019). https://doi.org/10.1038/s41586-020-2199-7

Tanaka, N. K., Awasaki, T., Shimada, T., & Ito, K. (2004). Integration of chemosensory pathways in the Drosophila second-order olfactory centers. *Current Biology : CB*, *14*(6), 449–457. https://doi.org/10.1016/j.cub.2004.03.006

Taruno, A., Vingtdeux, V., Ohmoto, M., Ma, Z., Dvoryanchikov, G., Li, A., … Foskett, J. K. (2013). CALHM1 ion channel mediates purinergic neurotransmission of sweet, bitter and umami tastes. *Nature*, *495*(7440), 223–226. https://doi.org/10.1038/nature11906

Tauber, J. M., Brown, E. B., Li, Y., Yurgel, M. E., Masek, P., & Keene, A. C. (2017). A subset of sweet-sensing neurons identified by IR56d are necessary and sufficient for fatty acid taste. *PLoS Genetics*, *13*(11), 1–18. https://doi.org/10.1371/journal.pgen.1007059

Teng, B., Wilson, C. E., Tu, Y. H., Joshi, N. R., Kinnamon, S. C., & Liman, E. R. (2019). Cellular and Neural Responses to Sour Stimuli Require the Proton Channel Otop1. *Current Biology*, *29*(21), 3647-3656.e5. https://doi.org/10.1016/j.cub.2019.08.077

Thistle, R., Cameron, P., Ghorayshi, A., Dennison, L., & Scott, K. (2012). Contact chemoreceptors mediate male-male repulsion and male-female attraction during Drosophila courtship. *Cell*, *149*(5), 1140–1151.

https://doi.org/10.1016/j.cell.2012.03.045

Thoma, V., Knapek, S., Arai, S., Hartl, M., Kohsaka, H., Sirigrivatanawong, P., … Tanimoto, H. (2016). Functional dissociation in sweet taste receptor neurons between and within taste organs of Drosophila. *Nature Communications*, *7*, 10678. https://doi.org/10.1038/ncomms10678

Thorne, N., Chromey, C., Bray, S., & Amrein, H. (2004). Taste Perception and Coding in Drosophila. *Current Biology*, *14*, 1118. https://doi.org/10.1016/j

Tobin, W. F., Wilson, R. I., & Allen Lee, W.-C. (2017). Wiring variations that enable and constrain neural computation in a sensory microcircuit. *BioRxiv*, 1–26. https://doi.org/10.1101/097659

Tomchik, S. M., Berg, S., Joung, W. K., Chaudhari, N., & Roper, S. D. (2007). Breadth of tuning and taste coding in mammalian taste buds. *Journal of Neuroscience*, *27*(40), 10840–10848. https://doi.org/10.1523/JNEUROSCI.1863-07.2007

Tordoff, M. G., Alarcón, L. K., Valmeki, S., & Jiang, P. (2012). T1R3: A human calcium taste receptor. *Scientific Reports*, *2*, 3–6. https://doi.org/10.1038/srep00496

Travers, S. P., & Geran, L. C. (2009). Bitter-responsive brainstem neurons: Characteristics and functions. *Physiology and Behavior*, *97*(5), 592–603. https://doi.org/10.1016/j.physbeh.2009.02.042

Tu, Y., Cooper, A. J., Teng, B., Chang, R. B., Artiga, D. J., Turner, H. N., … Liman, E. R. (2018). An evolutionarily conserved gene family encodes proton- selective ion channels, *3264*(January), 1–9.

Ueno, K., Kohatsu, S., Clay, C., Forte, M., Isono, K., & Kidokoro, Y. (2006). Gsalpha is involved in sugar perception in Drosophila melanogaster. *The Journal of*

Neuroscience : The Official Journal of the Society for Neuroscience, *26*(23), 6143–6152. https://doi.org/10.1523/JNEUROSCI.0857-06.2006

Van Buskirk, R. L., & Smith, D. V. (1981). Taste sensitivity of hamster parabrachial pontine neurons. *Journal of Neurophysiology*, *45*(1), 144–171. https://doi.org/10.1152/jn.1981.45.1.144

Van Giesen, L., Hernandez-Nunez, L., Delasoie-Baranek, S., Colombo, M., Renaud, P., Bruggmann, R., … Sprecher, S. G. (2016). Multimodal stimulus coding by a gustatory sensory neuron in Drosophila larvae. *Nature Communications*, *7*, 1–10. https://doi.org/10.1038/ncomms10687

Vijayan, V., Thistle, R., Liu, T., Starostina, E., & Pikielny, C. W. (2014). Drosophila Pheromone-Sensing Neurons Expressing the ppk25 Ion Channel Subunit Stimulate Male Courtship and Female Receptivity. *PLoS Genetics*, *10*(3). https://doi.org/10.1371/journal.pgen.1004238

Vosshall, L. B., & Stocker, R. F. (2007). Molecular architecture of smell and taste in Drosophila. *Annual Review of Neuroscience*, *30*, 505–533. https://doi.org/10.1146/annurev.neuro.30.051606.094306

Wang, Z., Singhvi, A., Kong, P., & Scott, K. (2004). Taste representations in the Drosophila brain. *Cell*, *117*(7), 981–991. https://doi.org/10.1016/j.cell.2004.06.011

Weiss, L. A., Dahanukar, A., Kwon, J. Y., Banerjee, D., & Carlson, J. R. (2011). The molecular and cellular basis of bitter taste in Drosophila. *Neuron*, *69*(2), 258–272. https://doi.org/10.1016/j.neuron.2011.01.001

Weiss, M. S., Victor, J. D., & Di Lorenzo, P. M. (2014). Taste coding in the parabrachial nucleus of the pons in awake, freely licking rats and comparison with the nucleus of

the solitary tract. *Journal of Neurophysiology*, *111*(8), 1655–1670. https://doi.org/10.1152/jn.00643.2013

Wickersham, I. R., Lyon, D. C., Barnard, R. J. O., Mori, T., Finke, S., Conzelmann, K. K., … Callaway, E. M. (2007). Monosynaptic Restriction of Transsynaptic Tracing from Single, Genetically Targeted Neurons. *Neuron*, *53*(5), 639–647. https://doi.org/10.1016/j.neuron.2007.01.033

Wilder, E. L., & Perrimon, N. (1995). Dual functions of wingless in the Drosophila leg imaginal disc. *Development*, *121*(2), 477–488.

Wisotsky, Z., Medina, A., Freeman, E., & Dahanukar, A. (2011). Evolutionary differences in food preference rely on Gr64e, a receptor for glycerol. *Nature Neuroscience*, *14*(12), 1534–1541. https://doi.org/10.1038/nn.2944

Wittstock, U., & Gershenzon, J. (2002). Constitutive plant toxins and their role in defense against herbivores and pathogens. *Current Opinion in Plant Biology*, *5*(4), 300–307. https://doi.org/10.1016/S1369-5266(02)00264-9

Wu, A., Dvoryanchikov, G., Pereira, E., Chaudhari, N., & Roper, S. D. (2015). Breadth of tuning in taste afferent neurons varies with stimulus strength. *Nature Communications*, *6*. https://doi.org/10.1038/ncomms9171

Wu, J. S., & Luo, L. (2006). A protocol for dissecting Drosophila melanogaster brains for live imaging or immunostaining. *Nature Protocols*, *1*(4), 2110–2115. https://doi.org/10.1038/nprot.2006.336

Yamaguchi, S., & Ninomiya, K. (2000). Umami and food palatability. *Journal of Nutrition*, *130*(4 SUPPL.), 921–926. https://doi.org/10.1093/jn/130.4.921s

Yao, C. A., & Carlson, J. R. (2010). Role of G-proteins in odor-sensing and CO2-sensing

neurons in Drosophila. *The Journal of Neuroscience : The Official Journal of the Society for Neuroscience*, *30*(13), 4562–4572. https://doi.org/10.1523/JNEUROSCI.6357-09.2010

Yapici, N., Cohn, R., Schusterreiter, C., Ruta, V., Vosshall, L. B., Yapici, N., … Vosshall, L. B. (2016). A Taste Circuit that Regulates Ingestion by Integrating Food and Hunger Signals. *Cell*, *165*(3), 1–15. https://doi.org/10.1016/j.cell.2016.02.061

Yarmolinsky, D. a, Zuker, C. S., & Ryba, N. J. P. (2009). Common sense about taste: from mammals to insects. *Cell*, *139*(2), 234–244. https://doi.org/10.1016/j.cell.2009.10.001

Ye, W., Chang, R. B., Bushman, J. D., Tu, Y. H., Mulhall, E. M., Wilson, C. E., … Liman, E. R. (2016). The K+ channel KIR2.1 functions in tandem with proton influx to mediate sour taste transduction. *Proceedings of the National Academy of Sciences of the United States of America*, *113*(2), E229–E238. https://doi.org/10.1073/pnas.1514282112

Yee, K. K., Sukumaran, S. K., Kotha, R., Gilbertson, T. A., & Margolskee, R. F. (2011). Glucose transporters and ATP-gated K+ (KATP) metabolic sensors are present in type 1 taste receptor 3 (T1r3)-expressing taste cells. *Proceedings of the National Academy of Sciences of the United States of America*, *108*(13), 5431–5436. https://doi.org/10.1073/pnas.1100495108

Yoshihara, Y., Mizuno, T., Nakahira, M., Kawasaki, M., Watanabe, Y., Kagamiyama, H., … Mori, K. (1999). A genetic approach to visualization neurotechnique of multisynaptic neural pathways using plant lectin transgene. *Neuron*, *22*(1), 33–41. https://doi.org/10.1016/S0896-6273(00)80676-5

Yu, J. Y., Kanai, M. I., Demir, E., Jefferis, G. S. X. E., & Dickson, B. J. (2010). Cellular organization of the neural circuit that drives Drosophila courtship behavior. *Current Biology*, *20*(18), 1602–1614. https://doi.org/10.1016/j.cub.2010.08.025

Zelle, K. M., Lu, B., Pyfrom, S. C., & Ben-Shahar, Y. (2013). The genetic architecture of degenerin/epithelial sodium channels in drosophila. *G3: Genes, Genomes, Genetics*, *3*(3), 441–450. https://doi.org/10.1534/g3.112.005272

Zhang, F., Klebansky, B., Fine, R. M., Xu, H., Pronin, A., Liu, H., … Li, X. (2008). Molecular mechanism for the umami taste synergism. *Proceedings of the National Academy of Sciences of the United States of America*, *105*(52), 20930–20934. https://doi.org/10.1073/pnas.0810174106

Zhang, H. J., Anderson, A. R., Trowell, S. C., Luo, A. R., Xiang, Z. H., & Xia, Q. Y. (2011). Topological and functional characterization of an insect gustatory receptor. *PLoS ONE*, *6*(8), 1–10. https://doi.org/10.1371/journal.pone.0024111

Zhang, J., Jin, H., Zhang, W., Ding, C., O'Keeffe, S., Ye, M., & Zuker, C. S. (2019). Sour Sensing from the Tongue to the Brain. *Cell*, *179*(2), 392-402.e15. https://doi.org/10.1016/j.cell.2019.08.031

Zhang, Y. V., Ni, J., & Montell, C. (2013). The molecular basis for attractive salt-taste coding in drosophila. *Science*, *340*(6138), 1334–1338. https://doi.org/10.1126/science.1234133

Zhang, Y., Hoon, M. A., Chandrashekar, J., Mueller, K. L., Cook, B., Wu, D., … Ryba, N. J. P. (2003). Coding of sweet, bitter, and umami tastes: Different receptor cells sharing similar signaling pathways. *Cell*, *112*(3), 293–301. https://doi.org/10.1016/S0092-8674(03)00071-0

Zhang, Y. Q., Rodesch, C. K., & Broadie, K. (2002). Living synaptic vesicle marker: Synaptotagmin-GFP. *Genesis*, *34*(1–2), 142–145. https://doi.org/10.1002/gene.10144

Zhao, G. Q., Zhang, Y., Hoon, M. A., Chandrashekar, J., Erlenbach, I., Ryba, N. J. P., & Zuker, C. S. (2003). The Receptors for Mammalian Sweet and Umami Taste. *Cell*, *106*, 381–390. https://doi.org/10.1016/S0092-8674(03)00844-4

Zheng, Z., Lauritzen, J. S., Perlman, E., Robinson, C. G., Nichols, M., Milkie, D., … Bock, D. D. (2018). A complete electron microscopy volume of the brain of adult Drosophila melanogaster. *Cell*, 140905. https://doi.org/10.1101/140905

Zingg, B., Chou, X., Zhang, Z., Mesik, L., Liang, F., Tao, H. W., & Zhang, L. I. (2017). AAV-Mediated Anterograde Transsynaptic Tagging: Mapping Corticocollicular Input-Defined Neural Pathways for Defense Behaviors. *Neuron*, *93*(1), 33–47. https://doi.org/10.1016/j.neuron.2016.11.045

Zocchi, D., Wennemuth, G., & Oka, Y. (2017). The cellular mechanism for water detection in the mammalian taste system. *Nature Neuroscience*, (May). https://doi.org/10.1038/nn.4575